## *Studies on the POLARIS gene of Arabidopsis*

MEHDI, SAHER

# Studies on the *POLARIS* gene of Arabidopsis

**Saher Mehdi B.Sc, M.Sc**

**School of Biological and Biomedical Sciences**

**University of Durham**

**September 2009**

# Declaration

I hereby declare that my submission as a whole is not substantially the same as any that I have previously made or am currently making, whether in published or unpublished form, for a degree, diploma, or similar qualification at any university or similar institution.

Dated: ……..  Signature……

# Abstract


## Studies on the *POLARIS* gene in Arabidopsis

The *POLARIS* (*PLS*) gene of *Arabidopsis* encodes a 36 amino acid peptide required for correct root growth and vascular patterning. Previous work indicates that PLS acts as a negative regulator of ethylene signalling. The *pls* mutant has enhanced ethylene signalling, which is the key determinant of its short root phenotype and results in a 'triple response' phenotype when seedlings are grown in the dark in air. The defects can be rescued by inhibition of ethylene signalling but not by inhibitors of ethylene biosynthesis, and *pls* does not over-produce ethylene, indicating a role for the peptide in ethylene signalling. Inhibition of ethylene signalling either by genetic or pharmacological methods restores *pls* mutant root growth. These data implicate ethylene as an important regulator of root development and PLS is hypothesised as a component of an ethylene regulatory mechanism to modulate root growth. This work establishes a direct interaction between ETR1, an ethylene receptor protein, and PLS by using both Yeast Two Hybrid and Bimolecular Fluorescence Complementation assays. In addition, the *pls* mutant has defective auxin transport and accumulation. The present work shows that PLS is required for correct gravitropic response, gene expression in the quiescent centre and columella patterning (each mediated in part at least by auxin) and also for ACC-mediated auxin synthesis. It is therefore proposed that PLS has two principal roles in root growth and development. First, PLS may act as a negative regulator of the ethylene signalling pathway by interacting with ETR1. Second, PLS is required for ethylene-mediated auxin synthesis; evidence is presented that suggests that PLS acts downstream of WEI2, an enzyme required for ethylene-mediated auxin synthesis. These roles function independently to regulate correct auxin distribution and concentration in the root tip, to control root growth and development.

# Acknowledgements

I would like to acknowledge and extent my heartfelt gratitude to the following persons who have made the competition of this thesis possible:

Foremost, to my supervisor, **Prof Keith Lindsey**, who not only gave me an opportunity to work in his group but also provided the much needed financial support to fund my PhD, offered his valuable time, advice and encouragement all along the way. I also appreciate Keith for giving me courage and independence to follow my mind in every aspect of my life.

My deepest, affectionate gratitude goes to the understated brilliance that is **Jen** (Dr Jennifer Topping). I thank her for laying the foundation of what turned out to be a thoroughly interesting, challenging and rewarding project. Her stimulating guidance and constant support throughout my time in Durham and even now is much appreciated. Her ability to simplify difficult ideas and immense patience is amazing and will always be idolised.

Special thanks, to **Stuart** (Dr Stuart Casson) and **Paul** (Dr Paul Chilley) for doing most of the background work of the POLARIS project and providing new objectives for this work. I am grateful to all the past and present members of the Lindsey and the Hussey lab: **Nick, John**, **Andrei**, **Mike** and **Tim** for their cooperation and support. I also thank **Prof Patrick Hussey**, for being my second supervisor and for giving unbiased advice on my work from time to time. Sincere thanks, to **Prof Jiri Friml** for doing the PIN work and, to **Dr Silin Zhong** for providing BiFC vector and valuable advice.

Last, this work would have never been completed without all the support, encouragement and love of all my family and friends. Affectionate thanks to my uncle Dr Haider Imam for not only bringing me into this country but also for all his support and love over these years. Deepest appreciation and love to Ellie for being a marvellous friend, Maher for being a lovely sister and to Manish for being my greatest critic and a true friend. To Mags, Kumari, Naomi, Nims, Lucy and others for being such good friends.

I will be indebted always....

To my parents,

Mrs Nikhat Mahdi and Colonel S Mahdi (Late)

Without them I would not have the goals to strive for and the will to follow my dreams……..

# Table of Contents

# List of figures

# List of tables

# Abbreviations

| | |
|---|---|
| ACC | 1-aminocyclopropane-1-carboxylic acid |
| ARFs | auxin response factors |
| AVG | aminoethoxyvinylglycine |
| Bp | base pairs(length of a mucleotide) |
| BSA | bovine serum albumin |
| CaMV35s | cauliflower mosaic virus 35S RNA gene |
| cDNA | complementary DNA |
| DNA | deoxyribonucleic acid |
| dNTPs | 2’ - deoxynucleotide 5’-triphosphates |
| d.a.g | days after germination |
| d.p.g | days post germination |
| DTT | dithiothreitol |
| EDTA | ethylenediaminetetracetic acid |
| GUS | β-glucoronidase |
| HCl | hydrochloric acid |
| IAA | indole-3-acetic acid |
| Kb | kilobase(s) |
| KCl | potassium chloride |

| | |
|---|---|
| KOH | potassium hydroxide |
| $MgCl_2$ | magnesium chloride |
| mRNA | messenger RNA |
| NAA | naphthaleneacetic acid |
| NaCl | sodium chloride |
| $Na_2HPO_4$ | disodium hydrogen orthophosphate |
| $NaH_2PO_4$ | sodium dihydrogen orthophosphate |
| NaOH | sodium hydroxide |
| NOS | nopaline synthase |
| NPA | 1-*N*-naphthylphthalamic acid |
| OD | optical density |
| PCR | polymerase chain reaction |
| RNA | ribonucleic acid |
| SDS | sodium dodecyl sulphate |
| SE | standard error |
| T-DNA | transferred DNA |
| Tris | tris (hydroxymethyl)aminomethane |
| µg | microgram |
| X-Gluc | 5-brom-4-chloro3-indoyl β-D-glucuronic acid |

# Chapter 1:

# Introduction

## 1.1: Introductory remarks

The life cycle of a flowering plant begins with a single cell and ends with a multicellular structure with discrete organs and tissues arranged in a highly precise manner. Primary meristems are laid down during the process of embryogenesis. They contribute to post-embryonic development upon germination by producing organs and secondary meristems. Cells within the primary shoot meristem give rise to various organs such as leaves, the stem, the inflorescence and the different floral organs. In contrast, the primary root meristem elaborates a single organ system, the primary root, with a stereotyped radial pattern of tissues (Scheres *et al*., 1995). The study of these processes of pattern formation, morphogenesis and cellular differentiation has been facilitated in recent years through the use of model plants such as *Arabidopsis thaliana*. Its elegant but simple structure, small size, rapid life cycle and the abundance of mutants has made *Arabidopsis* and its root a most attractive model to study growth and development (Scheres and Benfey, 2002; Casson and Lindsey, 2003).

## 1.2: Embryonic origin of Arabidopsis root

During Arabidopsis embryo development, cell division occurs in a fixed pattern, which makes it possible to trace the origin of seedling structures back to the region of the early embryo (Jürgens and Mayer, 1994; Laux and Wurchum, 2004).

First, the egg cell and the zygote display a polar organisation, with a large vacuole at the basal end and most of the cytoplasm and the nucleus at the apical end (Mansfield *et al*., 1991). After fertilisation the zygote undergoes a transverse asymmetric division resulting in a smaller apical cell and a larger basal cell. The apical daughter cell gives rise, after two rounds of longitudinal and one round of transverse divisions, to an eight-cell embryo proper (Figure 1.1). At the same time, the descendants of the basal daughter of the zygote divide transversely to form the suspensor and the uppermost cell, the hypophysis. At the eight-cell stage, four regions with different developmental fates can be recognized: (1) the apical embryo domain, composed of the four most apical cells of the embryo proper, will generate the shoot meristem and most of the cotyledons; (2) the central embryo domain, consisting of the four lower cells of the embryo proper, will form the hypocotyl and root and contribute to cotyledons and the root meristem; (3) the basal embryo domain (hypophysis) will give rise to the distal parts of the root meristem, the quiescent center, and the stem cells of the central root cap; and (4) the extra embryonic suspensor pushes the embryo into the lumen of the ovule and provides a connection to the mother tissue (Laux and Wurschum, 2004).

## 1.3: Cellular organisation of *Arabidopsis* root

The Arabidopsis root has a simple but highly ordered structure. One defining feature of the primary seedling root is its precise radial patterning which is set up in the heart stage, and comprises three fundamental tissues: dermal, ground and vascular tissues.

The principal tissues of the Arabidopsis primary root are arranged simply and in concentric rings. In the transverse sections of the mature root proximal to the root meristem the pattern presents itself as single cell-thick rings of epidermis, cortex, endodermis and pericycle tissues wrapped around the vascular tissues. The cortex and endodermal layers invariably contain eight cells whilst the pericycle averages twelve cells (Dolan *et al*., 1993). The epidermis lies on the outer side of the cortex and consist of two cell types, trichoblasts and atrichoblast. Trichoblasts overlay the anticlinal walls of two underlying cortical cells and differentiate into cells that produce root hairs, whereas atrichoblast cells are positioned above only one cortical cell and do not produce root hairs (Dolan *et al*., 1994). This radial pattern is maintained throughout the mature primary root and longitudinal sections shows cell files of each of the aforementioned cell types extending down to specific sets of cells in the meristematic zone, called initials, which act as the stem cells for these files (Figure 1.2 a & b).

The root meristem consists of these initials, which generate the specific tissue files by regulated cell division; and a central cluster of four cells called the quiescent centre, so called because of their low frequency of mitotic activity. The cells of the meristem are arranged in tiers with the lowest tier consisting of the initials for the root cap (both columella and lateral) and the epidermis, with the lateral root cap and epidermis appearing to originate from the same intials. The middle tier contains the central quiescent centre cells and flanking them are the initials for the cortex and endodermis, whilst the upper tier contains the vascular and pericycle initials, allied with the cells of the stele (Dolan *et. al*., 1993). The root meristem therefore provides new cells which add to the pre-existing files extending back into the mature root and into the root cap. Behind the root meristem is the so called expansion zone in which the newly added cells divide and expand before fully differentiating, in the maturation zone, into the varied cell types of the root. The primary root is therefore a good example of an organ in which all cell developmental stages can be easily identified along its axis. Because of the stereotypic organisation of the *Arabidopsis* primary root, any deviation from the basic pattern is easily detectable (such as in mutant screens). The highly organised and regular cellular patterning in the Arabidopsis primary seedling root makes it an attractive model system to study root development.

Some of the major questions that are being addressed currently are what is the nature of the signals that determine this ordered patterning? How is this defined cellular pattern maintained? And which genes are involved in controlling normal root growth and development. A number of different approaches have been used in order to address these problems and will be discussed.

## 1.4: The quiescent centre and its role in development

The quiescent centre and the columella of the root cap originate from direct derivatives of the hypophyseal cell in the developing embryo, whereas the more proximal initials which enclose the quiescent centre are derived from the apical cell of the globular embryo. The quiescent centre and enclosing initials comprise the promeristem, described by Scheres *et al*. (1996) as the "functionally integrated root meristem". Genetic studies of root meristem development in *Arabidopsis* demonstrate that roots which have a mutant *HOBBIT* (*HBT*) gene lack a quiescent centre. In addition the calyptrogen (root cap meristem) develops abnormally resulting in a root cap lacking a columella, demonstrating that the *HBT* gene is required for normal root meristem development (Willemsen *et al*., 1998). During normal embryogenesis in *Arabidopsis*, protoderm, ground meristem and provascular tissues become defined very early as clonal domains that appear to be derived from specific initials. This supports the viewpoint that these tissue regions are derived, initially, as cell lineages from specific initials or groups (tiers) of initials (Scheres *et al*., 1996). In a series of elegant experiments, it has been shown that following laser ablation (removal by killing) of initials from which a particular tissue type is directly derived, the adjacent cells that take over the role of the ablated cells, i.e they produce cells of the tissue type of the ablated initials. For example, following ablation of the quiescent centre in Arabidopsis, root cap columella cells, normally from the derived initials, are replaced by reprogrammed vascular tissue cells that "switch fate" to produce new quiescent centre and then columella cells (van der Berg *et al*., 1995). This supports the conclusion that, at least in some species, root meristem cells and their derivates develop according to position rather than as cell lineages. Additional evidence of the function of the quiescent centre has been provided by Ponce *et al*. (2000), who demonstrated that following excision of the root cap in *Zea mays*, genes that code for cell wall proteins or enzymes are expressed in the regenerating root cap only after the quiescent center has been re-established. Also, Aida *et al*. (2004) identified the *PLETHORA1* (*PLT1*) and *PLT2* genes encoding AP2 class putative transcription factors, which are essential for QC specification and stem cell activity in *Arabidopsis*. The *PLT* genes are transcribed indirectly in response to auxin accumulation

and are dependent on auxin response transcription factors. The quiescent centre also suppresses the differentiation of the surrounding initials, to maintain them in a 'stem cell-like' state (van den Berg *et al*., 1997)

These studies provide strong evidence for communication between the quiescent centre and the associated apical initials, the operation of system of positional information, and some control of development by the quiescent centre in both *Arabidopsis* and *Zea mays* (Scheres *et al*., 1996; Schiefelbein *et al*., 1997; Ponce *et al*., 2000).

## 1.5: The genetics of root patterning

### 1.5.1: Ground tissue patterning

In a transverse root section, there are four radially symmetric layers (from outside in, epidermis, cortex, endodermis and pericycle) that surround the bilaterally symmetric vascular tissue (consisting of pholoem, xylem and procambium) (Scheres *et al*., 1995). The vascular tissue and surrounding pericycle are termed the stele. Mutations that disrupt this radial pattern have been used to identify genes that play important roles in establishing and maintaining this pattern. Many of these mutations were isolated by screening for roots that were no longer able to grow in an indeterminate fashion. From these screens, mutations that disrupt patterning of the ground tissue and vascular cylinder were identified (Scheres *et al*., 2000).

In both the *scarecrow* (*scr*) and *short-root* (*shr*) mutants, instead of cortex and endodermis there is a single mutant layer between the epidermis and stele (Scheres *et al*., 1995). Both genes encode members of the GRAS family of putative transcriptional regulators. Analysis of tissue-specific markers revealed that the mutant layer is specified differently in the two mutants. In *scr*, markers for both cortex and endodermis are present in the mutant layer, indicating that SCR is required for the periclinal division of the initial cell, but does not play a role in cell specification (Di Laurenzio *et al*., 1996). In *shr*, only markers for cortex are found, indicating that SHR is required for both the longitudinal cell division as well as the endodermal cell specification (Benfey *et al*., 2000; Scheres *et al*., 2000).
Levesque et al (2006) carried out a meta-analysis of the results from microarray experiments of *shr-2*, an inducible *SHR* line in the *shr-2* background and cells sorted for SHR: GFP expression, and identified eight direct targets of SHR. Four of these were confirmed by ChIP-qPCR including *SCR*, two closely related C2H2 zinc finger genes *NUTCRACKER (NUC*) and *MAGPIE* (*MGP*) and the recently identified *JACKDAW (JKD*) (Welch *et al*., 2007, Scheres *et al*., 2000). *SCR* expression is ablated in *jkd* mutant roots

and it was demonstrated by yeast two hybrid and Bimolecular Fluorescent Complementation (BiFC) that JKD interacts with itself as well as with SCR and SHR (Welch et al., 2007).

*SCR* is transcribed in the cortex/endodermal initials, its daughter and all of the endodermal cells as well as in the QC (Di Laurenzio *et al*., 1996). Because *SCR* expression is downregulated in a *shr* mutant background, it was concluded that SHR is required for full transcriptional activation of *SCR* (Helaruitta et al., 2000). SHR action has been a topic of discussion since the vascular tissue (stele)-specific gene expression of *SHR* was first reported, with the loss of endodermis observed in the ground tissue of *shr-2* mutants (Nakajima *et al*., 2001). The SHR protein was later shown to move from stele to the adjacent ground tissue where it became nuclear localised (Sena *et al*., 2004; Nakajima *et al*., 2001). This ground tissue patterning research points to exciting downstream transcriptional targets that can be linked to later differentiation, and suggest mechanisms for how cell fate can be specified by a combination of protein interaction, movement and transcriptional control (Benfey *et al*., 2008).

## 1.5.2: Epidermal patterning

The epidermis is composed of two cell types (hair-bearing cells and hairless cells) whose identity is regulated by positional information. Trichoblasts develop into hair cells and are located in the cleft between underlying cortical cells (in transverse section) whilst atrichoblasts remain hairless and are located over single cortical cells (Dolan *et al*., 2006, Benfey *et al*., 2000).

Cell identity in the epidermis is regulated by a cascade of transcriptional regulators. The GLABRA 2 (GL2), GLABRA3 (GL3), ENHANCER OF GLABRA 3 (EGL3), TRANSPARENT TESTA GLABRA (TTG), and WEREWOLF (WER) transcriptional factors are required for the hairless fate, whereas the CAPRICE (CPC), TRIPTYCHON (TRY) are required for the hair fate (Benfey *et a*l., 2008). The exact model of non-hair cell and hair cell fate is a matter of controversy in this field.

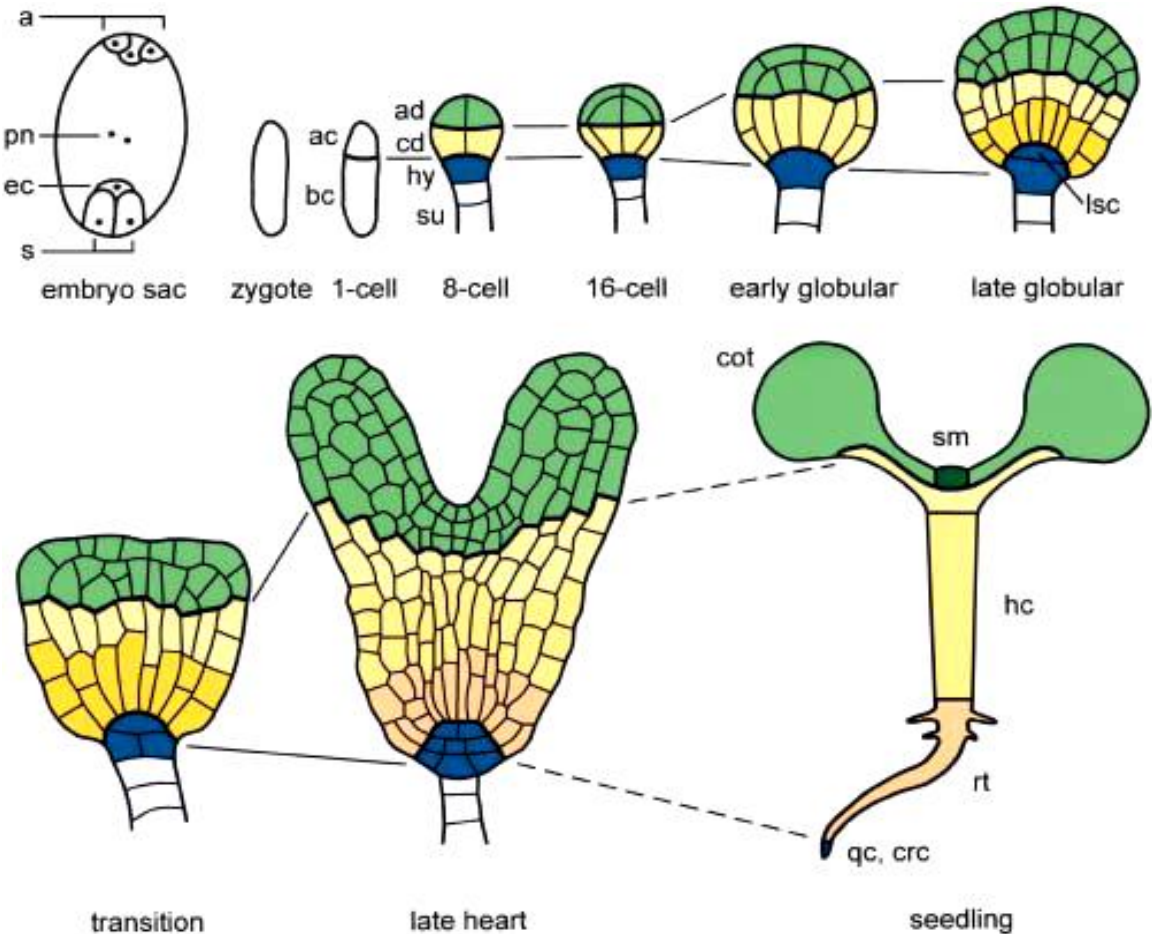


**Figure 1.1 Apical–Basal Arabidopsis Embryo Development**

Schemes of longitudinal median sections of the developing Arabidopsis embryo. The upper and lower thick lines represent clonal boundaries between the descendants of the apical and basal daughter cells of the zygote and between the apical and central embryo domains, respectively. a, antipodes; ac, apical daughter cell; ad, apical embryo domain; bc, basal daughter cell; cd, central embryo domain; cot, cotyledons; crc, central root cap; ec, egg cell; hc, hypocotyl; hy, hypophysis; lsc, lens-shaped cell; pn, polar nuclei; qc, quiescent center; rt, root; s, synergids; sm, shoot meristem; su, suspensor. (Adapted from Laux and Wurschum, 2004).

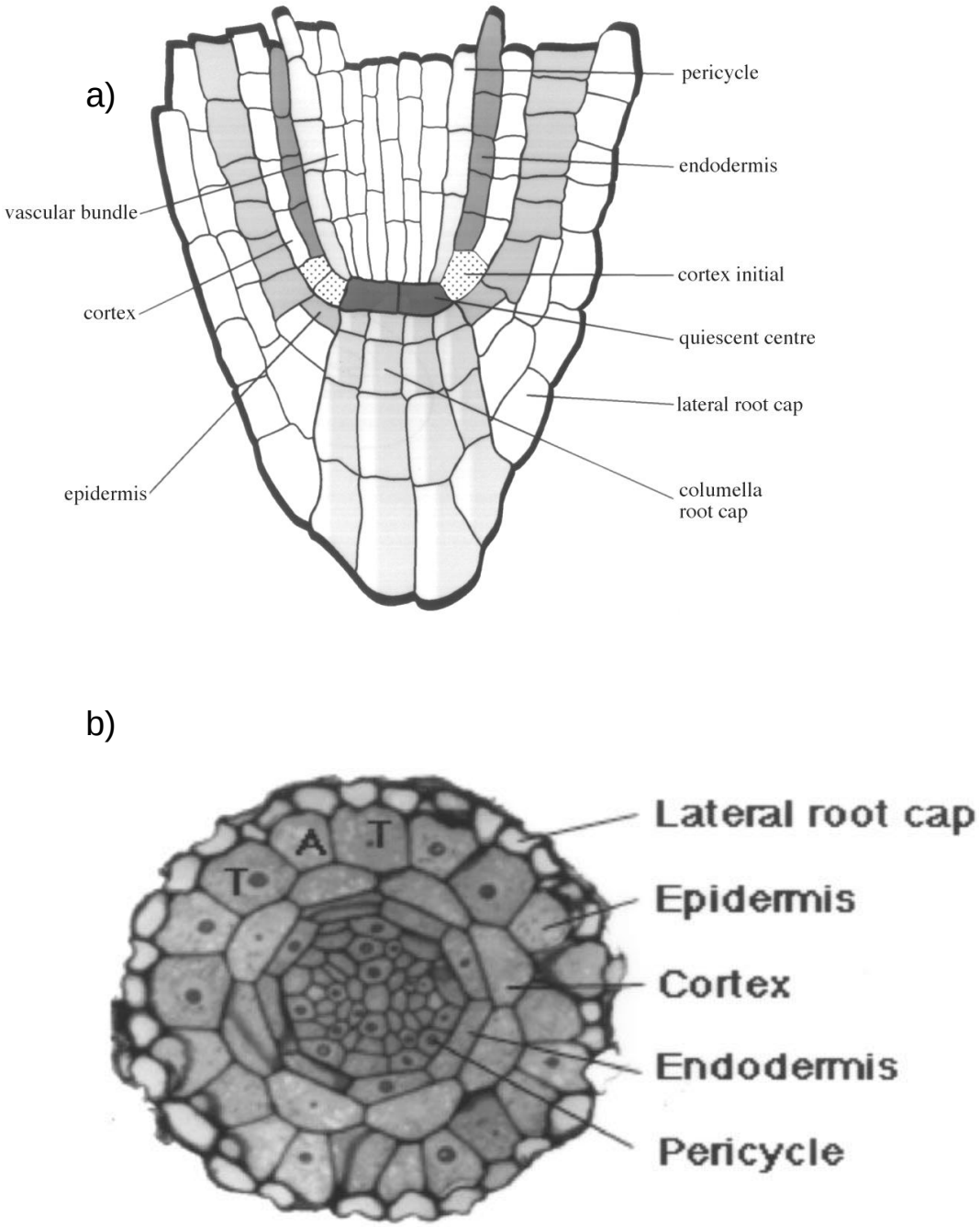


**Figure 1.2: (a) Longitudinal organisation of cells in the vicinity of the quiescent centre and initials. (b) Radial organisation of cells in the root (transverse section of a root made in the meristematic zone).** A shows the position of an atrichoblast and T indicates the location of two trichoblasts. Adapted from Dolan *et al*., (1998).

However, most models are based on the results from previous studies suggesting that a TTG/GL3/EGL3/WER transcriptional complex binds to the GL2 promoter to repress root hair cell fate, while the same complex activates *CPC* expression in non-hair cells. CPC then moves to neighbouring epidermal cell to repress *GL2* expression resulting in hair cells (Wada *et al*., 2008).

Kwak and Schiefelbein (2005) identified a receptor-like protein kinase named SCRAMBLED (SCM) that is required for cell-specific gene expression in the developing epidermis. It is proposed that SCM targets a cascade of transcriptional factor genes that, in complex interactions including cell–cell movement between non-hair cells and hair cells, regulates cell identity. A central role is this model is played by the MYB-type transcriptional factor WEREWOLF (WER), which in non-hair cells, forms a complex with GL3/EGL3/TTG. The WER-GL3-EGL3-TTG complex promotes the expression of the single repeat Myb protein CPC and of the homeodomain leucine zipper protein GL2. GL2 acts as a positive regulator of the non-hair cell fate. In hair cells the expression of *WER* is repressed by SCM. CPC moves from non-hair cells into the hair cells, suppressing the binding of WER to the GL3-TTG complex and a new complex composed of CPC-GL3-EGL3 and TTG is formed that blocks the expression of *CPC* and *GL2* in future hair cells (Perry et al., 2007)
Once hair cells have been specified, the hairs are initiated from the outer side of the hair cell nearest the meristem. The polar localisation of the hair cell is dependent on an ethylene and auxin pathway and coincides with the establishment of a high $Ca^{2+}$ gradient in the hair tip (Benfey et al., 2000; Grebe *et al.*, 2002).

## 1.5.3: Stele patterning in the roots

The phytohormone auxin plays a prominent role in this tissue and the action of PINFORMED (PIN) auxin transporters affects vascular patterning in the stele (Vieten *et al*., 2007). Recently, genes expressed in protophloem have been identified from enhancer trap screens (Bauby *et al*., 2007), including the previously characterised transcriptional factor BREVIS RADIX (BRX), that mediates between brassinosteroid and auxin action (Mouchel *et al*., 2004, 2006). Regulation of the bilateral symmetry within the stele was recently shown to be eliminated in *lonesome highway* roots (Ohashi-Ito *et al*., 2007). This gene encodes a protein with similarity to bHLH transcriptional factors and is predicted to interact with SHR or BRX to regulate stele patterning.

## 1.5.4: Stem cell niche patterning

Auxin transport and response are central to the patterning of the root's stem cell niche. A maximum of auxin response visualised by reporter genes upregulated by auxin corresponds to the position of the QC, suggesting the QC's position is defined by this maximum (Sabatini *et al*., 1999). Protonated auxin can move into cells by passive diffusion, and the AUX1/LAX family of influx carriers promote auxin uptake into cells (Bennett *et al*. 1996; Billy *et al*., 2001: Swarup *et al*., 2008). The PIN auxin transporters facilitate the movement of negatively ionized auxin out of cells because auxin is a weak acid and the extracellular pH is lower than the cytoplasmic pH in the root cells (Blakeslee *et al*., 2005). An 'inverted fountain model' has been proposed to describe auxin flux in the root tip, on the basis of the asymmetric distribution of PIN proteins within single root cells (Blilou *et al*., 2005).

Based on these models together with experimental information about the spatial localisation of the PIN family members in the root and accounting for simple diffusion of auxin, a recent mathematical model not only correctly predicted the position of auxin maximum but also proposed an auxin gradient in the roots (Grieneisen *et al*., 2007). This model simulates a variety of perturbations to the auxin maximum that correctly matches experimental observations, including laser ablation of the QC, high levels of auxin applied to the roots, and even decapitation of the plant removing the root's main source of auxin (Grieneisen *et al*., 2007). Decapitated plants were modelled to survive for 10-30 days depending upon the amount of 'reflux' that depend upon PIN localisation to the lateral face of cells to direct auxin flux back into the downward directed flow within the vascular tissue. The root can be considered to possess an 'auxin battery' that holds charge, but slowly loses it at a rate proportional to inefficient reflux (Benfey *et al*., 2008).

Remarkably, the PLETHORA (PLT) transcriptional factors are expressed in a pattern resembling this gradient (Galinha *et al*., 2007; Aida *et al*., 2004). Various *plt* double and triple mutants have reduced *PIN* expression, suggesting a connection between PLTs and an auxin gradient involving PINs (Xu *et al*., 2006; Benfey *et al*., 2008).

Xu *et al*. (2006) demonstrated in QC ablation experiments that there is a significant lag time between the appearance of the QC auxin maximum and PIN protein localisation. A host of transcriptional factors involved in QC specification and maintenance may function during this lag time including WUSCHEL-RELATED HOMEOBOX 5 (WOX5), SHR, and SCR, whose expression has already been show to appear during this lag time (Xu *et al*., 2006). Since SHR, SCR, WOX5 have roles in the QC, they represent attractive candidates

for connecting PLTs and PIN-derived gradients (Petricka and Benfey, 2008). Recently, double mutants in OBERON1 and OBERON2 plant homeodomain finger proteins were shown to lack PLT1, WOX5 and SCR expression, suggesting the nuclear-localised OBE1 and OBE2 may be upstream regulators in QC identity and specification (Saiga *et al*., 2008). Also the *MERISTEM-DEFECTIVE* (*MDF*) gene, which encodes a predicted DNA or RNA binding protein, is required for correct *PIN* expression, *PLT* expression and QC specification (Casson *et al.* 2009).

## 1.6: Hormonal signalling in root development

Hormonal signalling plays a pivotal role in almost every aspect of plant development, and of high priority has been the identification of the receptors that perceive these hormones. Genetic screens have been extremely useful in identifying genes involved in early hormone signal transduction. As more of these genes are cloned it has become apparent that a number of them are involved in regulating the distribution, synthesis and response to plant growth regulators. As such there is now increasing genetic evidence available to support the physiological information which indicates an important role of these compounds in plant development. This section will concentrate on the evidence supporting roles for the hormones auxin and ethylene in particular in normal root growth and development.

### 1.6.1: Auxin

Charles and Francis Darwin's experiments on the phototropic curvature of canary grass coleoptiles led them to propose the existence of a plant growth regulating substance that later came to be known as auxin (reviewed by Vietin *et al*., 2007). The chemical identification of auxin as indole-3-acetic acid (IAA), and the synthesis of non-natural analogues such as 2, 4-dichlorophenoxyacetic acid (2, 4-D) and 1-naphthylacetic acid (1-NAA) enabled physiologists to test the role of auxin in plant development (Friml *et al*., 2003). The results of such experiments were confusing because auxin seemed to affect a multitude of apparently unrelated processes in plants. A seemingly ever-expanding list of processes in which auxin is involved includes: embryogenesis (Shevell *et al*., 1994; Friml *et al*., 2003), root and shoot organogenesis (Laskowaki *et al*., 1995; Reinhardt *et al*., 2000), root meristem maintenance (Benkova *et al*., 2003; Kerk *et al*., 2000), vascular tissue differentiation (Sabatini *et al*., 1999; Friml *et al*., 2002), hypocotyl and root elongation (Jensen *et al*., 1998), apical hook formation (Lehman *et al*., 1996), apical dominace (Leyser *et al*., 2005) fruit ripening (Ellis *et al*., 2005), growth responses to environmental stimuli, and others (Marchant *et al*., 1999). These various function of auxin

suggested that it is a generally required factor rather than a specific signal. Pharmacological and genetic studies together with direct or indirect visualisation of auxin distribution suggested that a key to the problem might lie in a unique property of auxin – the directional intercellular and resulting local accumulation of auxin in certain tissue and cells (Morris *et al*., 2004). Auxin is distributed through the plant either through the phloem or by a more controlled, cell-to-cell transport system (Swarup *et al*. 2001). This polar auxin transport system is required for the local auxin accumulation observed in the different developmental contexts described above. These accumulations (gradients) have been observed using numerous different approaches, such as the auxin responsive promoter DR5, immunolocalisation of IAA, or by direct auxin measurement in tissue sections (Sabatini *et al*., 1999; Swarup et al., 2001; Avsian-Kretchmer *et al*., 2002).

### 1.6.1.1: Auxin transport

In an attempt to explain the auxin transport mechanism, Rubery & Sheldrake (1974) and Raven (1975) postulated the chemiosmotic hypothesis, based on known properties of auxin movement, namely that it is saturable, energy- and protein synthesis-dependent, and unidirectional. Three decades later it seems remarkable how accurately the molecular model – formulated with few clues from physiological experiments and no molecular data, fits the recent molecular genetic and cell biological findings (Vietin *et al*., 2007).

In the acidic environment of the cell wall (pH 5.5), the IAA molecule is present in both ionized and protonated forms. Hydrophobic, protonated IAAH enters a cell passively through the plasma membrane. Once inside the more basic cytoplasm (pH 7), the proton dissociates and the $IAA^-$ ion cannot passively move out of the cell and therefore becomes trapped inside. Specific auxin efflux carriers are then needed to transport $IAA^-$ ions out of the cell (Figure 1.3).

Recently, the molecular identification of auxin carriers and the demonstration of their polar localisation in the auxin transport – competent cells, as well as the importance of a pH difference between the apoplast and the symplast, have confirmed the basic predictions chemiosmotic hypothesis (Li *et al*., 2005).

### 1.6.1.2 Auxin Biosynthesis and distribution

The fate of developing tissue can be determined by the sensitivity of the growing cells to auxin, the concentration of active auxin and the relative concentration of other phytohormones. This can also vary widely in different tissues at different developmental stages. Auxin is readily conjugated to a wide variety of larger molecules, rendering it inactive. Indeed, the majority of IAA in the plants is in form of inactive conjugates. Auxin conjugation and catabolism can therefore decrease active auxin levels. *De novo* synthesis and hydrolysis of conjugates contribute to the developmental regulation of auxin homeostasis by increasing active auxin levels (Ljung *et al*., 2002; Ljung *et al*., 2005; Teale *et al*., 2006). There is a high capacity for auxin biosynthesis not only in young aerial tissues, but also in roots, particularly in the meristematic primary root tips (Ljung *et al*., 2005). Auxin is synthesised from indole through tryptophan-dependent and tryptophan-independent pathways, and the fact that no fully auxin-deficient mutant plants have been identified reflects the importance of auxin in plant development (Woodward et al., 2005).

### 1.6.1.3: PIN auxin efflux carriers

Most of our understanding of polar targeting has emerged from the study of the polar delivery of auxin efflux carriers from the PIN family (Figure 1.4). The family of PIN proteins have emerged in recent years from the genetic studies in Arabidopsis as key regulators of a plethora of auxin-mediated process, including root meristem maintenance (Friml *et al*., 2002; Blilou *et al*., 2005).

Because the chemical properties of IAA suggested that auxin efflux is the limiting step in its directional transport, the hunt for auxin efflux carriers started and became an area of focus. The physiological and biochemical approaches proved unsuccessful, but the *pin-formed1 (pin1)* mutant finally provided an answer. The *pin1* null mutant is characterised by bare, needle-like stems that lack flowers, a phenotype that can also be obtained in wild-type by inhibition of auxin transport (Okada *et al*., 1991). Molecular analysis of the corresponding *PIN1* gene revealed that it encodes a transmembrane protein with some similarity to a group of bacterial transporters (Galweiler *et al*., 1998). Subsequently, seven other genes similar to *PIN1* were found in *Arabidopsis*. PIN5 and PIN6 have not been functionally characterised yet, but PIN2, PIN3, PIN4 and PIN7 have been attributed functions in root gravitropism, tropic growth responses, root meristem patterning and early embryo development, respectively (Friml *et al*., 2003; Friml *et al*., 2002; Friml *et al*., Lusching *et al*., 1998; Muller *et al*., 1998), with PIN5 have a different role, in auxin homeostasis and localized to the endoplasmic reticulum (Mravec *et al*., 2009). Members of

the PIN protein family are considerably homologous and functionally redundant, as indicated by the increasingly severe phenotypes of the multiple *pin* mutants (Friml *et al*., 2003; Blilou *et al*., 2005; Vieten *et al*., 2005). Again, most aspects of the respective mutant phenotypes can be phenocopied by the chemical inhibition of polar auxin transport, and *pin* mutants have aberrant local accumulation patterns (Friml *et al*., 1998, 2002, 2003; Lusching et al., 1998; Muller et al., 1998).

The most exciting aspect of PIN proteins is their asymmetric localisation within auxin transport-competent cells (Figure 1.3). All PIN proteins except PIN5 show polar subcellular localisation, although some of them can be found in specific cell types without pronounced polarity. The polarity of PIN localisation correlates well with the direction of auxin transport and with the local accumulation of auxin in adjacent cells (Galweiler *et al*., 1996; Muller *et al*., 1998; Friml *et al*., 2002, 2003; Benkova *et al*., 2003; Blilou *et al*., 2005; Heisler *et al*., 2005), suggesting that PIN polarity determines the direction of intercellular auxin flow. This is one of the key issues in most models related to auxin transport-mediated development because it provides a connection between subcellular polar targeting at the level of individual cells and directional signalling within a specific tissue or organ. Indeed, a series of recent experiments involving the manipulation of PIN polarity and the monitoring of auxin translocation strongly suggested a link between the polar localisation of PINs and the direction of auxin transport (Wisniewska *et al*., 2006). The PIN2 protein typically localises to the upper cell side (facing the shoot apex) in epidermal cells of *Arabidopsis* root (Figure 1.4), whereas PIN1 ectopically expressed under the PIN2 promoter localised to the lower side of the same cells. This demonstrates that protein sequence-specific signal contribute to the control of polar PIN localisation.

Despite of increasing amount of evidence supporting the crucial role of PIN proteins in auxin transport, particularly efflux, there was no evidence for the molecular function of PINs, mainly because of the lack of clearly defined domains and homologies to known proteins. Finally, the use of cell cultures and heterologous systems has enabled researchers to address both the direct role of PIN proteins in auxin efflux and the requirement of other factors for this action.

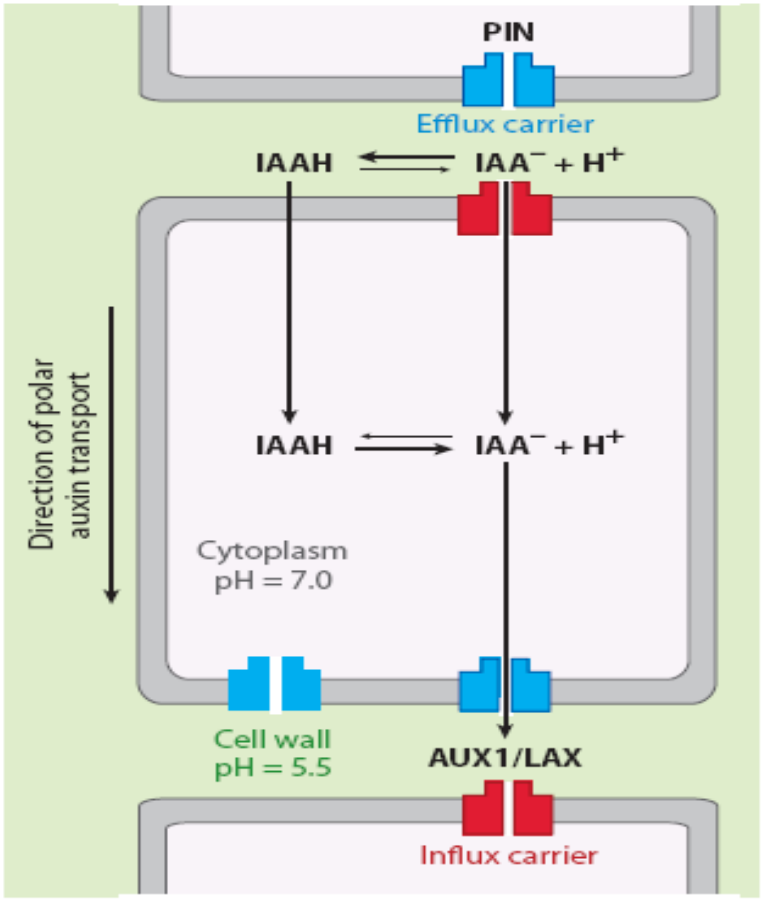


**Figure 1.3: Cellular model for polar, cell-to-cell auxin transport**

The auxin indole acetic acid (IAAH) is largely protonated at the lower pH of the cell wall and can pass through the plasma membrane into the cell. In the higher pH cytosol, part of the IAAH is deprotonated, and the resulting charged $IAA^-$ is largely membrane-impermeable and requires transport activity to exit the cell. The localisation of the PIN-FORMED (PIN) auxin efflux carriers at the plasma membrane determines the auxin exit site from individual cells. Coordinated polar localisation of PINs in a given tissue hence determines the direction of cell-to-cell auxin transport. AUX1/LAX1 denotes auxin influx carriers AUXIN RESISTANT 1/LIKE AUX1 (adapted from Kleine-Vehn and Friml, 2008).

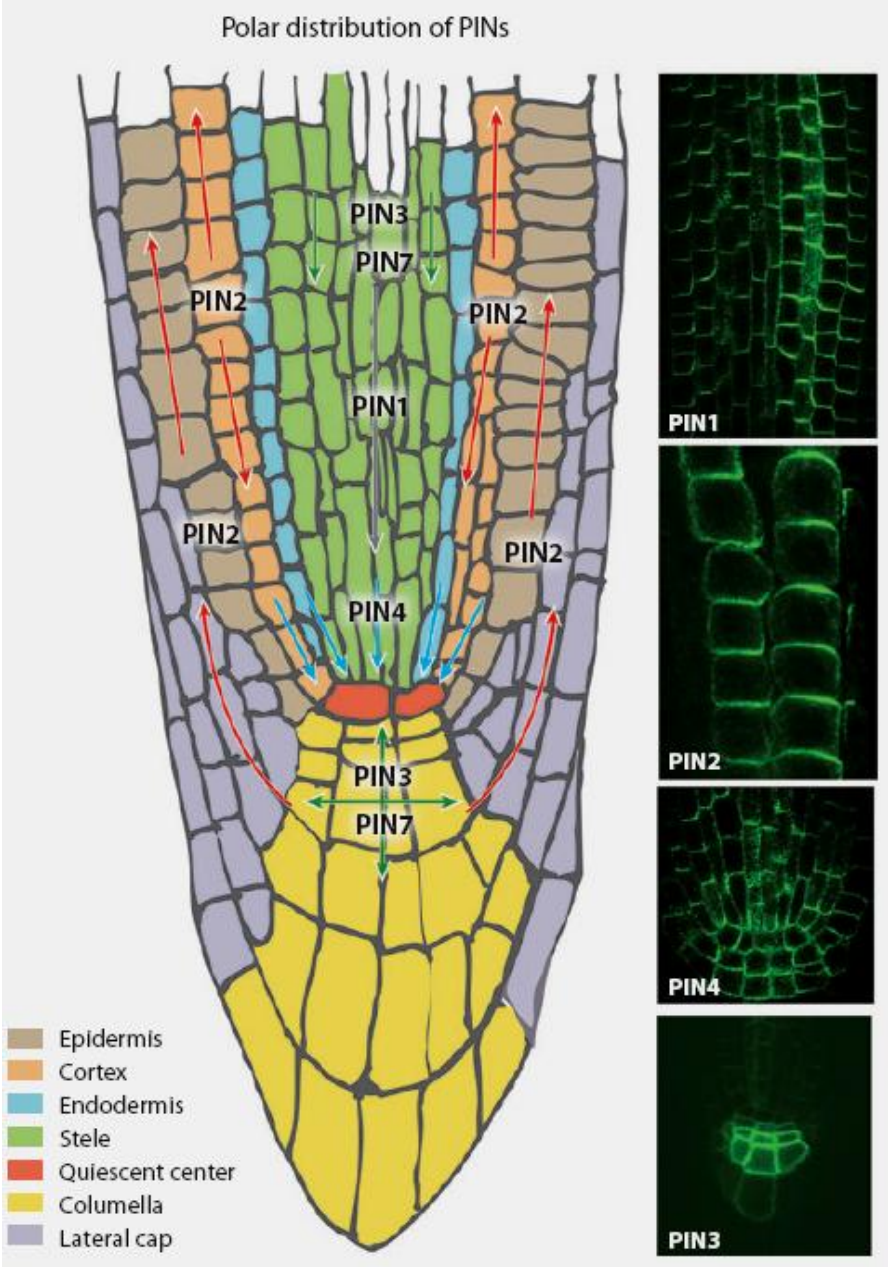


**Figure 1.4: Pattern of PIN protein localisation in the *Arabidopsis* root tip.** Schematic and immunolocalisation of PIN proteins in the *Arabidopsis* root tip. Arrows indicate polar PIN localization at the plasma membrane, illustrating cell type-dependent decisions in PIN polar localisation. To be noticed is the differential PIN2 targeting in the epidermis (apical) and young cortex (basal) cells (adapted from Kleine-Vehn and Friml, 2008).

The conditional overexpression of different PIN proteins in cultured *Arabidopsis* and tobacco BY-2 cells led to a lower retention and higher efflux of different radioactively labelled auxins, but not of related molecules such as benzoic acid or the auxin precursor tryptophan. This auxin efflux was saturable and sensitive to chemical auxin transport inhibitors. Its rate was dependent on the amount of overexpressed PINs in mammalian or yeast cells which also led to an increased efflux of IAA, although with decreased specificity. Given that mammalian and yeast cells are evolutionary divergent from plants and do not contain the transport or signalling machinery for auxin or related compounds, these experiments strongly suggest that PIN proteins themselves are capable of mediating auxin efflux (Petrasek *et al.*, 2006).

### 1.6.1.4: AUX1 (LAX) auxin influx carriers

Molecular genetic approaches in Arabidopsis were also instrumental in the discovery of auxin influx carrier. The *auxin resistant 1* (*aux1*) mutant was identified in a screen for auxin resistant and agravitropic mutants (Maher and Martindale, 1980 and Bleecker *et al*., 1987). The *aux1* mutant showed much stronger auxin resistance to the membrane-impermeable synthetic auxin 2,4-D than to membrane-permeable 1-NAA (Marchant *et al*., 1999; Yang *et al*., 2006). The *aux1* root agravitropic phenotype was rescued by supplying roots with 1-NAA, whereas 2,4-D, which needs to actively transported into cells, did not show this effect (Yomamoto *et al.*, 1998; Marchant *et al*., 1999). This suggested a role for AUX1 in auxin uptake. In support of this *aux1* root tips also incorporated less radioactively labelled 2,4-D than wild type, whereas 1-NAA was taken up at wild type levels (Marchant *et al.*, 1999). The *AUX1* gene was cloned and found to encode a protein related to amino acid permeases (Bennett *et al*., 1996). Given that IAA is derived from tryptophan and is structurally similar to it, the issue of AUX1 acting as an auxin influx carrier was largely settled. Further physiological studies came from the heterologous expression of *AUX1* in *Xenopus laevis* oocyte cells, which resulted in an elevated, saturable auxin uptake. This was a direct demonstration of specific, high affinity, pH-dependent auxin uptake, which is entirely dependent on AUX1 (Yang *et al*., 2006). .

Due to the lack of any previous prediction about the auxin influx carriers, asymmetrical localisation of AUX1 came as a surprise. More specifically AUX1 was enriched on the upper side of root protophloem cells, opposite to PIN1 in same cells, and often on the same side as PIN1 in the L1 layer cells of the shoot apical meristem (Swarup *et al*., 2001; Reinhardt *et al*., 2003). In the protophloem cells, AUX1 appears to play a crucial role in unloading auxin from the phloem based non-polar transport system (Swarup *et al*., 2001)

into the AUX1- and PIN-dependent polar transport of the root meristem (Bliliou *et al*., 2005). However, the root gravitropic response depends primarily on the activity of AUX1 in lateral root cap and in elongating epidermis cells but not in the stele (Swarup *et al*., 2005). In the shoot apical meristem, AUX1 might counteract lateral diffusion and confine auxin to the outer cell layer where patterning for phyllotaxis occurs (Reinhardt *et al*., 2003). However, it is unclear how important the polar distribution of AUX1 is for its function, and what would be the role of efflux and influx carriers positioned on the same cell side.

### 1.6.1.5: PGP auxin transporters

Members of the multi-drug-resistant/P-glycoprotein (MDR/PGP) subfamily of ATP-binding cassette (ABC) proteins have emerged as prominent players in the cellular efflux and influx of auxin. Loss-of-function mutation in several *PGP* genes cause diverse developmental defects that are related to altered auxin signalling and distribution, and some show aberrant polar auxin transport and altered auxin uptake or efflux from protoplasts (Geisler *et al*., 2005; Terasaka *et al*., 2005). PGP proteins localised within cells without any pronounced asymmetric distribution and importantly, in heterologous systems such as yeast or mammalian HeLa cells, some PGPs are capable of transporting different auxins across the plasma membrane (Geisler *et al*., 2005; Santelia *et al*., 2005). However, the connection between the function of PGPs in auxin transport and their role in plant development is not clear yet. But given that many *pgp* mutants show strong defects in multiple developmental processes, the genes are important factors in regulating plant development (Noh *et al*., 2001).

PGP function is not strictly required for PIN-dependent auxin efflux. However it is likely that the different auxin transport system in plants, be the phloem-based, PIN-, AUX1-, LAX- or PGP-driven are coordinated and interact functionally. Recently, an extensive and complex functional interaction between PIN- and PGP-based transport has been demonstrated (Blakeslee *et al*., 2007). However, the developmental role and molecular basis of such interaction still remains an important focus of auxin research.

### 1.6.1.6: Control of polar targeting of auxin transport components

A key feature of polar auxin transport that makes it such a unique mechanism for transmitting spatial and temporal signals in plant development is its controlled directionality. The polarity of auxin flow can be modulated by changes in the subcellular localisation of PIN efflux carriers within each auxin transporting cells (Weisniewska *et al*., 2006).

The molecular mechanisn of targeting auxin transport components to distinct sides of the cell is of fundamental interest, not only for auxin transport but also for the whole subject of cell and tissue polarity in plants. There are two different polar targeting machineries, given that AUX1 and PIN proteins are controlled by different sensitivities to various inhibitors (Kleine-Vehn *et al*., 2006). In addition the targeting of AUX1 requires an accessory protein AXR4, for the establishment and maintenance of plasma membrane localisation. The mode-of-action of AXR4 is unknown and it is localised in the endoplasmic reticulum. In *axr4* null mutants, AUX1 fails to arrive at the plasma membrane and is retained in the ER (Dharmasiri *et al*., 2006).

However, it has been the polar targeting of PIN proteins that has been genetically more accessible. A variety of different mutants identified by their general auxin-related phenotypes exhibit altered PIN localisation and has shed light on the mechanisms involved in PIN targeting. In *gnom* (*emb30*) mutant embryos, coordinated polar localisation of PIN1 is not established (Steinmann *et al*., 1999), resulting in embryos with poorly defined apical basal axes and a lack of bilateral symmetry (Mayer *et al*., 1991). *GNOM* encodes a guanine nucleotide exchange factor for small G-proteins of the ARF class (Shevell *et al*., 1994), which mediates formation of exocytic vesicles at endosomes responsible for carrying PIN proteins and possibly other cargos to the plasma membrane (Geldner *et al*., 2003).

Genetic suppression of the ARF-GEF function in *gnom* mutants, or chemical inhibition by the fungal toxin Brefeldin A (BFA) revealed that PIN proteins are normally constantly moving between endosomes and the plasmamembrane, in a process termed constitutive cycling (Geldner *et al*., 2001) (Figure 1.5). PIN cycling is argued to be a crucial part of auxin transport and is prerequisite for the rapid changes in PIN polar localisation observed during embryogenesis, organogenesis and tropic growth (Friml *et al*., 2002, 2003; Benkova *et al*., 2003).

Another important factor in the control of PIN localisation has been identified primarily through genetic studies. The *hydra/fackel* mutants of Arabidopsis, defective in sterol biosynthesis, show defective PIN localization, auxin responses and meristem organization (Souter *et al.* 2002, 2004). Similarly, a weak allele of the Arabidopsis *sterol methyltransferase1* (*smt1*) mutant called *orc* has defects in meristem patterning, cell polarity and auxin distribution in root tips (Willemsen *et al*., 2003). SMT1 is also required for the synthesis of membrane sterols (Schrick *et al*., 2002). Together with the finding that

the sterol-specific dye filipin labels the intracellular route of PIN1, these results link sterol membrane composition with the control of PIN polarity (Grebe *et al*., 2003).

In addition to sterols and *gnom*, the list includes another vesicle trafficking regulator, the ARF-GAP VAN3 (also called SCARFACE) (Koizumi *et al*., 2005; Sieburth *et al*., 2006) and components of the actin cytoskeleton, whereas microtubules seem to be only indirectly involved in PIN trafficking (Kleine-Vehn *et al*., 2006). However, the Ser/ Thr kinase PINOID (PID) is the only factor that has been identified unambiguously to mediate decisions about the polarity of PIN targeting. The phenotype of *pid* mutant is similar to that of pin1 mutants, a bare inflorescence shoot with limited lateral organs, which is indicative of auxin transport defects (Christensen *et al*., 2000; Benjamins *et al*., 2001). By contrast, plants overexpressing *PID (35::PID*) exhibit primary root collapse because of auxin depletion. The auxin accumulation and root meristem activity in *35S::PID* can be rescued by treatment with auxin transport inhibitors or in *pin2* or *pin4* mutant backgrounds (Friml *et al*., 2004). The simplest mechanistic explanation of PID function is that it directly phosphorylates PIN proteins, marking them as apical cargo, whereas dephosphorylated PIN would be preferred localized by a basal targeting route (Figure 1.6). Moreover, PID might be a component of a feedback regulation between auxin signalling and auxin transport given that PID expression, and therefore the level of PID activity, is controlled by auxin (Benjamins *et al*., 2001).

### 1.6.1.7: Feedback regulation in PIN-dependent auxin distribution

We have seen that local auxin accumulation patterns, which are the hallmarks of a plethora of developmental processes, are controlled by the cell-spanning, concerted action of nevertheless cell-autonomous PIN targeting machinery. For example, in embryo development, PIN7 localisation in the suspensor is apical early on, but reverses to basal later. This shift in PIN7 polarity, together with the onset of basal PIN1 accumulation in proembryo cells, correlates with a shift in the auxin maximum from an apical position in the proembryo to basal accumulation at the root pole (Friml *et al*., 2003). It was proposed decades ago that the underlying mechanism might involve a feedback of the actual auxin content of a cell or tissue on the regulation of directional auxin flow, thereby creating self-establishing, and self-propagating patterns.

In theory, the regulation of PIN-dependent polar auxin transport could occur at the level of PIN protein abundance (e.g. transcription, translation and silencing), PIN activity (e.g. post-translational modification and degradation) and targeting (PIN abundance at the specific cell side). Indeed, PIN proteins have been demonstrated to be regulated at all

these level (Figure 1.7). Among other factors, the transcription of various *PIN* genes has been shown to be regulated by auxin (Veiten *et al*., 2005; Peer *et al*., 2004). Although the details are not yet fully understood, this regulation depends in the auxin-dependent derepression of transcription factors of Auxin Response Factors (ARF) class (Woodward *et al*., 2005).

It seems that this mechanism also underlies changes in *PIN* expression, which corresponds to changes in auxin levels in *pin* mutants, and contributes to the observed extensive functional redundancy between different *PIN* genes (Vieten *et al*., 2005). Because *PIN* transcription is affected in multiple *plt* mutants and, conversely, *PLT* expression is expanded in some *pin* multiple mutant combination, it was proposed that auxin flow in the root meristem is established by the combined action of *PLT* and *PIN* genes (Blilou *et al*., 2005).

Another way to control PIN abundance, and therefore its activity, is by protein degradation. When *Arabidopsis* roots are turned sideways, an increase in auxin concentration in the epidermis and lateral root cap on the new lower side, and a decrease on the upper side of the root, coincides with a decrease in PIN2 levels on the upper side.

This decrease seems to be controlled post-transcriptionally through regulated degradation. Treatment with proteasome inhibitors, which affect root gravitropism and cause an increase in the ubiquitination status and level of PIN2, strongly suggests that the degradation of PIN2 occurs in a proteasome-dependent manner (Abas *et al*., 2006). Auxin itself seems to influence PIN2 levels in promoting PIN2 degradation (Sieberer *et al*., 2000), but whether this is the mechanism by which asymmetry in PIN2 abundance during the root gravitropic response occurs is still unclear.

Another significant point in the regulation of PIN activity is through the constitutive PIN cycling between the plasma membrane and endosomal compartments. On the one hand, constitutive PIN cycling probably facilitates rapid changes in PIN polarity in the columella cells in response to a gravitropic stimulus (Friml *et al*., 2002). On the other hand, endocytic cycling of PIN proteins also provides a means for controlling the occurrence of PINs at the plasma membrane and thus, for regulating the rate of auxin efflux from cells (Paciorek *et al*., 2005).

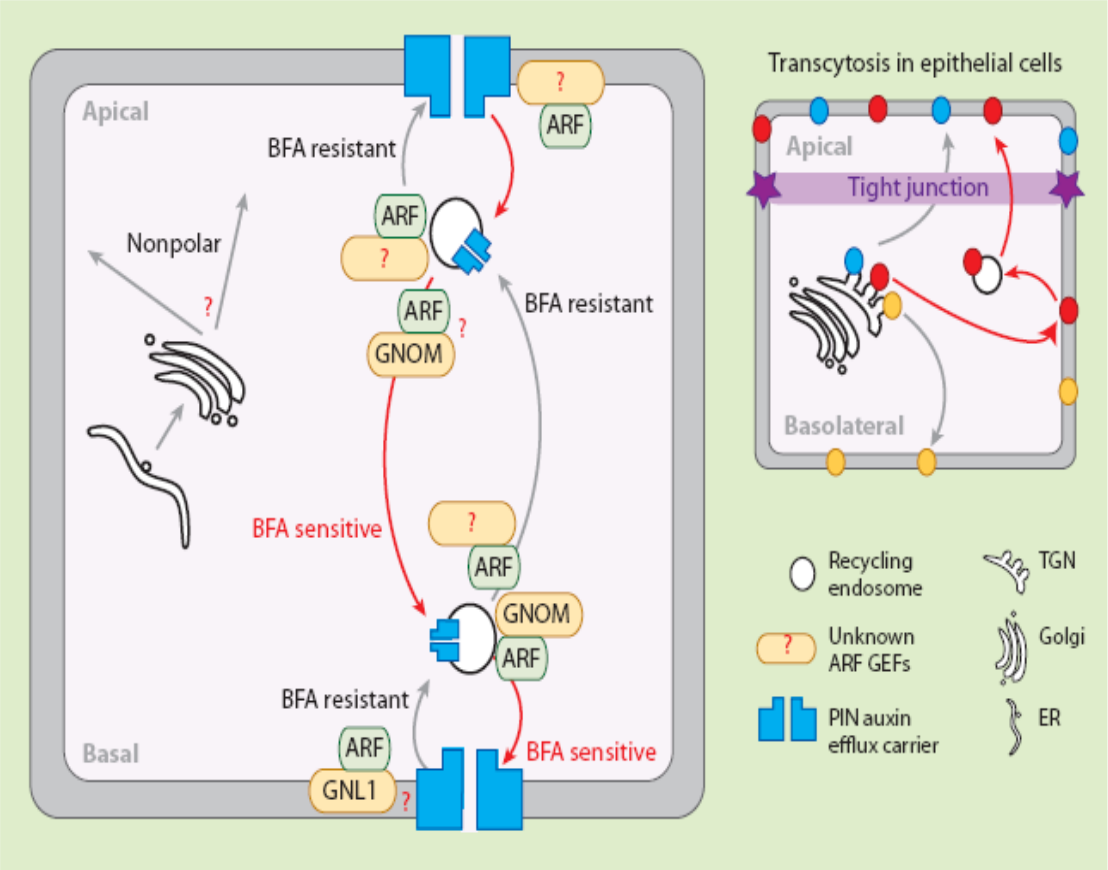


**Figure 1.5: Transcytosis and apical and basal targeting of PIN-FORMED (PIN) proteins**. Distinct ARF GEF-dependent apical and basal targeting pathways regulate polar PIN distribution. Alternative utilisation of both pathways by the same PIN molecules enables dynamic translocation of PIN cargos between different cell sides. Inhibition of the GNOM component of that basal targeting pathway genetically or by BFA leads to preferential recruitment of cargos by the apical pathways and to a reversible basal-to-apical PIN polarity shift. The top right panel illustrates that a similar process occurs in animal epithelial cells, in which several polar competent (depicted in red) are initially targeted to basolateral cell side and subsequently transcytosed to their final destination (the apical cell side). However, other polar cargos (depicted in yellow and blue) do not require transcytosis for polar localisation. Moreover, transcytosis in epithelial cells is also sensitive to BFA. ARF GEF, GDP/GTP – exchange factors for adenosyl ribosylation factors; BFA - brefeldin A; ER – endoplasmic reticulum; GNL1- GNOM-LIKE1; TGN- trans-Golgi network (adapted from Kleine-Vehn, 2008).

In plants, auxin negatively modulates the endocytic step of the cycling proteins such as $H^+$-ATPase and aquaporins. This effect was observed in mutants that have elevated auxin levels or after exogenous auxin application. The molecular mechanism controlling this process is unclear, and whether auxin regulates endocytosis by a known $SCF^{TIR1}$-Aux /IAA-ARF pathway, or by another unidentified pathway, is still open to debate (Vieten *et al*., 2007). The only molecular components directly or indirectly involved in this process is the protein BIG, given that in *big* mutants the inhibition of endocytosis by auxin is less pronounced (Paciorek *et al*., 2005).

Regardless of which hypothesis turns out to be correct for the pathway, this cellular mechanism enables auxin to influence the cycling of its own transporters, thereby controlling their abundance and therefore, their activity at the plasma membrane. One speculation can be that the auxin-dependent stabilisation of PIN proteins on a particular cell side would also be a part of the mechanism by which auxin influences the polar localisation of its transporters. Thus, auxin could influence both the rate and the directionality of its own flow (Vieten *et al*., 2007).

## 1.6.2: Auxin Signalling

Auxin signalling is assumed to start with the perception of auxin by its interaction with some kind of receptor. Evidence suggests that there are multiple sites for auxin perception, and in this sense, auxin can be considered to be multifunctional in that the auxin signal appears to be transduced through various signalling pathways.

### 1.6.2.1: Auxin Binding protein I

The search for auxin receptors has naturally focused on the isolation and characterization of proteins that bind auxin (Venis *et al.*, 1995). Although a variety of such proteins has been identified, conclusive evidence linking them to auxin response has proved difficult to obtain. The best-characterised auxin binding protein is ABP1 (Napier, 1995), which was first described in maize (Hertel *et al*., 1972). Excitement about the role of ABP1 in auxin perception is driven by the high specificity and affinity of its auxin binding, with a Kd for the synthetic auxin NAA of $5 \times 10^{-8}$ M (Napier, 1995). However, almost none of its other properties are characteristic of a typical receptor. The protein has no homology to any other known receptor family, and the vast majority of it is retained in the endoplasmic reticulum, where the pH is too high for strong auxin binding (Henderson *et al*., 1997; Tian *et al*., 1995). It is clear that ABP1 acts at the cell surface to mediate these responses because the exogenous addition of anti-ABP1 antibodies, which are unable to enter the

cell, can interfere with the ability of auxin to induce the responses. It is nevertheless interesting to note that PIN5 localizes to the endoplasmic reticulum (Mravec *et al*., 2009), though any possible link with ABP1 there is unknown.

In whole plants, transgenic approaches to change ABP1 levels have resulted in relatively modest phenotypic effects (Jones *et al*., 1998). Phenotypes are in general limited to effects on the balance between cell division and cell expansion. Many aspects of ABP1 biology remain mysterious, but recently two extremely important tools have been added to the collection available for the investigation of ABP1 function. First an insertion mutant in the Arabidopsis *ABP1* gene has been recovered, allowing the phenotype of complete loss of ABP1 function to be assessed for the first time (Chen et al., 2001). The phenotype of plants homozygous for the mutation is embryo lethality early in the globular stage. This demonstrates the essential role that ABP1 plays in plant growth, but it makes analysis of the postembryonic role of ABP1 difficult, requiring conditional mutations. The second major advance is the solving of the crystalline structure of ABP1 to a resolution of 1.9 Angstroms (Voges *et al*., 1999). The combination of these new genetic and biochemical tools will allow better analysis of the events immediately up- and downstream of ABP1 (Warwicker *et al*., 2001) so that its role in auxin signalling can be clarified.

### 1.6.2.2: Intracellular sites for auxin perception

The existing evidence suggests that there are multiple auxin receptors, and hence the work on ABP1 is expected to answer only part of the question of how the auxin signal is perceived. For example, although ABP1 appears to act at the cell surface, there is good evidence for intracellular perception of auxin, much of which is derived from comparing the effects of auxins that differ in their transport properties into and out of cells (Claussen *et al*., 1996). This approach has been strengthened by the isolation of mutants in *Arabidopsis* that differ in their ability to transport auxins. As indicated above, loss of *AUX1* function results in a variety of phenotypes including auxin-resistant root elongation and reduced root gravitropism (Bennett *et al*., 1996; Marchant *et al*., 1999). The roots of *aux1* mutants are resistant to the effects of membrane-impermeable auxins such as 2,4-D. However, *aux1* mutants respond normally to the membrane-permeable auxin NAA, and addition of NAA to *aux1* mutant roots can restore graviresponse (Marchant *et al*., 1999; Yamamoto *et al*., 1998). This suggests that intracellular auxin is important for root growth inhibition. Potential intracellular auxin binding proteins have been identified. For example, a 57-kDa soluble auxin binding protein has been identified in rice (Kim *et al*., 1998). This protein appears to interact directly with the plasmamembrane proton pumping ATPase,

suggesting a very short signal transduction pathway from auxin to increased proton pumping, cell wall acidification, and hence cell elongation (Kim *et al*., 2000, 2001).

## 1.6 2.3: Auxin signalling transduction

Rapid progress in the area of auxin signal transduction has been made recently through the use of genetic approaches in Arabidopsis (Leyser *et al*.,1997). Large screens for mutants with altered auxin sensitivity were used to define genes whose normal function is required for wild-type auxin response. Among the loci defined by these screens are *AXR1*, *AXR2, AXR3, AXR4*, and *AXR6*. A sixth locus, *TIR1*,was originally identified because mutations in it result in resistance to inhibitors of polar auxin transport, but these mutations were subsequently found also to confer auxin resistance (Ruegger *et al*., 1998).

## 1.6.2.4 The role of ubiquitin-mediated protein degradation

*Aux/IAA* genes encode transcriptional repressors of auxin responses; most are transcriptionally regulated by auxin, and in an ARF- and Aux/IAA-dependent manner (Abel *et al*., 1995, Tatematsu *et al*., 2004, Tian *et al*., 2002). Auxin-regulated expression of these repressors serves as a rapid negative feedback mechanism in auxin signalling. The Ub-proteasome pathway is responsible for the regulated degradation of diverse proteins in eukaryotes, including the Aux/IAA repressors. Ub is attached to substrate proteins through a series of highly conserved enzymatic reactions. Plants devote a remarkably large fraction of their genome to this pathway; suggesting that protein degradation is particularly important for cellular regulation in plants (Smalle and Vierstra, 2004). The Ub-protein conjugation pathway is initiated by an enzyme called the Ub-activating enzyme or E1 (Hershko and Ciechanoner, 1998). The enzyme catalyzes an ATP-dependent reaction that activates a Ub monomer and transfers it to the second enzyme in the pathway, the Ub-conjugation enzyme (E2) (Hershko and Ciechanover, 1998). A third protein or protein complex called the Ub-protein ligase (E3) interacts with both the Ub-E2 and specific substrate protein, thus promoting the transfer of Ub to the substrate (Hershko and Ciechanover, 1998; Pickart *et al*., 2001). The SCF (Skp1-Cul1-Fbox) protein complexes make up a major class of E3s in all eukaryotes and appear to be the most abundant type of E3 in plants (Moon *et al*., 2004, Smalle and Vierstra, 2004). Each SCF contains a highly conserved central scaffold protein, called a cullin, that is associated with the adaptor proteim Skp1 (a member of the ASK family in plants; Petroski and Deshaies, 2005; Smalle and Vierstra, 2004).

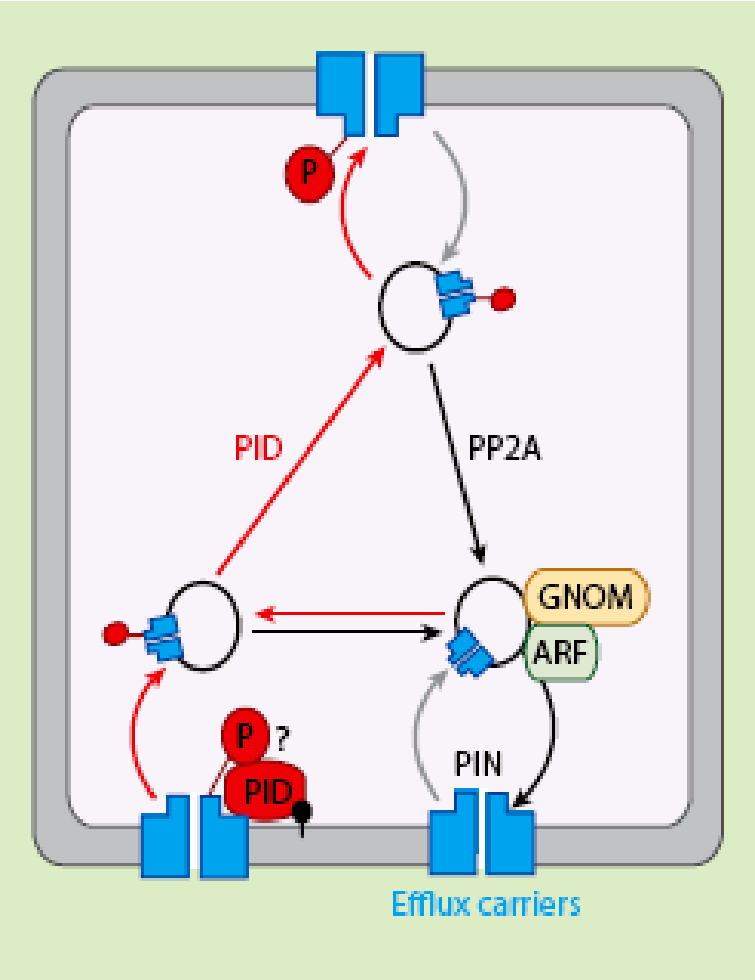


**Figure 1.6: Contribution of PIN-FORMED (PIN) phosphorylation to the decision on the PIN polar distribution.** PINOID (PID)-dependent phosphorylation of PIN proteins may affect affinity to distinct apical and basal targeting pathways. An increases in PID kinase or a decrease in protein phosphates 2A (PP2A) activities lead to a basal-to-apical PIN polarity shift. On the contrary, increased PP2A activity counteracts the PID effects and leads to prefential GNOM-dependent basal PIN targeting. ARF denotes adenosyl ribosylation factor (Kleine-Vehn *et al*., 2008)

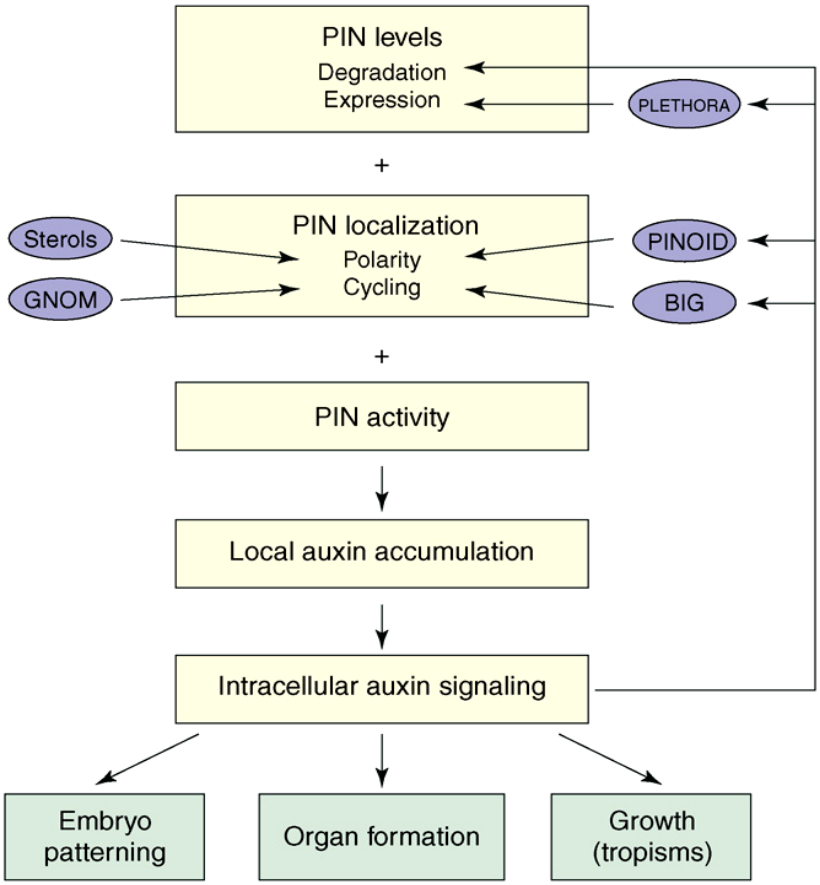


**Figure 1.7: Feedback regulation in PIN-dependent local auxin distribution**. The activity of the PIN-dependent auxin distribution network depends on PIN levels (the result of degradation and expression), PIN localization (the polarity and amount of PINs at the cell surface) and presumably the transport activity of the PIN-containing complex.

PIN-dependent transport mediates auxin accumulation in certain cells. In these cells, auxin is interpreted by signalling pathways (prominent among them the TIR1-Aux/IAA-ARF cascade) into various developmental responses. Auxin also feeds back on PIN expression, degradation, polarity and endocytic cycling through additional factors such as the transcription factor PLETHORA, the Ser/Thr kinase PINOID and the Callosin protein BIG, respectively. It is possible that other as yet unidentified feedback regulatory mechanisms are also operational. In addition, auxin influx carriers, including AUX1, and other transporters, such as PGPs, contribute to the regulation of auxin distribution, but the regulation of these components is less well characterised (adapted from Kleine-Vehn *et al.*, 2008).

This adaptor protein provides the binding site for the F-box protein, which functions as the substrate-binding component of the SCF. The fourth subunit, variously called RBX1, ROC, or Hrt1 binds the Ub-E2 and promotes transfer of Ub to the F-box-protein-bound substrate. Ub-E2 docking to RBX1 is thought to promote allosterically the transfer of Ub, indicating that the purpose of SCF-complex architecture is to position the protein substrate to receive the transferred Ub effectively (Petroski and Deshaies, 2005). Indeed, the structure of the CUL1 subunit establishes a critical distance between the substrate protein and Ub-E2. Upon transfer by the E2, AN isopetide bond is formed between a lysyl ε-amino group on the substrate protein and the C-terminal glycyl residue of Ub (Petroski and Deshaies, 2005).

Substrate marking for recognition by the 26S proteasome requires the addition of a chain of polymerized Ub (Petroski and Deshaies, 2005). It is not clear if polyubiquitination occurs through the successive addition of single Ub molecules to SCF-bound substrate or by the attachment of a preformed Ub chain (Hochstrasser, 2006). Members of a family of deubiquitinating enzymes (DUBs) assist in Ub recycling upon breakdown of polyubiquitinated substrates (Amerik and Hochstrasser, 2004). Some DUBs may have additional roles in selectively reversing the ubiquitination of substrates, thereby preventing substrate degradation. Diversity among subunits of the proteosome may also contribute complexity to proteasome substrate interaction (Brukhin *et al*., 2005, Demartino and Gillette, 2007, Smalle *et al*., 2002).

### 1.6.2.5: Ubiquitin-proteasome pathway is required for auxin signalling

The connection between auxin and the Ub pathway was established through a screen for Arabidopsis mutants with altered auxin response (Walker and Estelle 1998). The roots of Arabidopsis seedlings are inhibited by low levels of auxin in the growth medium, making it relatively straightforward to isolate large numbers of auxin-resistant mutants. The first auxin-resistant mutant to be characterized in detail was called *axr1* (Lincoln *et al.* 1990; Leyser *et al*. 1993). The *AXR1* gene encodes a subunit of the heterodimeric RUB-E1 enzyme, the first enzyme in the RUB-conjugation pathway (del Pozo *et al*. 1998). Because RUB modification of CUL1 is important for SCF function, these results suggested that auxin response depends on the action of a cullin-containing E3 ligase. This idea was supported by later studies of another auxin-resistant mutant called *tir1* (Ruegger *et al*. 1998). The *TIR1* gene encodes a leucine-rich-repeat (LRR)-containing F-box protein that interacts with CUL1, ASK1 or ASK2, and RBX1 to form $SCF^{TIR1}$ (Gray *et al*. 1999,

Ruegger *et al*. 1998). Typically the biggest challenge in characterizing a newly discovered E3 ligase is identifying its substrates. In the case of $SCF^{TIR1}$, there were some obvious candidates because the Aux/IAA proteins were known to be unstable repressors of auxin regulated transcription. Both genetic and biochemical studies confirmed that the Aux/IAAs are substrates of $SCF^{TIR1}$ (Gray *et al*. 1999). Several members of the Aux/IAA family are stabilized in the *axr1* and *tir1* mutants, and both mutants exhibit reduced auxin-regulated gene expression (Gray *et al*. 1999). Furthermore, *in vitro* studies demonstrated that Aux/IAA proteins interact with TIR1 and that auxin stimulates this interaction (Gray *et a*l. 1999). Taken together, these results indicate that auxin acts by promoting the degradation of the Aux/IAAs through the action of $SCF^{TIR1}$, a model that is summarized in Figure 1.8. Support for the model was provided by analyses of mutants that affect other proteins in the Ub pathway, including CUL1, ASK1, CAND1, and subunits of the CSN (Gray *et al*. 2001, 2003; Schwechheimer *et al*. 2001; Hellmann *et al*. 2003; Chuang *et al.* 2004; Moon *et al*. 2007; Quint *et al*. 2005).

Additionally, investigators have isolated mutants that affect an AXR1-like enzyme (AXL), the partner of AXR1 required for RUB-E1 activity (ECR1), the RUB-E2 (RCE1), and other SCF regulators (Dharmasiri *et al*. 2003, 2007; Chuang *et al*. 2004; Walsh et al. 2006; Woodward et al. 2007). Like *axr1* and *tir1*, these mutants are deficient in auxin response and show a variety of auxin related growth defects. For example, some *cul1* alleles (also called *axr6*) have a seedling-lethal phenotype that is similar to the phenotypes of *mp*/*arf5* and *bdl*/*iaa12*, contributing to evidence that SCF-mediated degradation of IAA12 is required for formation of the embryonic root (Hobbie *et al*. 2000; Hellmann et al. 2003). Taken together, characterization of these mutants demonstrates that the regulation of SCF function and the resulting Ub modification of Aux/IAA proteins are critical to auxin-regulated plant development.

## 1.6.2.6: Auxin perception through the SCF

The discovery that $SCF^{TIR1}$ promotes the degradation of the Aux/IAA proteins was a major breakthrough in plant hormone signaling. However, there were many unresolved questions, including the identity of the auxin receptor and how TIR1-Aux/IAA recognition is regulated. On the basis of studies of SCFs in animals and fungi, it was assumed that Aux/IAA recognition would require a posttranslational modification, probably phosphorylation (Petroski and Deshaies 2005).

However, in vitro studies strongly suggested that Aux/IAA modification was not required for recognition (Dharmasiri *et al*. 2003; Kepinski and Leyser 2004). For example, inhibitors of protein kinases and phosphatases do not affect the TIR1-Aux/IAA interaction (Dharmasiri *et al*. 2003; Kepinski and Leyser 2004). In addition, auxin promotes the interaction in membrane-depleted extracts, suggesting that the receptor and any intermediary components are not associated with cellular membranes (Dharmasiri *et al*. 2003). Two important papers confirmed that auxin regulates $SCF^{TIR1}$ through a novel mechanism (Dharmasiri *et al*. 2005a Kepinski and Leyser 2005). In these studies, partially purified $SCF^{TIR1}$ bound an Aux/IAA protein in an auxin-dependent manner, indicating that the receptor copurified with $SCF^{TIR1}$. Furthermore, labeled auxin ($^{3}$H-IAA) bound specifically to $SCF^{TIR1}$, or a closely associated protein, signifying that an auxin receptor was present in the complex. One explanation for these results, something that previously seemed very unlikely, is that TIR1 is the auxin receptor. That this is the case was strongly suggested by the discovery that TIR1 synthesized in insect cells or *Xenopus* embryos also binds recombinant Aux/IAA protein in the presence of auxin (Dharmasiri *et al*. 2005a; Kepinski and Leyser 2005). Because the only plant proteins in this assay are TIR1 and Aux/IAA, each synthesized in heterologous systems, the logical conclusion was that one of these two proteins binds auxin. Assays *in vitro* showed that Aux/IAA proteins do not bind auxin, leaving TIR1 as the best candidate.

## 1.6.2.7: A family of auxin receptors in plants

The *Arabidopsis* genome encodes five F-box proteins exhibiting 50–70% sequence identity with TIR1. These proteins have been named auxin signalling F-box protein 1 to 5 (AFB1–AFB5) (Table 1.6). Genetic and biochemical studies have implicated these proteins in auxin signalling (Dharmasiri *et al*. 2005b, Walsh *et al*. 2006). Moreover, binding of radiolabeled IAA is diminished in extracts from mutants lacking TIR1 and AFB1–3, confirming that these proteins are very likely to function as auxin receptors. As for the *tir1* mutants, single *afb* loss-of-function mutations do not cause dramatic developmental defects. Although the available evidence suggests that TIR1 and AFB1–3 have similar functions in development, it is likely that more detailed studies will reveal specific roles for one or more of these proteins. Such specific functions have already been demonstrated for AFB5. Genetic studies showed that loss of AFB5 results in resistance to the synthetic auxin (Walsh *et al*. 2006). Because *afb5* plants are only slightly resistant to IAA and other auxins, AFB5 appears to have important chemical selectivity.

## 1.6.3: Ethylene

The simple gas ethylene has been recognized as a plant hormone for over 80 years (Funke *et al*., 1938). It influences a diverse array of plant growth and developmental processes, including germination, leaf and flower senescence and abscission, cell elongation, fruit ripening, nodulation and the response to wide variety of stresses (Abeles *et al*., 1992). To understand how ethylene or any signalling molecule affects development, one needs to consider not only how it is transported and perceived but also how its level is controlled.

The biosynthesis of ethylene occurs through a relatively simple metabolic pathway that has been extensively studied and well documented in plants (Kende *et al*., 1993; Zarembinski and Theologis, 1994; Kieber *et al*., 2007). Ethylene is derived from amino acid methionine, which is converted to S-adenosylmethionine (AdoMet) by S-adenosylmethionine synthetase. AdoMet is then converted to 1-aminocyclopropane 1-carboxylic acid (ACC) and 5'-deoxy-5'methylthioadenosine (MTA) by the enzyme 1-aminocyclopropane-1-carboxylase synthase (ACS; Adam and Yang, 1979), which is first committed and in most instances the rate-limiting step in ethylene biosynthesis. Methylthioadenine is recycled to methionine through the Yang cycle, which allows high rates of ethylene production without depletion of the endogenous methionine pool (Yang *et al*., 1987).

ACC is converted into ethylene, $CO_2$ and cyanide by ACC oxidase (ACO). The cyanide produced by this reaction is detoxified into β-cyanoalanine by the enzyme β-cyanoalanine synthase, preventing toxicity to plants in condition of high ethylene biosynthesis. Besides being converted to ethylene, ACC can also be irreversibly conjugated to form N-malonyl-ACC (Kionka and Amrhein, 1984). Malonylation of ACC regulates the level of ACC and thus the production of ethylene. Ethylene can be metabolized by plant tissues to ethylene oxide and ethylene glycol (Sanders *et al*., 1989), but the physiological significance of this metabolism remains to be established. As a gas, ethylene can readily diffuse from plant tissues, so metabolism is not essential for its removal.

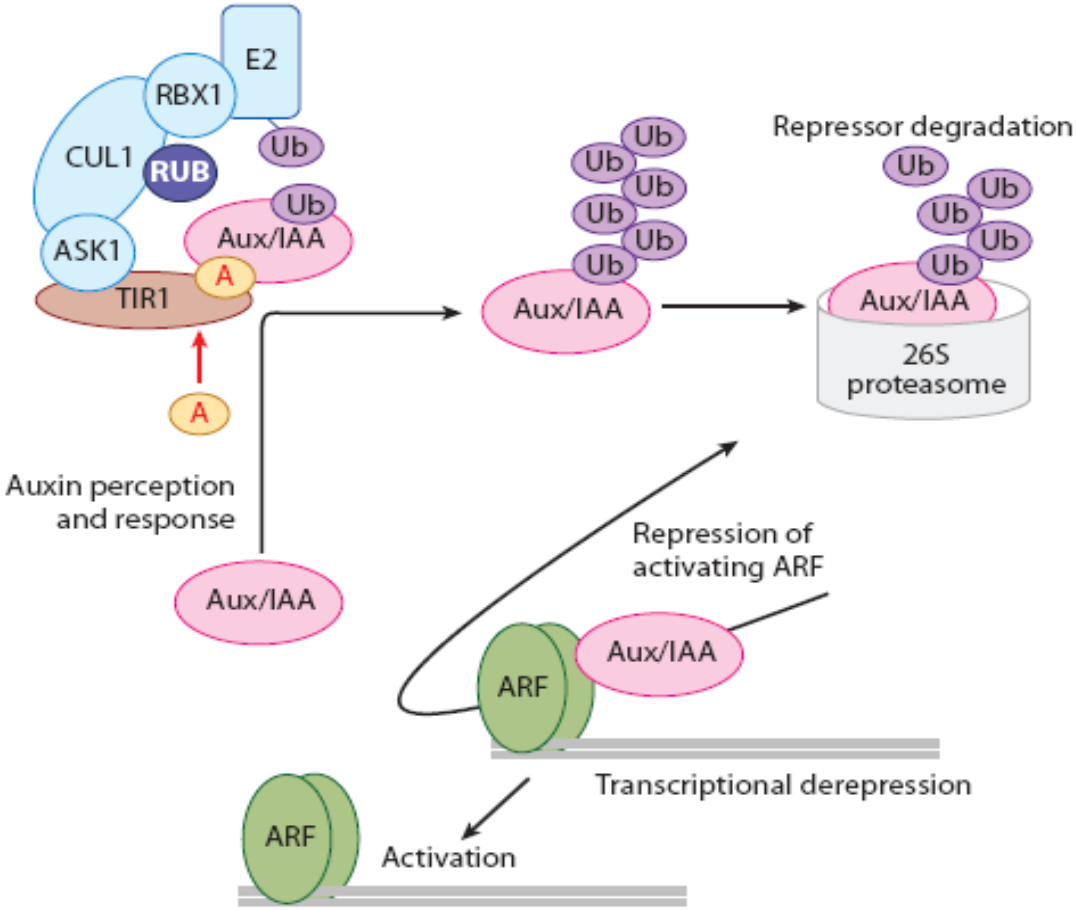


**Figure 1.8: Auxin regulates transcription by promoting ubiquitin(Ub)-mediated degradation of Aux/IAA repressors**. Auxin (A) binds to the F-box protein TIR1 in $SCF^{TIR1}$ and stabilises the interaction between TIR1 and an Aux/IAA substrate. The repressor is polyubiquitinated and degraded by the 26S proteasome. Loss of the Aux/IAA permits auxin response factor (ARF)-dependent transcription of auxin-regulated genes. E2, Ub -conjugating enzyme (Mockaitis and Estelle, 2008)

| Gene | Product | Function | Genetic evidence for role in auxin-mediated development | References |
|---|---|---|---|---|
| *TIR1* | Transport inhibitor response1, F-box protein | Interacts with ASK1; interacts with Aux/IAA; Auxin increases Aux/IAA affinity; crystal structure shows TIR-1-auxin-Aux/IAA complex | Loss-of-function mutations reduce multiple auxin responses | N. Dharmasiri et al. 2003, Dharmasiri et al. 2005b, Gray et al. 1999, Kepinski & Leyser 2005, Ruegger et al. 1998, Tan et al. 2007 |
| *AFB1* | Auxin F-box protein 1 (AFB1) | Member of TIR1/AFB family; auxin increases Aux/IAA affinity | Loss of function with *tir1*, *afb2*, *afb3* dramatically impairs development | Dharmasiri et al.2005b |
| *AFB2* | Auxin F-box protein 2 (AFB 2) | Member of TIR1/AFB family; auxin increases Aux/IAA affinity | Loss of function with *tir1* reduces multiple auxin responses | Dharmasiri et al. 2005b |
| *AFB3* | Auxin F-box protein 3 (AFB3) | Member of TIR1/AFB family; auxin increases Aux/IAA affinity | Loss of function with *tir1* and *afb2* dramatically impairs development | Dharmasiri et al. 2005b |
| *AFB4* | Auxin F-box protein 4 (AFB 4) | Member of TIR1/AFB family; auxin increases Aux/IAA affinity | | Dharmasiri et al. 2005b |
| *AFB5* | Auxin F-box protein 5 (AFB5) | Member of TIR1/AFB family; auxin increases Aux/IAA affinity | Loss-of-function mutation confers resistance to auxin analogs | Dharmasiri et al. 2005b<br><br>Walsh et al., 2006 |

**Table 1.9: Auxin receptors in Arabidopsis thaliana (adapted from Mockaitis & Estelle, 2008)**

## 1.6.3.1: Ethylene signal transduction

### 1.6.3.1.1: Components of ethylene signalling pathway

Many key components of the ethylene signal transduction pathway were identified from a genetic screen that made use of ethylene's effect on dark grown seedlings known as the 'triple response'. In Arabidopsis, the triple response is characterised by inhibition of hypocotyl and root elongation, a thickened hypocotyl and an exaggerated apical hook (Chen *et al*., 2005).

Populations of mutagenised Arabidopsis were screened for seedlings that displayed an altered triple-response phenotype, and this approach resulted in the identification of several ethylene-sensitive mutants. These mutants include *etr1* (ethylene response; Chang *et al*., 1993), *etr2* (Sakai *et al*., 1998), *ein2* (ethylene insensitive; Alanso *et al*., 1999), *ein3* (Chao *et al*., 1997) *ein4, ein5, ein6* (Roman *et al*., 1995), *hls1* (hookless; Guzman and Ecker, 1990), and *eir1* (ethylene insensitive root; Roman *et al*., 1995). Mutants were also identified that exhibited a triple response in the absence of ethylene. These include *ctr1* (constitutive triple response; Kieber *et al*., 1993) and *ran1* (responsive to antagonist; Hirayama *et al*., 1999). Genetic and molecular analyses of these mutants have defined a pathway for ethylene signal transduction leading from initial perception to transcriptional regulation. These components form the backbone of ethylene signalling pathway and much of the current research is aimed at determining how these components function in the pathway.

In Arabidopsis ethylene is perceived by a family of five membrane bound receptors (ETR1, ETR2, ERS1, ERS2, and EIN4) that have similarity to two-component receptors from bacteria (Bleecker, 1999; Schaller and Kieber, 2002). Loss-of-function (LOF) mutations in any single ethylene receptor have little or no effect on upon seedling growth, consistent with functional overlap within the receptor family (Hua and Meyerowitz, 1998). Plants with multiple LOF mutations in the receptors show a constitutive ethylene response, indicating that the receptors are negative regulators of ethylene signalling (Hua and Meyerowitz, 1998). This effect of LOF mutations in the receptors is due to their interaction with the downstream component CTR1 (Chen *et al*., 2002). Analysis of the ethylene receptor ETR1 supports localisation to the endoplasmic reticulum (Chen *et al*., 2002). Such a location is compatible with the ready diffusion of ethylene in both aqueous and lipid environments (Abeles *et al*., 1992).

CTR1 is the next downstream component identified in the signalling pathway (Kieber *et al*., 1993; Huang *et al*., 2003). CTR1 is a Raf-like ser/thr kinase with similarity to a mitogen-activated protein kinase kinase kinase (MAPKKK), suggesting the involvement of a MAP-kinase-like signalling cascade in the regulation of ethylene signalling. LOF mutation in CTR1 results in a constitutive ethylene-response phenotype, indicating that CTR1 is a negative regulator of ethylene signalling.

EIN2 has similarity to members of the Nramp metal-ion transport family (Alonso *et al*., 1999). EIN2 plays a major role in the ethylene response as LOF mutation result in complete ethylene insensitivity for all ethylene responses tested, indicating that EIN2 is a positive regulator of the pathway (Alonso *et al*., 1999). In addition EIN2 is predicted to be membrane-localised, the specific membrane system has not yet been determined. Thus the actual function of EIN2 in the pathway is still a mystery.

Functioning downstream of EIN2 is a small family of transcription factors that includes EIN3 and various EIN3-like (EIL) proteins (Roman *et al*., 1995; Chao *et al*., 1997). LOF mutations in *EIN3* cause partial ethylene insensitivity. This insensitivity can be rescued by expression of *EIN3*, *EIL1*or *EIL2* indicating that along with EIN3 at least two EILs can mediate an ethylene response (Chao *et al*., 1997). The EIN3/EIL family are involved in a regulatory cascade and stimulate the transcription of other transcription factors such as ERF1 (ethylene response factor; Solano *et al*., 1998; Alonso *et al*., 2003), a member of ERF family of transcription factors (Fujimoto *et al*., 2000). These transcription factors have been shown to act as activators or repressors of additional downstream ethylene-responsive genes (Ohme-Takagi and Shinshi, 1995).

## 1.6.3.1.2: Model of ethylene signal transduction

The genetically defined elements have been ordered into a proposed pathway for ethylene signal transduction based on double-mutant analysis (Kieber *et al*., 1993; Hua *et al*., 1995; Sakai *et al*., 1998). A pathway based on the genetic interactions may not always correspond to a biochemical or mechanistically based pathway. What we know about the biochemical nature of these elements does, however, support much of what has been defined genetically. An important feature of the ethylene signalling pathway is that it contain both positive and negative regulators, some proteins thereby serving to induce the response while others suppress them.

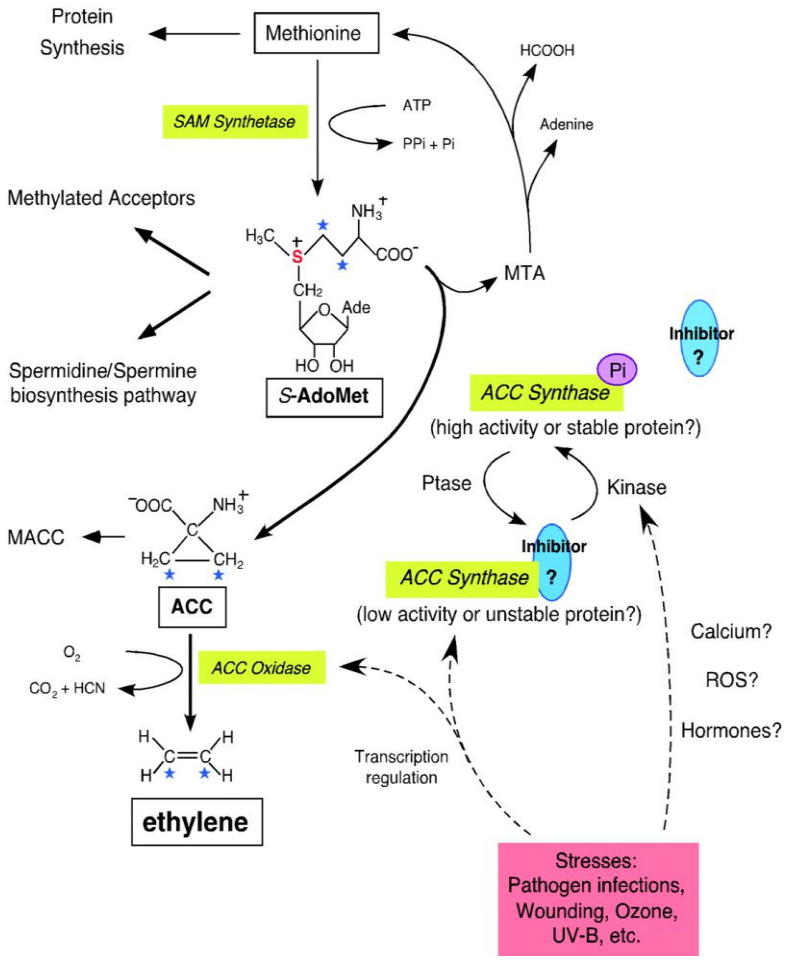


**Figure 1.10: Ethylene biosynthesis: Ethylene biosynthesis starts with methionine.**

The formation of *S*-AdoMet is catalyzed by SAM synthetase from the methionine at the expense of one molecule of ATP per molecule of *S*-AdoMet synthesized. *S*-AdoMet is the methyl group donor for many cellular molecules (Methylated Acceptors), including nucleic acids, proteins, and lipids. In addition, *S*-AdoMet is the precursor of the polyamine synthesis pathway (Spermidine/Spermine biosynthesis pathway). ACC is the immediate precursor of ethylene. The rate-limiting step of ethylene synthesis is the conversion of *S*-AdoMet to ACC by ACC synthase under most conditions. MTA is the by-product

generated along with ACC production by ACC synthase. Recycling of MTA back to methionine conserves the methylthio group and is able to maintain a constant concentration of cellular methionine even when ethylene is rapidly synthesized. Malonylation of ACC to malonyl-ACC (MACC) deprives the ACC pool and reduces the ethylene production. ACC oxidase catalyses the final step of ethylene synthesis using ACC as substrate and generates carbon dioxide and cyanide. Transcriptional regulation of both ACC synthase and ACC oxidase is indicated by dashed arrows. Reversible phosphorylation of ACC synthase is hypothesized and may be induced by unknown phosphatases (Ptase) and kinases, the latter presumably activated by stresses. Both native and phosphorylated form (ACC synthase-Pi) of ACC synthase are functional, although the native ACC synthase may be less stable or active in vivo. A hypothetical inhibitor is associated with ACC synthase at the carboxyl end and may be dissociated from the enzyme if it is modified by phosphorylation at the vicinity (adapted from Wang *et al*., 2002).

According to the basic working model, the ethylene receptors activate the kinase activity of CTR1 in the air (absence of ethylene). CTR1 then actively suppresses the downstream responses, such that EIN2 and EIN3/EIL transcription factors remain inactive. Upon binding ethylene, the receptors no longer activate CTR1, and so CTR1no longer suppresses the pathway. This relief of suppression allows for activation of EIN2, induction of the transcriptional cascade, and the establishment of ethylene responses. The presence of both positive and negative regulators result in a model for ethylene signalling that seems counterintuitive, because the binding of ethylene inactivates early component in the pathway.

Evidence indicates that the basic elements and mechanism of the ethylene signal transduction pathway are conserved in agronomically important dicots and monocots (Adam-Phillips *et al*., 2004; Klee, 2004). The ethylene receptors in other plant species such as tomato (*Solanum lycopersicum*; Klee, 2002), rice (*Oryza sativa*; Yau *et al*., 2004) and tobacco (*Nicotiana tabacum*), display properties in keeping with what has been found with the Arabidopsis ethylene receptors. As in Arabidopsis, the receptors show homology to prokaryotic two-component sensors, redundancy within a single plant species, act genetically as negative regulators of downstream responses, show differential expression throughout development with a subset of the genes induced by ethylene and regulate a broad spectrum of physiological processes.

Less information is available about the conservation of the downstream components of the ethylene signal transduction pathway such as CTR1, EIN2 and EIN3 in other plant species, although these have been found when looked for (Chen *et al*., 2005). Interestingly, in tomato there appears to be a three-member *CTR1*-like gene family (Adams-Phillips *et al*., 2004), compared to the single Arabidopsis *CTR1* gene.

### 1.6.3.1.3: An ethylene receptor-CTR1 signalling complex

Data indicate that the ethylene receptors form protein complexes with the downstream signalling component CTR1 (Chen *et al*., 2005). This physical interaction has been analysed in most detail for ETR1 and CTR1, but evidence suggests that the other ethylene receptors also interact with CTR1.

Like the ethylene receptors, CTR1 has been shown to associate primarily with the ER, as revealed by sucrose density-gradient centrifugation experiments (Gao *et al*., 2003). CTR1 has no predicted transmembrane domain or membrane attachment motifs, suggesting that the membrane association of CTR1 occurs due to interaction with integral membrane protein, the ethylene receptors being likely candidates. A pull-down assay demonstrated that CTR1 and ETR1 are in the same signalling complex in Arabidopsis (Gao *et al*., 2003). Several additional lines of evidences support a direct interaction between CTR1 and ETR1. Analysis using the yeast two-hybrid system indicated that CTR1 is able to interact with ETR1 as well as with ERS1 or ETR2 (Clark *et al*., 1998; Cancel and Larsen, 2002). In addition, CTR1 has been shown to be able to interact with ETR1 and ETR2 using proteins transgenically expressed in *E.coli* and yeast (Clark *et al*., 1998; Gao *et al*., 2003).

The mechanism by which the activity of CTR1 is regulated by the ethylene receptors is still unclear. Based on the model for signalling by the protein kinase Raf (Heidecker *et al*., 1990), the N-terminal of CTR1 might be able to autoinhibit its C-terminal Ser/kinase activity. In air (absence of ethylene), the receptor would maintain the N-terminus of CTR1 in a conformation such that CTR1 is active and able to repress downstream ethylene responses. Ethylene binding would induce a conformational change such that the N-terminal of CTR1 could autoinhibit its kinase activity, thereby releasing the repression on downstream ethylene responses. Because of the physical interaction between the ethylene receptor and CTR1, it is possible that regulation of CTR1 could occur due to conformational changes induced in the receptor by binding ethylene then being passed on to CTR1. There is a possibility that such regulation could be mediated through changes in the phosphorylation of the ethylene receptors and CTR1 (Zhang *et al*., 2004; Chen *et al*.,

2005). The ethylene receptors ETR1 and ERS1 have been shown to contain the predicted histidine kinase activity (Gamble *et al*., 1998; Moussatche and Klee, 2004).

### 1.6.3.1.4: Recently proposed components of the signal transduction

A number of recent studies have implicated new components in the regulation of ethylene signal transduction. Their role in ethylene signal transduction is, however, not clear as those components previously identified by forward genetics analysis. The proposed role of these new components is based on loss-of-function mutant phenotypes that result in slight modification of ethylene responses or phenotypes resulting from over-expression. Thus these components are not necessarily part of the primary ethylene signal transduction pathway (Chen *et al*., 2005).

#### 1.6.3.1.4.1: MAPK and MAPKK

A MAPK kinase pathway has been proposed to function in ethylene signalling because CTR1 is similar to Raf, a member of the MAPKKK (mitogen-activated protein kinase kinase kinase) family (Kieber *et al*., 1993; Huang *et al*., 2003). In fact, a MAPK pathway involving SIMK (salt-stress-inducible MAPK) in *Medicago* or MAPK6 in *Arabidopsis* was recently implicated in operating downstream of CTR1 as a positive regulator of the ethylene response (Ouaked *et al*., 2003). Nonetheless, the reduction or elimination or elimination of *Arabidopsis MPK6* expression/function by RNA interference or the T-DNA insertion approach does not have an appreciable defect on ethylene responses (Ecker *et al*., 2004; Menke *et al*., 2004). Through a series of biochemical studies, another group of investigators failed to observe any significant difference of MPK6 activity upon ACC treatment in *Arabidopsis* between wild-type and mutant plants (Liu and Zhang, 2004). In addition, the same group presented convincing evidence to indicate that MPK6 regulates ethylene biosynthesis rather than the signalling pathway (Liu and Zhang, 2004). Overall, other than the sequence similarity of CTR1 to MAPKKK, there is so far no conclusive evidence to support a MAPK kinase cascade operating in the ethylene signal transduction pathway.

#### 1.6.3.1.4.2: RTE1/GR, a novel regulator of the ETR1 receptor

Genetic studies indicate that the ethylene receptors serve as negative regulators of the ethylene-signalling pathway (Hua and Meyerowitz, 1998). However, it is not clear how ethylene binding turns off the receptor activity. Recently, a newly identified regulator of ethylene responses, RTE1 (*REVERSION TO ETHYLENE SENSITIVITY1*) is likely to provide some hints on how the biological function of the receptors is regulated (Resnick *et*

*al*., 2006). RTE1 was identified by genetic screen for suppressors of the dominant gain-of function allele *etr1-2*.

Loss-of-function *rte1* mutants show an enhanced response to ethylene, similar to the *etr1* null mutant or the *rte1*/*etr1* double null mutant, suggesting that RTE1 is a negative regulator of the ethylene response, and that RTE1 and ETR1 act in the same pathway. Moreover, although loss of *rte1* function can suppress ethylene insensitivity of etr1-1, or gain-of-function mutation in the four other ethylene-receptors genes, implying that RTE1 is required specifically for the *etr1-2* mutant receptor to repress the downstream ethylene pathway. No biochemical function has been assigned to this interesting protein yet, except that RTE1 appears to be a membrane protein based on the sequence prediction (Resnick *et al*., 2006).

## 1.6.3.1.5: Role of auxin and ethylene in inhibition of root growth

Inhibition of root growth is one of the characteristic ethylene responses in *Arabidopsis* seedling. Interestingly, many auxin response or transport mutants also show clear defects in the ethylene-mediated root inihibition, leading to the hypothesis that ethylene-induced inhibition of root growth is mediated by accumulation of auxin in the root tissues (Stepanova and Alonso, 2005). Experimental proof of this hypothesis came from the recent identification of two root-specific ethylene-insensitive mutants *wei2* (*weak ethylene insensitive 2*) and *wei7* (Stepanova *et al*., 2005). *WEI2* and *WEI7* encode α and β subunits of anthranilate synthase, repectively, which is a rate-limiting enzyme in tryptophan biosynthesis pathway, and subsequently the auxin synthesis pathway (Bartel *et al*., 1997). Ethylene treatment can induce the expression of *WEI2* and *WEI7* specifically in root tip, and simultaneously increases auxin accumulation, manifest with auxin-driven reporter gene expression. Loss-of-function *wei2* and *wei7* mutants prevent auxin accumulation upon ethylene treatment (Stepanova *et al*., 2005; Swarup et al., 2007; Stepanova et al., 2007). Therefore a simple explanation for ethylene-triggered inhibition of root growth is that ethylene induces *WEI2/7* expression specifically in the root tips, which in turn accelerates auxin biosynthesis, and consequently inhibits root elongation.

## 1.7: POLARIS peptide

To identify new genes involved in the regulation of root development and to gain insight into hormonal interactions, a population of Arabidopsis promoter-trap transgenic lines were screened for genes expressed in roots and defective root phenotype. The tagging of genes by promoter-trap insertional mutagenesis potentially facilitates expression analysis

of genes, the investigation of tagged gene function by mutant analysis, and the cloning of genes (Topping *et al*., 1991). This strategy was used to identify a novel GUS-expression line of the tagged gene called *POLARIS (PLS)* (Topping *et al*., 1994) (Figure 1.10).

GUS (β-glucuronidase) expression by the *PLS* promoter was identified in the heart-stage embryos, in the basal region of the embryo that corresponds to the embryonic root primordium (Scheres *et al*., 1994). In the developing embryo, GUS activity is maintained in the embryonic root and in the young seedling and mature GUS activity is found in both primary and lateral root tips with low expression in the aerial parts (Figure 1.10). GUS expression in the root tips is found in all the cell types (i.e. columella, lateral root cap epidermis, meristem, and immature vasculature) and occurs from the earliest stages of the pericycle division in the lateral root development (Topping and Lindsey, 1997).

Further sequencing of the *pls* locus revealed that the T-DNA insertion occurred in an open reading frame (ORF) encoding a predicted 36-amino acid polypeptide with a predicted molecular mass of 4.6 kDa and limited homology to known proteins (Casson *et al*., 2002). The N-terminal 24 amino acids are predicted to form two *β*-sheets and the remaining 12 amino acids are likely to form a *α*-helix. Between the two *β*-sheets are three basic arginine residues, which may form a possible cleavage site. The C-terminal *α*-helix also contains the repeat KLFKLFK. The lysine residues and a terminal histidine residue represent the only charged residue in this helical region. The 3 amino acid spacing between each of the lysine residues indicate that they would lie in the same face of the *α*-helix, creating an amphipathic helical region with both hydrophobic and charged faces. The fact that the predicted helical region is leucine-rich indicates the potential for a leucine zipper motif, suggesting the possibility for protein-protein interactions (Casson *et al*., 2002).

The PLS peptide is yet to be detected by western blotting using polyclonal antibodies to the N-terminal 18 amino acids, but has been detected in cell extracts by proteomic analysis (Angus Murphy and Wendy Peer, personal communication). Genetic evidence demonstrates a partial *PLS* cDNA is functional and that functionality of the cDNA requires that *PLS* ORF contains an ATG codon (Casson *et al*., 2002). Therefore, these data suggest that the *PLS* gene encodes a functional polypeptide.

Evidence of the function of the PLS peptide came from the investigation of the *pls* mutant root phenotype when compared to the wild type. The primary root of the *pls* mutant was found to be 50 % shorter than the wild type, and microscopic studies revealed that the cells of the root meristem and cortex of the primary root were shorter and more radially

expanded. Longitudinal cell expansion and increased radial expansion could potentially be related to auxin, ethylene or cytokinin signalling defects (Casson *et al*., 2002) (Figure 1.11).

It is known that enhanced ethylene responses reduce axial growth in light-grown seedlings (Guzman and Ecker, 1990, Kieber *et al*., 1993) and could potentially contribute to the short-root phenotype of the *pls* mutant. When *pls* seedlings are grown in the dark, they exhibited an abnormal etiolation response, typical of ethylene effect on seedlings. *pls* seedlings were found to exhibit a triple response phenotype when grown in air, similar but less severe than that of the ethylene -overproducing *eto1* or the constitutive response mutant *ctr1-1* (Figure 1.12) (Chilley *et al*., 2006). The enhanced ethylene response in *pls* was confirmed by measuring the abundance of the ethylene inducible transcript, *AtGSTF2* (Smith et al., 2003) by RNA gel blot analysis and was found to be greater in air-grown *pls* compared to the wild type. Similarly, the expression of the primary ethylene response gene *ERF10*, was increased in air-grown *pls* seedlings (Figure 1.11) (Chilley *et al*., 2006).

This short-root phenotype was rescued by genetic or pharmacological inhibition of ethylene signalling: here, *pls* seedlings were either crossed with the gain-of-function ethylene insensitive receptor mutant *etr1-1* or treated with silver ions (1 µM) to inhibit ethylene signalling (Figure 1.13). These data show that *pls* mutant exhibits enhanced ethylene responses and this determines the short-root phenotype, indicating that PLS acts as a negative regulator of ethylene responses. The failure of *pls* mutation to suppress the *etr1-1* mutation suggested that PLS may act at or upstream of the ETR1 receptor (Chilley *et al*., 2006).

To determine whether these enhanced ethylene responses of *pls* is attributable to increased ethylene biosynthesis, the level of ethylene production was measured using gas chromatography. These experiments revealed no significant difference in ethylene production between *pls* mutants and wild type seedlings (Figure 1.14). Also, *pls* seedlings did not exhibit increased sensitivity to ethylene or its precursor, ACC (1-aminocyclopropane-1-carboxylic acid) (Casson *et al*., 2002).

## 1.7.1: *pls* is defective in ethylene signalling

In another experiment, a transgenic *PLS* overexpresser was crossed with the *ctr1-1* mutant, to find the point of PLS action in the ethylene signalling pathway. The *PLSOx*/*ctr1*

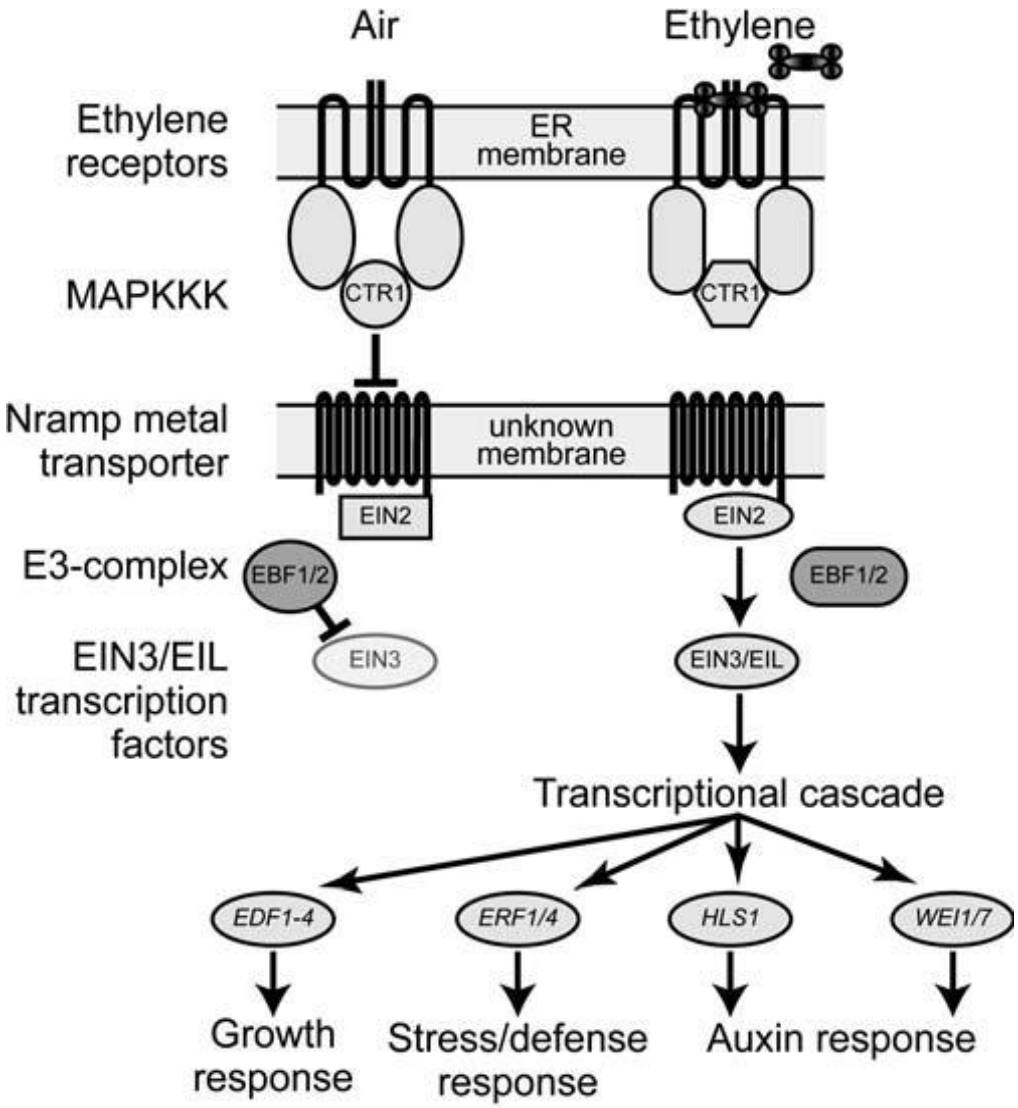


**Figure 1.11: A model of the ethylene signal transduction pathway in Arabidopsis.**
In the absence of ethylene, the receptors activate CTR1, a negative regulator that suppresses downstream signalling. CTR1 is related to the MAPKKKs, but it is unclear whether CTR1 functions as the first step in a MAP kinase cascade. Downstream of CTR1, EIN3 levels are reduced by proteasome-mediated degradation, involving action of the E3 complex components EBF1 and EBF2. Perception of ethylene results in the inactivation of CTR1 and prevents EIN3 degradation, thus activating the ethylene-signalling pathway. Activation of the EIN3/EIL family of transcription factors induces a transcriptional cascade to establish ethylene responses. (Adapted from Etheridge *et al*., 2006)

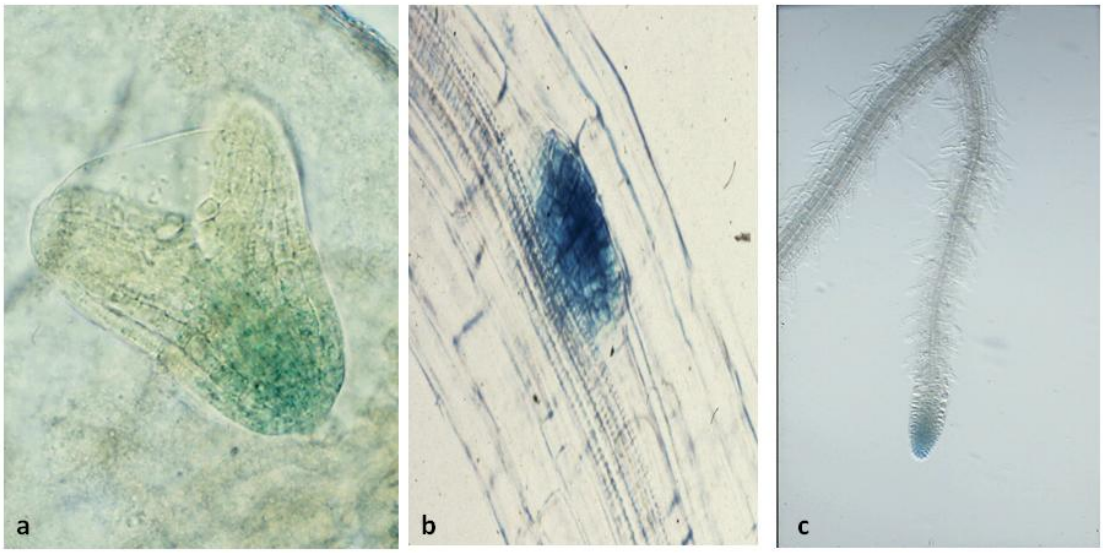


**Figure 1.12: PLS: GUS expression in (a) heart stage embryo (b)lateral root primodia (c) lateral root (Topping and Lindsey, 1997)**

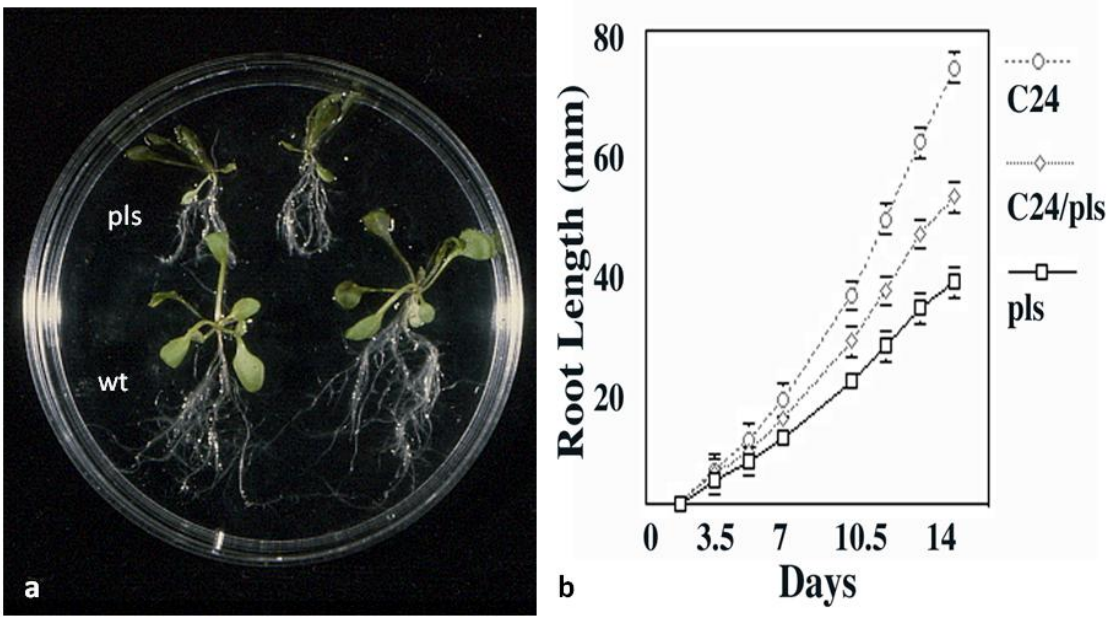


**Figure 1.13: (a) Short root phenotype of the *pls* mutant as compared to wild-type, (b) Primary root growth of wt C24, *pls* mutant and C24/*pls***

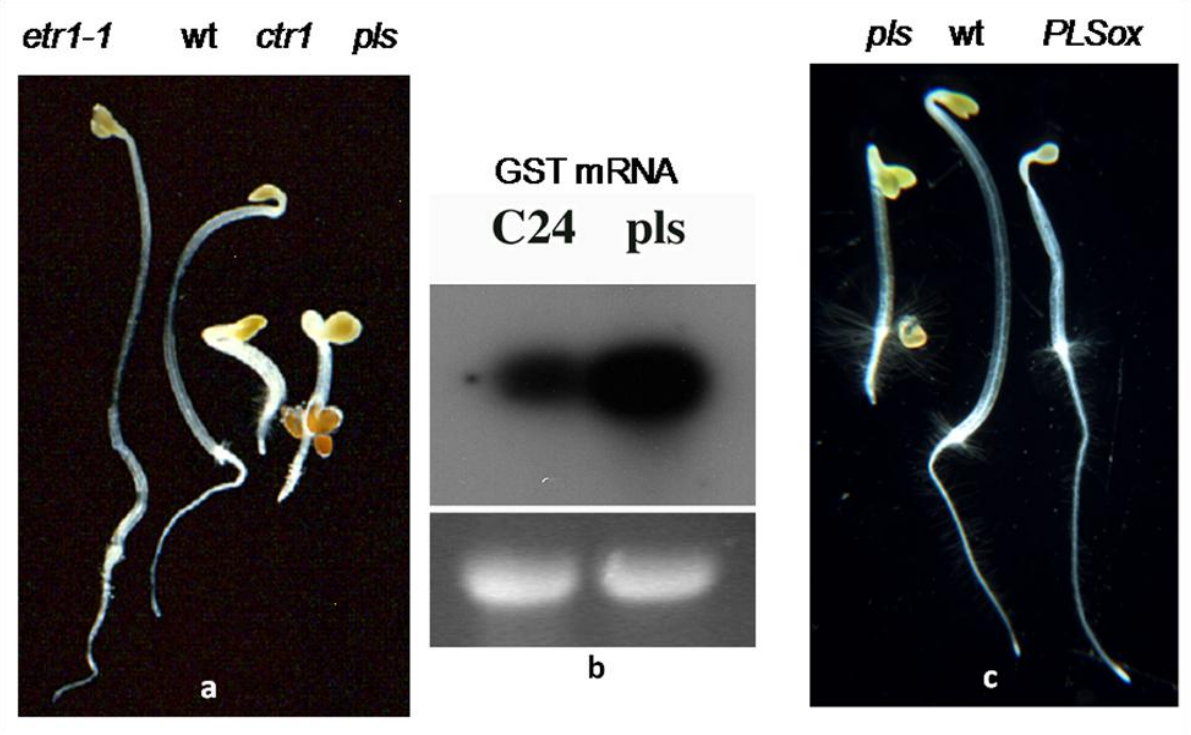


**Figure 1.14: (a) *pls* mutant showing triple response similar to *ctr1*, (b) *pls* is unregulated in ethylene responsive gene; (c) triple response phenotype is rescued in *PLS*ox**

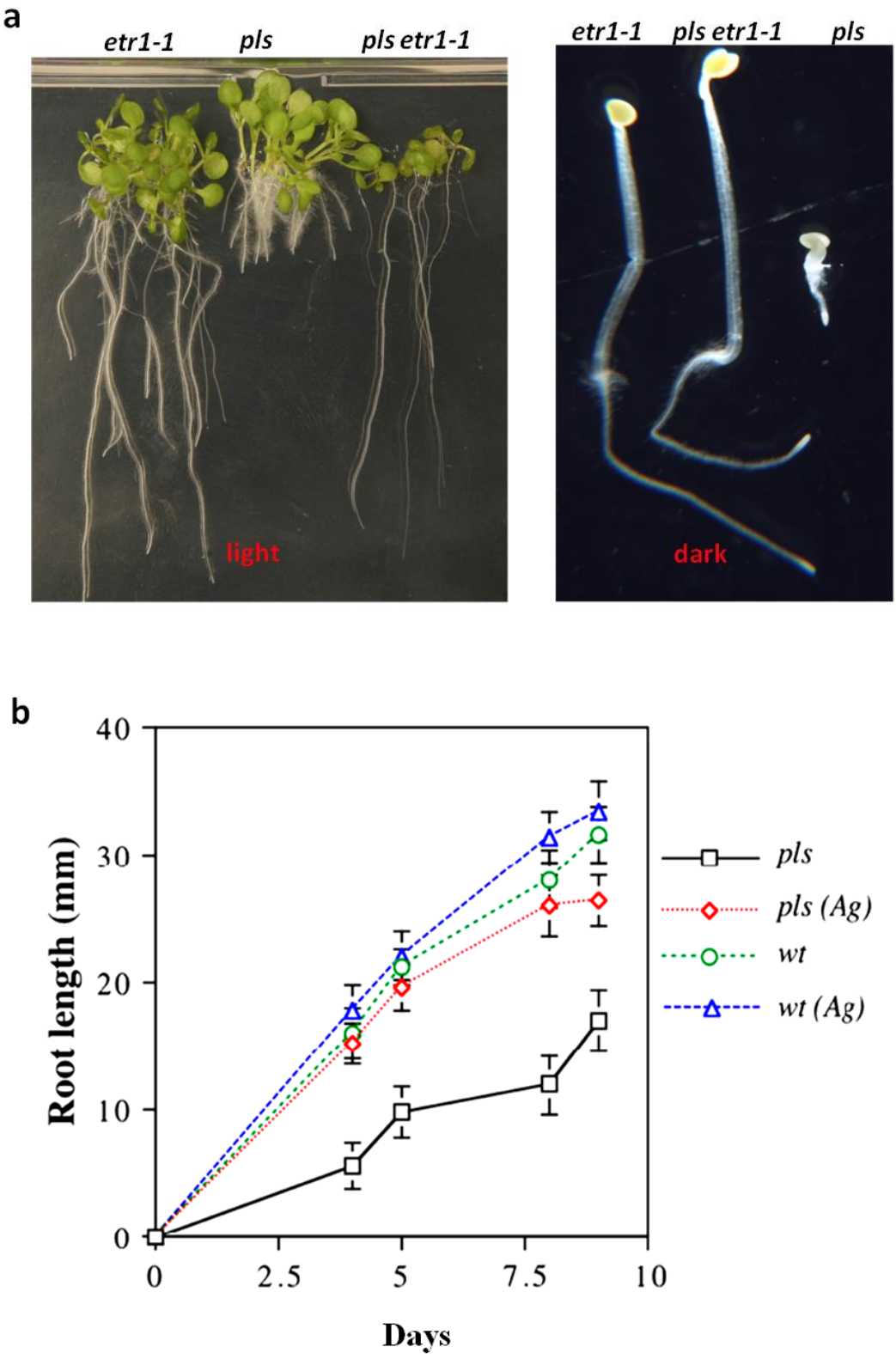


**Figure 1.15: (a) Rescue of *pls* root growth by inhibition of ethylene action, either by either genetic methods ie by crossing with *etr1-1* (a), or by pharmacological methods (silver treatment, b)**

mutants showed an intermediate phenotype (i.e., longer roots in both light and dark grown seedlings than *ctr1* but much shorter than *PLSOx*). These findings suggested that *ctr1* partially suppresses *PLSOx*.

Moreover, the roots of PLSOx/*ctr1* seedlings grown in dark were approximately 50% shorter than those of PLSOx seedling grown on 100 µM ACC, suggesting that CTR1 acts downstream of PLS. These data suggested that PLS and CTR1 may interact to modulate root growth in response to ethylene, but not necessarily in a single linear pathway. It was pointed out the PLS may act at one or more places in the ethylene signalling pathway to modulate root growth (Chilley *et al*., 2006).

## 1.7.2: Auxin transport and accumulation in *pls*

Ethylene is known to inhibit auxin transport in stems (Suttle, 1988). Therefore, the enhanced ethylene signalling in *pls* could cause reduced auxin responses (Casson *et al*., 2002). The free IAA content of *pls* was measured to determine auxin level in the root tip of *pls* as compared to the wild type, and was found to be significantly lower than in wild-type (Figure 1.16). Free IAA concentrations were also found to be 70% lower in *pls* seedlings as compared to wild type, whereas PLSOx had higher free IAA concentration than the *pls* mutant suggesting a link between PLS and auxin accumulation.

To determine whether the low auxin levels in *pls* are attributable to defective transport from the shoot, the auxin transport in term of [$^3$H] IAA was measured in isolated stem tissue. The *pls* mutant had much reduced auxin transport level as compared to wild type (approximately 24 % of the level of wild type) (Figure 1.15). Therefore, it was concluded that the *PLS* gene is required for correct auxin transport, accumulation and root growth (Chilley *et al*., 2006). The auxin transport level in the double mutant between *pls* and *etr1-1* was also measured to investigate the role of ethylene signalling in auxin transport and accumulation. It was found that in these double mutants the auxin transport levels were greatly rescued (~85 % of the wild type levels). Moreover, the number of lateral roots was restored to ~ 80 % of wild-type in the double mutant (Chilley *et al*., 2006).

Together, these data indicate that the low-auxin phenotype and reduced polar auxin transport and reduced numbers of the lateral roots of *pls* can be restored to approximately wild-type levels in a double mutant with ethylene-resistant *etr1-1.* This suggests that the enhanced ethylene signalling phenotype of *pls* is most likely responsible for the repression of auxin synthesis and transport (Figure 1.17). This indicates that ethylene can have an

inhibitory effect on auxin synthesis, transport, and biological function and that PLS is a new molecular component of this signalling interaction (Chilley *et al*., 2006).

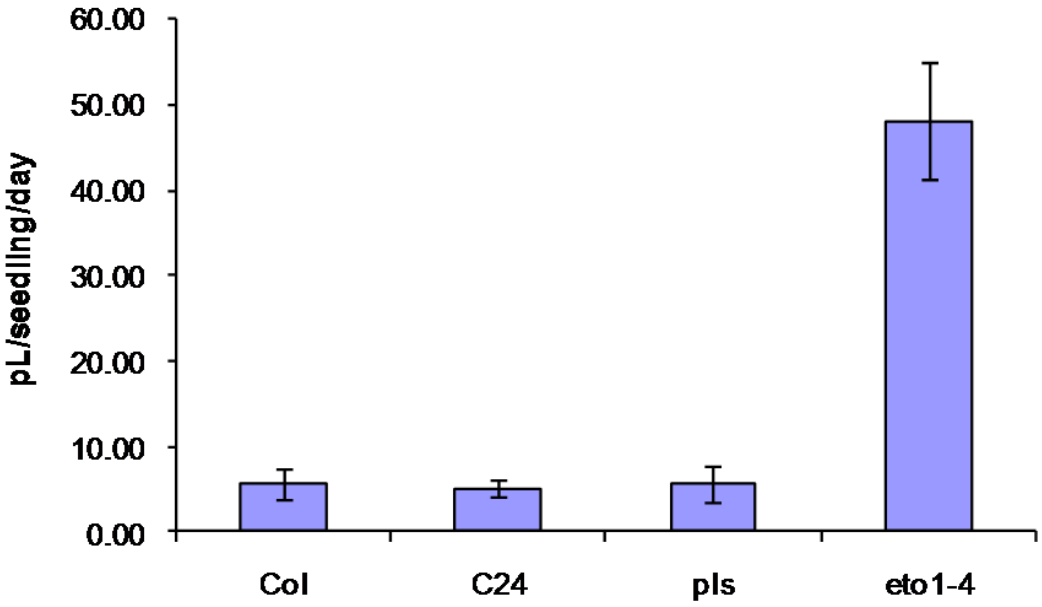


**Figure 1.16: Ethylene production in *pls* , eto1, wild-types Col and C24**

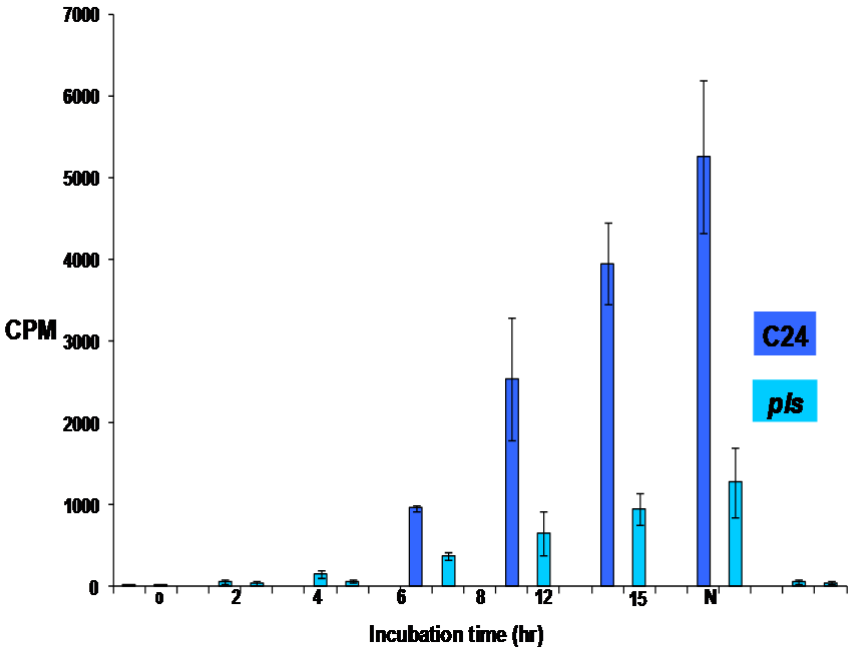


**Figure 1.17: Polar auxin transport activity in C24 and *pls***

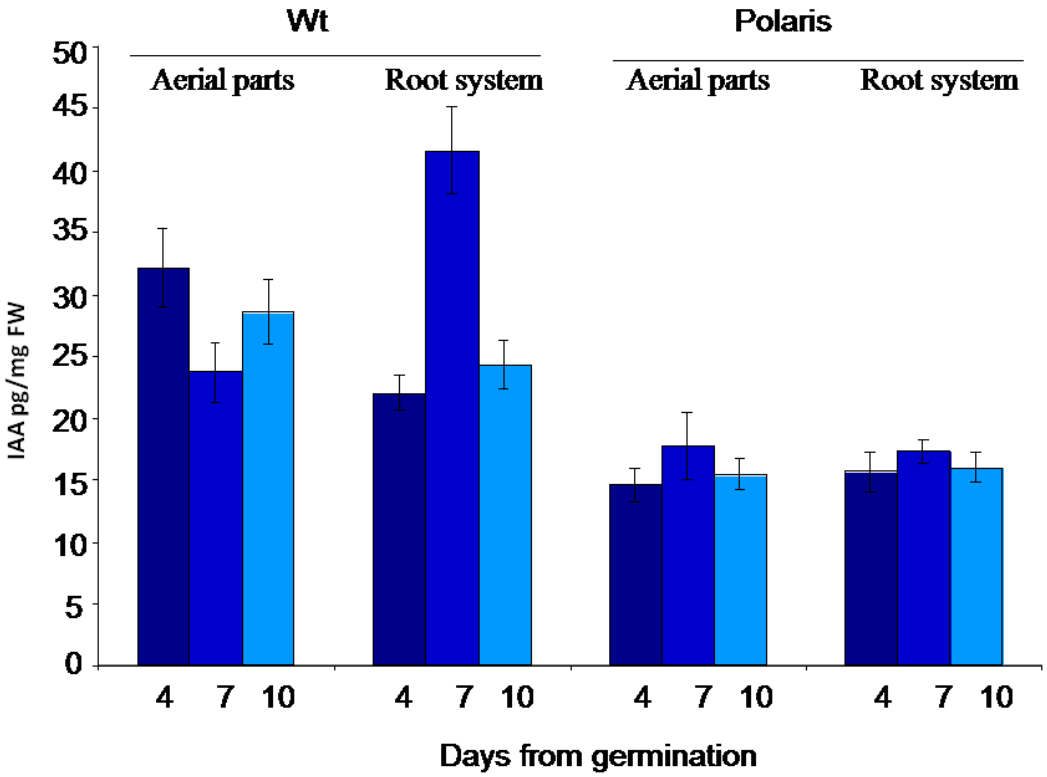


**Figure 1.18: *pls* mutants shows reduced IAA content as compared to Wt**

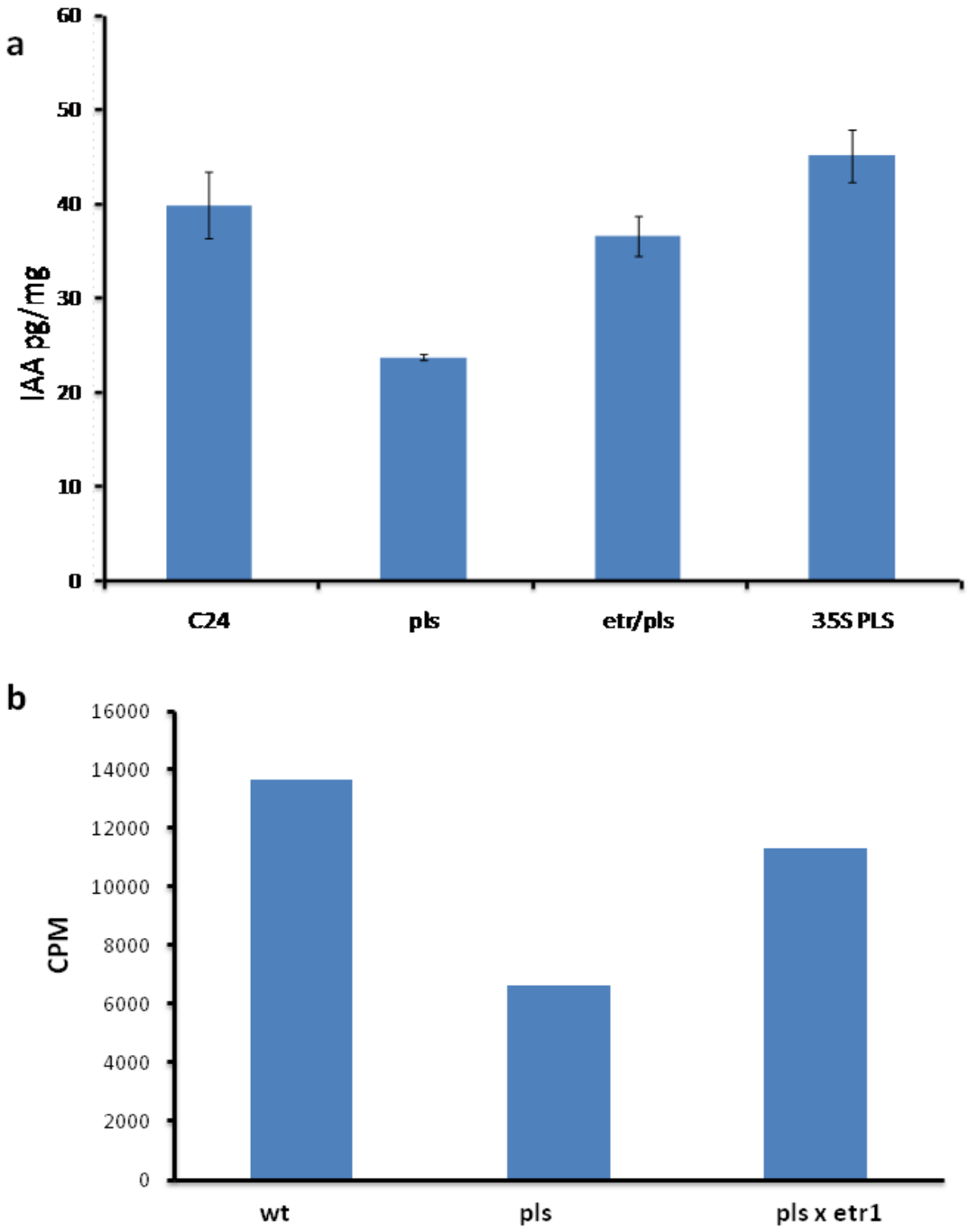


**Figure 1.19: Reduced ethylene signalling (*pls/etr1* mutant) rescues (a) free IAA content and (b) polar auxin transport**

## 1.7.3: A Model for PLS function in root development

Chilley *et al*. (2006) proposed a model to explain the role of PLS in root development specifically in root growth (elongation) and lateral root formation. According to this model, *PLS* transcription is activated at the root tip by the relatively high auxin concentration that accumulates and is required for correct cell division at that position (Friml *et al*., 2002; Blilou *et al*., 2005). Here, PLS acts as a negative regulator of ethylene signalling, which is inhibitory to cell division and expansion, and therefore affects root growth (Souter *et al*., 2004). This model explains the suppression of the inductive effects of auxin and cytokinin on ethylene biosynthesis at the root tip (Vogel *et al*., 1998).

Mechanical stress in the soil that can induce relatively high levels of ethylene synthesis/signalling could produce thicker and potentially mechanically stronger roots to allow better soil penetration. *PLS* expression would also suppress the ethylene-mediated inhibition of auxin transport in the root tip, again ensuring correct auxin signalling for cell division and patterning. PLS is also required for correct lateral root initiation, presumably via ethylene-mediated control of auxin transport to the pericycle.

The model concludes that PLS is an essential component in the regulation of auxin homeostasis and root growth by restricting ethylene signalling. It also shows that one downstream component of the cellular machinery that transduces these hormonal signals in the modulation of cell division and expansion at the root tip is the microtubule cytoskeleton. This model further suggests a number of experiments for the elucidation of the roles of auxin and ethylene interaction at the root tip.

## 1.8: Aims and objectives

The project aims to study the molecular mode of action of PLS and its role in the ethylene and auxin signalling pathway to regulate root growth and development in Arabidopsis. The major objectives of this project are:

1) **Characterisation of root patterning by generating pls mutant root cell marker lines and PLS sub-cellular localisation.** This involved generating *pls* mutants root cell marker lines. Five different root cell GFP marker lines: Q12::GFP, Q6::GFP (Quiescent centre marker lines), *SCR::GFP* (*SCARECROW* ::GFP lines) and two Hasseloff lines J1092 and J2341 were used to study any abnormalities in cellular patterning in the *pls* mutant and in *PLSOx.* Also, in order to determine the

subcellular localisation of the PLs peptide, a GFP::*proPLS:PLS* translational fusion has been generated.

2) **Study of the auxin responses in the *pls* mutant.** To investigate the auxin distribution in the *pls* mutant, *DR5::GFP* fusion construct has been generated. Detailed study of gravitropic response of *pls* mutant and other ethylene signalling mutant was carried out. Also, the expression of PIN1::GFP and PIN2::GFP in *pls* mutant backgrounds was analysed to find answers for the defective auxin accumulation and transport.
3) **Genetic and molecular studies to investigate the role of PLS in ethylene signalling.** This involved study of the expression of major ethylene signalling genes (ETR1, ERS1, EIN2, EIN3, CTR1 and HSL1) in *pls* and *PLSOx* using real time PCR and semi-quantitative PCR. The direct interaction of PLS with the ethylene receptor ETR1 was analysed using Yeast two hybrid and BiFC assays.
4) **Analyse the cross-talk between PLS, ethylene and auxin.** To examine the effect of ethylene on auxin synthesis, the WEI2 expression pattern in *pls* mutant backgrounds were studied using real time PCR.

Overall, the project intends to enhance our understanding of the crosstalk between ethylene, auxin and PLS to control root growth and development in Arabidopsis.

# Chapter 2:

# Materials and Methods

This chapter presents an ordered account of all the materials and procedures used to obtain the results discussed in the following chapters.

## 2.1: Materials

### 2.1.1: Chemicals

All the chemicals used in the following experiments were analytical grade reagents. All the chemicals were obtained from Sigma-Aldrich (Poole,UK), Fisher Scientific Ltd (Loughborough, UK) and BDH (Lutterworth, UK) unless otherwise stated. X-Gluc and IPTG were obtained from Melford Laboratories Ltd (Suffolk,UK), and X-Gal from Bioline (London, UK)

### 2.1.2: Enzymes

Restriction endonucleases, T4 DNA ligase, RNase-free DNase , MMLV reverse transcriptase, RNasin ribonuclease inhibitor and polynucleotide kinase were obtained form Promega Ltd. (Southampton, UK). The Expand High Fidelity PCR system and Proteinase K were from Boehringer Mannheim (Lewes, UK). Shrimp alkaline phosphatase was obtained from Sigma Chemical Company Ltd. *Taq* DNA polymerase was from Bioline.

### 2.1.3: Kits and Reagents

The Wizard$^{TM}$ Plus SV Minpreps DNA purification system was from Promega (Southampton, UK). The *High Pure* PCR Product purification kit was from Roche (Mannheim, Germany). The TOPO-TA cloning kit was from Invitrogen (Paisley, UK). The RNeasy Plant RNA extraction kit and the QIAGEN® Plasmid Midi Kit were from Qiagen Ltd (Surrey, UK).

Oligodeoxynucleotide primers used in PCR reactions were obtained from MWG-Biotech (Ebersberg, Germany).

### 2.1.4: Bacterial Strains

The *E.coli* strain XL1-Blue MRF' (Jerpseth, 1992) was used to prepare competent cells, and as a plasmid host.
The TOP-10 *E.coli* strain used as a host for pCR2.1-TOPO was supplied as a part of the TOPO-TA cloning kit.

*Agrobacterium tumefaciens* LBA4404 (Ooms *et al.*, 1982; Hoekema *et al*., 1983) and C58C3 (Dale *et al*., 1989) were used for plant transformations. Both strains have been disabled so that they do not cause crown-gall disease but they still have the virulence factors required for T-DNA transfer and insertion into plant genomic DNA.

LBA4404 has a rifampicin (Rf) resistance marker located chromosomally allowing selection with the presence of 100 µg/ml rifampicin.

C58C3 carries a chromosomal streptomycin resistance marker, allowing antibiotic selection using 100 µg/ml streptomycin.

## 2.1.5: Plasmids

The following plasmids were used during this project: pCR®2.1 TOPO (Invitrogen), pBIN19 (Bevan, 1984), pCIRCE (a derivative of pBIN19, Bevan 1998), pRK2013 (Ditta *et al*., 1980) and pDH51 (Pietrzak M. *et al*., 1986). The pCR®2.1 TOPO is used for cloning DNA fragments generated by PCR. pRK2013 provides mobilisation. pDH51 contains the CaMV 35S promoter and terminator and was used in the overexpression of the *POLARIS* transcript. pBIN19 and pCIRCE are wide range binary cloning vectors for *Agrobacterium* – mediated gene transfer into plant cells.

## 2.1.6: Culture media

All the culture media were sterilised by autoclaving at 121°C for 20 minutes.

## 2.1.6.1: Bacterial culture media

**Luria-Bertani (LB) medium:** 10 g/litre tryptone or peptone, 5 g / litre yeast extract, 10 g NaCl and pH adjusted to 7.2 using 0.1M NaOH (Ausubel *et al*., 1997)

**LB agar:** 15 g bacto-agar to a litre of LB prior to autoclaving.

All the antibiotics and reagents were added after cooling the media to 40-50 °C in a water bath.

The following antibiotics and reagents were used at different stages of this project:

| Antibiotic / Reagent | Stock solution concentration | Working concentration | Storage temperature |
|---|---|---|---|
| Ampicillin | 25 mg/ml in water | 35 - 50 µg/ml | -20 °C |
| Kanamycin | 25 mg/ml in water | 50 µg/ml | -20 °C |
| Chloramphenicol | 34 mg/ml in ethanol | 10 µg/ml | -20 °C |
| Tetracycline | 12.5 mg/ml in 50% ethanol | 12.5-15.0 µg/ml | -20 °C |
| Carbenicillin | 5 mg/ml in water | 50-100 µg/ml | -20 °C |
| Gentamycin | 10-50 mg in water | 10 -50 µg/ml | -20 °C |
| Streptomycin | 20 mg/ml in water | 25 µg/ml | -20 °C |
| Rifampicin | 20 mg/ml in methanol | 100 µg/ml | -20 °C |
| X- Gal | 40 mg/ml in Dimethylformamide | 40 µl/100 mm agar plate | -20 °C |
| IPTG | 100 mM in water | 10 µl/100 mm agar plate | -20 °C |
| Nalidixic acid | 5 mg/ml in 70% ethanol | 25 mg/l | -20 °C |

**Table 2.1: Antibiotic and selection reagents usage for resistant *E.coli* cells**

**SOC medium:** 20 g/l Tryptone, 5 g/l Yeast extract, 5.84 g/l NaCl, 10 mM $MgCl_2$, 10 mM $MgSO_4$, 2 g/l glucose and pH adjusted to 6.8 -7.0 using 1 M KOH/HCl. $MgCl_2$, $MgSO_4$ and glucose were added after autoclaving**.**

**Glycerol stock:** Aliquots from fresh overnight cultures of bacterial strains were combined with an equal volume of sterile 50% glycerol in Eppendorf tubes, and stored either at -20 °C for short-term use, or flash-frozen in liquid nitrogen and kept at -80 °C for long term storage.

## 2.1.6.2: Yeast culture media

**YPAD agar and broth (per litre):** 20 g peptone, 10 g yeast extract and 15-20 g agar. Deionised $H_2O$ was added to a final volume of 960 ml and pH adjusted to 5.8. 40 mg of adenine sulphate was added to the medium to reduce the reversion rate of the *ade2-101* mutation, thereby reducing the amount of reddish pigments in the yeast colonies. 40 ml of 50% glucose solution was added to media after cooling to 55 ° C.

**SD agar and broth (per litre):** 6.7g Difco yeast nitrogen base without amino acids (Difco catalog no. 0919-15-3), 182.2 g D-sorbitol, 15-20 g agar. Deionised $H_2O$ was added to make the final volume of 860 ml and pH adjusted to 5.8. 100 ml of the appropriate 10x dropout solution and 40 ml of a 50% glucose solution was added to the medium after cooling to 40-50°C. For making SD broth agar is omitted from this recipe.

**Amino acid dropout solution:** 10x dropout solutions were prepared by simply omitting the amino acid required for selection (for example, L-histidine HCl monohydrate was omitted for selection of interacting proteins). A detailed account of the type of selection used in this work is provided under the Yeast Two Hybrid section (Section 2.14). All the dropout solutions were sterilised by autoclaving at 121°C for 20 minutes. After sterilisation, the 10x dropout solutions were stored in 100 ml aliquots at 4°C.

| Component | Weight ( mg/ L ) | Sigma Catalog No. |
|---|---|---|
| L-Isoleucine | 300 | I 2752 |
| L-Valine | 1500 | V 0500 |
| L-Adenine hemisulphate salt | 200 | A 9126 |
| L-Arginine HCl | 200 | A 5131 |
| L-Histidine HCl monohydrate | 200 | H 8125 |
| L-Leucine | 1000 | L 8000 |
| L-Lysine HCl | 300 | L 5626 |
| L- Methionine | 200 | M 9625 |
| L-Phenylalanine | 500 | P 2126 |
| L-Threonine | 2000 | T 8625 |
| L- Tryptophan | 200 | T 0254 |
| L- Tyrosine | 300 | T 3754 |
| L- Uracil | 200 | U 0750 |
| L- Glutamic acid | 1000 | G 1251 |
| L- Aspartic acid | 1000 | A 9256 |
| L- Serine | 4000 | S 4500 |

**Table 2.2: Components of 10x amino acid dropout solutions**

## 2.1.6.3: Plant culture media

**½ MS10 medium (Germination medium) per litre:** 2.2 g half strength Murashige and Skoog medium (Sigma M5519), 10 g sucrose, 2 g phytogel**,** pH 5.7 adjusted with 1M KOH and autoclaved (121 ° C, 20 min)

**MS30 (per litre):** 4.4 g Murashige and Skoog medium (Sigma M5519), 30 g sucrose, 8 g agar. pH was adjusted to 5.8 using 1M KOH and autoclaved (121°C, 20 min)

**Shooting medium 1:** 1 mg/L BAP (6-benzylamino-purine, 10 mM stock solution) was added to the molten MS30 after cooling it to 50-60 ° C.

**Shooting medium 2:** 1 mg/L of BAP, 100 mg/L of kanamycin sulphate and 200 mg/L of cefotaxime (100 mg/ml stock solution in water) were added to molten MS30 after cooling it to 50-60 ° C.

**Rooting medium:** 200 mg/L of cefotaxime and 100 mg/L of kanamycin sulphate were added to molten MS30 after cooling to 50-60 ° C.

## 2.1.7: Plant materials

*Arabidopsis thaliana* var. C24 and Columbia (Col-0) were kindly supplied by Prof. Keith Lindsey (Durham University), as were seeds from the promoter trap line AtEM101 (C24 background) and *etr1*, *ctr1*, *eto1* mutant lines. SCR::GFP (NASC ID – N3999, donated by Philip Benfey), J1092 (NASC ID – N9147 - donated by Jim Haseloff) and J2341 (NASC ID – N9118 – donated by Dr. Jim Haseloff) were purchased from NASC (The Nottingham Arabidopsis Stock Centre). Q12::GFP and Q6::GFP quiescent centre markers were supplied by Prof Philip Benfey – Duke Institute of Genome Sciences).

Seeds were germinated and grown for 2-3 weeks in deep 9 cm Falcon® Petri dishes (Becton and Dickinson, Loughborough UK). Transformed seedlings were grown initially in 60 ml Polypots (Northern Media, Loughborough UK). Older seedlings were transferred to larger (250-500 ml) vessels. Magenta boxes (Sigma) were used for growing tobacco seedlings (SR1 variety; seeds provided by Prof. Keith Lindsey, Durham University).

Good ventilation was maintained by sealing the Petri dishes with Micropore$^{TM}$ medical tape (Industricare Ltd., Leicestershire UK).

## 2.2: Plant tissue culture

This section describes the plant tissue culture procedures and growth conditions used during the course of this project:

### 2.2.1: Seed sterilisation

Surface-sterilisation of seeds is necessary for germination on nutrient rich medium to prevent contamination by fungi or bacteria. Sterilisation was carried out in a laminar flow cabinet, and solutions were transferred using a fresh sterile transfer pipette for each seed sample. Aliquots of seeds were placed in Eppendorf tubes and treated with 70% v/v ethanol for 30-60 seconds to partially de-wax the testa. Seeds were then immersed for 20 minutes in 10% v/v commercial bleach solution with a drop of Tween 20 detergent to enhance wetting and penetration. The seeds were then washed thoroughly in 4-6 changes of sterile distilled water before being plated onto germination medium (½ MS10).

All the washings were collected and filtered through paper towels to remove stray seeds, for autoclaving and disposal.

### 2.2.2 Plant growth conditions

#### 2.2.2.1: Soil based greenhouse culture

*Arabidopsis* plants used for genetic crosses, segregation of mutant lines and bulking of seeds, were grown in a 5:1 mixture of Gem multipurpose compost and horticultural silver sand (both from LBS Horticulture Ltd., Lancashire UK) to ensure adequate drainage. Seeds were sown in small pots and pre-chilled at 4 °C for three days to break dormancy, before transfer to standard growing conditions (22 °C, 16 hours light: 6 hours dark). Germination seedlings were transferred at 5-10 days after emergence (dae) into 24-well standard tray inserts (LBS Horticulture Ltd., Lancashire UK) containing the standard compost-sand mixture, placed on damp capillary matting. Plants were watered from above using a fine nozzle water dispenser. Separate pools of seeds from individual plants were obtained using the Aracon system (BetaTech, Belgium).

All compost was treated as standard with “Intercept” systemic insecticide (Levinton Horticulture Ltd., UK), at a concentration of 64 mg/24- well tray. The mite *Amblyseius*

*cucumeris* (Syngenta, UK) was introduced every 6 weeks onto the aerial parts of the plant as a biological control against thrips.

### 2.2.2.2: Culture under sterile conditions

Seedlings for analysis were grown in sterile Petri dishes using ½ MS10 media, with plate margins sealed using Micropore$^{TM}$ tape. Prior to germination, seeds were stratified for 3-4 days in the dark at 4°C to promote and synchronise germination. Plates were then transferred to a growth chamber at 22 ± 2 °C set at 'long days' (16 hours light: 6 hours dark). 'Dark-grown' plates were treated exactly as those in the light, except that Petri dishes were wrapped in aluminium foil prior to placement in the growth chamber.

## 2.2.3: Mobilisation of plasmids into *Agrobacterium* by triparental mating

**Preparation**

Two days before the triparental mating, 10 ml of LB broth was set up with 100 µg/ml rifampicin for LBA4404 culture and with 100 µg/ml streptomycin for C58C3 culture. The cultures were left to grow for 48 hours at 30 °C with constant shaking. The day before the mating, overnight cultures of pRK2013 and of the *E.coli* strain containing the construct to be transformed into either tobacco or *Arabidopsis* were each set up in 10 ml LB broth plus 100 mg/ml kanamycin sulphate to grow at 37 °C, with constant shaking.

**Method**

For triparental mating, 100 µl aliquots from each 10 ml culture were mixed together in a sterile 1.5 ml Eppendorf tube. The remaining liquid cultures were stored at 4°C for future use. The cells were then spun down in a microcentrifuge at 12, 000 rpm for 5 minutes. Supernatants were discarded and the pellets were resuspended in 10 µl of 10 mM $MgSO_4$. The 10 µl droplets were placed onto LB agar plates and incubated overnight at 28-30°C. During this time mobilisation of the plasmids takes place. A patch of the bacterial droplets was streaked on an LB plate containing 100 µg/ml kanamycin sulphate and 100 µg/ml for LBA4404, and 100 µg/ml of streptomycin for C58C3. The plates were then incubated at 28-30°C overnight. The parental strains were streaked on duplicate plates, as a control.

## 2.2.4: Arabidopsis transformation using the floral dipping method. After Clough and Bent (1998).

**Solution and media**

5% sucrose (w/v) and 0.05% Silwett L-77 (v/v) (Lehle Seeds, Texas, USA), which acts as a detergent

½ MS10 plates supplemented with 35 mg/l kanamycin sulphate (pBin19 and pCIRCE based constructs) and 850 mg/l vancomycin was added to kill the residual Agrobacteria.

**Preparation**

*Arabidopsis thaliana* var. C24 was grown in soil in 3.5'' pots (10-15 plants per pot) with a plastic mesh placed over the soil. Plants were grown for 3-4 weeks until they are 10-15 cm tall and displaying a number of immature, unopened buds. 2-3 days prior to dipping, open flowers and any young siliques were removed.

The *Agrobacterium tumefaciens* strain C58C3 was used for all binary vector constructs. The Agrobacteria were grown for 48 hours at 30 °C in 200 ml LB supplemented with 25 mg/l nalidixic acid, 100 mg/l streptomycin and 50 mg/l kanamycin sulphate. The culture was pelleted by centrifugation and resuspended in 1 litre of freshly made solution of 5% sucrose. Once resuspended, Silwett L-77 was added to final concentration of 0.05% (v/v).

**Method**

Plants were then fully dipped into the solution and gently agitated for 10-15 seconds before removal. Dipped plants were placed in transparent bags to maintain humidity and placed back in the greenhouse in a shaded place overnight. Occasionally a second dipping was carried out 6 days after the first. Following removal from the bags plants were allowed to set seeds and dry out in the greenhouse. Seeds were collected from individual pots of plants and allowed to dry for 2 weeks at 25 °C. Seeds were then surface sterilised and germinated on ½ MS10 with antibiotic selection. Antibiotic-resistant plants were transferred to soil and seeds from these plants were tested for segregation of the resistanc trait on selective plates.

## 2.2.5 Tobacco transformation using the leaf explant method

Adapted from 'Methods in Molecular Biology', Vol. 81, Plant Virology Protocols (Foster G. D and Taylor S.C., 1998)

This is the most efficient and technically most simple method of transforming tobacco where the leaf explants are infected with disarmed strain of naturally occurring soil-borne bacterium *Agrobacterium tumefaciens*, which contains a disabled (nononcogenic) Ti plasmid. The gene construct (PLS: 35S) to be transferred was integrated between the T-DNA borders of a binary vector (pCIRCE) which was introduced into the *Agrobacterium*. This method was specifically designed for *Nicotiana tabacum* cv.Petit Havana SR1(commonly abbreviated to SR1).

**Method**

SR1 tobacco seeds were surface sterilised (using the method mentioned in 2.2.1) and grown on MS30 plates until they are 2-3 weeks old, when they are big enough to be transferred into Magenta pots. The plants are grown for 4-5 weeks, until they have shoots with fully expanded leaves. These fully expanded leaves are cut from the parent plant and were placed on a sterile Petri dish in laminar flow cabinet (sterile environment). The leaf midrib and the leaf edge were removed using sterile scapel. The lamina is then cut into 1 $cm^2$ pieces and 5-6 explants were placed adaxial-side up on a plate of shooting medium 1 (see section 2.1.6.3). 20-30 leaf explants were prepared for each construct; the plates were sealed with Micropore$^{TM}$ tape and incubated for 2 days under constant light at 22 °C.

On the day before the inoculation, 75 ml of LB broth culture of strain LBA4404 harbouring the DNA construct was set up from a fresh overnight culture. Both 100 mg/l kanamycin sulphate and rifampicin were added to the LB broth and incubated overnight at 28-30°C, with constant shaking (200 rpm). The optical density of the LB broth was measured at 600 nm to an $OD_{600}$ of 1.0 and was then poured into a sterile beaker. The leaf explants were removed from the plate using a sterile forceps and were immersed in the bacterial suspension. The leaves were left in for a minute and mixed by swirling. The explants were removed and blotted dry on a piece of sterile filter paper. The explants were then replaced on the same shooting medium plates and were incubated as before for 2 days. After 2 days, the explants are transferred to the shooting medium 2 (see section 2.1.6.3) and were returned back to the growth room for another two days. The first regenerating shoots were visible after 3-4 weeks.

When the shoots were big enough to handle (approx. 1 cm in length) they were removed from the explants and were transferred to the rooting medium in Magenta pots. Only single and well separated shoots were removed from each explant, to avoid propagation of genetic clones. The pots were returned to the growth room and were grown there until the roots appear in 2-3 weeks, at this stage the plants were transferred directly to compost and further grown there until ready to harvest.

### 2.2.6: Genetic crosses

Genetic crosses between Arabidopsis plants were made under the Zeiss STEMI SV8 dissecting stereomicroscope (Carl Zeiss Ltd., Welwyn Garden City, Herts, UK). Flowers were selected on the basis of age; examples were chosen for relative maturity of the stigma prior to dehiscence of pollen from the anther, and all other siliques and unsuitable flowers were removed from the stem. Young flowers were emasculated using fine watchmaker forceps (BDH, UK) to gently remove immature anthers, and then mature pollen from the male parent was transferred manually to the stigma, again with forceps. The stem below the crossed flower was labelled, and the plants were returned to the greenhouse for siliques development. Siliques were harvested upon maturity, but prior to senescence and pod shatter.

## 2.3: Screening

### 2.3.1: Screening for mutant seedlings

The *pls* mutation is semi-dominant in nature, which means for the null *pls* phenotype the mutant must be homozygous. Therefore, all the *pls* mutants or crosses were genotyped for the homozygous *pls*. This was done by extraction the genomic DNA from the mutant leaves using a quick genomic DNA extraction method (Edward *et al*., 1991) followed by a standard PCR using the following primers:

POL-RT: GAA AAT GAT AGG GTG ATC AAT GG

BIN19-Tail: GGA GTC CAC GTT CTT TAA TAG TG

Pol5'- Test:GGA GAC TAA AGC GAA AAC ATA TAA AAC C

Two set of PCR reaction were performed, PCR-1 with BIN19-Tail and Pol5'-Test giving a product of 760 base pairs (bp) containing the T-DNA insertion and, PCR-2 with POL-RT and Pol5'-Test generating a product of 430 bp. Mutants were screened using the results from the two PCR reactions, explained in the following table:

| Lines | BIN19-Tail+Pol5'-Test<br>PCR-1, Product ≈ 760 bp | POL-RT+ Pol5'-Test<br>PCR-2, Product ≈ 430 bp |
|---|---|---|
| Homozygous | Product | No Product |
| Heterozygous | Product | Product |
| Wild type | No Product | Product |

**Table 2.3: Illustration of genotyping results for screening *pls* homozygous mutant**

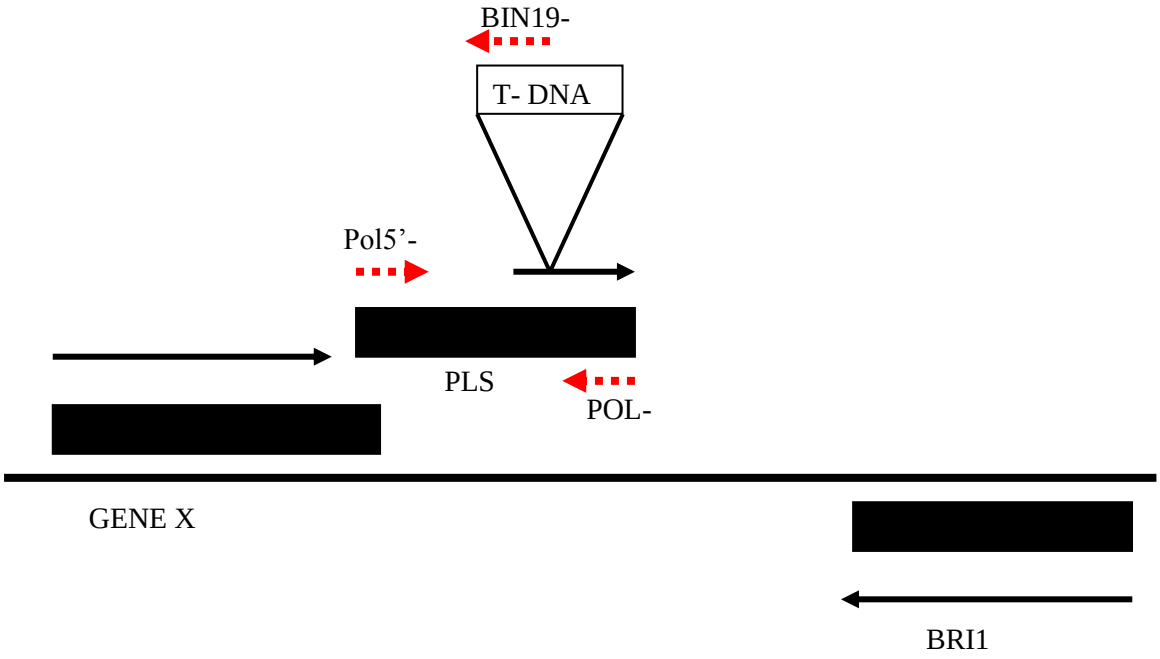


**Figure 2.4: *PLS* locus. Closed rectangles indicate transcripts, and black arrows indicate ORFs (for *GENE X* and *PLS*). The three genotyping primers are indicated by red arrows.**

## 2.3.2: Screening for molecular markers

Molecular markers that demonstrate a response to certain signalling pathways or gene activities can be used to gain insight into the positioning of cell types and cellular responses within wild-type plants with those in the *pls* mutant. Markers were used in this study to analyse the cellular patterning in *pls* mutant roots. Some protein-fusion markers, such as those highlighting intracellular components by fusing native protein with GFP, again in comparison with wild-type results are able to reveal aspects of the internal functioning of the mutant cells.

Seedlings expressing GFP constructs were mounted in water and viewed under epifluorescence using the BY2A (GFP) filter on a Nikon Optiphot-2 stereomicroscope, (Nikon UK Ltd, Surrey, UK) prior to bulking seed for confocal analysis.

## 2.3.2.2: GUS enzyme analysis

Adapted from Stomp (1990).

**Solutions**

**X–Gluc stock:** 20 mM (5-bromo-4-chloro-3-indolyl –β- D-Glucuronide) in N, N –dimethlylformamide, stored at -20 ° C.

**X–Gluc buffer:**100 mM $Na_2H_2PO_4$ , 10 mM EDTA , 0.1% (v/v) Triton X-100, 0.5 mM potassium ferricyanide ($K_3Fe(CN)_6$), and 0.5 mM potassium ferrocyanide $K_4(Fe(CN)_6)$), pH adjusted to 7.0.

**X–Gluc staining solution:** prepared by mixing 1 volume of X–Gluc stock with 19 volumes of X-Gluc buffer to give a final concentration of 1mM X-Gluc.

**Chloralhydrate solution:** 8 g Chloralhydrate, 3 ml water and 1 ml glycerol.

**Method**

Localisation of GUS enzyme activity was determined by staining root tips for 1-2 hours in 1 mM X-Gluc staining solution at 37°C. Stained root tips were cleaned in chloralhydrate solution for 10 minutes. Excised roots were then mounted on microscope slides under a coverslip with a drop of chloralhydrate solution. Root tips were then examined for staining using DIC (Differential interference contrast / Normarski) optics on a Nikon Optiphot-2 microscope fitted with Nikon FX-35 camera containing Ektachrome 160 tungsten –balanced film (Kodak).

## 2.4: Root gravitropic response experiments

Tip curvature response (root gravitropic response) experiments were performed to investigate defective auxin signalling in the *pls* and ethylene signalling mutants. When roots are accidently or experimentally reoriented within the gravity field they undergo a tip-curvature response that ultimately results in a resumption of growth towards gravity (Boonsirichai et al., 2002).

The seeds of the mutant lines were plated on ½ MS10 (hard set) and were allowed to germinate. For tip curvature response, 2 day old seedlings were reoriented at 90° angle and the angle of curvature toward gravity was measured after 2, 4, 6, 8 , 10, 24 hours.

## 2.5: Exogenous hormone response experiments

Exogenous hormone response experiments provide a rapid, though crude means of assessing the responsiveness of seedlings to known plant signalling molecules. It is noted that under these circumstances the applied compounds may be present at levels unrepresentative of the seedling's usual physiology, and many of the compounds themselves are analogues of natural active forms of the relevant pathway components. However in comparison between the mutants and their control backgrounds, these treatments may reveal qualitative differences in responses which can indicate differences in the mutant's physiology in relation to its respective wild-type control.

All phytohormone and inhibitor compounds were made up as 10mM stock solutions in the relevant solvents, and filter-sterilised using 0.2 µm Minisart® (Sartorius, Germany) filters prior to use. These chemicals were introduced into molten media, cooled to 55°C, before square plates were poured and allowed to cool. Seeds were plated individually on these square plates and seedlings were grown vertically (by standing the square plates 70-90° angle). Response was assessed by changes in the shoot and root morphology, in relation to seedling grown on un-supplemented media or to the wild-type seedling grown on the same media.

### 2.5.1: Ethylene

ACC (1-aminocyclopropane-1-carboxylic acid) is also known as ACPC, and is used in this thesis as a proxy for ethylene treatment. ACC is the ethylene precursor, produced during biosynthesis of ethylene in plants, and the enzyme ACC synthase is the rate-

limiting step in the pathway. ACC oxidases are in all tissues, and convert ACC to ethylene. A stock solution of ACC was made in sterile $dH_2O$.

## 2.5.2: Silver Nitrate ($AgNO_3$)

Silver ions are know to inhibit ethylene responses when applied to plant tissues (Beyer, 1976, 1979), and are thought to block the signalling pathway by binding to the ethylene receptor ETR1, in competition to the $Cu^{++}$ cofactor used by this protein (Rodriguez et al., 1999). A 10 mM stock solution of silver ions was made by dissolving 0.017 g of $AgNO_3$ in 10ml of sterile $dH_2O$.

## 2.6: Extraction and purification of nucleic acids

## 2.6.1. Miniprep of plasmid DNA using the Wizard Plus SV Minpreps DNA purification system

Plasmid DNA from small culture volumes (1-10 ml) was isolated using the SV minipreps DNA purification system from Promega. The resulting plasmid DNA was suitable for DNA sequencing and all cloning purposes.

**Method**

The bacteria containing the plasmid of interest were grown overnight at 37°C with vigorous shaking in LB containing the appropriate antibiotic in a 15 ml test tube. 1.5 ml of overnight culture was transferred to an Eppendorf tube and the bacterial pellet was obtained by centrifugation at 10,000 rpm or 2 minutes. The supernatant was discarded and the pellet was resuspended in 250 µl of cell resuspension solution. 250 µl of cell lysis solution was added to each sample and tubes were inverted 4 times to mix the contents. 10 µl of alkaline protease solution was added to tubes, inverted 4 times, and incubated at room temperature for 5 minutes. 350 µl of Neutralisation solution was added and tubes were inverted 4 times to mix the contents properly. Eppendorf tubes were centrifuged at 13, 000 rpm for 10 minutes at room temperature. Minicolumns were assembled by inserting the spin column into the collection tube and clear lysate was decanted into the spin column. 750 µl of column wash solution was added to the tubes, centrifuged at 14, 000 x g for 1 minute. Washing was repeated with 250 µl of column wash solution and centrifuged at 14, 000 x g for 2 minutes. The spin column

was transferred to a 1.5 ml centrifuge tube. 100 µl of nuclease free water was added and centrifuged at 14, 000 x g for 1 minute at room temperature. The purified DNA was stored at -20 °C until used for further analysis.

## 2.6.2: Midiprep of plasmid DNA using the QIAGEN® Plasmid Midi Kit

The pCIRCE vector is a low copy number plasmid, and so was extracted from a large bacterial culture volume (100-200 ml) using the Qiagen Midi Prep Kit. The resulting DNA was suitable for sequencing, PCR and all other cloning purposes.

A flask of 100 ml of selective LB liquid medium was inoculated with bacteria carrying the plasmid of interest, and grown overnight with vigorous shaking at a temperature to suit the bacterial host. The culture was then transferred to sterile 50 ml Falcon centrifuge tubes, and the cells pelleted by centrifugation at 6,000 x g for 15 minutes at 4°C. The supernatant was discarded, and the cells re-suspended in 4 ml of buffer P1, after which 4 ml of lysis buffer P2 was added. The tube was inverted several times to mix the contents thoroughly, and then left to incubate at room temperature for 5 minutes. A further 4 ml of neutralisation buffer P3 was added and mixed by inversion, prior to incubation on ice for 15 minutes. The mixture was centrifuged at 20, 000 x g for 30 minutes at 4°C to pellet cell debris before the plasmid-containing supernatant was removed to a clean tube, and centrifuged again for a further 15 minutes at 20,000 x g, 4°C.

Before the last centrifugation step was completed, a QIAGEN-tip 100 column was prepared to receive the cleared supernatant, by adding 4 ml of buffer QBT to the column and allowing it to drain by gravity flow. The supernatant was removed from the centrifuge tube promptly and applied to the column, where it was also allowed to drain though the membrane under gravity. The QIAGEN-tip 100 was then washed twice, each with 10 ml with of buffer QC, before the DNA was eluted into a sterile 15 ml Falcon tube with 5 ml of buffer QF. The plasmid DNA was precipitated by mixing with 3.5 ml of room temperature isopropanol, the suspension was transferred to Eppendorf tubes and the DNA pelleted by centrifugation at 15, 000 x g, 4 °C for 30 minutes. The pellets were washed with room temperature 70 % (v/v) ethanol, centrifuged for a further 15 minutes at 15,000 x g , 4°C, and the supernatant removed. The pellets were air-dried until all visible droplets of liquid had disappeared, re-suspended in 100 µl sterile distilled water, and stored at -20 °C.

## 2.6.3: A quick genomic DNA extraction method for PCR (Edwards *et al.*, 1991)

This method is for extraction of genomic DNA from individual mutants using leaf tissues.

**Materials**

Extraction buffer: 200 mM Tris.HCl (pH 7.5), 200 mM NaCl, 25 mM EDTA, 0.5 % (w/v) SDS, Sterile water, isopropanol and dry ice or liquid nitrogen.

**Method**

A small leaf or leaf disc was placed in an Eppendorf tube, frozen on dry ice or in liquid nitrogen and ground. 400 µl of extraction buffer was added and tissues were ground further for 20 sec whilst tissues were thawing. The mixture was centrifuged at 14,000 x g for 1 minute. 300 µl of the supernatant was removed and mixed with equal volume of isopropanol. The DNA pellet was precipitated by spinning for 5 minutes at 14,000 x g and then the pellet was air dried. Dried pellet was redissolved in 50 µl of TE. Genomic DNA obtained from this method was stored at – 20° C until further use. 0.5 – 2 µl of this DNA is sufficient for PCR amplification.

## 2.6.4: Total RNA extraction from plant tissues using QIAGEN RNeasy® Plant Kit

The RNeasy kit from Qiagen was used to prepare total RNA from small amount of tissue (50 - 100 mg). Tissues were frozen in liquid nitrogen prior to RNA extraction.

**Method**

The sample was ground under liquid nitrogen to fine powder in a mortar and pestle and transferred to an Eppendorf tube containing 450 µl of buffer RLT ( 10 µl of β-mercaptoethanol added per 1 ml of buffer RLT) and vortexed vigorously. The sample was transferred to the QIAshredder spin column sitting in a 2 ml collection tube and centrifuged for 2 minutes at 14, 000 x g. The supernatant was carefully transferred into a new centrifuge tube. 0.5 volumes (225 µl) of 100 % ethanol was added to the supernatant and mixed immediately by pipetting. The sample was then applied to a pink binding RNeasy mini column and centrifuged for 15 seconds at 10, 000 x g. Flow-through was discarded. 700 µl of buffer RWI was added to the column and centrifuged

at 10, 000 x g for 15 seconds. The column is then transferred to a new tube, 500 µl of buffer RPE was added onto column and centrifuged for 15 second at 10,000 x g. The wash was repeated twice. 30-50 µl of RNase free water was added for elution and centrifuged for 1 minute at 14, 000 x g. The extracted RNA was stored at -20° C for short term storage and at 80° C for long term storage.

## 2.6. 4.1: Spectrophotometric analysis of RNA

RNA in solution was analysed and quantified using a UniCam UV2 UV/Vis spectrophotometer (ATI, Cambridge, UK). A 1/100 dilution was made of RNA samples in sterile distilled water, and same water was used a blank. The absorbance of the samples was scanned from 200 nm to 300 nm. If good quality RNA has been obtained, there should be a peak at 260 nm on the trace. The purity of RNA sample was calculated by measuring the ratio of absorbance at 260 nm and 280nm. A pure RNA should have a ratio of 1 or above. The concentration of RNA sample was calculated using the following formula:

Concentration of RNA samples = 40 x $A_{260}$ x dilution factor

Total yield = concentration x volume of sample in millilitres

## 2.6.5: Purification of DNA from agarose gels using *High Pure* PCR Product purification kit

The *High Pure* PCR product purification kit was obtained from Roche Applied Science and was used to purify DNA fragments from agarose gels following restriction enzyme digestion or PCR. The following procedure was used for the purification of DNA from a 100 mg agarose gel slice.

The DNA of interest was isolated using agarose gel electrophoresis. The band of interest was cut from the gel using an ethanol-cleaned scalpel or razor blade. The excised gel slice was placed in a sterile 1.5 ml microcentrifuge tube. The weight of the gel slice was determined by first pre-weighing the tube and then reweighing the tube with the excised gel slice. 300 µl of Binding Buffer was added for every 100 mg of agarose gel slice to the microcentrifuge tube. The agarose slice was dissolved by vortexing for 15-30 seconds, incubating the suspension for 10 minutes at 56°C, and further voxtexing the tube for 2-3 minutes. After the agarose gel slice was completely

dissolved, 150 µl isopropanol was added for every 100 mg gel slice and the tube was voxtexed thoroughly. *High Pure* filter tubes were inserted into the collection tube. The entire contents of the microcentrifuge tube were pipetted into the filter tube. The tubes were centrifuged at 13, 000 rpm for 30-60 seconds. The flowthrough was discarded and 500 µl of wash buffer was added to the filter tube, and centrifuged for 1 minute at 13, 000 rpm. The wash was repeated with 200 µl of washing buffer, and centrifuged again at maximum speed for 1 minute. The filter tube was transferred into a new microcentrifuge tube, and 50-100 µl of elution buffer was added to it, and the tube was centrifuged at 13, 000 rpm to pellet the DNA. The eluted DNA was stored at -20° C until further analysed.

## 2.7: Agarose gel electrophoresis

**Solutions**

1x TAE buffer: 40 mM Tris-acetate, pH 8.0, 1mM EDTA

10x Loading buffer: 0.25% (w/v) bromophenol blue, 0.25% (w/v) xylene cyanol FF, 0.25% acridine orange (w/v), 25% Ficoll (type 400) in water.

DNA marker: Hyperladder I and Hyperladder II (Bioline) were used according to the manufacturer's instructions.

**Method**

Gels of 0.7% to 2% (w/v) agarose were prepared in 1x TAE buffer depending on the size of the DNA fragments to be separated. Gels were melted in a microwave, allowed to cool to approximately 50°C before 0.1 µg/ml of ethidium bromide was added and mixed. The molten agarose was immediately poured into a gel tray and allowed to solidify at room temperature for 20-40 minutes. DNA samples were mixed with 1/10 volume of 10x loading buffer and loaded into gel wells by pipetting. DNA markers were mixed with 1/10 volume of 10x loading buffer and loaded into gel wells by pipetting. DNA markers were run alongside sample DNA to enable approximate sizing of fragments. Electrophoresis was performed at 5-10 V/cm in 1x TAE buffer. DNA was visualised on a UV transilluminator (Gel Doc 1000 system with Molecular Analyst version 2.1.1 software, Biorad) and photographed.

## 2.8: Rubidium chloride method for making competent *E.coli* cells

The following method of making chemically competent *E.coli* for transformation is as described by Ausubel *et al.* (1994). Buffer Tfbl and Tfbll were made up as detailed

below, and filter sterilised using 0.2 µm Minisart® filters (Sartorius,Germany) prior to use.

Buffer TfbI
30 mM potassium acetate
100 mM rubidium chloride
10 mM calcium chloride
50 mM manganese chloride
15 % v/v glycerol
pH adjusted to 5.8 (with dilute acetic acid)

Buffer TfbII
10 mM MOPS
75 mM calcium chloride
10 Mm rubidium chloride
15 % v/v glycerol
pH adjusted to 6.5 (NaOH)

To prepare competent cells, a single colony from a fresh LB plate of *E.coli* strain XL1-blue was used to inoculate 100 ml of sterile LB broth, and grown overnight at 37°C with vigorous shaking to provide aeration. The culture was transferred to 50 ml Falcon centrifuge tubes, and chilled on ice for 15 minutes before at 4000 x g for 5 minutes at 4°C. The supernatant was discarded, and the cells were resuspended gently in 40 ml of buffer TfbI before resting on ice for 15 minutes. The supernatant was then discarded and the cells re-suspended in 4 ml of buffer TfbII. The cell suspension was rested on ice for 15 minutes before 250 µl aliquots were flash frozen in liquid nitrogen and stored at -80°C until required.

## 2.9: DNA cloning into plasmid vectors

### 2.9.1: Digestion of vector and insert DNA with restriction endonucleases

Restriction enzymes and 10 x reaction buffer were obtained from Promega Ltd., and reactions were carried out according to the manufacturer's instructions. Typically, a digestion reaction contained 1-5 µg of DNA, 3 µl of 10 x reaction buffer, 1 µl restriction enzymes (10 units/µl) and made to 30 µl with sterile, distilled water. Reactions were left at the required temperature for 1-4 hours (upto an overnight). Following digestion

reaction vector DNA was phosphorylated prior to ligation. Insert DNA was purified by using High Pure PCR clean up kit (Roche labs).

## 2.9.2: Dephosphorylation of vector DNA

Following restriction digestion, vector DNA was treated with shrimp alkaline phosphatase (Sigma Chemical Company) to dephosphorylate the 5' ends prior to ligation to prevent re-ligation of vector ends. This was only performed if the vector DNA had been treated with just one restriction enzyme. After digestion, 1 unit of shrimp alkaline phosphatase was added to 1-5 µg of vector DNA with the relevant restriction enzyme in a total volume of 30 µl. The reaction was incubated at 37°C for 30 minutes followed by 10 minutes at 70° C to inactivate the phosphatase.

## 2.9.3: T- tailing of vector DNA

After Finney *et al*. (1995)

T-tailing of the vector involves the addition of a thymidine nucleotide to the 3' end of DNA stand following vector linearization. This facilitates the cloning of PCR products since *Taq* DNA polymerase adds a 5' adenosine nucleotide. After, cutting the DNA with the restriction enzymes and purifying the DNA fragment from agarose gel. The DNA (10 µl) was mixed with 10 µl of $Mg^{++}$-free 10x PCR buffer (supplied with *Taq* DNA polymerase from Bioline), 3 µl of 50 mM $MgCl_2$, 20 µl of 5 mM dTTP, 1 µl of *Taq* DNA polymerase (5 units) and made up to 100 µl with sterile distilled water. The reaction was incubated at 75°C for 2 hours and was used in ligation reaction without further purification.

## 2.9.4: Ligation of DNA fragment

The enzyme T4 DNA ligase catalyses the formation of a covalent phosphodiester bond between a 5'-phosphoryl group and adjacent 3'- hydroxyl group. In a typical ligation reaction 50-100 ng of vector DNA (cut with suitable restriction enzymes) was mixed with an equal molar amount of insert DNA. To this were added 2 of 5x ligation buffer and 1 µl (3 units) of T4 DNA ligase and the volume made upto 10 µl with sterile, distilled water. The contents were mixed and incubated at 14° C overnight before transformation of competent *E.coli* cells.

## 2.9.5: Ligation of PCR fragments pCR®2.1-TOPO

DNA fragments generated by PCR were generally cloned into the pCR® 2.1-TOPO vector from Invitrogen. The vector is supplied linearized with 3' thymidine overhangs for efficient ligation of PCR products. It also utilises the ligation activity of the topoisomerase enzyme resulting in fast, high efficiency ligation. To 1 µl of the pCR® 2.1-TOPO vector was added 1-2 µl of fresh, unpurified PCR product and the reaction made up to 5 µl. the reactants were mixed and left at room temperature for 5 minutes to allow ligation to proceed. The tube was then placed on ice until ready for transformation into TOP10 competent cells (Invitrogen).

## 2.9.6: Transformation of TOP10 One shot ™ competent cells

TOP10 One shot™ competent cells were supplied with the TOPOTA Cloning® kit (Invitrogen) along with the ligation ready pCR® 2.1-TOPO vector. Following the ligation of PCR products a tube of TOP10 One shot™ competent cells was defrosted on ice. The TOPO cloning reaction was set up by mixing 2 µl of ligation reaction with 1 µl of salt solution and 3 µl of sterile water in an Eppendorf tube. The reaction mix was incubated on ice for 25-30 minutes before heat shocking at 42° C for 30 seconds. The tube was then returned to ice for 2 minutes, followed by addition of 250 µl of SOC medium. The tube was then incubated for 30 minutes (ampicillin selection) to an hour (kanamycin selection at 37° C with gentle shaking). 50-100 µl of the transformation mix was spread onto LB plates containing either 100 µg/ml ampicillin or 50 µg/ml kanamycin sulphate and 37.5 µg/ml of X-Gal. Recombinant appear as white colonies following overnight growth at 37° C.

## 2.9.7: Transformation of XL1- Blue MRF' competent cells

XLI-blue MRF' competent cells were made by using the procedure mentioned earlier (Pg. 31). 250 µl of XL1-Blue MRF' competent cells were defrosted on ice. 2µl of ligation mixture was then added to these competent cells. The tube was incubated on ice for an hour followed by heat shock at 42°C for 2-3 minutes. The tube was placed back on ice for another 10 minutes, followed by addition of 1 ml LB or SOC media, and incubated at 37°C for an hour. After an hour, the tube was spun down and the pellet was resuspended in 100 µl of LB. The transformation was then plated on LB plates containing appropriate selection and 37.5 µg/ml of X-Gal.

## 2.10: Polymerase chain reaction

### 2.10.1: Standard PCR

For standard PCR reactions, *Taq* DNA polymerase was obtained from Bioline and was supplied with 10x reaction buffer with $MgCl_2$ and 50 mM $MgCl_2$ stock solution. Oligodeoxynucleotide primers were obtained from MWG-Biotech as lyophilised pellets and resuspended to the desired concentration in sterile distilled water. The template for amplification was either genomic DNA, a cloned fragment of DNA in a plasmid, cDNA or a bacterial colony. A standard PCR reaction contains:

10-100 ng of DNA sample
0.2 µM of each primer
1.5 µl of 50 mM $MgCl_2$ (1.5 mM final concentration)
5 µl of 10x reaction buffer
1mM dNTP mix
2.5 units of *Taq* DNA polymerase, the volume is made upto 50 µl with sterile, distilled water in a 0.5 ml Eppendorf tube. Reactions were then placed in a GeneAmpR PCR System 9700 Thermal Cycler (Applied Biosystems, California, USA). A typical amplification was carried out using following conditions:

Denaturation at 94° C for 2 minutes - 1 cycle; followed by
30 cycles of denaturation at 94° C for 30 seconds, annealing at 55° C for 30 seconds, 1 minute of extension at 72° C and final extension step of 10 minutes at 72° C.
When the reaction was complete, 10-20 µl of reaction mix was run on an agarose gel (0.7-2%) to check the size and concentration of the product.

### 2.10.2: PCR using Expand™ High Fidelity PCR system

The Expand™ High Fidelity PCR system consists of a mix of both *Taq* and *Pwo* DNA polymerase. Due to the proofreading activity of *Pwo* DNA polymerase, the Expand™ High Fidelity PCR system results in a 3-fold increase in the fidelity of DNA synthesis ($8.5 \times 10^{-6}$ error rate). This system was therefore used when a high degree of sequence fidelity was required. A typical reaction contains:
10-100 ng of DNA sample
0.2 µM of each primer
6 µl of 25mM $MgCl_2$ (3.0 mM final concentration)

5 µl of 10x reaction buffer
1mM dNTP mix
2.5 units of enzyme mix, the volume is made upto 50 µl with sterile, distilled water in a 0.5 ml Eppendorf tube. Reactions were then placed in a pre-heated block at 90° C in a Thermal Cycler. A typical amplification was carried out using the following conditions:
Denaturation at 94° C for 2 minutes; followed by
30 cycles of denaturation at 94° C for 30 seconds, primer annealing at 60 °C for 30 seconds, 2 minute of extension at 72 °C and final extension step of 10 minutes at 72° C. If the expected product was grater than 3 kb in length then the extension step was carried out at 68° C instead of 72 °C with a general rule of 1 minute extension per kilo base of target.
When the reaction was complete, 5-10 µl of reaction mix was analysed on a 0.7-1% agarose gel.

## 2.10.3: Colony PCR

Bacterial colonies from single cells transformed with plasmid DNA were patched onto a numbered grid on selective plates, and grown overnight at 37°C before checking for the desired insert by colony PCR. The reaction mixture was set up on ice in bulk without *Taq*, in a 1.5 ml sterile Eppendorf tube, allowing 20 µl for each N+1 reaction (the extra quantity allowed for pipetting errors).

The following formula was used to calculate the volumes of the various components.

| | |
|---|---|
| 10x $Mg^{++}$ free 10x reaction buffer | (N + 1) x 2 µl |
| 10 mM dNTP mix | (N +1) x 0.5 µl |
| Primer 1 (forward) | (N +1) x 0.5 µl |
| Primer 2 (reverse) (N + 1) x 0.5 µl | |
| 50 mM $MgCl_2$ ] (N + 1) x 0.5 µl | |
| $dH_2O$ to make the total volume up to | ( N + 1 ) x 0.5 µl |

The cocktail was mixed gently then pipetted into 20 µl aliquots in 0.5 ml sterile microcentrifuge tubes, 0.1 µl *Taq* was added, the tube contents overlain with mineral oil, and the PCR thermal cycle reaction carried out under the condition described above. 10 µl of each reaction product was checked using agarose gel electrophoresis.

## 2.10.4 DNase treatment of RNA

After Sanyal et al., (1997)

Total RNA was extracted from 7 day old seedlings of all the plant lines required (Col-0, C24, *pls*, PLSOx, *pls x etr, etr1*, *ctr1* and *eto1*) using the QIAGEN, RNeasy Plant Mini Kit. 2 µg of RNA from each sample was DNase treated in 20 µl reactions to give a 100 ng/ µl of each RNA sample. The required volumes of each RNA sample, depending upon their concentrations, were mixed with 2 µl of 10 x DNase buffer, 1 µl of RQ1-DNase (RNase free, Promega Ltd.) and the volume was made up to 20 µl. The reaction was incubated at 37°C for 30 minutes. DNase was inactivated by adding 2 µl of RQ1 DNase stop solution and the reactions were incubated for further 10 minutes at 65 °C.

## 2.10. 5 cDNA synthesis

Reverse transcription reaction was used to synthesise or copy the RNA into its complementary DNA (cDNA) sequence. The cDNA so obtained can serve as a template for amplification by PCR. The RETROscript™ RT-PCR kit from Ambion was used to synthesise cDNA from the RNA.

**Method**

1 µg of total RNA (extracted using Qiagen RNAeasy kit) was mixed with 2 µl of Oligo (dT), the mixture was spun briefly and heated at 70-85° C for 3 minutes. Generally 85°C is more appropriate for targets that are GC-rich or that have a predicted high degree of secondary structure. The tubes are then removed to ice, spun briefly, and replaced on ice. The remaining reverse transcription components are then added to the mixture: 2 µl of 10X RT buffer, 4 µl of dNTPs mix, 1 µl of RNase inhibitor, 1 µl reverse transcriptase, and nuclease free water, to make up the volume of the reaction upto 20 µl. All the components are mixed gently, spun briefly, and incubated at 42-44°C for an hour (slowly elevating the temperature to 55°C). The reaction is further incubated at 92°C for 10 minutes to inactivate the Reverse Transcriptase. The cDNA obtained was stored at -20°C until required for PCR.

## 2.10.6: Semi-quantitative PCR or Reverse Transcription-mediated Polymerase Chain Reaction (RT-PCR)

Semi-quantitative RT-PCR allows a fairly accurate determination of the realative abundance of specific transcripts within either the same or different cDNA populations. It was important to have a base line against which the results were normalised. This was done by keeping the amount of RNA in the cDNA synthesis reaction the same (i.e. normalised per mg RNA), using the same level of a specific actin transcript in each cDNA population as a base line (assuming that this will remain unchanged in the different samples) and by extracting the RNA from same amount of starting material (both in terms of age and weight). The results from the semi-quantitative PCR were confirmed using the Real time PCR.

**Method**

The total RNA from each plant was extracted using the QIAGEN RNeasy Kit. The integrity of the RNA was checked by running an agarose gel and was quantified using a spectrophotometer. Equal amounts of RNA from each sample (5 mg) were used to synthesize cDNA. The cDNA synthesis was done using the Ambion Retroscript Kit and the cDNA was diluted to 1:2 to give produce a working stock. The efficiency of the primers was checked using a standard PCR reaction. The primers were optimised for $MgCl_2$ concentration and PCR product abundance. Keeping all the parameters the same as the optimisation PCR reaction, the abundance of product produced at defined time points was determined by running the products on a 4% agarose gel. A cocktail of all the cDNA samples was made, and the number of genes to be screened was taken as 'n'. Six time points of 10, 15, 20, 25, 30, 35 and 40 cycles were used. Two separate cocktails were made, one with all the components of PCR without primers in 15 µl $dH_2O$ and other with forward and reverse primers in 5 µl $dH_2O$. The tubes were labelled with name of the gene and the cycle number. The composition of the two cocktails used was:

Cocktail 1: PCR components without primers (15 µl)

| | |
|---|---|
| cDNA | (nx7)* 0.5 µl |
| 10x PCR buffer | (nx7) 2 µl |
| dNTPs (10 mM) | (nx7) 0.5 µl |
| $MgCl_2$ (50 mM) | (nx7) 0.5 µl |
| Taq DNA polymerase | (nx7) 0.1 µl |

| | |
|---|---|
| $dH_2O$ | (nx7) 11.4 µl |
| **Total** | (nx7) 15 µl |

* (n x7) where n is the number of genes and 7 is 6+1 for six different time points plus one for pipetting errors.

Cocktail 2: One cocktail per gene (eg: cocktail for 10 reactions)

| | |
|---|---|
| Forward primer | 0.5 µl x 10 |
| Reverse primer | 0.5 µl x 10 |
| $dH_2O$ | 4 µl x 10 |
| **Total** | 5 µl x10 |

15 µl cocktail-1 and 5 µl of cocktail-2 were mixed together in Eppendorf tubes labelled before with gene name and cycle number, and spun briefly in a microcentrifuge. The PCR reaction was performed using the same parameters as optimisation reactions which were:

94 °C for 4 minutes

94 °C for 1 minute
56 °C for 1 minute
72 °C for 30 seconds
} The first set of tubes was taken out at the end of 10 cycles, next at end of 15 cycles and so on until the finish of 40 cycles.

72 °C for 10 minutes

The removed tubes were put on ice to stop the reaction, stored at 4°C if required and loaded on 4% gel to quantify the product. Once the optimum number of cycles was decided for an exponential amplification of product, those time points were used to compare the transcript levels of different in a particular line. The same sets of primers were used for doing the semi-quantitative PCR and Real-time PCR. The primers used in this experiment are listed below:

| Name | Sequence 5'-3' | Length (bp) | $T_m$ (°C) |
|---|---|---|---|
| act2_rev | AAC GAT TCC TGG ACC TGC CTC | 22-mer | 62.1 |
| act2_for | TCA CAG CAC TTG CAC CAA GCA | 21-mer | 59.8 |
| ctr1_for | ATG GCT CGG ATG TTG CTG TGA AAA | 24-mer | 61.0 |
| ctr1_rev | TTG CTC CCT TGC TCC ACT TTT ATG | 24-mer | 61.0 |
| etr1_for | TGC TTT GAT GGT TTT GAT GCT TCC | 24-mer | 59.3 |
| etr1_rev | GAT TGC TGT TTC TGC TTC TCG TCT | 24-mer | 61.0 |
| ein3_for | GAA CAT CCC AAA CAG AGC AAA CAA | 24-mer | 59.3 |
| ein3_rev | TCG TTC CTA CTA CTC CTG GCA TCG | 24-mer | 64.4 |
| erf10_for | CCG AGA CGG TGA GTG ATG GAA ATG | 24-mer | 64.4 |
| erf10_rev | GAT GGT GCA AGA AAA TGG AGA GAC | 24-mer | 59.3 |
| ers1_for | GAT GGT GCA AGA AAA TGG AGA GAC | 24-mer | 61.0 |
| ers1_rev | TCG ATC ATA ACT CTT TGC TCT GGA | 24-mer | 59.3 |
| hls1_for | GAG TCA CGG TTA TCA AGT TAG AGC | 24-mer | 61.0 |
| hls1_rev | CTC GCG TCG TTT TAG CCA CCA CAC | 24-mer | 66.1 |
| ein2_for | CCG TGC TTT TGC CTT CAG ATT | 21-mer | 57.9 |
| ein2_rev | ACC GGG TCC ATC CTG ATT CAT | 21-mer | 59.4 |
| eto2_rev | TGC TTC TTG ATA TCA TTC GTC | 21-mer | 54.0 |
| eto2_for | GCC AAT ACC TCG AAG AGA ACC | 21-mer | 59.8 |
| ers2_rev | CAC CGC CTC TCG ACA TCA TC | 20-mer | 61.4 |
| ers2_for | GGA AAG ATA TTC AAG AAG CGG | 21-mer | 55.9 |
| SMpin1_for | TAC TCC GAG ACC TTC CAA CTA CGA | 24-mer | 62.7 |
| SMpin1_rev | CTC CTC CAC CGC CGA ACA CAT CTG | 24-mer | 67.8 |
| SMpin2_for | GAG TAG GAG TAG GAG GAC AAA ACA | 24-mer | 61.0 |
| SMpin2_rev | CTT TCC CCC GTT ATT ACC GTC TTG | 24-mer | 62.5 |
| SMpin3_for | TCT CTT CAA CCA CCA CAT CTA CCG | 24-mer | 62.7 |
| SMpin3_rev | GAT TGA TCT GGG ACT AAC ATA C | 22-mer | 56.5 |
| SMpin4_for | CGG AAC AAT CTG AAC AAG GTG CTA | 24-mer | 61.0 |
| SMpin4_rev | AGC CCA TAT GAG ACC GAT TAG ACT | 24-mer | 61.0 |
| SMpin7_for | GGA GCC AAT GAA CAA GTC GGA AAA | 24-mer | 61.0 |
| SMpin7_rev | TCA ATA TCA GCC GAG TCA TCA CAC | 24-mer | 61.0 |
| pin1_for | AAC TCT AAC TTT GGT CCT GGA GAA | 24-mer | 59.3 |
| pin1_rev | CGT GCC TCC ACC ACC GCC AGT GTT | 24-mer | 69.6 |
| pin2_for | AGT TAT GAA GAC GGC GAA GAA AGC | 24-mer | 61.0 |
| pin2_for | TGT TCA TCT CCT TGT TTT GTC CTC | 24-mer | 59.3 |

**Table 2.5: List of Primer used for the real time PCR analysis**

## 2.11: Real-time PCR

The real-time PCR is based on the quantitative relationship between the starting target DNA and the amount of amplification product during the exponential phase of a cycling program. The real-time instruments comprise a fluorometer and a thermal cycler for the detection of fluorescence during the cycling process. A computer communicates with the real-time machine and collects fluorescence data. This data were displayed in graphical format software developed for real-time analysis.

Fluorescence data were collected once during each cycle of amplification allowing for real-time monitoring of amplification. These data help to determine which samples are amplifying on a cycle-by-cycle basis. This allows visualization of how individual samples amplify in relation to a known standard, positive controls and negative controls. After the raw data were collected, the analysis was started. The software for the real-time instrument normalises the data to account for differences in background fluorescence. Once normalisation was complete, a threshold level was set. This was the level at which the fluorescence data was analyzed.

Sybr-Green (SG), a fluorescent dye that binds to the minor groove of the double helix, was used as an intercalating dye. The unbound dye exhibits little fluorescence in solution, but upon binding to the double-stranded DNA the fluorescence enhances. This was utilised in real-time amplification. As the DNA amplifies during an amplification reaction, the dye binds to amplified products and the fluorescence signal increases. This increase was analysed against the background fluorescence level. Multiple molecules of fluorescent dye bind to the dsDNA based on amplicon length.

SG is not a sequence specific intercalating dye and binds to any dsDNA including non-specific products and primer dimers. Therefore it was necessary to differentiate between target and artifact signals. Intercalating dyes allow for the melting of amplification product at the end of the run. This is called the melt curve analysis. During the melt curve, the real-time machine continuously monitors the fluorescence of each sample as it is slowly heated from a temperature below the melting point of the product to a temperature above the melting point of the products. This range was set from 55°C to 99°C. As products melt, a decrease in fluorescence was realised and measured. The melt peaks reflect the product amplified during the reaction. These peaks are analogous to the bands on an electrophoresis gel.

## 2.11.1: Optimisation of primer concentration

The primers used for real-time were designed using Oligo® primer designing software. The primers were made to give an amplicon of 200-300 bp over the intron from the cDNA of the gene of interest. The primer concentrations were between 2 µM to 10 µM and the optimisation was performed with a fixed amount of DNA template.

The melt curves were obtained for primers optimised using the standard PCR to further confirm their specificity. A specific primer should give a single peak, and no additional peaks, at lower melt temperature in the melt curve analysis. Additional peaks at lower temperature could also be due to an excessive amount of primers in the reaction. In the reaction where excessive primer were resulting in additional peaks at lower temperature, the amount of the primers were reduced to a minimum.

## 2.11.2: Optimisation of $MgCl_2$ concentration

Several aspects of the amplification are affected by $MgCl_2$ concentration in a reaction. These include DNA polymerase activity, which can affect specificity. The dNTPs and templates bind magnesium and reduce the amount of free magnesium necessary for enzyme activity. Greater yields of amplification can be achieved with higher concentration of free magnesium, albeit this can also increase non-specific amplification. Therefore, the optimal level of $MgCl_2$ was achieved by using a range of $MgCl_2$ concentrations from 1.5 mM to 3.5 mM from a 50 mM $MgCl_2$ stock solution in a standard PCR reaction.

## 2.11.3: Optimisation of Sybr-Green (SG) concentration

All the parameters of an amplification reaction (i.e $MgCl_2$, dNTPs, Taq-Polymerase and primer concentration) were optimised prior to optimisation of SG concentration. The result was obtained as a single band on an agarose gel. To achieve an optimal SG concentration, a dilution series reaction containing different dilution from 1: 200 to 1:1000 of SG was performed. The ability of SG to intercalate into a dsDNA interferes with the amplification reaction. An excessively high SG concentration can lead to an inhibition of the reaction and a low SG concentration may not provide enough SG to label the amplicon sufficiently. Therefore, the optimal SG concentration has to be a compromise between the two.

## 2.11.4: Real-time reaction

A cocktail of following components was made in 20 µl reaction. The cDNA synthesised from the total RNA was diluted in a 1:2 ratio with sterile nuclease-free water and was used as a template for the real-time reaction:

| | | |
|---|---|---|
| 10 x PCR buffer | | 2 µl |
| $MgCl_2$ (50 mM) | | 1 µl |
| dNTPs (25 mM) | | 2 µl |
| Forward primer (10pmol/µl) | 1 µl | |
| Reverse primer (10pmol/µl) | | 1 µl |
| Taq Polymerase (5 U/µl) | | 0.2 µl |
| SG (1:500) | 0.3 µl | |
| Sterile $dH_2O$ | | 7.5 µl |
| Total | 15 µl | |

} Multiplied by the number of reactions needed.

0.5 µl of template was mixed with 4.5 µl of sterile water (multiplied by the number of reactions to make up 5 µl with the rest of the reaction mix. The two cocktails were mixed together in flat topped real-time PCR tubes, spun briefly and were run in the RotorGene using the following parameters.

## 2.11.5: Cycling parameters

A typical profile of SG run used in this experiment was as follows:

Denaturing: (depends upon the enzyme used in the reaction)
95°C for 2 minutes

Cycling: (40 cycles)
95°C for 20 seconds
56°C for 20 seconds (annealing temperature)
72°C for 40 seconds

Melt:
55°C-99°C, hold 30 seconds on the 1st step, and 5 seconds on subsequent steps.

The data from the run was acquired at the annealing temperature using the multi channel, emission at 470 nm and detection at 510 nm.

## 2.11.6: Analysis of quantitative data

There are two main ways of analyzing the quantitative data, absolute quantification and relative quantification, based on the application and the aim of the analysis. In this experiment, relative quantitation method was used to analyse the data.

## 2.11.6.1: Absolute quantification

Absolute quantification refers to an analysis where unknown samples are compared to a standard curve. A standard is a known DNA sample whose absolute concentration is known. An ideal standard must be extracted in same ways as the known samples for the accuracy of the absolute quantification assay. Unfortunately this is not always possible. Alternatively, the amplicon being studied can be cloned or a synthetic oligonucleotide can be used. There are several criteria for absolute standards. The standard must be amplified using the same primers as the gene of interest and must amplify with the same reaction efficiency.

There are several ways of analysing absolute quantification data on the rotor gene. Beside the standard curve, the R-value, the slope, the intercept and the efficiency of the standard curve are displayed on the RotorGene software. One of the major drawbacks of absolute quantification is that the standard curve can degrade, so for each reaction a new standard curve has to be made with the same threshold as the first one. Also, the accuracy of the absolute quantitation assay is entirely dependent on the accuracy of the standards.

## 2.12.6.2: Relative quantification

The term relative quantitation is used when two or more genes are compared to each other with the result being a ratio. No absolute numbers are detected. An endogenous or a housekeeping gene is normally compared to the gene of interest. Comparative quantification software of the Rotorgene was used to analyse the data in this experiment using *Actin2* as a housekeeping gene.

The transcript abundance of eight different ethylene signalling genes (i.e *etr1*, *ctr1, ein2, ein3, ers2, eto1, hls1, and gst1)* in eight plant lines (ie Col-0, C24, *pls*, *pls*Ox, *pls*

x *etr1*, *etr1*, *ctr1*, and *eto1*) were analysed using the comparative quantification method. Once the primers were optimised using standard PCR and all the parameter of a real-time were optimised, the real-time reaction for each gene in all the different lines was carried out in quadruplicates. After the completion of the run, the concentration of each reaction sample was calculated by the software, which was then normalised using a 'no template' control. The amplification value for each sample must be above 1 for the amplification to be considered real. These concentrations (in quadruplicates) for each sample are then copied to Microsoft Excel, where the mean of the quadruplicates for each sample was calculated and then divided by the mean of the corresponding *actin2* sample. The results were finally plotted in a graphical format.

## 2.13: DNA sequencing

The DNA sequencing was performed by the DNA sequencing lab at Durham University, using an ABI 373 DNA sequencer and dye terminator labelling reaction (Perkin Elmer Applied Biosystems). Samples were normally supplied in plasmid form prepared using the Wizard™ SV minipreps DNA purification system from Promega at a concentration of 0.2 µg/µl. Primers for sequencing were supplied at a concentration of 3.2 pmoles/ µl.

## 2.14: Yeast Two-Hybrid assay using Stratagene® GAL4 Two-Hybrid Phagemid Vector Kits

The yeast two-hybrid system is a reverse proteomic approach to identify and study protein-protein interactions (Fields and Song, 1989; Vidal and Legrain, 1999; Walhout and Vidal, 2001). The system is based on the functional reconstitution of an intact transcription factor that activates reporter gene expression.

In this project, I used the GAL4 two-hybrid phagemid vector system to detect protein-protein interaction *in vivo*. The system is based on the ability to separate eukaryotic transcriptional activators into two separate domains, the DNA-binding domain (BD) and the transcriptional activation domain (AD). In the GAL4 two-hybrid phagemid vector system, proteins that interact with the bait protein were identified by generating hybrids of yeast GAL4BD and the bait protein (PLS) and the GAL4AD and a target protein (ETR1). Neither hybrid protein is capable of initiating specific transcription of reporter genes in yeast in the absence of a specific interaction with the other hybrid protein. When a hybrid protein (PLS) was expressed in yeast, the GAL4BD binds PLS to specific DNA sequences in the yeast defined by GAL4 upstream activating

sequences ($UAS_{GAL4}$) which regulate the expression of reporter gene. Binding of PLS to the UAS was not sufficient to initiate transcription of the reporter gene. When ETR1 was expressed in yeast, the AD interacted with the other components of the transcriptional machinery required to initiate transcription of the reporter gene. However, ETR1 alone was not localised to the reporter gene UAS and therefore does not activate transcription of the reporter gene. When a specific interaction between PLS and ETR1 localises both the GAL4-BD and GAL4-AD to the reporter UAS, transcriptional activation of the reporter gene occurred. The reporter genes in the GAL4 two-hybrid phagemid vector system are β-galactosidase *(lacZ)* and histidine (*HIS3*).

## 2.14.1: Vectors

### 2.14.1.1:The pAD-GAL4-2.1 Vector

The pAD-GAL4-2.1 phagemid vector contains a multiple cloning site (MSC) with *Bam*H I, *Nhe* I, *Eco*R I, *Xho* I, *Sal* I, *Xba* I , *Pst* I and *Bgl* II restriction sites. The *Xba* I site in the pAD-GAL4-2.1 AND pBD GAL4 Cam is not unique and contains the UAG amber suppressor in the same translational reading frame as the GAL4 domain. Therefore, the DNA was inserted such that the *Xba* I site is not between the GAL4 domain and the DNA insert.

The unique *Eco*R I and *Sal* I, and *Xho* I and *Sal* I cloning sites were used for cloning of *ETR1* and *CTR1* respectively into the pAD-GAL4-2.1 phagemid vector. The pAD-GAL4 2.1 and pBD-GAL4 Cam phagemid vectors contain the pUC origin for replication and an f1 origin for production of single stranded DNA in *E.coli*. The two vectors also contain the 2µ origin of replication. The pAD-GAL4 2.1 phagemid vector contains ampicillin resistance gene, β-lactamase (*bla*) for selection with ampicillin in *E. coli* and the *LEU2* gene for selection in yeast.

| Feature | Nucleotide position |
|---|---|
| Yeast *ADH1* promoter | 4-408 |
| GAL4 activation domain (114 amino acids) | 488-829 |
| Multiple Cloning Site | 839-935 |
| Yeast *ADH1* terminator | 1168-1318 |
| Yeast *LEU2* selection marker ORF | 1615-2709 |
| f1 origin of ss-DNA replication | 3483-3789 |

| | |
|---|---|
| pUC origin of replication | 4427-5094 |
| Ampicillin resistance (bla) ORF | 5245-6102 |
| 2µ yeast origin of replication | 6489-7653 |

2.13.1.2 The pBD-GAL4 Cam Vector

The pBD-GAL4 Cam phagemid vector contains an MCS with *Eco*R I, *Srf* I, *Sma* I, *Xho* I, *Sal* I, *Xba* I , and *Pst* I restriction sites. The unique *Eco*R I and *Xho* I cloning sities was used to clone *PLS* into the pBD-GAL4 Cam phagemid vector. The pBD-GAL4 Cam contains the chloramphenicol acetyltransferase gene for selection with chloramphenicol in *E.coli* and *TRP1* gene for selection in yeast. The hybrid protein was expressed by the *ALCOHOL DEHYDROGENASE 1* (*ADH1*) promoter and is terminated by the *ADH1* terminator (T *ADH1*).

| Feature | Nucleotide position |
|---|---|
| Yeast *ADH1* promoter | 4-408 |
| GAL4 DNA-binding domain (148 amino acids) | 434-877 |
| Multiple Cloning Site | 878-941 |
| Yeast *ADH1* terminator | 948-1154 |
| Yeast *TRP1* selection marker ORF | 1197-1871 |
| f1 origin of ss-DNA replication | 2322-2628 |
| pUC origin of replication | 2970-3637 |
| chloramphenicol resistance ORF | 4174-4725 |
| 2µ yeast origin of replication | 5330-6489 |

## 2.14.2: Host Strains

## 2.14.2.1: Bacterial strain

The RecA⁻ *E.coli* host strain XLI-Blue MRF´ was used for amplification and excision. The stored cells were revived by scraping off splinters of solid ice with a sterile loop and streaking the splinters onto a agar plate containing tetracycline, and incubated overnight at 37°C.

## 2.14.2.2 Yeast strain

The YRG-2 strain, a yeast strain with two reporter genes for detection of *in vivo*-protein-protein interaction was used in this assay. YRG2 is a derivative of the HF7c strain and was selected for its ability to generate high-efficiency competent cells. The

YRG-2 strain carries a mutation which ensures that the endogenous *GAL4* gene is not expressed. YRG-2 also carries the auxotropic markers leucine (*leu2*) and tryptophan (*trp1*), for selection of yeast which have been transformed with the AD and the BD vectors respectively, and the autotrophic marker, histidine (*his3*), for selection of yeast which has been transformed with interacting protein. The YRG-2 strain contains a dual selection system with *lac*Z and *HIS*3 reporter genes constructs. The *HIS3* reporter gene construct, including the *URA3* yeast gene, was integrated into the non-functional *ura* locus. Expression of the functional *URA3* gene allows the YRG-2 strain to grow in the absence of uracil.

The stored cells were revived by streaking the splinters of cells onto YPAD agar plates, and incubated at 30°C for 2-3 days until colonies appear. The plates were sealed with Parafilm laboratory film and stored at 4°C. The colonies were re-streaked onto fresh YPAD plates every week.

Yeast host strain phenotype

The phenotype of the YRG-2 yeast host strain was verified prior to the screening assays. Fresh plates of YRG2 on YPAD agar plates were prepared from the yeast glycerol stock stock, and incubated at 30°C for 2-3 days. The SD plates were prepared using the appropriate 10x dropout solution to test the yeast host strain for nutritional requirements of tryptophan (Trp), leucine (Leu), histidine (His) and uracil (Ura). The YRG-2 strain was streaked onto the SD plates with the appropriate 10x dropout solution and incubated at 30°C for 2-3 days. The colonies of yeast host strain should only grow on SD plates without Ura, if showing functional protein interactions. Some yeast colonies also grow on SD plates without His, due to the leaky expression of the *HIS3* gene. After verifying the phenotype, the tested colonies were used to inoculate the medium for the preparation of competent yeast cells.

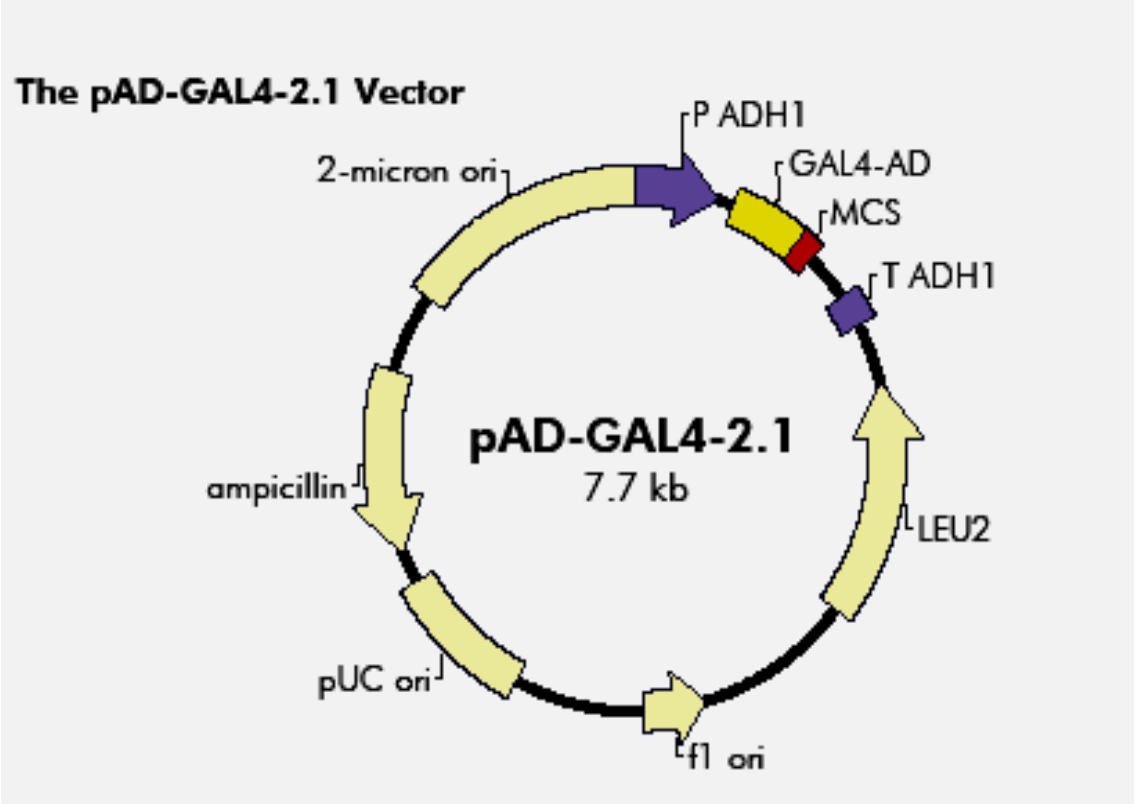


**Figure 2.6: Circular map features of the excised pAD-GAL4-2.1 phagemid**

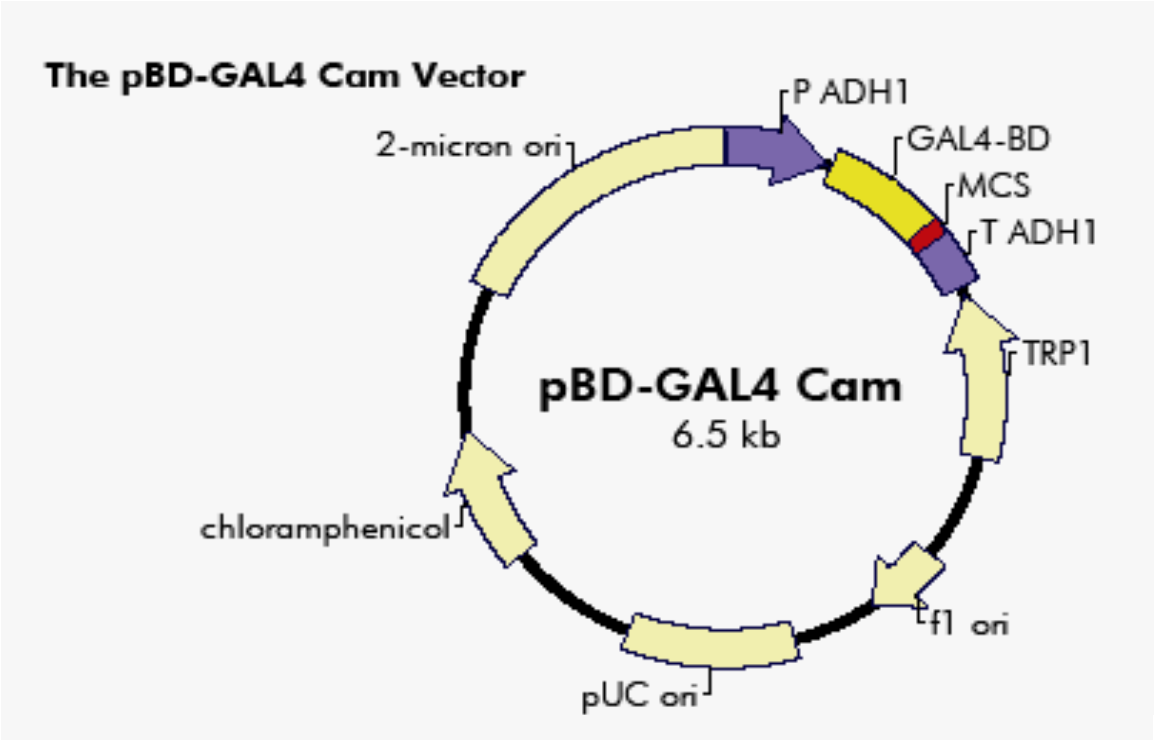


**Figure 2.7: Circular map of the pBD-GAL4 Cam phagemid vector**

## 2.14. 3: Control plasmids

The GAL4 two-hybrid vector system contains six control plasmids listed below:

| Control plasmid | Insert description | Vector | Genotype | Function |
|---|---|---|---|---|
| pGAL4 | Wild-type, full length GAL4 | pRS415 | LEU2, $Amp^r$ | Positive control |
| pBD-WT | Wild-type fragment C of lamda cl repressor (aa 132-236) | pAD-GAL4 Cam | TRP1, $Cam^r$ | Interaction control |
| pAD-WT | Wild-type fragment C of lamda cl repressor (aa 132-236) | pBD-GAL4 2.1 | LEU2, $Amp^r$ | Interaction control |
| pBD-MUT | E233K mutant fragment of lamda cl repressor (aa 132-236) | pBD-GAL4 Cam | TRP1, $Cam^r$ | Interaction control |
| pAD-MUT | E233k mutant fragment of lamda cl repressor (aa 132-236) | pAD-GAL4 2.1 | LEU2, $Amp^r$ | Interaction control |
| pLaminC | Human Lamin C (aa 67-230) | pBD-GAL4 | TRP1, $Amp^r$ | Negative control |

The pGAL4 control plasmid expresses the entire coding sequences of the wild type GAL4 protein. The pBD-WT control plasmid expresses the DNA-binding domain (BD) of GAL4 and amino acids (aa 132-236) of the wild-type lamda cI, fragment C as a hybrid protein. The pAD-WT control plasmid expresses the activation domain (AD) of GAL4 and amino acids (aa 132-236) of the wild-type lamda cI, fragment C as a hybrid protein.

These plasmids were used alone or in pairwise combination as positive and negative controls for the induction of the *HIS3* and *lacZ* genes. Induction of the *HIS3* gene enables the transformed host to grow on SD medium without His. Similarly, induction of the *lacZ* gene was detected by cleavage of the chromogenic substrate causing the transformed host to turn blue in colour. The pGAL4 control plasmid was used alone to verify that induction of the *lacZ* and *HIS3* genes has occurred and that the gene products are detectable in the assay used. The pLamin C control plasmid was used in pairwise combination with the pAD-WT control plasmid or with the pAD-MUT control

plasmid to verify that the *lacZ* and *HIS3* genes are not induced as the protein expressed by each of these pairs do not interact *in vivo*. The degree of colour development of the transformed host depends on the strength of interaction of the expressed proteins. The pBD- WT and pAD-WT control plasmid express proteins that interact strongly *in vivo* and the host turns blue in colour. The pBD-MUT and pAD-MUT control plasmids express proteins that interact weakly *in vivo*, and the transformed colonies turn light blue in colour.

## 2.14.4: Activation Domain and DNA-Binding Domain vector construction

DNA that encodes the target (ETR1) and bait (PLS) was inserted into the pAD-GAL4-2.1 A and pBD-GAL4 Cam phagemid vectors respectively and expressed as hybrid protein. The hybrid proteins were then assayed for protein-protein interaction.

### 2.14.4.1: Target and Bait Protein Insert preparation

DNA encoding the target and bait proteins were prepared by PCR amplification using primer designed the specifically for the DNA encoding the target (ETR1) and bait (PLS). Each set of primer contained specific endonucleases on the ends of primer corresponding to the endonucleases in the MCS of pAD-GAL4-2.1 A and pBD-GAL4 Cam phagemid vectors. The DNA construct of the target (ETR1) and bait (PLS) with specific restriction sites on the ends was then transformed into the TOPO 2.1 vector to check the sequence of the amplified DNA by sequencing with M13 forward (CTG GCC GTC GTT TTA C) and M13 reverse (CAG GAA ACA GCT ATG AC). The two vectors, pAD-GAL4-2.1 and pBD-GAL4 Cam were digested using specific restriction endonucleases and dephosphorylated prior to ligating the insert DNA. The DNA encoding the target (ETR1) and bait (PLS) was then ligated into the same reading frame as the GAL4 AD of the pAD-GAL4-2.1 phagemid vector and the GAL4 BD of the pBD-GAL4 Cam phagemid vector.

The following primers were used for PCR amplification:

ETR1:

Forward primer GAA TCC ATG GAA GTC TGC AAT TGT A (Eco RI on 5’ end)

Reverse primer GTC GAC TTA CAT GCC CTC GTA CA (Sal I on 5’end)

PLS:

Forward primer CTG GAG ATG AAA CCC AGA CTT TGT (Xho I on 5’ end)

Reverse primer GTC GAC ATG GAT TTT AAA AAG TTT (Sal I on 5’ end)

## 2.14.4.2: Ligation

In ligation, the ideal ratio of insert-to-vector DNA can be variable. In general a 3:1 and 2:1 (vector: insert) ratio was used for ligation in this experiment. For different inserts, the concentration of the insert with a vector of known size and concentration was calculated using the following formula:

$$\text{Insert (ng)} = \frac{\text{vector (ng)} \times \text{insert (kb)}}{\text{vector (kb)}} \times \text{ratio of insert}$$
$$\text{ratio of vector}$$

Ligation reactions were incubated at 4°C overnight.

## 2.14.4.3: Transformation

1-5 µl of ligation mix was transformed into XL1- Blue MRF' competent cells and plated on selective media. 3-4 isolated colonies were selected for miniprep analysis to identify transformed colonies containing the pAD-GAL4 2.1 and pBD-GAL4 Cam phagemid vector with the DNA insert. The following oligonucleotide primers were used to identify recombinants and to determine the nucleotide sequence of the DNA insert:

| Vector | Primer | Binds to nucleotide | Nucleotide sequence (5' -3') |
|---|---|---|---|
| pAD-GAL4-2.1 | 5' AD | 745-765 | AGGGATGTTTAATACCACTAC |
| | 3' AD | 962-982 | GCACAGTTGAATGTAACTTGC |
| pBD-GAL4 Cam | 5' BD | 816-836 | GTGCGACATCATCATCGGAGG |
| | 3' BD | 1021-1041 | CCTAAGAGTCACTTTAAAATT |

## 2.14.5: Yeast Transformation

The control plasmids were transformed into the YRG-2 strain prior to the initial transformation of the bait and the target plasmids. The control plasmids were used separately or in pairwise combination in the transformation of the YRG-2 yeast strain. The yeast competent cells were cotransformed with the bait and target plasmids by sequential transformation. First, yeast were transformed with the bait plasmid and

assayed for expression of reporter genes. Second, yeast competent cells containing the bait were prepared and transformed with the target plasmid.

### 2.14.5.1: Preparation of Yeast Competent Cells

The yeast culture was prepared as follows:

1 ml of YPAD broth was inoculated with 2-4 YRG-2 yeast colonies in a 1.5 ml microcentrifuge tube. The culture was vortex mixed vigorously until no cell clumps were visible. This 1 ml yeast culture was added to 50 ml of YPAD broth in a 250 ml flask. The diluted culture was incubated for 18-24 hours at 30°C with constant shaking at 225-250 rpm.

The optical density of the culture was measured at 600 nm wavelength to 1.2.

The 50 ml yeast culture was added to 300 ml of YPAD broth in a 1-litre flask and incubated for 3 hours at 30°C with constant shaking at 225-250 rpm. The cells were harvested at 1000 xg for 5 minutes at room temperature. The supernatant was discarded and the cells were resuspended in 50 ml of deionized water. The cells were spun again at 1000 xg for 5 minutes at room temperature. Finally the supernatant was discarded and the cells were resuspended in 1.5 ml of freshly prepared TE-LiAc solution. The yeast competent cells were freshly prepared prior to transformation.

### 2.14.5.2: Transformation of yeast competent cells

The carrier DNA was prepared by boiling salmon sperm DNA (20 mg/ml) for 20 minutes followed by cooling on ice.

100 µl of yeast competent cells and 100 µg of carrier DNA were aliquoted per microcentrifuge tube using a wide-bore pipette tips.

100 ng of the desired plasmid for single transformation and 200 ng of each plasmid for pairwise transformation were added to each tube.

600 µl of TE-LiAc-PEG solution was added to each and the contents were mixed together by vortexing.

The microcentrifuge tubes containing the transformation reaction were incubated at 30°C for 30 minutes with constant shaking at 225-250 rpm.

70 µl of DMSO was added to each tube and mixed gently.

The samples were heat-shocked for 15 minutes in a 42°C water bath and the tubes were then replaced on ice for 10 minutes.

The samples were centrifuged for 10 seconds at 3000 rpm to pellet the cells. The supernatant was carefully removed and the pellet was resuspended in 0.5 ml of 1x TE buffer.

The transformed cells were plated on appropriate SD-selective plates using wide-bore pipet tips. 150 µl of transformed cells for single transformation and 125 µl of transformed cells for pairwise transformation were plated on two 100 mm plates.

The plates were incubated at 30°C for 2-4 days until colonies appear.

The colonies were then picked and screened to confirm the interaction.

Result expected for interaction between control plasmid are outlined in the following table:

| Yeast transformation | Purpose of control | SD medium | Expected results |
|---|---|---|---|
| pBD-WT and pAD-WT | Positive interaction | SD agar plates without Leu, Trp and His | Growth, Blue colonies |
| pBD-MUT and pAD-MUT | Positive interaction | SD agar plates without Leu, Trp and His | Growth, Light blue colonies |
| pLamin C and pAD-WT | Negative interaction | SD agar plates without Leu, Trp and His | No growth |
| pLamin C and pAD-MUT | Negative interaction | SD agar plates without Leu, Trp and His | No growth |
| pGAL4 | Positive interaction for *lacZ* expression | SD agar plates w/o Leu | Growth, Blue colonies |
| pBT-WT | Negative interaction for *lacZ* expression | SD agar plates w/o Trp | Growth, White colonies |

Once the expected results were obtained, the yeast competent cells containing the bait plasmid were prepared for transformation with the target plasmid. The following modifications were incorporated into the protocol for the target plasmid transformation:

1 ml of SD medium lacking Trp was inoculated 2-4 yeast colonies containing the bait plasmid, followed by inoculation of 50 ml of SD medium lacking Trp with this 1 ml bait plasmid culture.

1 ml yeast competent cells containing the bait plasmid was added to each 50 ml conical tube. 2 mg of salmon sperm was also added to the same conical tube.

40 µg of each target plasmid to be transfected was added to each conical tube.
6 ml of TE-LiAC-PEG solution was added to each tube, vortexed to mix the content.
Followed by addition of 700 µl of DMSO and centrifugation of the tubes at 1000 x g for 5 minutes.

The pellet was resuspended in 10 ml 1 x TE and 1 µl, 10 µl and 100 µl of the transformed cells were plated to SD plates lacking Leu and Trp. The remaining transformed cells were plated on SD agar plates lacking His, Leu and Trp at 250 µl of transformation/100-mm plate.

## 2.14.6: Assay for expression of reporter genes

Colonies that grow on SD agar plates without His, Trp and Leu are either due to leaky expression of the *HIS3* reporter gene or because of the specific interaction between the bait and the target protein resulting in expression of the *HIS3* gene.

To distinguish between leaky expression cand specifically interacting proteins, detection of the expression of the second reporter gene (*lacZ*) was determined by a filter lift assay.

### 2.14.6.1: Filter lift assay

**Solutions:**

Z Buffer stock solution (per litre)

16.1 g of $Na_2HPO_4.7H_2O$

5.5 g of $NaH_2PO_4.H_2O$

0.75 g of KCl

0.246 g of $MgSO_4 . 7H_2O$

1 litre of $dH_2O$ was added and the pH was adjusted to 7.0. Autoclaved and stored at 4 °C.

Z buffer with X-gal (100 ml)
98 ml of Z buffer
0.27 ml of β-mercaptoethanol
1.67 ml of X-gal stock solution

**Method:**

The transformed colonies were allowed to grow for 3-7 days until the colonies were 1-2 mm in diameter.

The Z buffer was prepared with X-gal and 2 ml of Z buffer with X-gal to the bottom of a 100 mm Petri dish. A sterile qualitative filter paper was added to the dish.

A separate piece of sterile piece was labelled. The paper was held with forceps and was slowly placed on the wet filter paper on the plate ensuring that it touched all the colonies on the plate.

The filter paper was lifted carefully from one side and dipped in liquid nitrogen for 10 seconds. The filter paper was removed from liquid nitrogen and was allowed to thaw (colony side up). This step was repeated two or three times with each.

The thawed filter papers with colony side up were placed carefully onto the filter paper soaked in the Z buffer with X-gal.

The plates containing the filter paper were incubated at room temperature for 6 hours.

During the incubation, the colonies containing the pGAL4 control turned blue. The pAD-WT and pBD-WT cotransformants turned to a similar shade of blue. The pAD-MUT and pBD-MUT cotransformant turned light blue. No colour change was observed in the pAD-WT and the pLaminC cotransformants.

## 2.15: Gateway Cloning using Invitrogen Gateway® Technology

Gateway® Technology is a universal cloning method based on the site-specific recombination properties of bacteriophage lamda (Landy, 1989). It provides a rapid and highly efficient way to move DNA sequences into multiple vector system for function analysis and protein expression (Harley et al., 2000). Gateway® Technology provides the following advantages:

- Enables rapid and highly efficient transfer of DNA sequences into multiple vector systems for protein expression and functional analysis while maintaining orientation and reading frame.
- Permits use and expression from multiple types of DNA sequences.
- Easily accommodates the transfer of a large number of DNA sequences into multiple destination vectors.

Lamda recombination is catalyzed by a mixture of enzymes that bind to specific sequences (*att* sites), bring together target sites, cleave them and covalently attach the DNA. Recombination occurs following two pairs of strand exchanges and ligation of the DNAs in a novel form. The recombination proteins involved in the reaction differ depending upon whether lamda utilizes the lytic or lysogenic pathway.

The lysogenic pathway (BP reaction) is catalysed by the bacteriophage λ Integrase (Int) and *E.coli* Integration Host Factor (IHF) proteins (BP Clonase$^{TM}$ enzyme mix) while the lytic pathway (LR reaction) is catalysed by the bacteriophage λ Int and Excisionase (Xis) proteins, and the *E.coli* Integration Host Factor (IHF) protein (LR Clonase$^{TM}$ enzyme mix).

## 2.15.1 Designing *attB* PCR Primers

The *attB* sites were introduced into the PCR product to make it suitable substrate in a BP reaction with a donor vector. The forward primer must contain following structure, to enable efficient Gateway® cloning:

- Four guanine (G) residues at the 5' end followed by
- The 25 bp *attB* site followed by
- At least 18-25 bp of template or gene-specific sequences

The *attB1* site ends with a thymine (T). In order to fuse the PCR product in frame with an N-terminal tag, the primer must include two additional nucleotides to maintain the proper reading frame with the *attB1* region. These two nucleotides cannot be AA, AG, or GA, because these additions would create translation termination codon.

In order to fuse the PCR product in frame with a C-terminal tag, the primers must include one additional nucleotide to maintain the proper reading frame with the *aatB2* region and any in-frame stop codons between the *attB2* site and the gene of interest must be removed.

The following primers were designed using the above mentioned features for Gateway® cloning to construct vectors for the BiFC and localisation experiment:

1. **Bifc_nt-fusion:**
   GGGGACAAGTTTGTACAAAAAAGCAGGCTTCACCATGAAACCCAGACTTT
   GTTTTAATTTCAG

2. **Bifc_ct-stop:**
   GGGGACCACTTTGTACAAGAAAGCTGGGTCCTAATGGATTTTAAAAAGTTTAAACAATTTTGCTACTAATAAATAAG
3. **Bifc_ct:**
   GGGGACCACTTTGTACAAGAAAGCTGGGTCATGGATTTTAAAAAGTTTAAACAATTTTGCTACTAATAAATAAG
4. **PLS_Prom**
   **forward:**GGGGACAAGTTTGTACAAAAAAGCAGGCTTCAAGCTTTAGCCCGTGCGG

## 2.15.2: Producing *attB*-PCR products

The *attB*-PCR products were prepared by amplification of *pls* sequence from TOPO 2.1 vector containing the cloned *pls* sequence using the Bifc_nt-fusion, Bifc_ct and Bifc_ctstop primers. The PLS_Prom forward and Bifc_ct primers were used to amplify the *pls* sequence with 1.5 kb *pls* promoter sequences.

Finnzymes' Phusion $^{TM}$ High-Fidelity DNA polymerase from New England BioLabs was used to perform a PCR reaction as follows:

Reaction Mixture (50 µl reaction):

| | |
|---|---|
| 5 x Phusion HF Buffer | 10 µl |
| 10 Mm dNTPs | 1 µl |
| Forward primer (10pM/ µl) | 2.5 µl |
| Reverse primer (10Pm/ µl) | 2.5 µl |
| Phusion DNA Polymerase | 0.5 µl |
| Template DNA | 1 µl |
| $dH_2O$ | 33.5 µl |

Due to the novel nature of Phusion DNA polymerase, optimal reaction conditions differ from standard enzymes. Phusion DNA polymerase tends to work better at elevated denaturation and annealing temparatures due to a higher salt concentration in its buffer.

**Cycling:**

| | | | |
|---|---|---|---|
| Intial denaturation | 98 °C | 30 seconds | 1 cycle |
| Denaturation | 98 °C | 5-10 seconds | 25-35 cycles |

| | | | |
|---|---|---|---|
| Annealing | 55°C | 1 minutes | |
| Extension | 72 °C | 15-30 seconds | |
| Final extension | 72 °C | 10 minutes | 1 cycle |
| Hold | 4 °C | - | |

5 µl of PCR product was removed from each tube and was quantified using agarose gel electrophoresis.

The BP recombination facilitates transfer of a gene of interest in an *att*B-PCR product to an *att*P-containing donor vector to create an entry clone. Once the entry clone was created, the gene of interest was shuttled into a large selection of destination vector using the LR recombination reaction.
The entry clone was generated by:

- Performing a BP recombination reaction using the appropriate *att*B- and *att*P-containing substrates
- Transformation of the BP reaction mixture into a suitable *E. coli* host ( DH5α)Selection of the entry clone.
- Procedure:
- Following components were added to a 1.5 ml microcentrifuge tube and mixed together at room temperature:

| | |
|---|---|
| attB-PCR product (100 ng) | 5 µl |
| Donor vector (pDONR™207, 150 ng/µl) | 1 µl |
| TE buffer, pH 8.0 | 2 µl |
| BP Clonase™II enzyme mix | 2 µl |

The reaction was incubated at 25°C for an hour. 1 µl of Proteinase K solution was added to each tube to terminate the reaction, vortexed and incubated at 37 °C. The reaction mixture is then transformed into suitable E. coli competent cells.

## 2.15.3: Transformation of DH5α competent cells

The DH5α™ E.coli cells were made competent using Rubidium Chloride Method (see method 2.9) to make competent cells.

**Method**

5 µl of the BP reaction was added to 250 µl of DH5α competent cells and mixed gently. The competent cells are then incubated on ice for 30 minutes, followed by heat-shock at 42°C for 30 seconds without shaking. The cells were immediately transferred to ice after heat-shock and incubated for 10 minutes. 1 ml of room temperature S.O.C medium was added to the cells and tubes were incubated at 37°C for 1 hour with constant shaking (200 rpm). The cells were spun in a bench top centrifuge for 1 minute at 12000 rpm and 1 ml of the supernatant was removed. The cell pellet was then resuspended in the remaining supernatant. 50 µl and 100 µl of each transformation mix was then spread on selective media plate and incubated overnight at 37°C.

**Sequencing Entry Clones**

M13 sequencing primers were used to check the entry clones derived from BP recombination with pDONR 207.

## 2.15.4: The LR recombination reaction

After generating the entry clone, the LR reaction was performed to transfer the gene of interest into an attR-containing destination vector to create an attB-containing expression clone.

An expression clone was generated by:

Performing an LR recombination reaction using the appropriate attL and attR containing substrates

Transforming the reaction mixture into a suitable E.coli host

Selection for expression clone using suitable antibiotic selection

**Procedure:**

Following components were added to a 1.5 ml microcentrifuge tube and mixed together at room temperature:

| | |
|---|---|
| Entry clone (100 ng) | 5 µl |
| Destination vector (150 ng/ µl) | 1 µl |
| TE buffer, pH 8.0 | 1 µl |
| LR Clonase™ II enzyme mix | 2 µl |

LR Clonase™ II enzyme mix was thawed on ice for 2 minutes and vortexed briefly before being added to the reaction mix. The reaction was incubated at 25°C for 1 hour

and 1 µl of Proteinase K solution was added to the reaction mixture to terminate the reaction with 10 minutes incubation at 37°C.

5 µl of LR reaction mixture was transformed in 250 µl of DH5α™ competent cells using the protocol described above and 100 µl of each transformation mix was then spread on selective media plates and incubated overnight at 37°C.

## 2.15.5: "One-Tube" Protocol for cloning attB-PCR products directly into the destination clone

1. 25 µl of BP reaction was prepared in a 1.5 ml microcentrifuge tube:

| | |
|---|---|
| *att*B DNA (100-200 ng) (PCR product) | 5.0 µl |
| *att*P DNA (pDONR™ vector, 150 ng/ µl) | 2.5 µl |
| 5 X BP reaction buffer | 5.0 µl |
| BP Clonase™ enzyme mix | 5.0 µl |
| TE buffer, pH 8.0 (added to make the final volume of | 25 µl |

2. The BP reaction was mixed well by vortexing briefly and then incubated at 25°C for 4 hours. After 4 hours 5 µl of the reaction was removed into a separate tube and was used to assess the efficiency of BP reaction by transforming into DH5α™ competent cells.
3. The following were added to the remaining 20 µl reaction:

| | |
|---|---|
| Destination vector (150 ng/ µl) | 3.0 µl |
| LR Clonase™enzyme mix | 6.0 µl |
| 0.75 M NaCl | 1.0 µl |
| Final volume | 6.0 µl |

The LR reaction mix was mixed well by vortexing and incubated at 25°C for 2 hours. 3 µl of Proteinase K solution was added and the reaction mix was incubated at 37°C for 10 minutes. 5 µl of the reaction mix was transformed into 500 µl of DH5α™competent cells and finally 50 µl of transformed cells were plated on LB plates containing the appropriate antibiotic.

## 2.16: Bimolecular florescence complementation (BiFC) assay

BiFC is a method of visualising protein-protein interaction *in vivo* (Hu et al., 2002). It is based on the principle of reassembly of yellow fluorescent protein (YFP) fragments. Each of the N- and C-terminal halves of the protein is fused to the putative interacting partners which leads to restoration of the restoration of the fluorescence within a cell

by reconstitution of the split flurophore. The advantage of the BiFC assay over other methods is that it gives an indication of the interaction as well as the cellular localisation of the complex.

## 2.16.2: Construction of Expression clones

Gateway cloning protocol was used to make the expression clones, by fusing the target and the bait protein to N- and C-termini of YFP

## 2.16.3: Binding DNA to Gold particles

DNA samples for transient expression and BiFC analysis were introduced into plant (onion) tissues by particle bombardment. Onion tissues were used because they lack chlorophyll, allowing clear visualization of YFP. 1 cm sections of gold-coat tubing were covered with DNA bound to the gold particles to function as cartridges for the Helios™Gene gun.

**Reagents required:**

Fresh 100 % ethanol

PVP (Polyvinylpyrrolidone) 360,000 MW (hydrophilic polymer)

Fresh 0.05M Spermidine free-base NOT complexed with HCl

1M $CaCl_2$

Gold particles 1.0 micron (cat no. 1652262)

Plasmid -1 µg/µl concentration, buffered in 10mM Tris, pH-8.0

**Preparation:**

A stock solution of 20 mg/ml PVP in 100 % ethanol was prepared and stored in a screw-cap tube by sealing the lid with parafilm. From this stock solution a working stock of 0.05 mg/ml of PVP in 100 % ethanol was prepared.

25 mg of Gold particles were weighted in a 1.5 ml tube.

**Method:**

500 µl of freshly made spermidine was added to 25 mg gold particles and the gold suspension was vortexed for few seconds.

500 µl of plasmid DNA (1µg/ µl) was added to the mixture of spermidine and gold particles. In the case of adding multiple plasmids, the plasmids were mixed together

before adding to the gold suspension to ensure even coating. The final concentration of the plasmid DNA was maintained at 1 µg/ µl to avoid clumping of particles.

The gold suspension together with the plasmid was vortexed for 5 seconds. While vortexing, 500 µl of 1 M $CaCl_2$ was added drop-by-drop to this gold suspension.

The mixture was allowed to precipitate at room temperature for 10 minutes and was spun at 5,000 rpm for 15 seconds to remove the supernatant.

The pellet was washed twice with 1 ml of 100 % ethanol and centrifuged for 5 seconds at 5, 000 rpm between each wash.

The pellet was finally resuspended in 3ml of 0.05 mg/ml PVP and was stored at -20°C until used in a screw-cap tube.

## 2.16.4: Loading suspension onto the plastic tubing

The tubing prep station (from Bio Rad™) was attached to the nitrogen cylinder using the luer barb fitting on the machine.

A 65 cm-long section of the plastic tubing was inserted to from the right hand side of the machine into the O-ring at the other end of the cylinder. The ends were trimmed using the Bio Rad™tubing cutter.

The plastic tubing was dried by blowing nitrogen through the tube for 15 minutes. The valve on the top of the nitrogen cylinder was turned anti-clockwise to feed into the regulator. The regulator was turned clockwise until the left-hand gauge registers 2 psi of pressure. The output valve of the tubing prep station was turned anti-clockwise to allow the nitrogen to pass into the tube. 0.3 -0.4 LPM (litres per minute) of nitrogen was allowed to flow in to the tubing prep station. After 15 minutes the nitrogen was disengaged by closing both the regulator and the output valve.

The plastic tubing was removed from the tubing prep station and one end of the tubing was attached to a syringe.

The gold suspension was vortexed and the free end of the tubing was dipped into the suspension and it was sucked slowly avoiding any bubbles using the syringe. The plastic tubing containing the gold suspension is immediately replaced on the tubing prep station and the gold left to settle at the bottom of the tubing for 5 minutes.

Once the gold settled at the bottom of the tubing, the ethanol was removed from the tubing at the rate of 1.5-3 cm per second. It takes 30 to 45 seconds to remove all the ethanol of the tubing.

The tubing prep station switch was briefly turned to position II to rotate the tube 180°. The syringe was then detached of the tubing and the switch was tuned to position I.

The tube was left to rotate for 30 seconds to allow the gold to smear evenly around the tube.

The nitrogen flow was turned on and maintained at 0.35 to 0.4 lites per minute to dry the tube for 5 minutes.

After 5 minutes the rotating tube was stopped and the nitrogen flow was shut down. The tubing was removed from the tubing prep station and the uncoated section of the tubing was chopped using the tubing cutter. 1 cm sections of gold coated tubing were made using the tubing cutter and were used as bullets for the Helios™ Genegun.

## 2.16.5: Bombarding gold particles on onion peel cell using Helios™ Genegun

The onion peel cells were prepared by taking out the inner transparent layer on an onion peel. The thin layer of the onion peel was then carefully placed on a ½ MS10 plate, with the inner side of the peel on the media and avoiding any air bubbles between the peel and the media.

The gold coated bullets were then inserted into a cartridge holder, leaving the position 1 empty. The cartridge holder was then fitted into the breach of the gun by opening the cylinder lock and push bar. The two O-rings on either side of the breach were quickly checked to ensure that the cartridge holder sits properly and safely. The push bar and the cylinder lack were closed. The cylinder advance lever was squeezed to move to position 1.

The battery was then inserted into the handle of the gun to turn it on. The Swagelok connector from the helium cylinder was attached to the base of the gun and pushed in until it makes a clicking sound. The helium cylinder was opened by turning anti-clockwise. The regulator was adjusted to 250 psi pressure of helium by turning it clockwise. The advance level was squeezed in to allow the helium to kick in the valve and the gun was fired twice to ensure it was pressurised correctly.

The Helios™Gene gun was then placed on to the onion peel on ½ MS10 and the trigger was pulled while holding the safety interlock button to fire. 5-10 bullets were fired onto small section of onion peel.

The ½ MS10 plates containing the bombarded onion peel were covered with aluminium foil and incubated at 22° C in the tissue culture room for 10-15 hours. All the control and the samples must be incubated for equal time to detect the difference in the fluorescence.

After incubation, the onion peel was placed on a glass slide with a drop of water, covered with coverslip and viewed under a Bio Rad confocal microscope to detect fluorescence in the samples.

## 2.17: Propidium iodide (PI) staining:

The seedlings to be analysed were grown 4-5 d.a.g. Before viewing under confocal microscope, the root tips of the seedlings were cut and were stained with 10 mg/ml propidium iodide for 1 minute on a glass slide. The root tips were then carefully washed with water and were transferred to a glass slide with a drop of water. The glass slides were then covered with cover glass and viewed under confocal microscope.

## 2.18: Confocal Microscopy:

BioRad Microradiance confocal microscope was used analyse the seedling root tips of the mutants expressing GFP root cell marker lines and to view the results from Bimolecular florescence compartmentation (BiFC) assay.

### 2.18.1: Starting up the Microscope

The steps were simple but it was important to switch the machine in the right sequence in order for it function effectively. The U.V lamps were first switched on, followed by starting the computer and the monitor. Then at the next prompt the username and password were entered into the system. The main switch A on the instrument control unit switch panel was turned on causing the adjacent LED power indicator B to lid up. The green LED power indicator on the scan head of the microscope should lid up at the same time as the LED power indicator B. The laser key switch C was tuned clockwise at 90 degrees to enable all the lasers. The button D for Argon and button E for Helium/Neon were then switched on to enable the required lasers. Once the microscope and the laser are switched on, the icon of LaserSharp 2000 on the desktop was clicked and the username and password were entered to login the software. At this point the computer goes through a built-in checklist and the various individual hardware components were checked to work properly by the system.

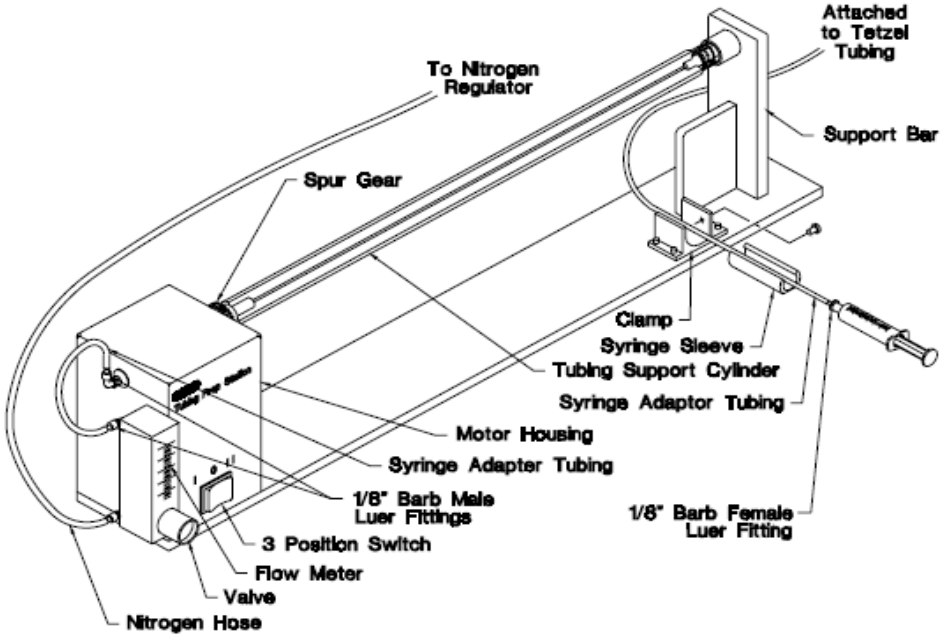


**Figure 2.8: Components and control on the tubing prep station, fully assembled**

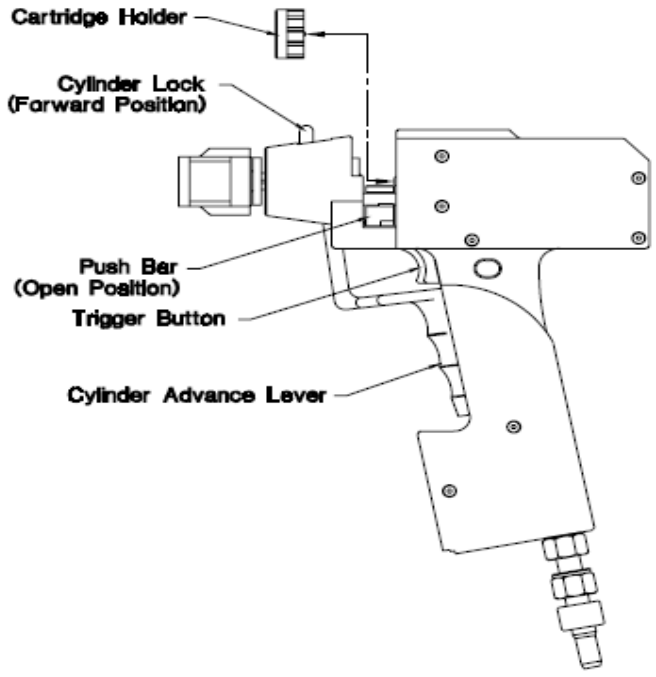


**Figure 2.9: Inserting a cartridge holder into the Gene gun**.

## 2.16.2: Collecting a single image

The sample to be viewed was freshly prepared on a microslide and covered with a glass coverslip. The sample was then viewed under the light microscope on 10x magnification. Once the correct area of the sample was found, a drop of oil was placed on the slide to view the sample on 20x magnification under the UV light. After finding the region of interest under the UV light path, the UV light path was closed and the laser light path was opened by pulling the scan head lever out and putting either the Dapi filter or no filter in place as required. A new experiment window was opened from the file menu on the tool bar of the Lasersharp 2000. The appropriate objective was selected in the Objective box in *scan control panel* (i.e 40x Oil). The Box Size was set as 1024 x 1024, Zoom = 1 and Speed = 500 lps. In the *detector control panel*, the sensitivity of instrument was increased by opening Iris to about 5 or 6 mm, setting Gain to 40-50% and adjusting laser Power to 50 %. Scanning was started by clicking on the blue starburst button. This opens a rough image in the main window. The image was further improved by optimisation.

## 2.18. 3: Optimisating the image

The single rough image collected was optimised by adjusting the setting of Iris diaphragm and laser intensity in PMT1. The Gain and Offset was adjusted with *setcol lut* loaded. The gain was increased until the structures in focus were almost gray, with few pixels of red and the offset until most of the background is green. This was repeated for PMT2 and the scanning was stopped by clicking on the blue star burst again. The Scan speed was then reduced to 100 lps and an image was scanned by clicking the blue star burst button. The scan was stopped when a smoothed and clear image was acquired.

# Results

# Chapter 3:

# Cellular patterning in the *pls* mutant root

As discussed in the Introduction to this thesis, the highly organised and stereotypic arrangement of radial cells and longitudinal cell files in the Arabidopsis root serves as an excellent tool to screen for the mutants that are divergent from this simple set pattern. A number of short root mutants have been identified in screen for genes controlling root development (Benfey *et al*., 1993; Hauser *et al*., 1995; Scheres *et al*., 1995; Helaruitta *et al*., 2000). Some of these mutants, such as *short root*, have been found to be defective in radial patterning and cause loss of internal root cell layers while others such as *cobra* and *lion's tail* mutations lead to abnormal growth of epidermal and stele cells respectively. The *sabre* mutation causes abnormal cell expansion in the root cortex cell layer and is independent of root growth rate. The short root phenotype of the *pls* mutant (Casson *et al*., 2003), coupled with short fat cells of the mutant root, is indicative of a possible defect in cellular patterning of the *pls* mutant root meristem. This chapter describes the analysis of the *pls* mutant seedling root using different GFP root cell marker lines to investigate for any patterning defects.

## 3.1: Generation of GFP root cell marker lines in the *pls* mutant

To examine the arrangement and pattern of cells in the *pls* seedling root in detail, *pls* homozygous mutant lines were crossed with five different GFP root cell marker lines (Section 2.2.6). The quiescent centre markers Q6::GFP and Q12::GFP show the patterning of the quiescent centre cells and the surrounding cortex initials and columella cells. The *SCR*::*GFP* (*SCARECROW*) marker gene encodes a putative transcription factor that controls asymmetrical cell division within ground tissues, and is expressed in the endodermis, the ground tissue stem cells and the quiescent centre (Scheres *et al*., 1995). Two Haseloff lines, J2341::GFP and J1092::GFP highlight the patterning of the endodermal cells, cortex cells and arrangement of vascular bundles in the primary seedling root of *pls* mutant.

All these *pls* x marker plant crosses were grown to the F2 generation and were genotyped for the *pls* homozygous lines to avoid any contamination in the population by heterozygotes, as the *pls* mutation is semi-dominant. Genomic DNA was extracted from the leaves of these plants using the Rapid Method for the preparation of DNA for PCR (Edward *et al*., 1991; Section 2.6.4), and following oligonucleotides were used in a PCR reaction to screen the plants for *pls* homozygous:

Pol RT: GAA AAT GAT AGG GTG ATC AAT GG; Bin 19-Tail: GGA GTC CAC GTT CTT TAA TAG TG; Pol5'-Test: GGA GAC TAA AGC GAA AAC ATA TAA AAC C (described in Section 2.3.1).

Plants homozygous for the *pls* mutation (generated by a T-DNA insertion) gave a 760 base pair product with Bin 19 -Tail and Pol5'-Test primers, and no product with the Pol RT and Pol5'- Test (data not shown). The confirmed homozygous plants were grown to the next generation (F3) and the seeds of these plants were sterilised (Section 2.2.1), plated on ½ MS10 (hard set) (Section 2.1.6.3) and were grown on vertical plates for 4-5 days post germination. The fully grown seedling roots were used for further analysis. The tips of seedling roots were cut, stained with a drop propidium iodide (10mg/ml) for 1 minute and immediately viewed under the confocal microscope (Section 2.16).

## 3.2: Expression of quiescent centre marker lines in the *pls* mutant

Primary root tissues are organised in concentric cylinders of epidermis, ground tissues and stele from outside to in (Benfey *et al*., 2005) These, in turn are made up of longitudinal cell files that originate from single cells termed initials (Scheres *et al*., 1994). Initials fulfil the minimal definition of a stem cell by producing two cells in every division; the regenerated initial and a daughter cell that differentiates progressively upon displacement by further rounds of division. Two distal tissues, the columella (central root cap) and the lateral root cap are also produced by the activity of initials. Together, initials for all tissue types surround a group of four to seven mitiotically less active cells in Arabidopsis, and other species, known as the quiescent centre (QC). The two QC GFP maker lines used here, namely Q12::GFP and Q6::GFP were kindly supplied by Prof. Philip N. Benfey, Department of Biology, Duke University.

### 3.2.1: The expression of both Q6::GFP and Q12::GFP is reduced in the *pls* mutant

The homozygous lines of the wild type (C24) and of the *pls* mutant expressing Q6::GFP were generated and analysis as described in Figure 3.1. The screened primary root tips (5 d.a.g) showed a much weaker and diffused expression of Q6::GFP in the *pls* mutant as compared to wild type (Figure 3.1). The expression of Q6::GFP in C24 is localised (as seen in longitudinal section) in the two central quiescent center cells, four initial cells under (distal to) the QC and in four layers of cells of columella. In contrast, in the *pls* mutant the expression of Q6::GFP can be seen strongly only in the QC cells, with weak expression in the initials and in only two layers columella.

In the case of the Q12::GFP marker, it is expressed in C24 in the two central QC cell and the initials of endodermis, cortex and stele in the primary root tips (five days after

germination). However, the level of expression of Q12::GFP in the *pls* mutant is barely detectable (Figure 3.2).

Little is known about the molecular mechanism that determines the properties of the QC or initial cells. However, stem cell fate has been correlated with the position of a local maximum of auxin phytohormone perception in the QC and columella root cap initials (Sabatini *et al*., 1999), which regulates expression of the *PLT* genes that control cell identity at that position (Aida *et al.* 2004). SCR and SHR also play roles in QC specification (Sabatini *et al*., 2003).

## 3.3: Expression of *SCR::GFP* in the *pls* mutant

The *SCARECROW* (*SCR*) gene encodes a putative transcription factor (Di Laurenzio *et al*., 1996) that is expressed in QC precursor cells during embryogenesis, after which it extends to the initial cells for the ground tissues (cortex and endodermis) (Wysocka-Diller *et al*., 2000). In *scr-1* mutants, the asymmetric division of the daughter of the cortex/ endodermis initial does not occur, resulting in a single cell layer with mixed identity (Di Laurenzio *et al*., 1996). Importantly, the cells in the *scr-1* region are aberrant in shape and roots ultimately cease growth (Scheres *et al*., 1995; Di Laurenzio *et al*., 1996). In the primary root of the *pls* mutant (at 5 d.a.e.), *SCR*::GFP expression is lower and diffuse but still confined to a single endodermis layer, compared to wild-type (C24) primary root (Figure 3.3). Interestingly, the size of the cells of columella in the *pls* mutant root is smaller and their organization is more constricted in comparison to wild-type (Figure 3.4). The number of layers of columella cells in *pls* was reduced to four compared to six layers in wild type (C24) (Figure 3.4).

## 3.4: Expression patterns of J2341 and J1092 enhancer trap lines in the *pls* background

To investigate the patterning of the cells around the QC in the *pls* mutant, two enhancer trap lines from the Jim Haseloff enhancer trap collection (http://www.plantsci.cam.ac.uk/Haseloff) were used, J2341 and J1092; these mark the ground tissue and vascular initials (Figure 3.5) and the lateral root cap and QC (Figure 3.6) respectively.

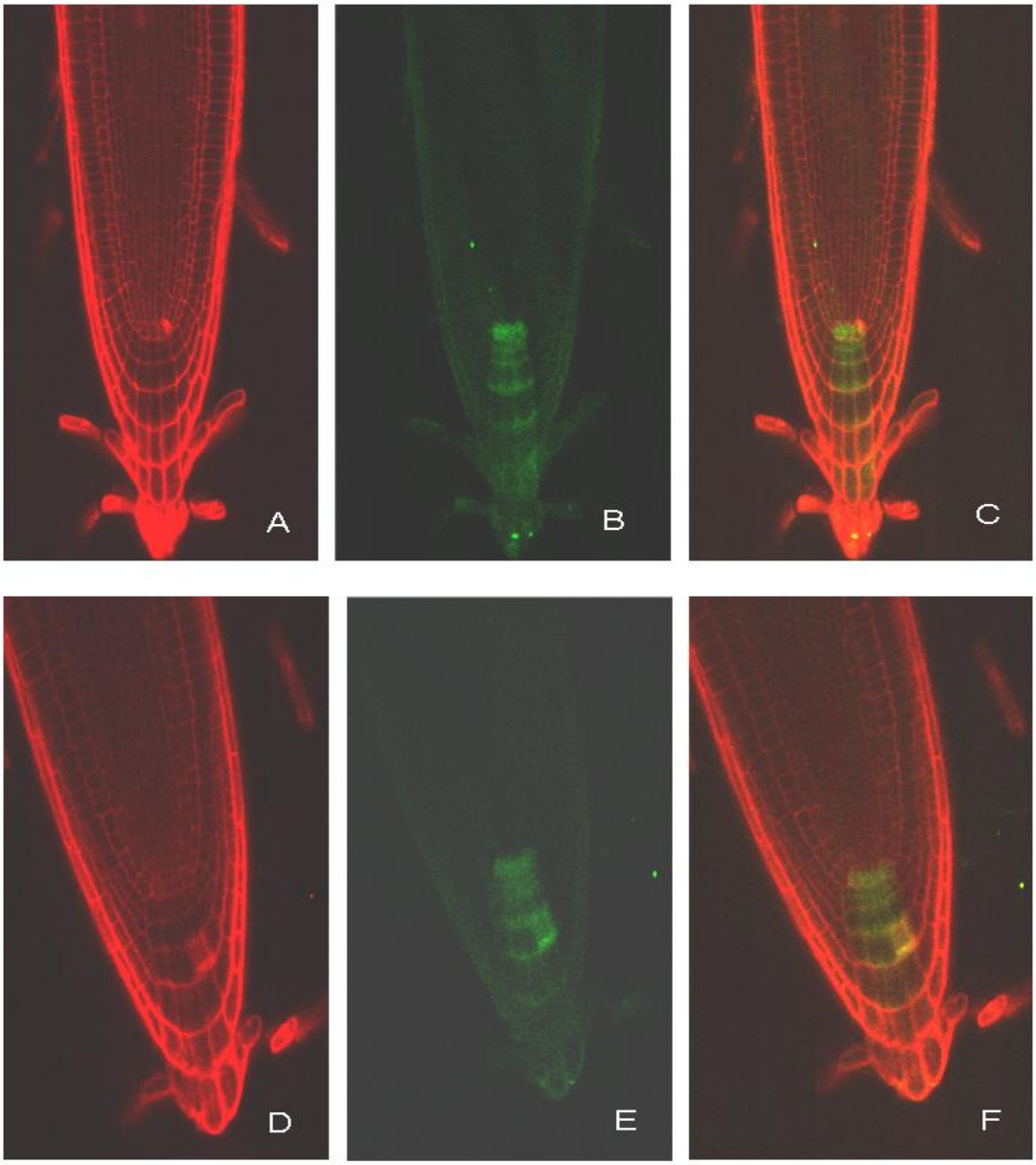


**Figure 3.1: Expression of Q6::GFP in wild type (C24) and in the *pls* mutant seedling root (5 d.a.g).** A) Wild type (C24) seedling root stained with propidium iodide (10mg/µl). B) Wild type seedling root showing Q6::GFP expression in the two central QC cells and in the surrounding initials and columella cells. C) Wild type seedling root showing Q6::GFP expression counterstained with propidium iodide. D) Root tip of the *pls* mutant stained with propidium iodide. E) *pls* mutant root showing reduced Q6::GFP expression in the QC cells and columella initials. F) Root tip of the *pls* mutant showing Q6::GFP expression counterstained with propidium iodide.

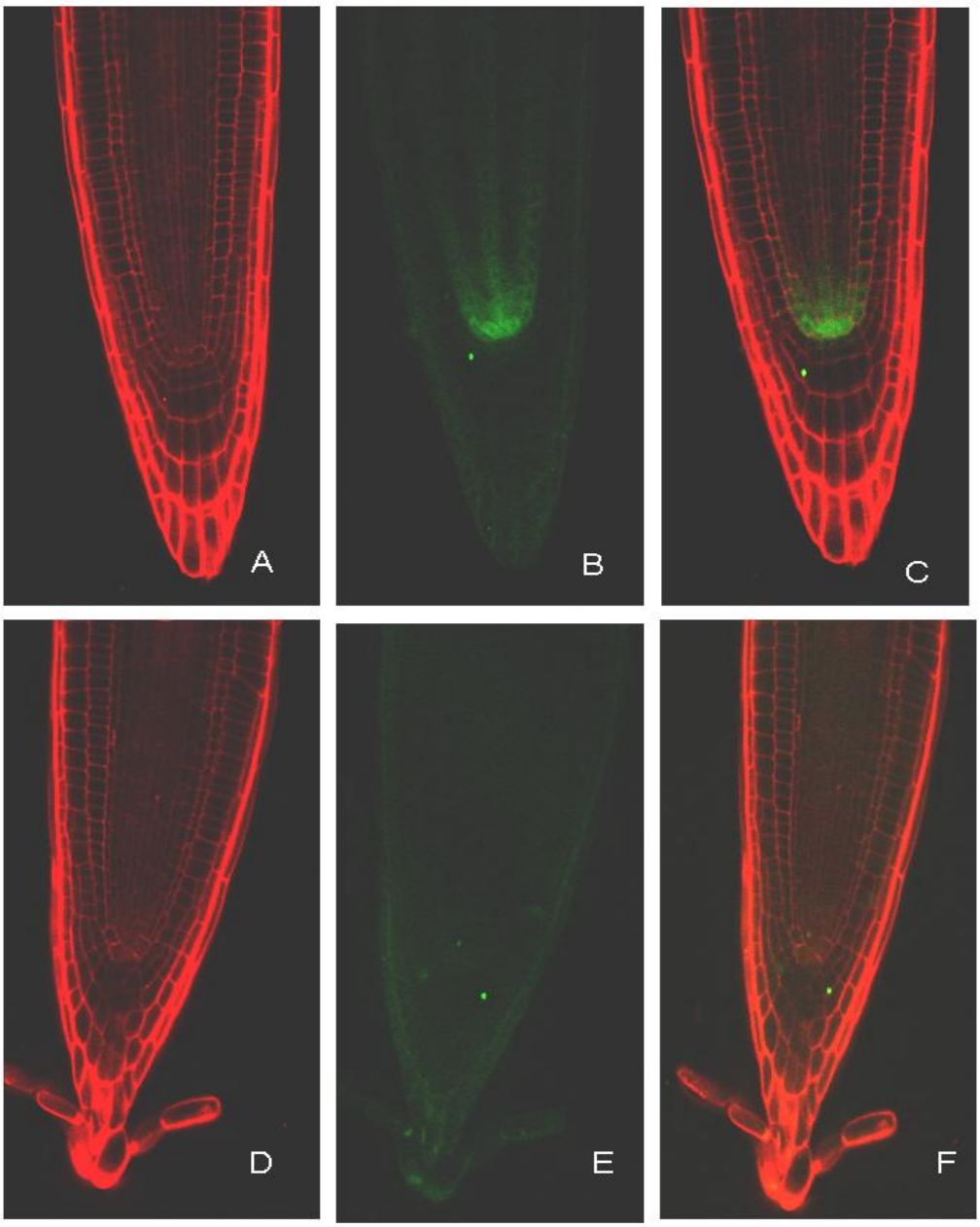


**Figure 3.2: Expression of Q12::GFP in wild-type (C24) and in the *pls* mutant.** A) Wild type (C24) seedling root stained with propidium iodide (10mg/µl). B) Wild type seedling root showing Q12::GFP expression in the two central QC cells and in endodermal and stele initials. C) Wild type seedling root showing Q12::GFP expression counterstained with propidium iodide. D) Root tip of the *pls* mutant stained with propidium iodide. E) *pls* mutant root showing undectectable Q12::GFP expression F) Root tip of the *pls* mutant showing no Q12::GFP expression counterstained with propidium iodide.

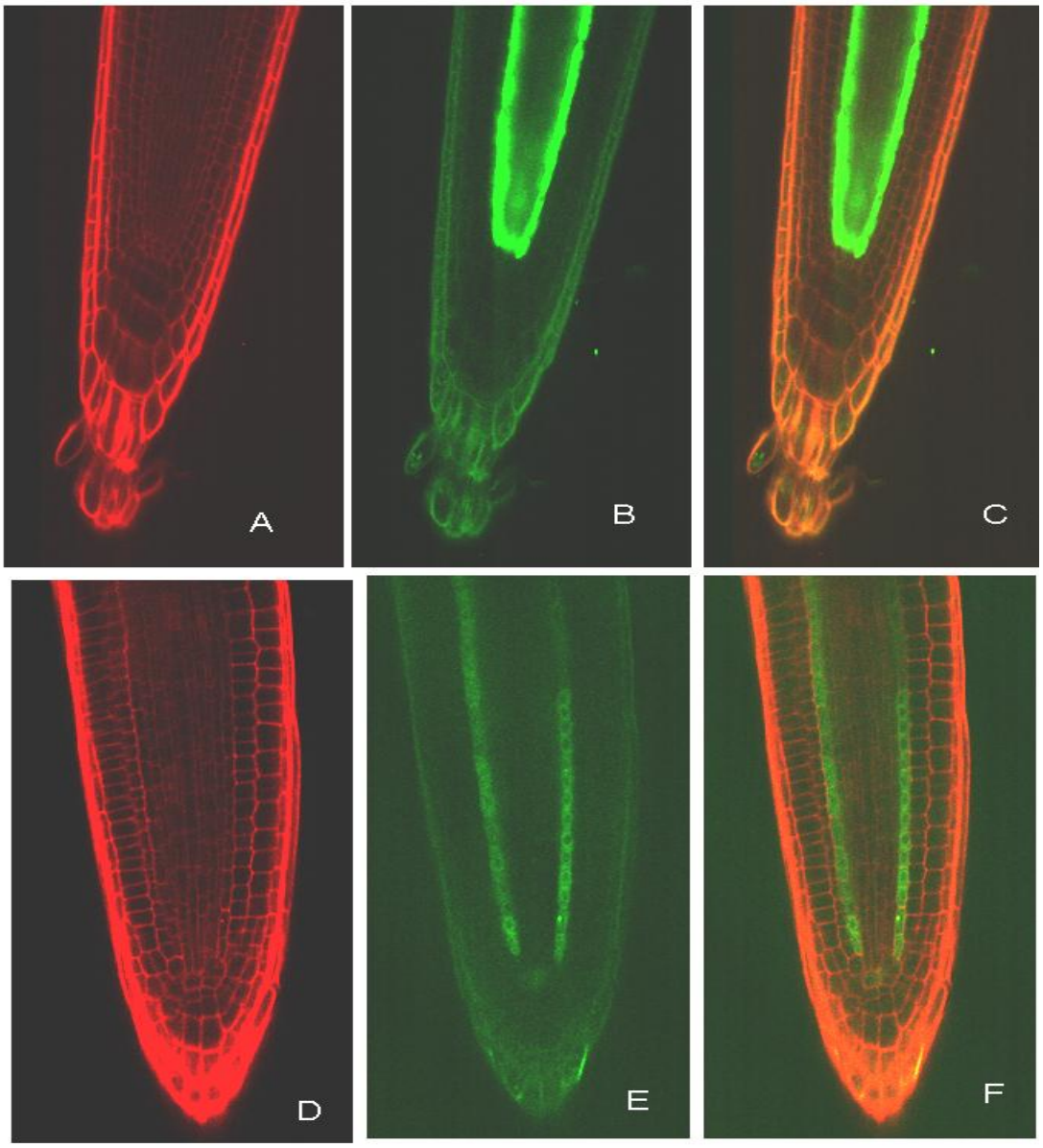


**Figure 3.3: Expression of *SCR*-GFP in C24 and *pls* mutant primary root (5 d.a.g).** A) Wild type (C24) seedling root stained with propidium iodide (10mg/µl). B) Wild type seedling root showing SCR::GFP expression in the endodermis and QC region C) Wild type seedling root showing SCR::GFP expression counterstained with propidium iodide. D) Root tip of the *pls* mutant stained with propidium iodide. E) *pls* mutant root showing reduced expression of SCR::GFP F) Root tip of the *pls* mutant showing reduced SCR::GFP expression counterstained with propidium iodide.

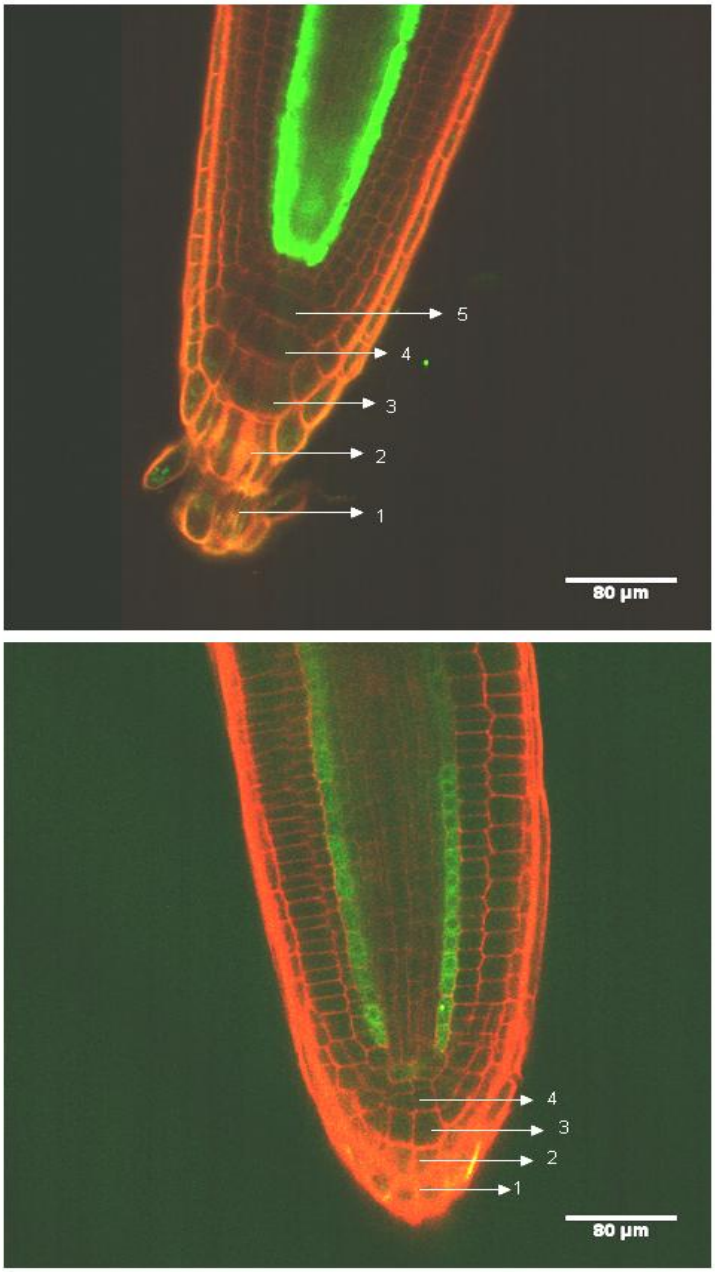


**Figure 3.4: Comparison of columella cell layers between wild type and pls mutant seedling (5 d.a.g).** Top**:** Wild type seedling root showing SCR::GFP expression and five tiers of columella cells. The cells of the columella are arranged in a characteristics pattern with small initials adjacent to the QC and larger, differentiated cells toward the root cap. Bottom: *pls* mutant root showing only four layers of columella. Columella cells are smaller and more condensed compared to wild type.

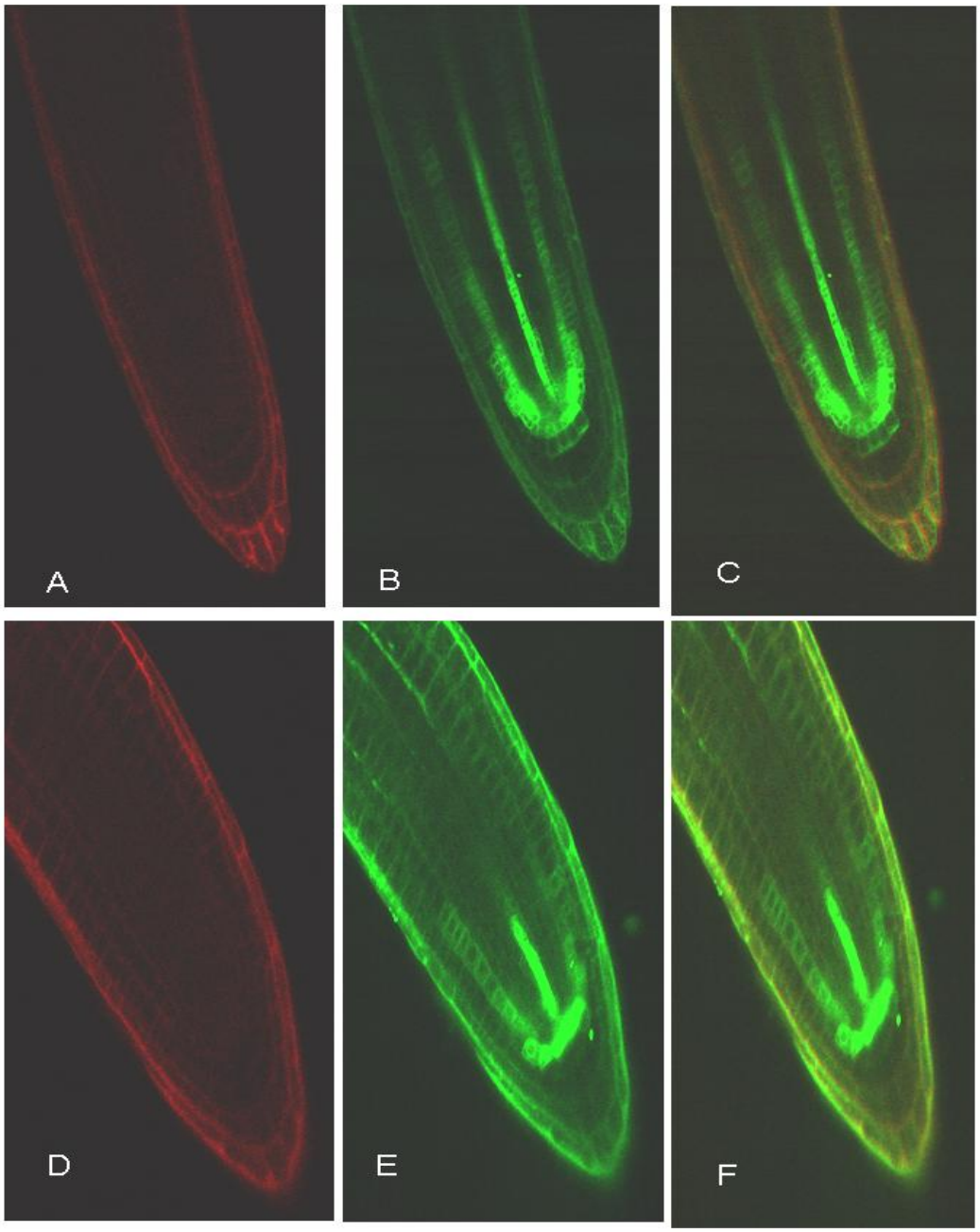


**Figure 3.5: Expression of J2341 enhancer trap line in wild-type and *pls* mutant seedling roots (5 d.a.g).** A) Wild type (C24) seedling root stained with propidium iodide (10mg/µl). B) Wild type seedling root showing J2341 expression in the ground tissue and vascular initials C) Wild type seedling root showing J2341 expression counterstained with propidium iodide. D) Root tip of the *pls* mutant stained with propidium iodide. E) *pls* mutant root showing J2341 expression. F) Root tips of the *pls* mutant showing J2341 expression counterstained with propidium iodide.

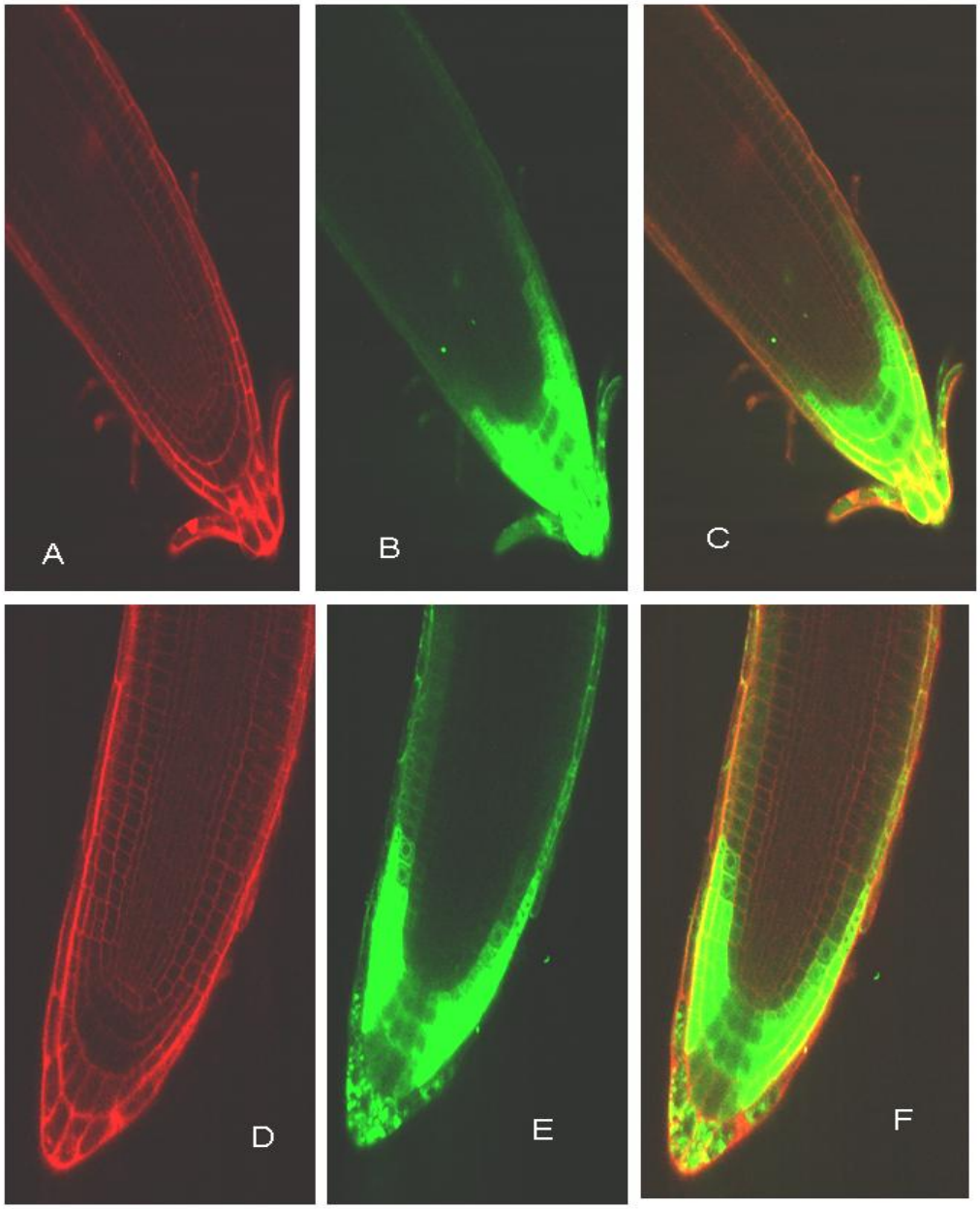


**Figure 3.6: Expression of J1092 enhancer trap line in wild type and *pls* mutant background (5 d.a.g).** A) Wild type (C24) seedling root stained with propidium iodide (10mg/µl). B) Wild type seedling root showing J1092 expression in QC cells and lateral root cap cells C) Wild type seedling root showing J1092 expression counterstained with propidium iodide. D) Root tip of the *pls* mutant stained with propidium iodide. E) *pls* mutant root showing enhanced J1092 expression in lateral root cap cells but reduced in the central file of the columella and QC. F) Root tip of the *pls* mutant showing J1092 expression counterstained with propidium iodide.

The expression of J2341 in the *pls* mutant was similar to expression in the wild-type, though confined to fewer vascular and cortical cells compared to the wild-type (Figure 3.5). In the case of J1092, the expression in the *pls* columella cells and outer root cap cell was reduced compared to wild-type, but enhanced expression was observed in the *pls* lateral root cap (Figure 3.6).

## 3.5: Sub-cellular localisation of the PLS peptide

To determine the subcellular localisation of the PLS peptide, a *proPLS::GFP:PLS* translational fusion (ie with the GFP fused to the N-terminal sequence of the PLS peptide) was generated using the Gateway™ recombinational cloning technology (Invitrogen, Carlsbad, CA, USA) and analysed using confocal microscopy. Only N-terminal fusion was used as the C-terminal fusion as found to be inactive in an earlier attempt.

The PLS ORF, together with 1.5 kb of promoter sequence, was cloned into the pMDC107 plant expression vector (supplied by Prof P. Hussey, Durham University) as a translation fusion with GFP. This involved amplifying an *attB*-PCR product, comprising the PLS ORF with 1.5 kb promoter, from the TOPO 2.1 vector which contained the PLS gene sequence with promoter, using following oligonucleotides:

PLS_Prom forward:
GGGGACAAGTTTGTACAAAAAAGCAGGCTTCAAGCTTTAGCCCGTGCGG
Bifc_ct:
GGGGACCACTTTGTACAAGAAAGCTGGGTCATGGATTTTAAAAAGTTTAAACAATTTT
GCTACTAATAAATAAG

Subsequently, the attB-PCR product was cloned into the Entry vector pDONR 207, via the BP reaction (see Section 2.14.2). The BP reaction product was then transformed into a chemically competent *E.coli* strain (DH5α) by heat shock transformation (Section 2.14.4). 100 µl of transformation mix was plated on to LB plates containing 25 µg/ml gentamycin. M13 sequencing primers were used to check the entry clones derived from BP recombination with pDONR 207. Bacterial cultures containing entry clones were grown from single colonies in 5 ml LB containing 25 µg/ml gentamycin overnight at 37 °C with 250 rpm shaking. Entry clones were isolated using the SV miniprep DNA purification system from Promega (Section 2.6.1). The LR reaction was performed to transfer the *PLS* ORF into the pMDC107 vector to generate expression clones.

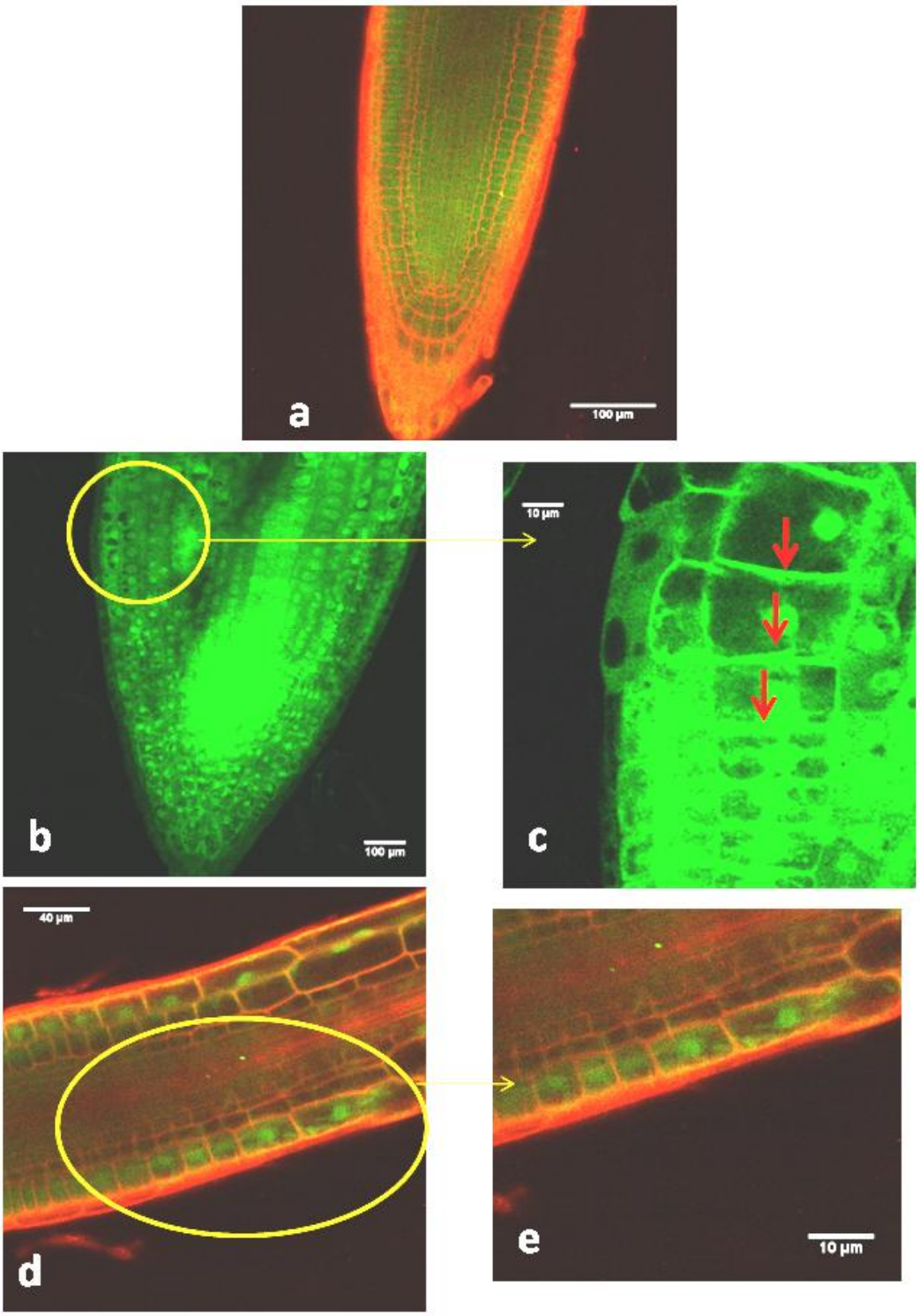


**Figure 3.7: Sub-cellular localisation of PLS peptide.** a) Wild-type showing diffused expression of *proPLS::GFP* (lacking PLS ORF sequence) localised to the cytoplasm. b - e) Localization of *proPLS*::*GFP::PLS* protein fusion in cells of root tip of transgenic plants.

For expression analysis in plants, these expression clones were mobilised into *Agrobacterium* using triparental mating (Section 2.2.3), followed by *Arabidopsis* (C24) transformation using the dipping method (Clough and Bent, 1998).

The seeds from the F1 generation were collected, sterilised and plated on ½ MS10 plates supplemented 50 µg/µl kanamycin to select for plant expressing the expression clones and 850 mg/l vancomycin was added to kill residual Agrobacterium. The selected plants were transferred to soil and the F2 generation seeds were plated on ½ MS10 plates for analysis of these seedlings by confocal microscopy (Section 2.16).

Analysis of root cells of the GFP-positive seedlings (2 d.a.g) revealed that GFP:PLS (N-terminal) fusion peptide is localised to membranous compartments of the cell, including the periphery (possibly plasmamembrane), the endoplasmic reticulum (ER) and around the nucleus. In comparison, *proPLS*::*GFP* (lacking the PLS ORF sequence) localised diffusely in the cytoplasm, and was cytosolic as expected. *proPLS*::*GFP* also shows expression in the root tip, as found previously for PLS promoter-GUS fusions (Casson *et* al., 2002) with gradient of GFP at the base of cortical cells (indicated by red arrows in Figure 3.7 c) similar to PIN1 localisation.

## 3.6: Summary

Described in this chapter is the characterisation of *pls* mutant root tip using five different GFP root cell marker lines. These GFP marker lines facilitated a detailed investigation of patterning of cells in the root meristem of the *pls* mutant. The QC marker lines Q6::GFP and Q12::GFP showed reduced expression in the mutant compared to wild type, indicating a role of *pls* in regulating, directly or indirectly, the expression of the genes required for QC identity and fate (i.e *PLT*, *SHR* and/or *SCR*). The expression of *SCR*::GFP is absent in the *pls* mutant. Also, the cells of the columella are smaller and reduced in number in the mutant compared to wild type. This could be due to the repression of cell expansion and division in mutant, as *PLS* acts as a negative regulator of ethylene signalling (Chilley *et al*., 2006). Although radial pattern appeared normal, J2341 and J1092 enhancer trap lines both showed defective expression in the mutant indicating an inability to specify and maintain correct gene expression levels in particular cell types in the *pls* mutant. Further illustrated in this chapter is the subcellular localisation of *PLS* in the root tip. The GFP::PLS peptide appears localised in membranous compartments, though future co-localization studies are required to define precisely which membrane compartment(s).

# Results

# Chapter 4:

# Characterisation of auxin responses in the *pls* mutant

The dynamic and differential distribution of the hormone auxin within plant tissues controls a wide variety of developmental processes (discussed in detail in Chapter 1), which tailor plant growth and morphology to environmental conditions. The establishment of an auxin gradient has been attributed to local auxin biosynthesis (Chen *et al*., 2006, 2007; Stepanova *et al*., 2008; Tao *et al*., 2008) and directional intercellular auxin transport (Tanaka *et al*., 2006), which are both controlled by diverse environmental and developmental signals. Therefore the modulation of auxin distribution provides a means to integrate efficiently these signals (Vanneste *et al*., 2009).

Ethylene can inhibit auxin transport in stems (Suttle, 1988), and as observed previously, enhanced ethylene signalling in *pls* causes reduced auxin responses (Casson *et al*., 2002) and represses auxin transport and accumulation in inflorescence stems (Chilley *et al*., 2006). Auxin is also known to affect root architecture, as demonstrated by *aux1* (Bennett *et al*., 1996; Ljung *et al*., 2001) and the *pls* mutant (Chilley *et al*., 2006), both of which have defective polar auxin transport, reduced levels of auxin in the root tip, and reduced lateral root formation.

The work described in this chapter aimed to investigate further the auxin distribution pattern in the *pls* mutant, using the auxin-responsive *DR5::GFP* fusion construct. Differential auxin distribution can mediate tropic changes in the response to environmental stimuli such as light and gravity (Tanaka *et al*., 2006). Depending on concentration and tissue, auxin either stimulates or inhibits cell elongation (Thimann, 1938). Thus, a stimulus-induced differential auxin distribution across the organ, such as a root, leads to differential growth resulting in bending. Based on this principle, this chapter looks in-depth into gravitropic responses of the *pls* mutant and other ethylene mutants. Also presented is an account of the expression PIN protein in the *pls* mutant and PLSOx transgenic, to further characterize auxin transport and accumulation patterns in the *pls* mutant.

## 4.1 Analysis of auxin distribution in the *pls* mutant using *DR5::GFP*

To investigate the defective polar auxin transport and accumulation in the *pls* mutant, the homozygous mutant lines were crossed with *DR5::GFP* transgenics. The crosses were grown to the F2 generation and were genotyped for *pls* homozygosity to avoid any heterozygous contamination. Genomic DNA was extracted from the leaves of plants using Section 2.6.4. The identified homozygous plants were grown to the next generation (F3) and the seeds of these plants were sterilised (Section 2.2.1), plated on ½ MS10 (hardset) (Section 2.1.6.3) and grown on vertical plates for 4-5 days (post

germination). The seedling roots were used for further analysis. The tips of seedling roots were cut, stained with a drop of propidium iodide (10 mg/ml) for 1 minute and immediately viewed under the confocal microscope (Section 2.16 & 2.17).

To examine the expression pattern of *DR5::GFP* in the *pls* mutant, the primary seedling roots at 2, 4, 6 and 8 days after germination (d.a.g.) were analysed. 2 d.a.g wild type seedling roots show *DR5::GFP* expression in the QC and columella, whereas in the *pls* mutant the signal was much weaker and diffuse, and reduced expression was seen in the QC and columella (Figure 4.1). In 4 d.a.g. *pls* mutant seedlings, the *DR5::GFP* expression level was lower compared to the 4 d.a.g. wild type (Figure 4.2). The *DR5::GFP* expression level in 4 d.a.g *pls* mutants was similar to that seen in 2 d.a.g wild type, and the same pattern was observed in 6 d.a.g *pls* mutant seedling roots (Figure 4.3 & Figure 4.4), where the *DR5::GFP* expression levels were comparable to 4 d.a.g wild types.

Enhanced *DR5::GUS* gene expression was reported in the wild-type seedling root when grown in the presence of 1-aminocyclopropane-1-carboxylic acid (ACC) (Ruzicka *et al*., 2007; Swarup *et al*., 2007; Muday *et al*., 2008). To determine whether the *pls* mutant responded in the same way as wild type, *pls* mutants and wild type (Col-0) seedlings were grown in presence of 10 µM ACC and 5 d.a.g seedlings were screened for *DR5::GFP* expression (Figure 4.5). Wild type showed enhanced *DR5::GFP* expression in columella, root cap, QC cells and stele in presence of 10 µM ACC, whereas *pls* mutants had reduced *DR5::GFP* expression together with constriction of the elongation zone, and formation of cone shaped root tip suggestive of abnormal cell expansion (Figure 4.5).

To determine whether the reduced *DR5::GFP* response in *pls* in response to ACC was due to enhanced ethylene signalling in *pls* (as distinct from some other potential signalling effect of ACC), ethylene signalling was blocked using silver nitrate, which acts at the ethylene receptor (Beyer *et al*., 1976; Rodriguez *et al*., 1999). Both the *pls* mutants and wild type were grown in presence of 100 µM $AgNO_3$ and were screened for *DR5::GFP* expression at 4 d.a.g (Figure 4.6). Wild type seedling roots showed no increase in *DR5::GFP* expression, and there was a slight decrease in root cortical cells. This suggests that the ACC effect on wild type acts via the ethylene receptor. The *DR5::GFP* expression in presence of 100 µM $AgNO_3$ in the *pls* mutant was not obviously altered compared to the *DR5::GFP* expression in *pls* seedling roots grown in

absence of silver nitrate. This suggests that the *PLS* gene product is required for ACC-mediated activation of the *DR5::GFP* signal in the root tip, which is independent of the ethylene response pathway activated in the *pls* mutant, in turn suggesting that PLS regulates a subset of ethylene responses.

Root elongation is synergistically inhibited by IAA and ACC because of the translocation of inhibitory concentrations of ethylene induced auxin back up the root from the tip to the elongation zone (Ruzicka *et al*., 2007; Stepanova *et al*., 2007; Swarup *et al*., 2007). The inhibition of root elongation by ACC is lost in the *aux1* mutant (Rahman *et al*., 2001; Ruzicka *et al.,* 2007), which is consistent with AUX1's central role transporting the increased auxin, produced by ACC/ethylene, to the elongation zone. AUX1 is an auxin influx carrier, and mutations within the *AUX1* gene confer an auxin-resistant root growth phenotype and abolish root gravitropic curvature (Bennett *et al*., 1996).

The failure of *pls* to show an increase in *DR5::GFP* signal in response to ACC in the root tip could potentially be explained by either a failure to synthesise auxin; or a failure to respond to auxin synthesized; or could be due to a rapid removal of auxin from the tip to a proximal region, following ACC treatment. Previously it has been shown that the *pls* root responds to exogenous auxin, in terms of root growth effects, and so is not insensitive to auxin (Casson *et al*., 2002). The possible rapid removal of auxin in ACC-treated *pls* was also considered unlikely, given that there was no activation of *DR5::GFP* in the elongation zone of the root. Neverthless, to investigate this further, the fact that *aux1* does not transport auxin out of the root tip was exploited. The rationale was that a double mutant between *pls* and *aux1* would exhibit a trapping of newly synthesized auxin in response to ACC treatment, reflected in a rescue of the observed swelling of the elongation zone of the *pls* root to the wildtype response. Alternatively, if *pls* still showed the abnormal swelling in response to ACC, this must be due to a response to ACC independent of a mechanism involving enhanced auxin transport out of the root tip.

Seedlings of *aux1*, *pls* and the *aux1 pls* double mutant were grown in presence of 10 µM ACC and the phenotype of the root tip was examined (Figure 4.7). The *aux1* mutant seedling root treated with 10 µM ACC showed a slight constriction and reduction in the elongation zone of the root (Figure 4.7 a), whereas the *pls* mutant had an even shorter elongation zone, defective cellular patterning and slightly cone shaped root apex (Figure 4.7 c). The *aux1 pls* double mutant treated with 10 µM ACC similarly developed a defective elongation zone and short, cone shaped root apex similar to both *pls* and *aux1* (Figure 4.7 e), indicating that *aux1* does not rescue the inhibitory effect of ACC on the

*pls* mutant. It can be concluded that the abnormal defect in root tip phenotype of ACC-treated *pls* is not due to the transport of auxin out of the root tip, and so this mechanism is unlikely to be responsible for the lack of enhanced *DR5::GFP* signal in response to ACC. The results are consistent with a failure of ACC-mediated auxin synthesis in the *pls* mutant. As previously found (Casson *et al*. 2002), the primary root length of *pls* was reduced when grown in the presence of 10 µM ACC, compared with growth on ½ MS10 (Figure 4.8), and was partially rescued on 100 µM $AgNO_3$. Growth on low auxin concentrations (50 nM NAA) had no clear effect on *pls* root length, confirming previous data (Casson *et al*., 2002). Interestingly, introduction of the *aux1* mutation, which confers ethylene resistance, to *pls* as the *aux1 pls* double mutant conferred some ethylene resistance to *pls* when grown on 10 µM ACC (Figure 4.9). This suggests that part of the ethylene-mediated short root phenotype in *pls* may be rescued by inhibition of auxin transport.

## 4.2: Characterisation of the gravitropic response in the *pls* mutant

It has been demonstrated that polar auxin transport is important for gravitropic responses. The auxin efflux carrier PIN-FORMED2 (PIN2), which is distributed asymmetrically within the root epidermal and cortical cells, and the influx carrier AUX1, play important roles in basipetal auxin transport in the gravitropic response of root elongation zone (Muller *et al*., 1999; Marchant *et al*., 1999). Further, Chilley *et al*. (2006) demonstrated that *pls* mutant has defective and reduced auxin transport and accumulation in the inflorescence stem. Therefore, in order to determine whether the observed defects in auxin transport in *pls* affected tropic responses, gravitropic curvature was investigated.

*pls*, wild type and *PLS*-overexpressing (PLSOx) seedlings (2 d.a.g) were grown on hard set ½ MS10 agar plates for 2 d.a.g and turned to a 90° angle to measure the angle of bending towards the gravity (Section 2.4). The angle towards gravity was measured after 24 hours. *pls* mutants were found to be less gravitropic than wild type, whereas PLSOx rescues this defect (Figure 4.10). Only 23% of *pls* mutants roots showed true gravitropic response compared to 53% wild type and 73% PLSOx seedling roots (Figure 4.11).

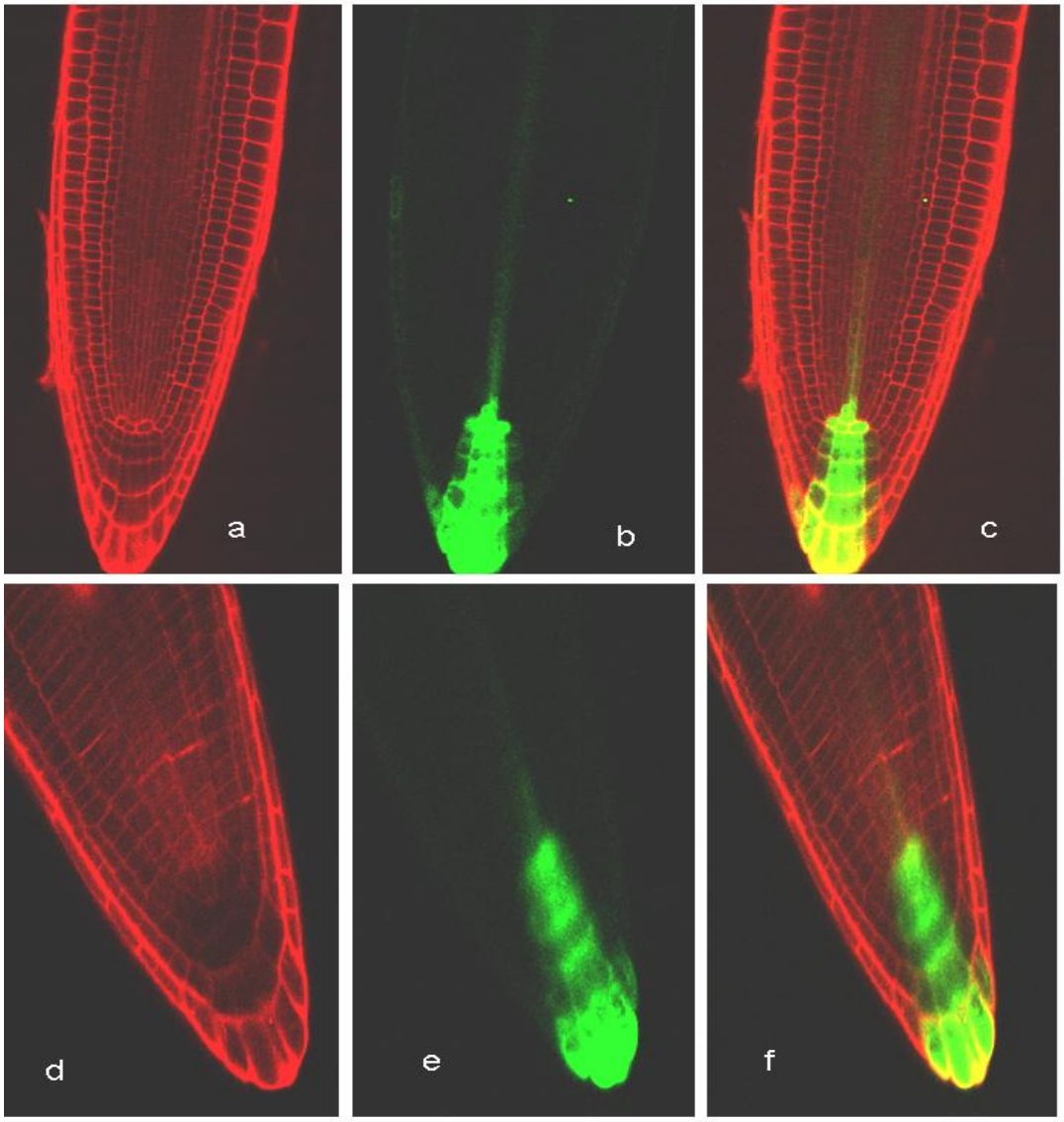


**Figure 4.1: *DR5::GFP* expression in 2 d.a.g. primary roots of *Arabidopsis.***

a) Propidium iodide stained wild type root, b) *DR5::GFP* expression in columella, and QC cells of wild type root, c) merged image (a & b), d) *pls* mutant root stained with propidium iodide, e) *pls* mutant root showing weaker *DR5::GFP* expression in columella and QC cells compared to wild type, f) merged image (d & e).

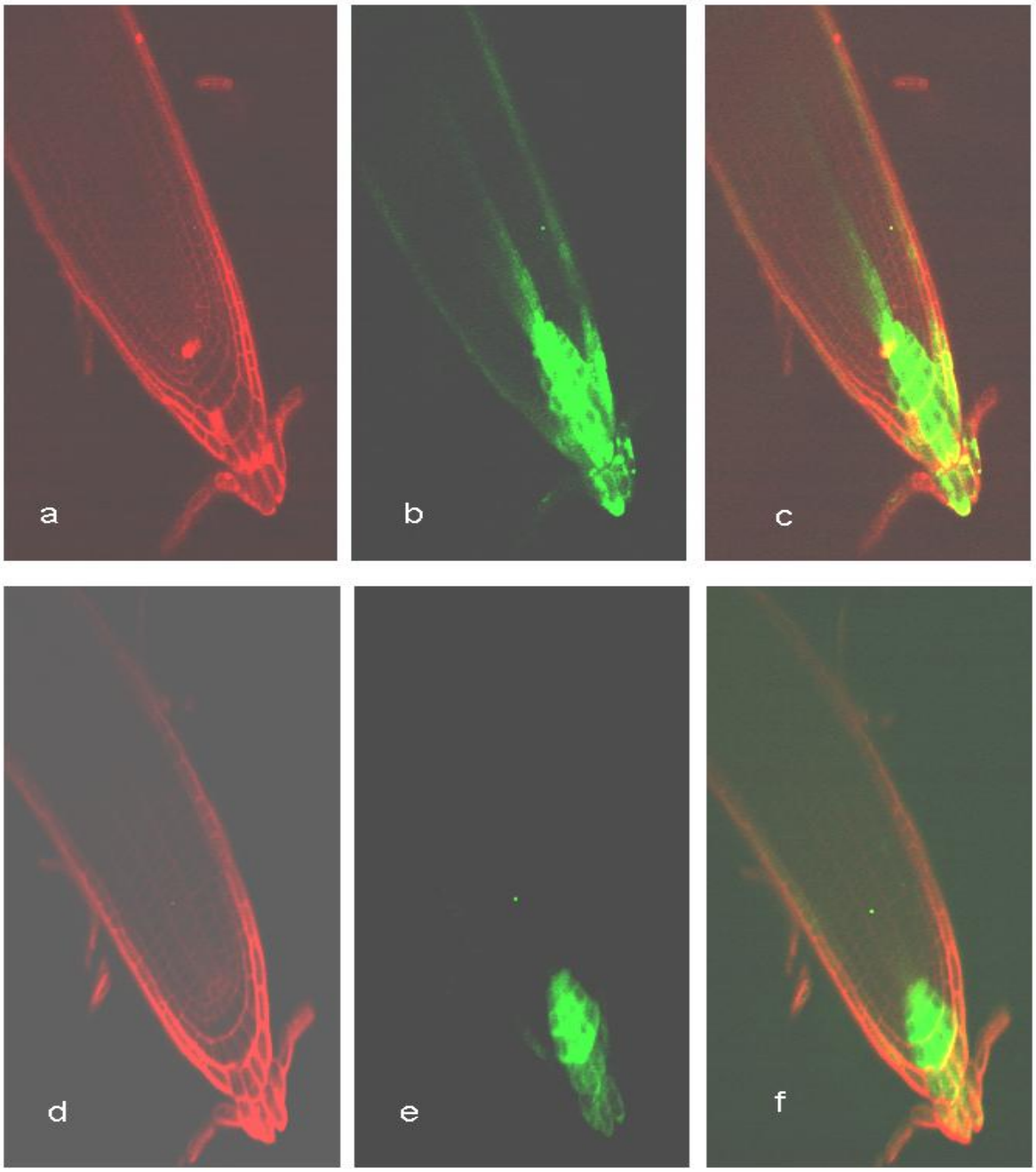


**Figure 4.2: *DR5::GFP* expression in 4 d.a.g. primary roots of *Arabidopsis.***

a) Propidium iodide stained wild type root, b) *DR5::GFP* expression in columella, root cap cells and QC cells of wild type root, c) merged image (a & b), d) *pls* mutant root stained with propidium iodide, e) *pls* mutant root showing reduced *DR5::GFP* expression in columella and QC cells compared to wild type, f) merged image (d & e).

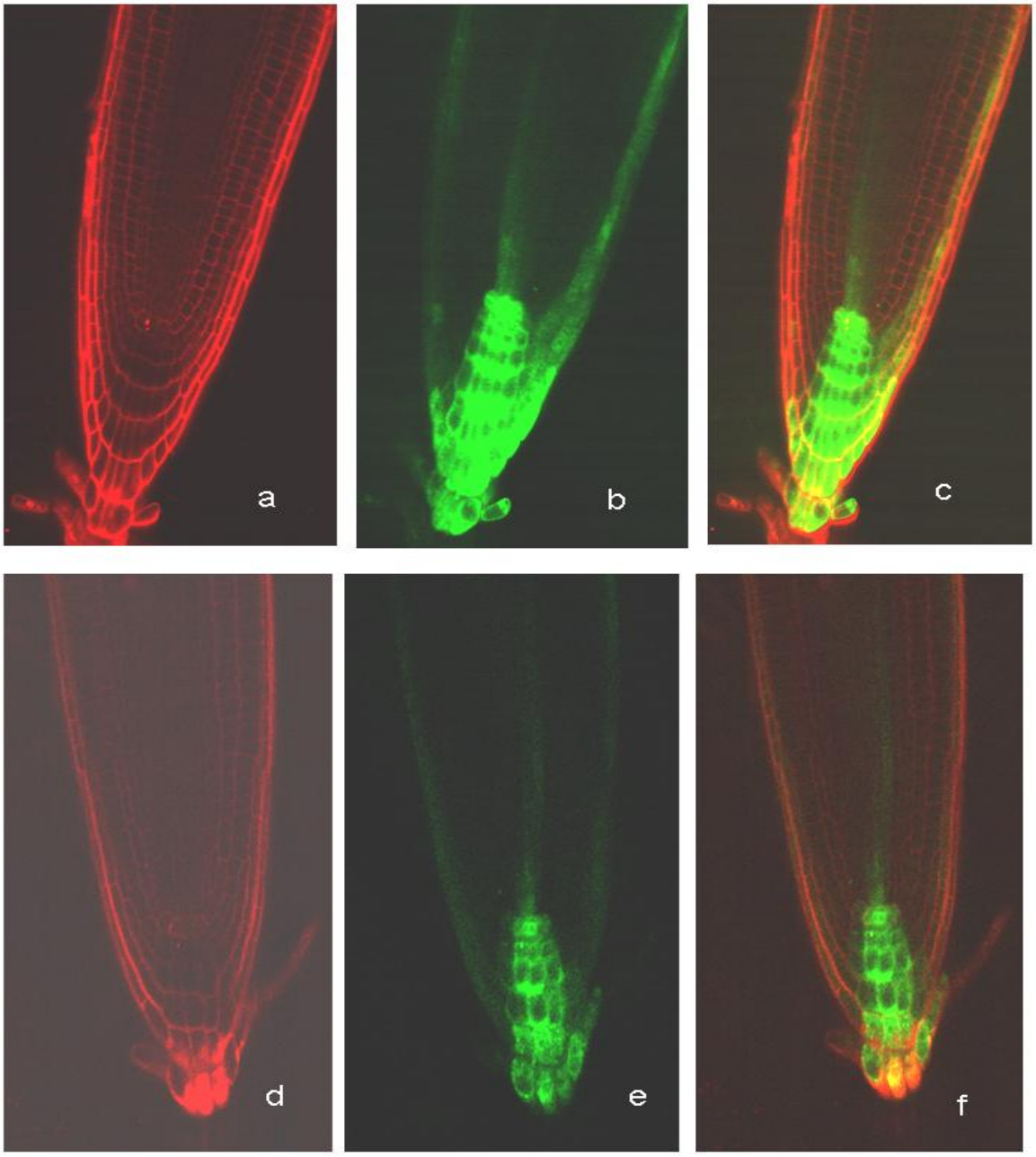


**Figure 4.3: *DR5::GFP* expression in 6 d.a.g. primary roots of *Arabidopsis.***

a) Propidium iodide stained wild type root, b) Pronounced *DR5::GFP* expression in columella, root cap cells and QC cells of wild type root, c) merged image (a & b), d) *pls* mutant root stained with propidium iodide, e) *pls* mutant root showing reduced *DR5::GFP* expression in columella and QC cells compared to wild type, f) merged image (d & e).

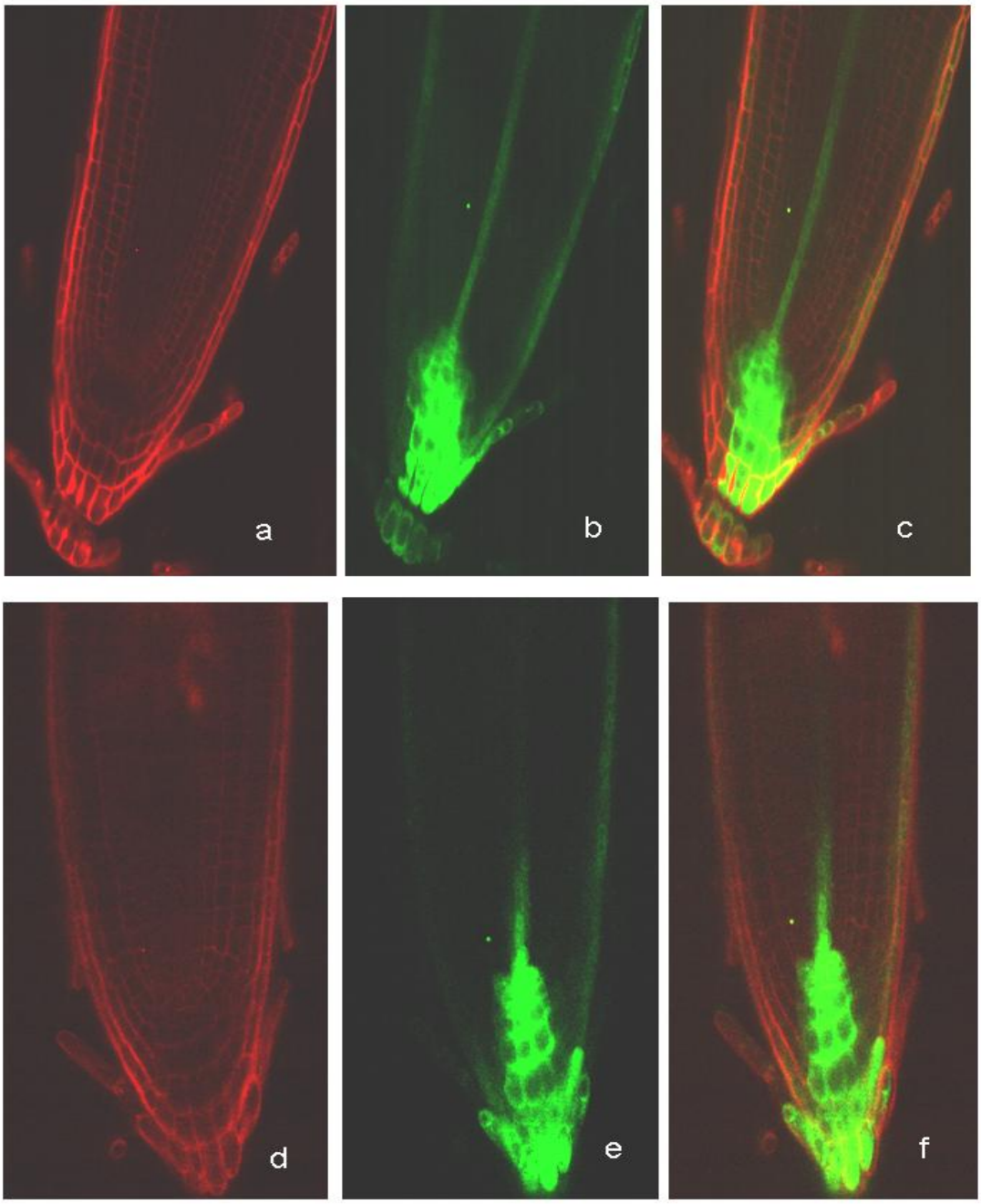


**Figure 4.4: *DR5::GFP* expression in 8 d.a.g. primary roots of *Arabidopsis.***

a) Propidium iodide stained wild type root, b) *DR5::GFP* expression in columella, root cap and QC cells of wild type root (similar to 6 d.a.g. *DR5::GFP* expression), c) merged image (a & b), d) *pls* mutant root stained with propidium iodide, e) *pls* mutant root showing reduced *DR5::GFP* expression in columella and QC cells compared to wild type, f) merged image (d & e).

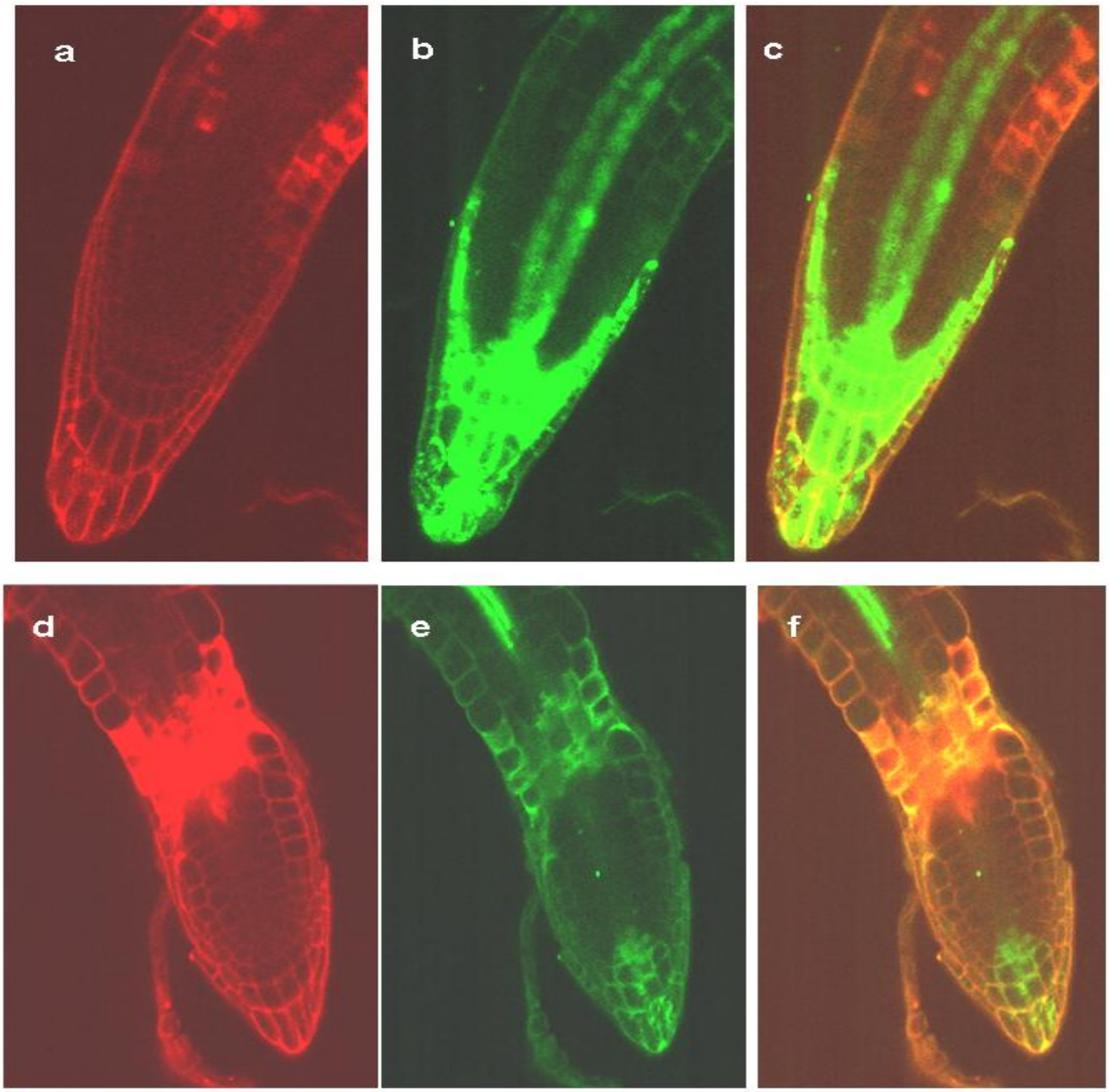


**Figure 4.5: Seedling root (4 d.a.g.) showing *DR5::GFP* expression in presence of 10 µM ACC.** a) Propidium iodide stained wild type root, b) Wild type root showing *DR5::GFP* expression in columella, root cap, QC cells and stele in presence of 10 µM ACC. c) merged image (a & b), d) *pls* mutant root stained with propidium iodide, e) *pls* mutant root showing reduced *DR5::GFP* expression together with constriction of elongation zone and cone shaped root tip in presence of 10 µM ACC, f) merged image (d & e).

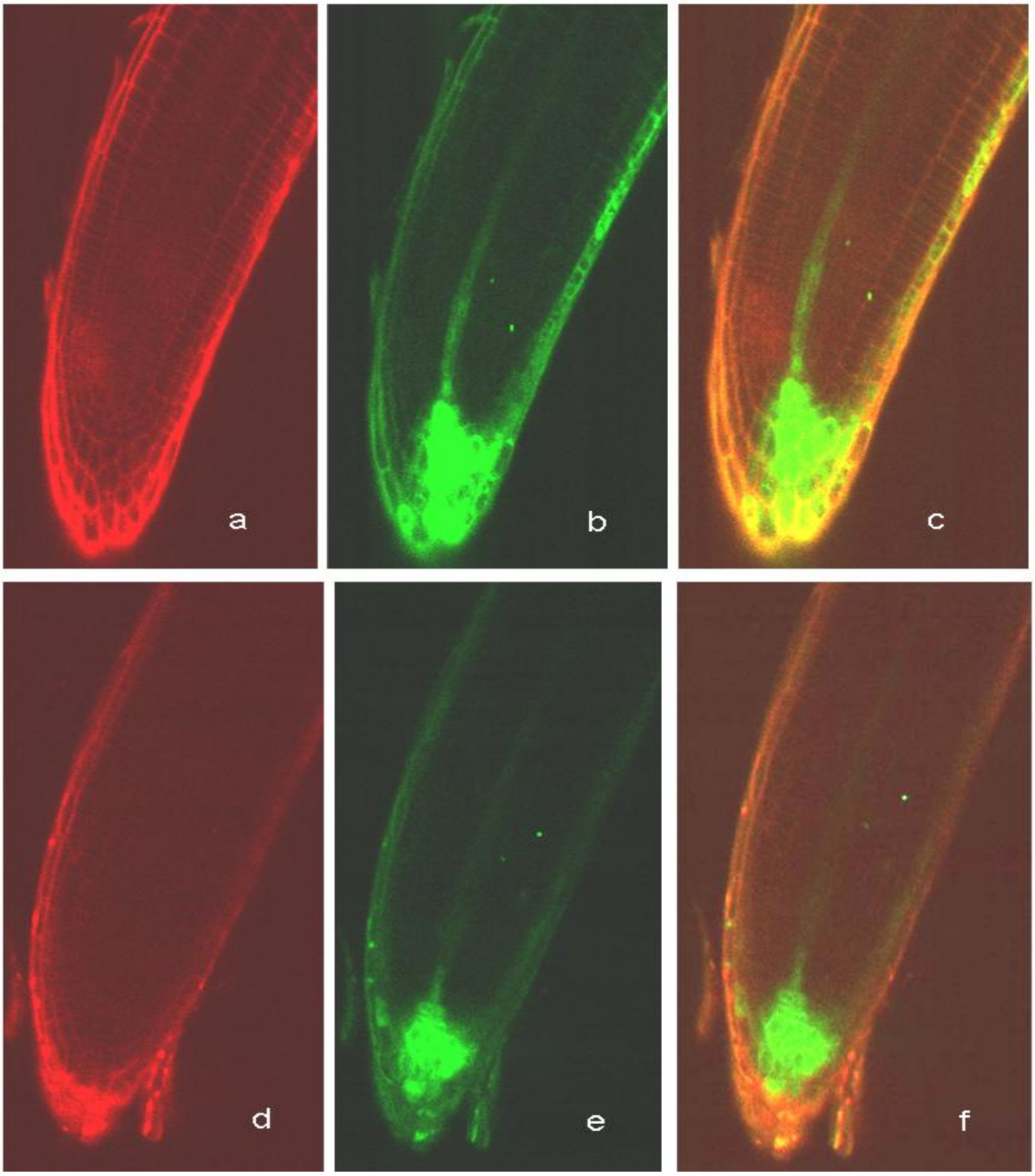


**Figure 4.6: Seedling roots (4 d.a.g.) showing DR5::GFP expression in presence 100 µM silver nitrate.** a) Propidium iodide stained wild type root, b) wild type root showing no change in *DR5::GFP* expression in presence of 100 µM $AgNO_3$, c) merged image (a & b), d) *pls* mutant root stained with propidium iodide, e) *pls* mutant root in presence of 100 µM $AgNO_3$ showing *DR5::GFP* expression, f) merged image (d & e).

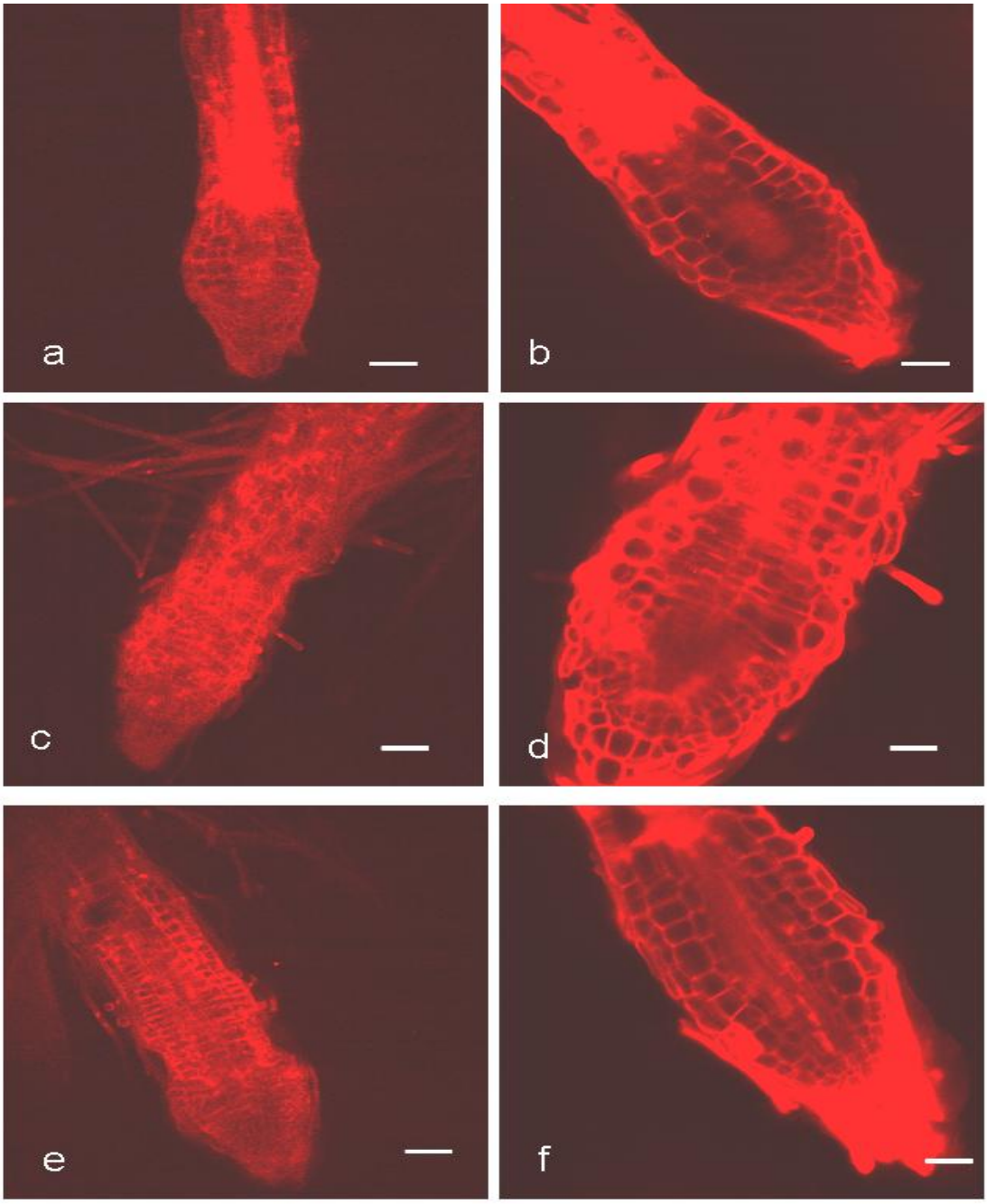


**Figure 4.7: Seedling roots of *aux1*, *pls* and *pls aux1* in presence of 10 µM ACC.**

a) *aux1* mutant seedling root treated with ACC showing constriction and reduction in elongation zone of the root with characteristic cone shaped root apex, b) higher magnification image of ACC treated *aux1* root, c) ACC treated *pls* mutant primary root showing shorter elongation zone, cone shaped root apex, swollen epidermal cells and defective cellular patterning, d) higher magnification image of *pls* root apex, e) *pls aux1* double mutant root treated with ACC depicting shorter and condensed elongation zone, cone shaped root apex and defective cellular patterning, f) higher magnification image of root apex of *pls aux1* treated with ACC .( a, c, & e Bar = 50µm ; b, d, & f Bar = 20µm).

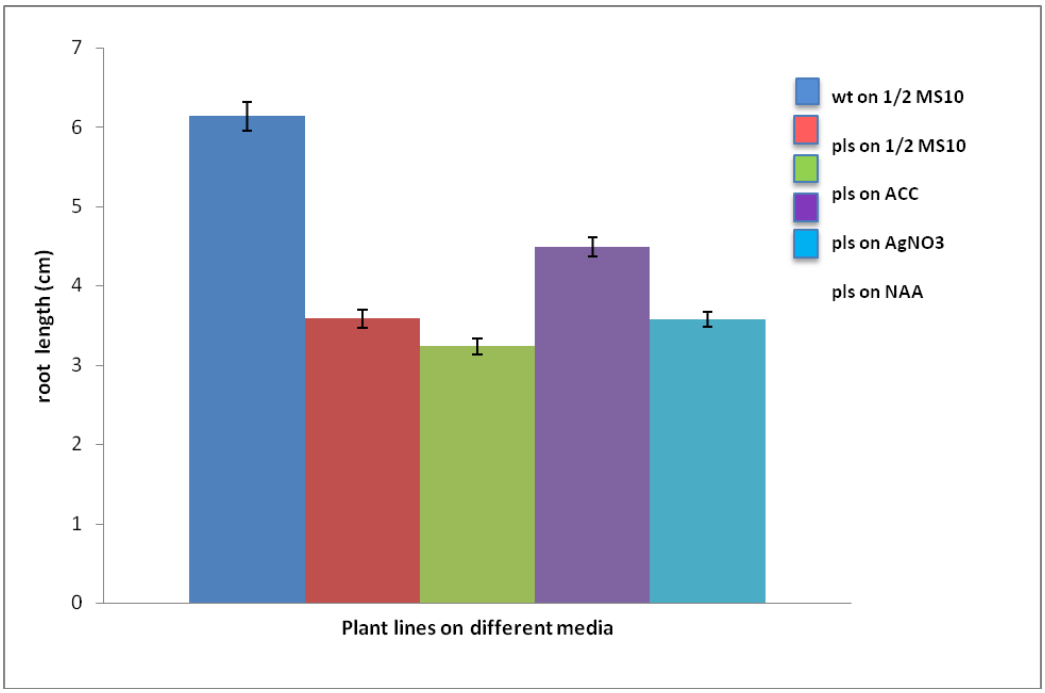


**Figure 4.8: Comparison of *pls* root length on different media.** *pls* mutants grown on ½ MS10, 10 µM ACC and 10 nm NAA are 50 % shorter than the wild type grown on ½ MS10. *pls* mutants grown on 50 nm $AgNO_3$ rescues the short root phenotype of *pls* to ca. 70 % of wild type length. (n=16 ± SE).

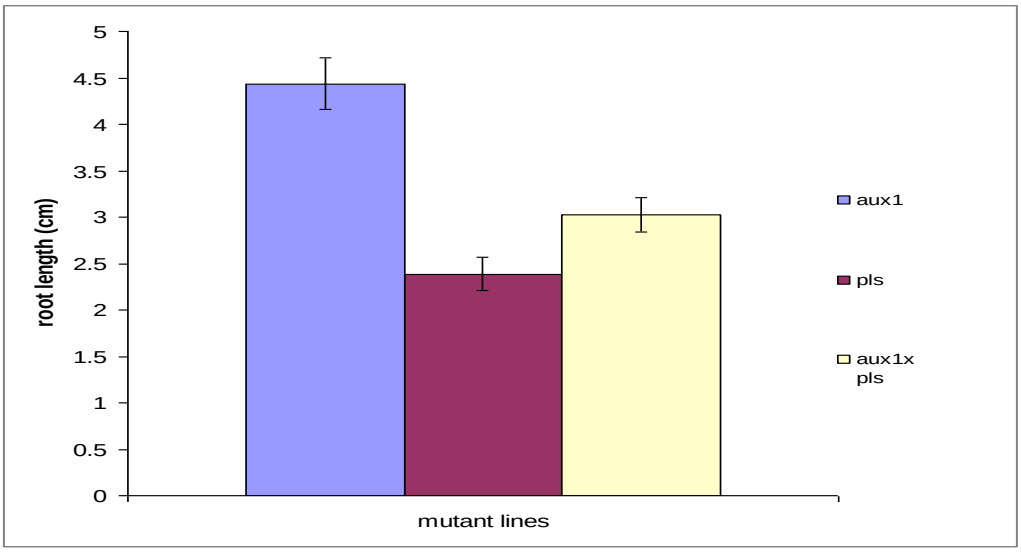


**Figure 4.9: Rescue of *pls* root length on ACC using *aux1.*** *pls* mutant seedling roots treated with 10 µM ACC are 50% shorter than the *aux1* mutant root. The *aux1 pls* double mutant partially rescues the *pls* short root phenotype. ( n = 7 ± SE).

Interestingly, most of the auxin resistant mutants that exhibit an altered gravitropic response like *aux1* (Bennett *et al*., 1996), *axr1*, *axr2* and *axr3* (Lincoln *et al*., 1990; Wilson *et al*., 1990; Leyser *et al*., 1996) are also resistant to ethylene. However, small amounts of ethylene have been reported to restore a normal gravitropic response (Zobel, 1974). Therefore, in order to compare the gravitropic responses of ethylene mutants with the *pls* mutant, three ethylene mutants, *etr1*, *ctr1* and *eto1*, together with *pls*, PLSOx, *pls etr1* double mutant and two wild types (Col-0, C24) were grown simultaneously on vertical hard set ½ MS10 plates. Seedlings were grown for 2 d.a.g. and then turned at a 90º angle towards gravity to measure their gravitropic response (Figure 4.12). The angle of bending towards gravity was measured at 2 hours, 4 hours, 6 hours, 8 hours, 10 hours, and 24 hours (Figure 4.13 and Figure 4.14). The angles were used to compare the degree of bending towards gravity (Figure 4.15) and the rate of bending towards gravity (Figure 4.16). The *pls* mutant showed less bending towards gravity compared to wild type, but a higher degree of bending compared to *eto1* (Figure 4.15). Both *eto1* and *pls* showed less and relatively slow bending towards gravity, but the effects were less severe in the latter case. Interestingly, *pls etr1* double mutants showed the highest degree of bending closely followed by *ctr1* which also had a high degree of bending towards gravity and the fastest response to gravity compared to others. Both PLSOx and *pls etr1* rescue the slow and defective gravitropic response in *pls* (Figure 4.15 and 4.16), suggesting a role of PLS upstream of auxin and downstream of ethylene in gravitropic signal transduction.

## 4.3: Expression of PIN proteins in *pls*

PIN proteins act as the efflux carrier of auxin and polar PIN localisation directs auxin flow in plants (Petrasek *et al*., 2006). PIN proteins exhibit synergistic interactions, which involve cross-regulation of *PIN* gene expression in *pin* mutants or plants with inhibited auxin transport. Auxin itself positively feeds back on *PIN* gene expression in a tissue-specific manner through an AUX/IAA-dependent signalling pathway. This regulatory switch is indicative of a mechanism by which the loss of a specific PIN protein is compensated for by auxin-dependent ectopic expression of its homologues (Vieten *et al*., 2005). Since *pls* has defective auxin transport and accumulation (Chilley *et al*., 2006), the possible basis of this was investigated by analysis of PIN1 and PIN2 immunolocalisation, which was kindly carried out by Prof Jiri Friml, Gent University.

Investigation into the expression level and localization of PIN1 in *pls*, PLSOx, *pls x etr1* and *etr1*, was examined in at least three independent experiments. The results revealed

that PIN1 is localised intracellularly normally in all lines, at the basal and lateral end of the vascular cells with weaker expression in epidermal and cortical cell. Interestingly, the *pls* mutant shows upregulation of expression in the root cortex, with strongest signal in the endodermis (Figure 4.16). Both *etr1* and PLSOx showed weaker PIN1 signal in endodermis, cortex and vascular tissue. The *pls etr1* double mutant shows downregulation of PIN1 expression with no signal in the cortex (Figure 4.16). Similarly, PIN2 expression at the apical end of epidermal cells and the basal end of cortical cells in wild type was found to be slightly upregulated regulated in the *pls* background (Figure 4.16). PIN2 signal in epidermis and cortex was weaker in *PLSOx*, and slightly weaker in *etr1-1*, compared to wild-type and *pls*, whereas in *pls etr1* the expression is weaker than in wild type but stronger than in *etr1*. These data suggest that the enhanced ethylene responses in *pls* lead to enhanced PIN1 and PIN2 levels, which can be rescued by introduced *etr1* or by overexpressing the *PLS* gene.

## 4.4: Study of transcript abundance of *WEI2* in *pls* and ethylene mutants

Inhibition of root growth by ethylene is mediated by the action of the *WEI2 (WEAK ETHYLENE INSENSITIVE2*) and *WEI7* (*WEAK ETHYLENE INSENSITIVE7*) genes that encode α- and β-subunits of anthranilate synthase, a rate-limiting enzyme of Trp biosynthesis. Upregulation of *WEI2* and *WEI7* results in the accumulation of auxin in the tip of the primary root, whereas downregulation prevents the ethylene-mediated auxin increase (Stepanova *et al*., 2005). In view of the observations that the *pls* mutant fails to show evidence of increased auxin accumulation in the root (as indicated by *DR5::GFP* expression), it is possible that this effect could be mediated by defective *WEI2* expression or enzyme activity in *pls*; or by the expression or activity of other enzymes upstream or downstream of WEI1 in the *pls* mutant. As a first step to investigate this, the mRNA abundance of *WEI2* in *pls*, PLSOx, the *pls etr1* double mutant, *eto1* and wild type were measured by quantitative real time PCR (Section 2.12) using *WEI2* primers, with *ACTIN2* expression as a control (Figure 4.18).

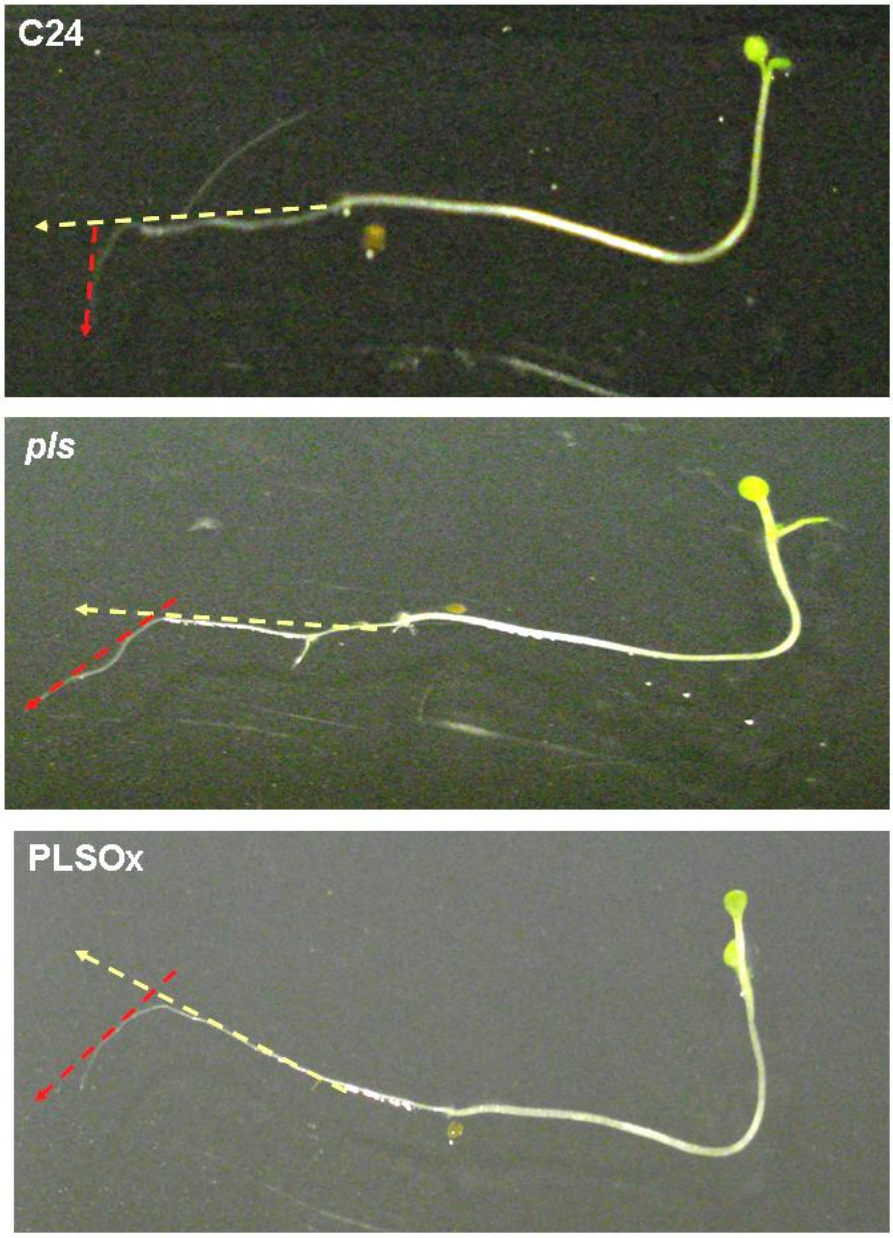


**Figure 4.10: Comparison of gravitropic response of wild-type (C24), *pls* and PLSOx.** *pls* mutants show weaker gravitropic response (less bending towards gravity when turned at 90° angle to gravity) compared to wild type seedlings, whereas PLSOx shows normal gravitropic response (n=20)

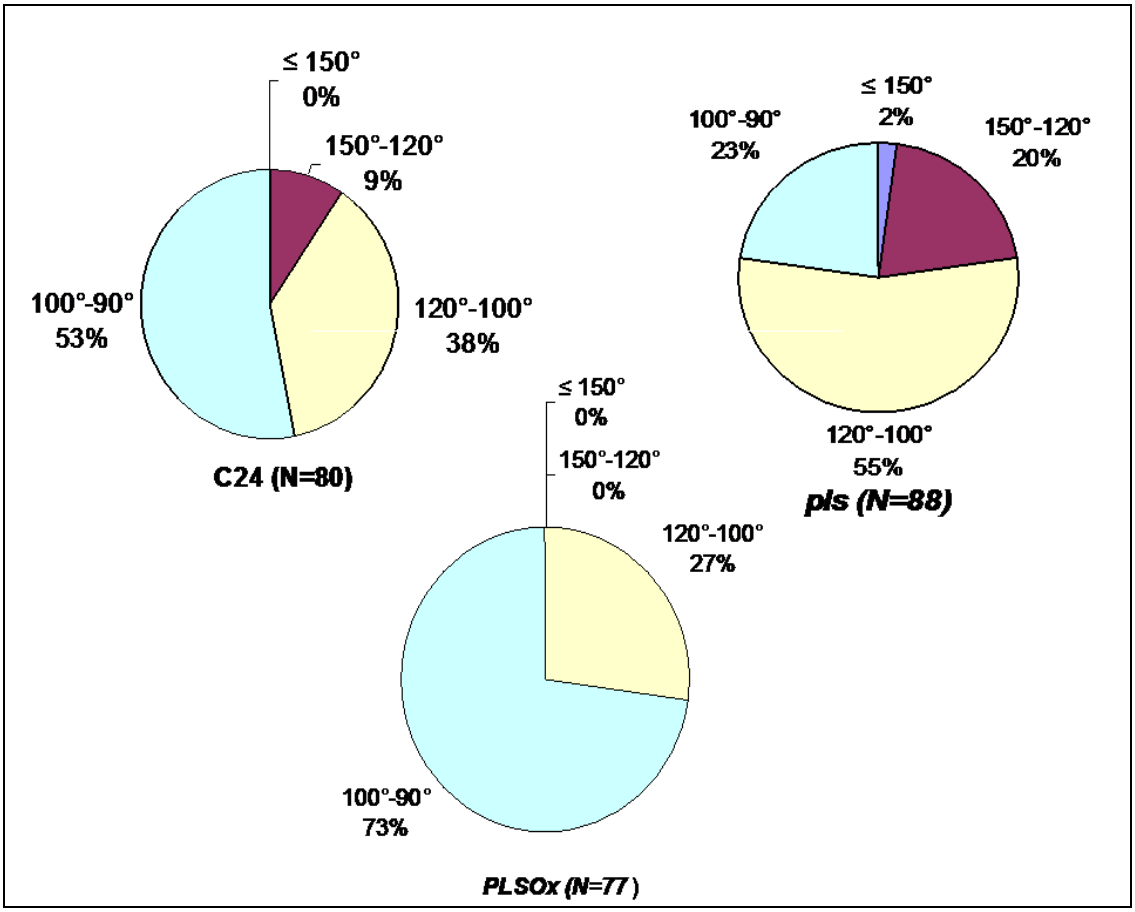


**Figure 4.11: Diagrammatic representation of the frequency of wild type (C24), *pls* and PLSOx seedlings showing different gravitropic responses.** Only 23 % of *pls* mutants show true gravitropic response (100°- 90° degree bending towards gravity) compared to 53% of wild type and 73% of PLSOx seedlings.

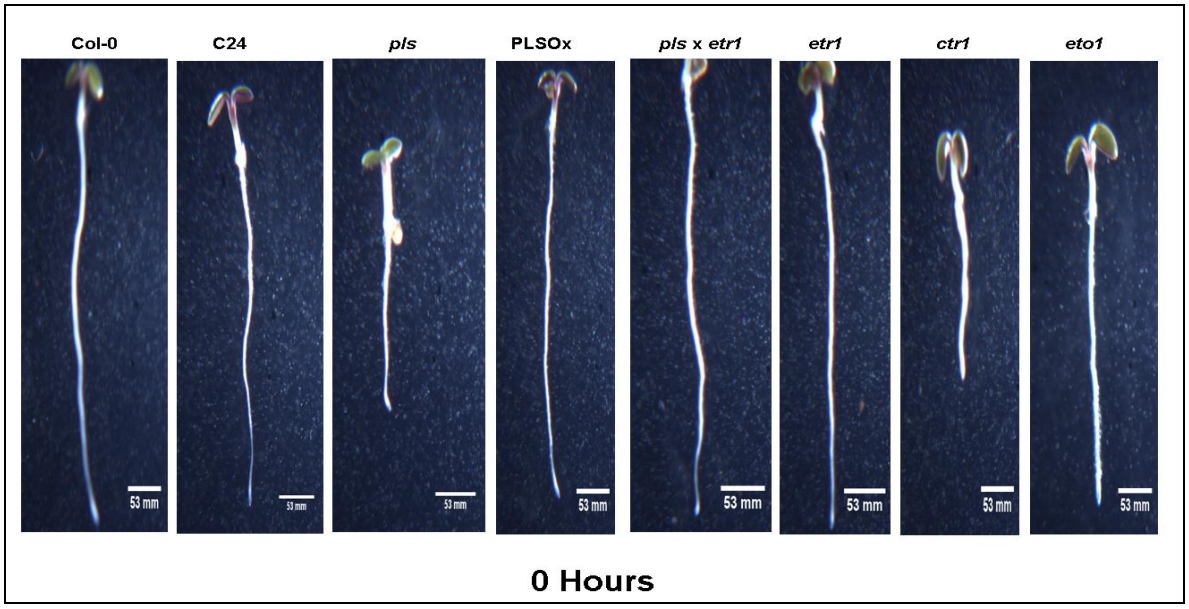


**Figure 4.12: Seedlings of eight different plant lines showing root length and orientation prior to measuring their gravitropic response (i.e. before turning them at a 90° angle).**

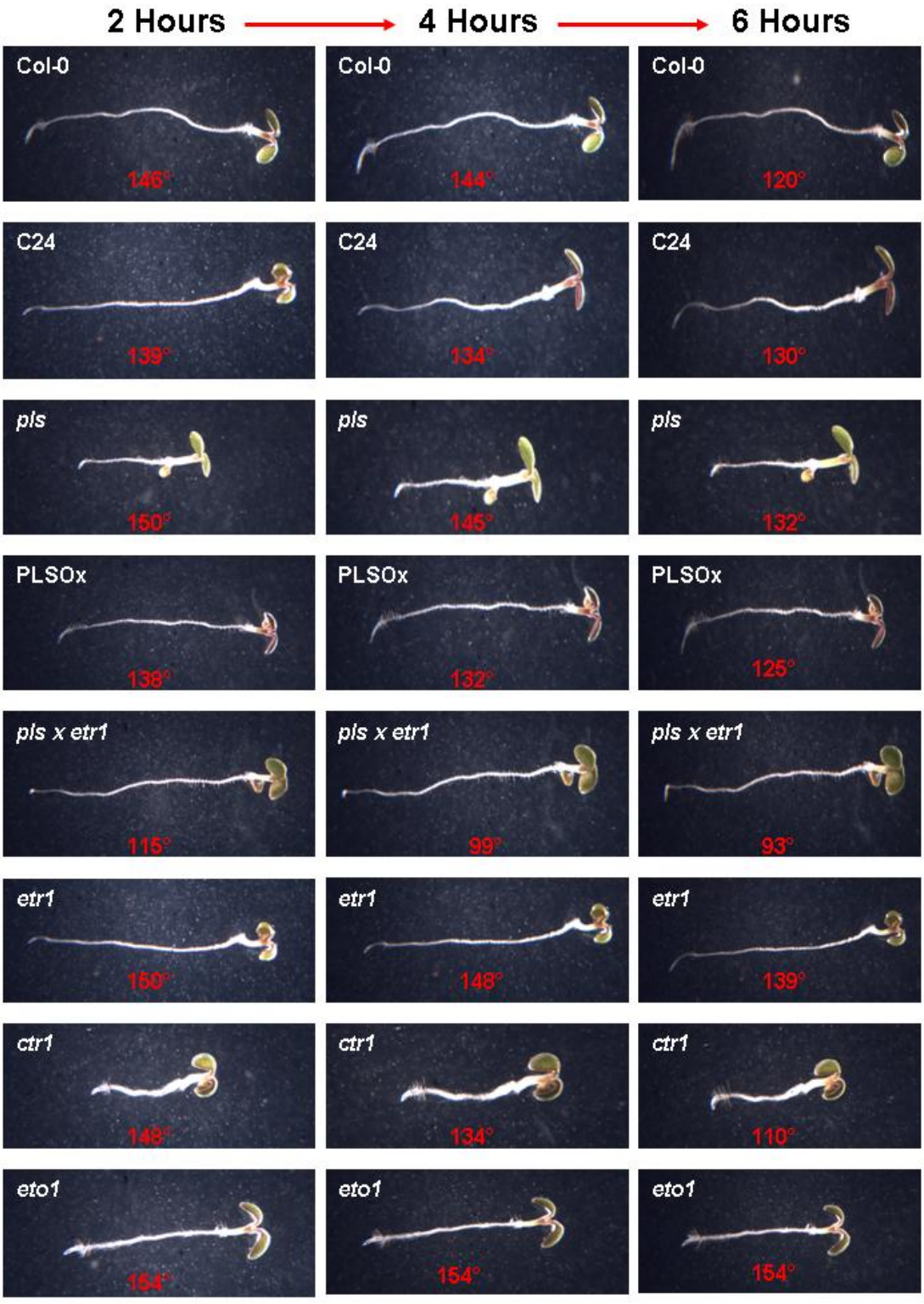


**Figure 4.13: Gravitropic responses of eight different plant lines by measuring the angle of bending toward gravity (in red, bottom centre) at 2 hours, 4 hours and 6 hours after turning them at a 90° angle.**

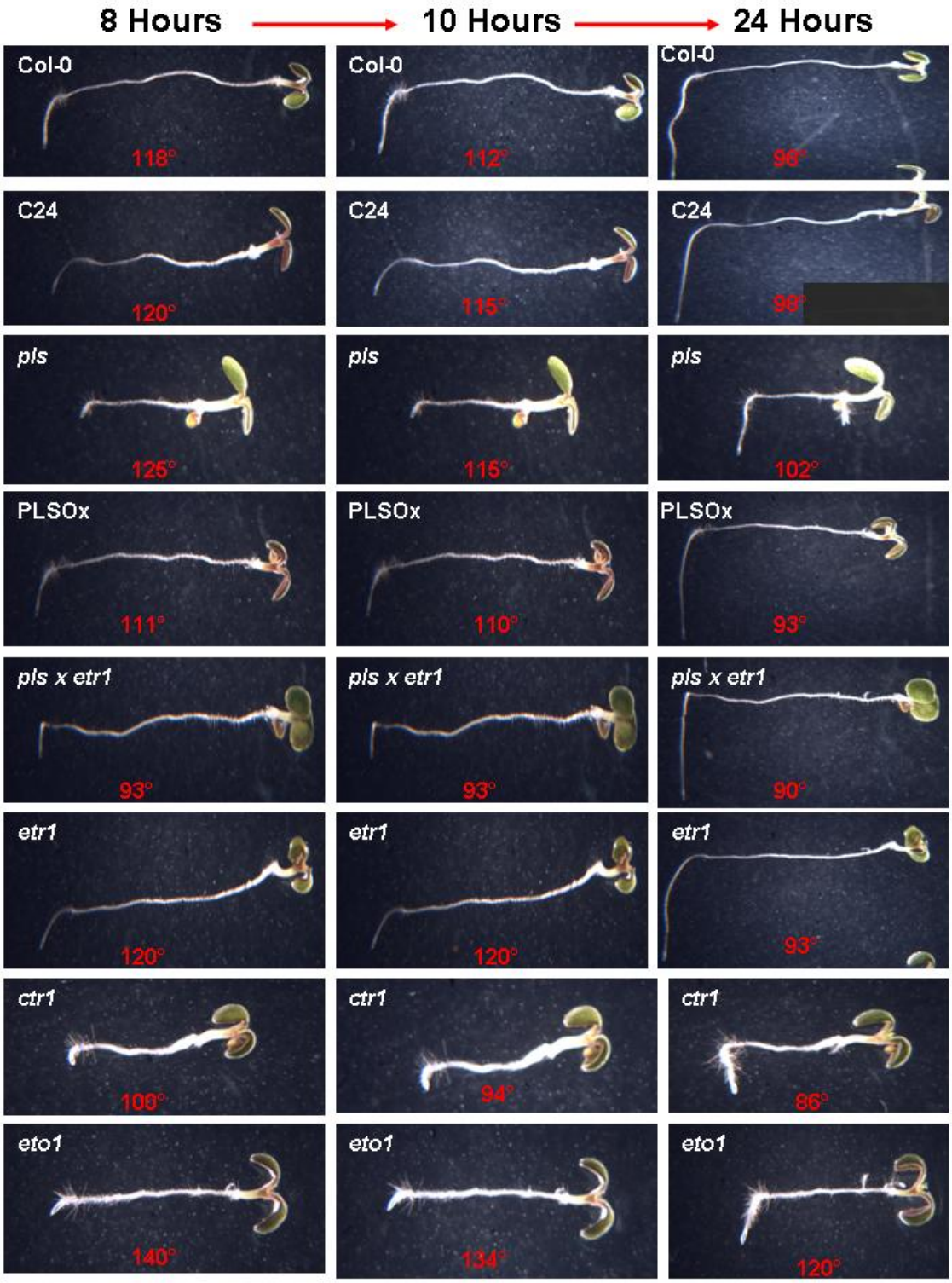


**Figure 4.14: Gravitropic responses of eight different plant lines by measuring the angle of bending toward gravity (in red, bottom centre) at 8 hours, 10 hours and 12 hours after turning them at a 90° angle.**

**A**

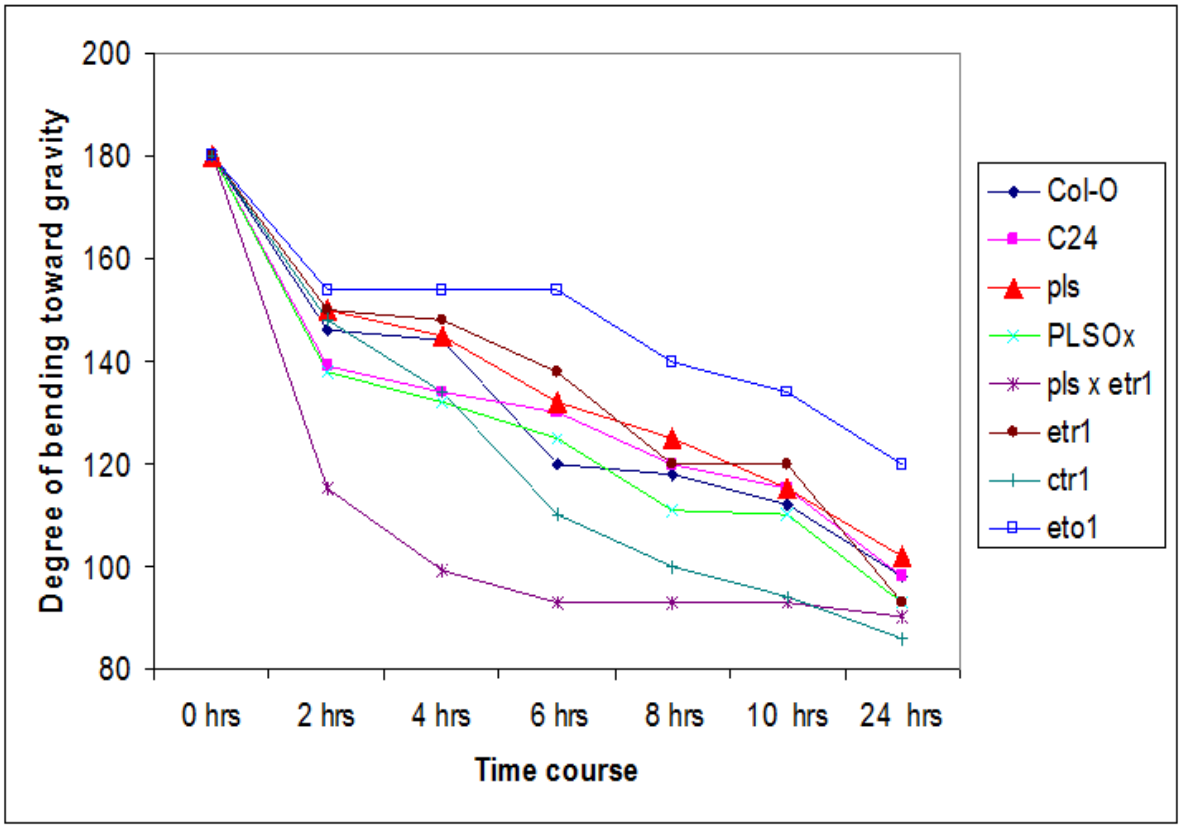


**B**

Angle of bend toward gravity

| Plant lines | 0 hrs | 2 hrs | 4 hrs | 6 hrs | 8 hrs | 10 hrs | 24 hrs | Rate of bending (Change in angle per hour) |
|---|---|---|---|---|---|---|---|---|
| Col-O | 180 | 146 | 144 | 120 | 118 | 112 | 98 | 3.41 |
| C24 | 180 | 139 | 134 | 130 | 120 | 115 | 98 | 3.41 |
| *pls* | 180 | 150 | 145 | 132 | 125 | 115 | 102 | 3.25 |
| PLSOx | 180 | 138 | 132 | 125 | 111 | 110 | 93 | 3.625 |
| *pls x etr1* | 180 | 115 | 99 | 93 | 93 | 93 | 90 | 3.75 |
| *etr1* | 180 | 150 | 148 | 138 | 120 | 120 | 93 | 3.625 |
| *ctr1* | 180 | 148 | 134 | 110 | 100 | 94 | 86 | 3.91 |
| *eto1* | 180 | 154 | 154 | 154 | 140 | 134 | 120 | 2.5 |

**Figure 4.15: A) Graph depicting the degree of bending of towards gravity (Y-axis) for eight different plant lines in 24 hours (x- axis). B) Table showing the rate of bending (change in angle per hour) for eight different plant lines.**

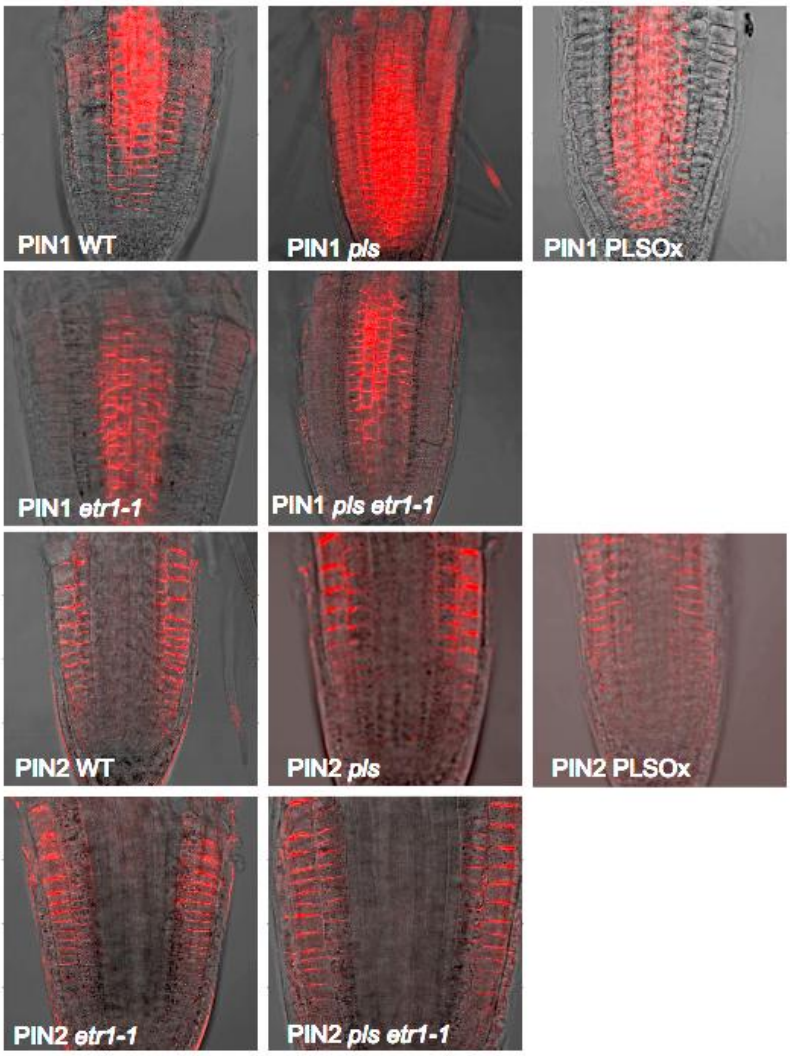


**Figure 4.16: PIN1 and PIN2 immunolocalization in different mutant lines (data kindly provided by Prof. Jiri Friml).**

**PIN1:** Wild type shows PIN1 localization at the basal and lateral ends of vascular cells and weaker expression in endodermal and cortical cells; *pls* mutant shows stronger (than control) PIN1 levels in the epidermal, endodermal and cortical cells; PLSOx shows weaker (compared to wild type and *pls*) PIN1 signal at the basal and lateral ends of the endodermal and vascular tissue with no signal in the epidermis and weak basal signal in the cortex. *etr1* mutant seedling root showing weak PIN1 signal residing at the basal side of endodermal and vascular cells, with no signal in the epidermis and slight up-regulation in the cortex but weak signal; *pls etr1* double mutant exhibits PIN signal intensity intermediate between *pls* and *etr1* but weaker than wild-type in the vascular and endodermal cells, no up-regulation in the cortex.

**PIN2:** Wild type seedling root shows PIN2 localization at the apical end of epidermal cells and at the basal end of cortical cells; *pls* mutant root shows slightly stronger PIN2

expression at the apical end of the epidermis and in the basal end near the epidermal side of cortex compared to wild type; *PLSOx* shows weaker PIN2 expression in epidermal and cortical cells compared to the wild type and pls; *etr1* mutant has slightly weaker PIN2 signal in both epidermis and cortex compared to wild type; *pls etr1* shows PIN2 levels that are higher than *etr1*, but weaker than *pls* and wild type in both epidermis and cortex.

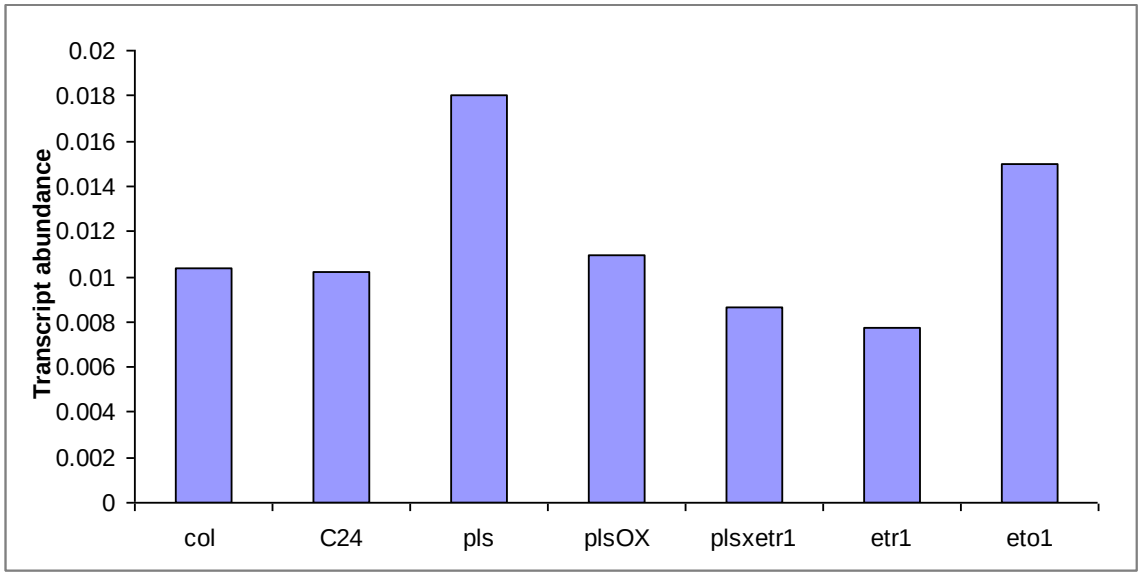


**Figure 4.17: Relative transcript abundance of WEI2 in *pls* and ethylene mutants (data values detailed in Appendix 3)** WEI2 expression is upregulated in pls mutant but down to wt levels in *PLSOx* and *pls etr1* double mutant.

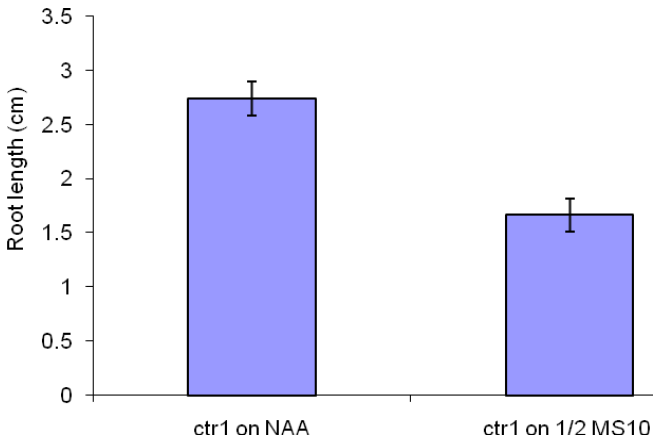


**Figure 4.18: Root length of the *ctr1* mutant is rescued on 1-NAA.** Roots of *ctr1* mutant seedlings (5 d.a.g) grown on 50nM 1-NAA are longer than those grown on ½ MS10

Intriguingly, it was found that the *WEI2* transcript level is upregulated in the *pls* and *eto1* mutants compared to wild type, *PLSOX*, *etr1* and *pls etr1* (each of which contrasts in ethylene response with *pls* and *eto1*), while *ACTIN2* levels were similar between all lines (Figure 4.17). One interpretation of this is that the *pls* and *eto1* mutations prevent auxin synthesis or accumulation in the root tip, and feedback regulation may lead to upregulation of these genes in an attempt by the plant to ensure correct auxin homeostasis in the root tip.

It has previously been found that PLS overexpressing seedlings largely, but not entirely, suppress the short root phenotype of *ctr1* (Chilley *et al*., 2006). The *PLSox ctr1* combination seedlings have slightly longer roots than *ctr1* seedlings. One possible explanation could be that, if PLS is required for auxin biosynthesis in response to ACC/ethylene, PLS overexpression may give rise to more auxin accumulation in the *PLSOx ctr1* root, leading to an increase in length compared to the length of the *ctr1* mutant.

To test this hypothesis, *ctr1* seedlings were germinated on 50 nM 1-NAA and length of the primary root was compared at 5 d.a.g. with seedlings grown in the absence of 1-NAA. The results show that exogenous 1-NAA treatment leads to a ca. 70% increase in primary root length of *ctr1* (Figure 4.18, consistent with the view that PLS overexpression leads to increased root growth in a *ctr1* background by promoting auxin accumulation in the root).

## 4.5: Summary:

The above chapter gives an account of auxin responses of the *pls* mutant and highlights its role in the cross talk between auxin and ethylene. First, it is shown that *pls* exhibits a reduced *DR5::GFP* signal, consistent with previous auxin assays in the mutant (Chilley *et al*., 2006). Interestingly, *pls* does not show an enhanced *DR5::GFP* signal following treatment with exogenous ACC, suggesting PLS is required for ACC-mediated auxin biosynthesis or accumulation in the root tip. *pls* does show an altered root phenotype following ACC treatment, with enhanced swelling of the elongation zone, and crosses with *aux1*, which is unable to transport auxin basipetally to the elongation zone, does not rescue this phenotype, supporting the view that *pls* does not fail to exhibit a *DR5::GFP* response following ACC treatment by rapidly removing newly synthesized auxin from the root tip, and the root swelling may be the consequence of a direct effect of ACC on cell shape in that region. Transcription of the gene encoding WEI2 (anthranilate synthase),

which is required for ACC-mediated auxin synthesis, was defective in *pls*, reflecting the defective response of the mutant to ACC.

It is also shown that the *pls* mutant exhibits a weak gravitropic response, with a reduced and slower curvature towards gravity than wild type. PLSOx seedlings have a strong gravitropic response, similar to *etr1* and the *pls etr1* double mutant; the rescue of the *pls* gravitropic defect by *etr1* further supports the view that *pls* exhibits an enhanced ethylene response phenotype, which may affect root bending through effects on cell shape. *eto1* also exhibited a defective gravitropic phenotype, whereas, surprisingly, *ctr1* was most gravitropic amongst the mutants studied.

Analysis of PIN levels by immunolocalization revealed that PIN1 was relatively strongly and ectopically expressed (in the root cortex) in *pls* compared with wild type, and downregulated in *etr1*, *PLSOx* and the *pls etr1* double mutant. PIN2 levels were slightly increased in *pls*, and are reduced in *PLSOx*, *etr1* and *pls etr1* compared to the wild type and *pls*. This suggests that the enhanced ethylene responses in *pls* are responsible for enhanced PIN levels, as reported previously (Ruzicka *et al*., 2007).

The new evidence presented in this chapter for altered ethylene responses and the cross-talk with auxin in *pls* lays the foundations for further studies into the ethylene response and role of PLS into the ethylene signalling pathways, described in the following chapter.

# Results

# Chapter 5:

# Role of PLS in the ethylene signalling pathway

Ethylene and auxin have a long history of interaction at both the physiological and molecular levels. The antagonistic effects in the control of abscission of fruits and flowers (Brown, 1997), and conversely their synergistic effects in the regulation of root elongation, root hair formation and lateral root growth in Arabidopsis (Pitts *et al*., 1998; Rahman *et al*., 2002; Swarup *et al*., 2002; Ruzicka *et al*., 2007; Swarup et al., 2007) illustratrate the complex nature of ethylene-auxin crosstalk. Mutant analysis has uncovered additional levels of complexity in the relationship between these two hormones. Use of genetic approaches in Arabidopsis has helped to dissect deeper the molecular basis of ethylene action (Alonsa and Stepanova, 2004) and its interaction with auxin (Swarup *et al*., 2007).

The isolation of a series of ethylene response mutants led to the identification and better understanding of key signal transduction components. *ETR1* encodes a histidine kinase-like receptor protein that mediates ethylene perception (Chang *et al*., 1993). ETR1 and its related proteins directly regulate the activity of the Raf-like kinase protein CTR1, to repress ethylene signalling (Kieber *et al*., 1993). Ethylene binding to ETR1 causes inactivation of CTR1 (Clark *et al*., 1998), releasing the repression of EIN2, resulting in the up-regulation of downstream genes by the transcription factor, EIN3.

Intriguingly, mutations in many auxin transport or signalling components also cause aberrant responses to ethylene, indicating crosstalk between these two growth regulators (Pickett *et al*., 1990; Roman *et al*., 1995; Luschnig *et al*., 1998; Rahman *et al*., 2001; Stepanova *et al*., 2005; Chilley *et al*., 2006). Chilley *et al*. (2006) have shown that *pls* mutant seedlings exhibit enhanced ethylene responses, confirmed by the triple response phenotype of seedlings grown in the dark in air, and enhanced expression of both *GSTF2*, an ethylene upregulated gene and *ERF10*, a primary ethylene response gene. Interestingly, inhibition of ethylene signalling rescues the defective *pls* phenotype, seen as restoration of a longer primary root, increased polar auxin transport in stem tissue, increased numbers of lateral roots and increased auxin accumulation. Moreover, transgenic overexpression of the *PLS* gene reduces the inhibitory effects of exogenous ACC on primary root growth. Furthermore, the *pls* mutation cannot suppress the *etr1-1* phenotype, whereas *ctr1-1* significantly suppresses the PLS overexpression phenotype (Chilley *et al*., 2006), suggesting PLS acts at or close to the ethylene receptor, upstream of CTR1. These data strongly indicate a role for PLS in the ethylene signal transduction pathway.

Based on this rationale, the work described in this chapter analyses the possible function of PLS in the ethylene signalling pathway by investigating the potential interaction

between PLS and components of ethylene signalling pathway. Also described is a transcriptional analysis of major ethylene signalling pathways genes and some ethylene regulated genes in the *pls* mutant and in PLS overexpressing seedlings.

## 5.1: PLS may interact with ETR1

Previously, the interaction between ethylene receptors (ETR1 and ERS1) and the negative regulator of the ethylene signalling pathway, CTR1, a Raf-like kinase, was demonstrated by using the yeast two hybrid system (Clark *et al*., 1998). Nevertheless, the mechanism by which the interaction between ETR1 and CTR1 controls the regulation the expression of the components of ethylene signalling pathway downstream of CTR1 remains unclear. The ability of *ctr1-1* to at least partially suppress the PLS overexpression phenotype, and the rescue of *pls* phenotype by *etr1-1*, together suggest a role for PLS in the ethylene signalling pathway close to the ethylene receptor.

As a first step to investigate possible physical interactions between the PLS peptide and one of the ethylene receptors, ETR1, the GAL4 yeast two hybrid (Y2H) assay was used. The results were then followed up using bimolecular fluorescence complementation, BiFC.

The Y2H assay was performed by using Stratagene® GAL4 Two-Hybrid Phagemid vector system, as described in detail in Method Section 2.14. The PLS peptide was cloned as an *EcoR* I–*Xho* I fragment into the binding domain vector pBD-GAL4 Cam, and ETR1 was inserted into the activation domain vector pAD-GAL4-2.1 as an *EcoR* I –*Sal* I fragment, to test the interaction. ETR1 was also cloned into both the pBD-GAL4 Cam and pAD-GAL4-2.1 vectors as a positive control, because ETR1 can interact with itself to form a homodimer.

The two vectors pBD-GAL4 Cam and pAD-GAL4-2.1, containing PLS and ETR1 respectively were co-transformed into YRG-2 yeast strain to check the expression of two reporters genes, *lacZ* (β-galactosidase) and *HIS3* (histidine) (detailed in Section 2.14). Reconstitution of the two domains of transcriptional activator as a result of interaction between PLS and ETR1, led to the expression of the two reporter genes *lac*Z and *HIS3* (Figure 5.1). To test for possible leaky expression of *HIS3* gene, colonies obtained for yeast transformation were grown on SD media plates (Section 2.14) lacking the amino acids leucine, tryptophan and histidine. Colonies grown on these plated were further checked for leaky expression of *HIS3* by the *lacZ* assay (Section 2.14.6). The colonies of two positive controls pBD-wt::pAD-wt and pBD- mut::pAD-mut; two negative controls

pLaminC::pAD-mut and pLaminC::PAD-wt; pBD-PLS::pAD-ETR1 and pBD-ETR1::pAD-ETR1, were grown on SD media plates lacking Leu and Trp, containing X-GAL to confirm the interaction (Figure 5.1(b)).

The result of Yeast two hybrid assay (summarised in Figure 5.1) suggests an interaction between ETR1 and PLS. These results are consistent with the putative ER subcellular localisation of PLS (discussed in Chapter 3). Previously, the ethylene receptor ETR1 was found to contain a transmembrane domain responsible for ethylene binding and ER localisation (Chen *et al*., 2002). Hence, the interaction of PLS-ETR1 either localised at the ER or elsewhere in the cell, further indicates a possible role for PLS in the ethylene signalling pathway.

To further investigate a possible interaction between PLS and ETR1, BiFC was used. In this technique, two halves of the fluorescent protein YFP (the N- and C- termini) are fused to two possible interacting proteins, and any detectable interaction between the two protein permits the fusion of N and C terminal resulting in YFP fluorescence within the plant cell (Illustrated in Figure 5.2). The detailed BiFC protocol is described in Section 2.16. The Gateway vectors used in BiFC assay were kindly supplied by Dr. Silin Zhong, Nottingham University. Standard Gateways cloning techniques were used to clone PLS into the YFPc Gateway vector (Method 2.15). One negative control of YFPc alone plasmid (Figure 5.3), two positive controls, whole YFP containing plasmid and ETR1-YFPn and CTR1-YFPc containing plasmids; and the PLS-YFPc and ETR1-YFPn plasmids, were adhered to the gold particles to make gold-coated cartridges. 5-10 of these cartridges were used for bombarding onion peel cells. The MS plates containing bombarded onion peels were incubated for 8-hours in dark and then a 1 cm section of the peel was stained with propidium iodide (10 mg/ml) for 1 min was viewed under confocal microscope.

The onion peel cells bombarded with the PLS-YFPc::ETR1-YFPn plasmid showed YFP expression in internal membranes, possibly the ER (Figure 5.5) and weaker YFP signal in the plasma membrane. The positive control of ETR1-YFPn:: CTR1-YFPc interaction showed YFP expression in internal membranes, expected to be the ER ( Figure 5.4). The negative control of YFPc showed no YFP expression (Figure 5.3 a-c). The positive control of whole YFP was found to be localised in the cell wall of onion peel cells (Figures 5.3 d-f). Therefore, the results of Yeast Two Hybrid and BiFC assays indicate that the PLS peptide interacts with the ethylene receptor ETR1, and the two might co-localise in the ER. The results also support the existing view that ETR1 interacts with itself and with CTR1. In order to establish more precisely the role of PLS in the ethylene signalling pathway,

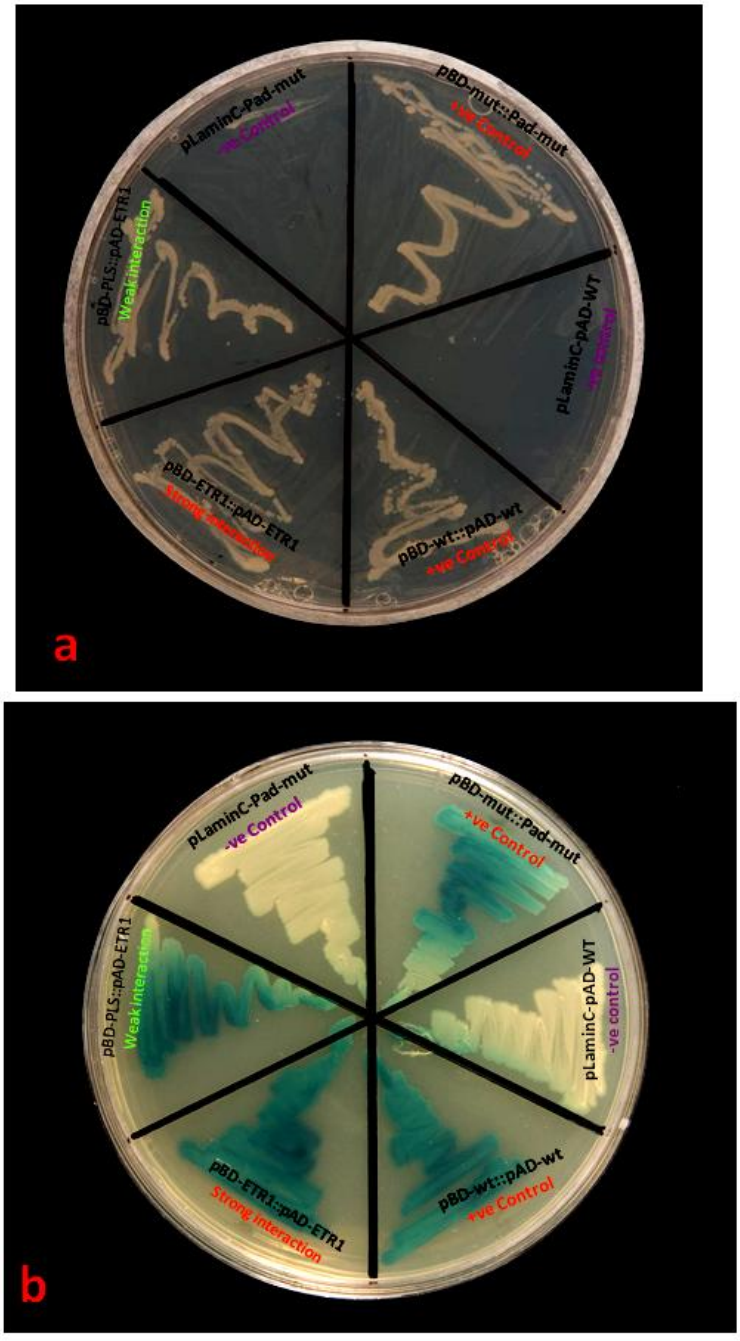


**Figure 5.1: PLS interacts with ETR1 in Y2H assays:** GAL4 two hybrid vector systems were used to detect interaction between PLS and ETR1, with the help of two reporter genes, β galactosidase (*lacZ*) and histidine *(HIS3)*. a) SD agar plate without His,Trp or Leu, showing colonies growing due specific interaction between the bait and the target protein, resulting in expression *HIS3* gene. b) SD agar plate with Trp and Leu, containing X-GAL showing expression of the *lacZ* gene (blue colonies) due to interaction between bait and target protein.

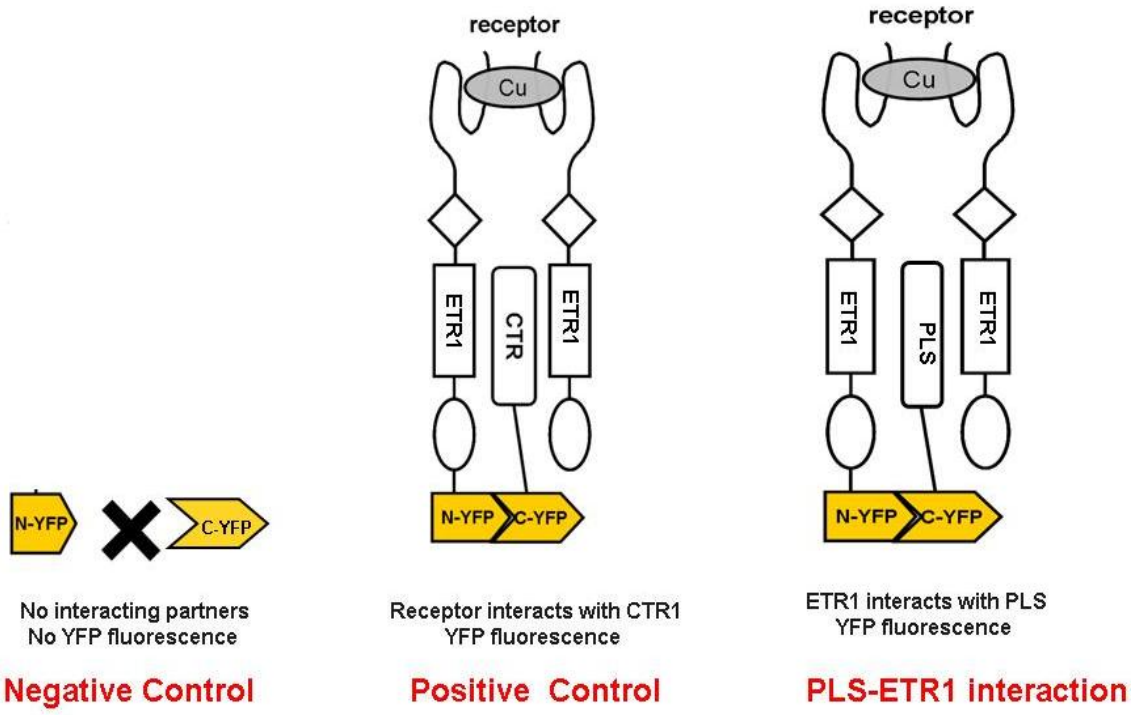


**Figure 5.2: Principle behind BiFC (Bimolecular Fluorescence Complementation) assay.** When YFP fluorescent protein is split into N and C terminal halves, the YFP does not produce fluorescence. Two interacting proteins (ETR1-CTR1) attached to the N- and C-termini of YFP result in its reconstitution, causing YPF to fluoresce.

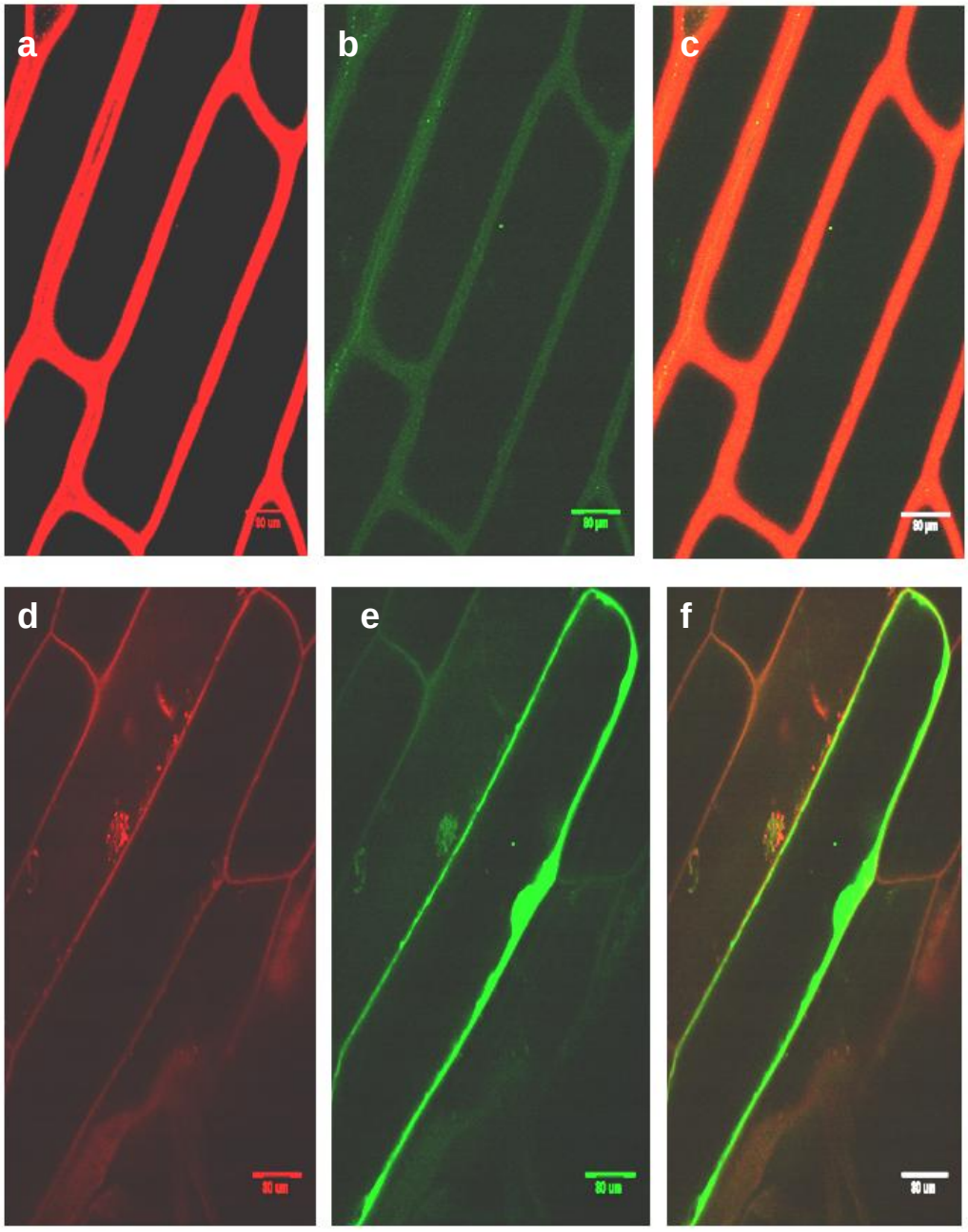


**Figure 5.3: Controls used in BiFC assay**. a, b, c ) YFPn alone was used as a negative control, showing no YFP fluorescence in the onion peel cells, with the background counter stained with propidium iodide. d, e, f) Intact YFP plasmid containing both N- and C-termini was used as a positive control. The positive controls shows YPF florescence (in green) localised in the cell periphery of onion peel cells, background counterstained with propidium iodide.

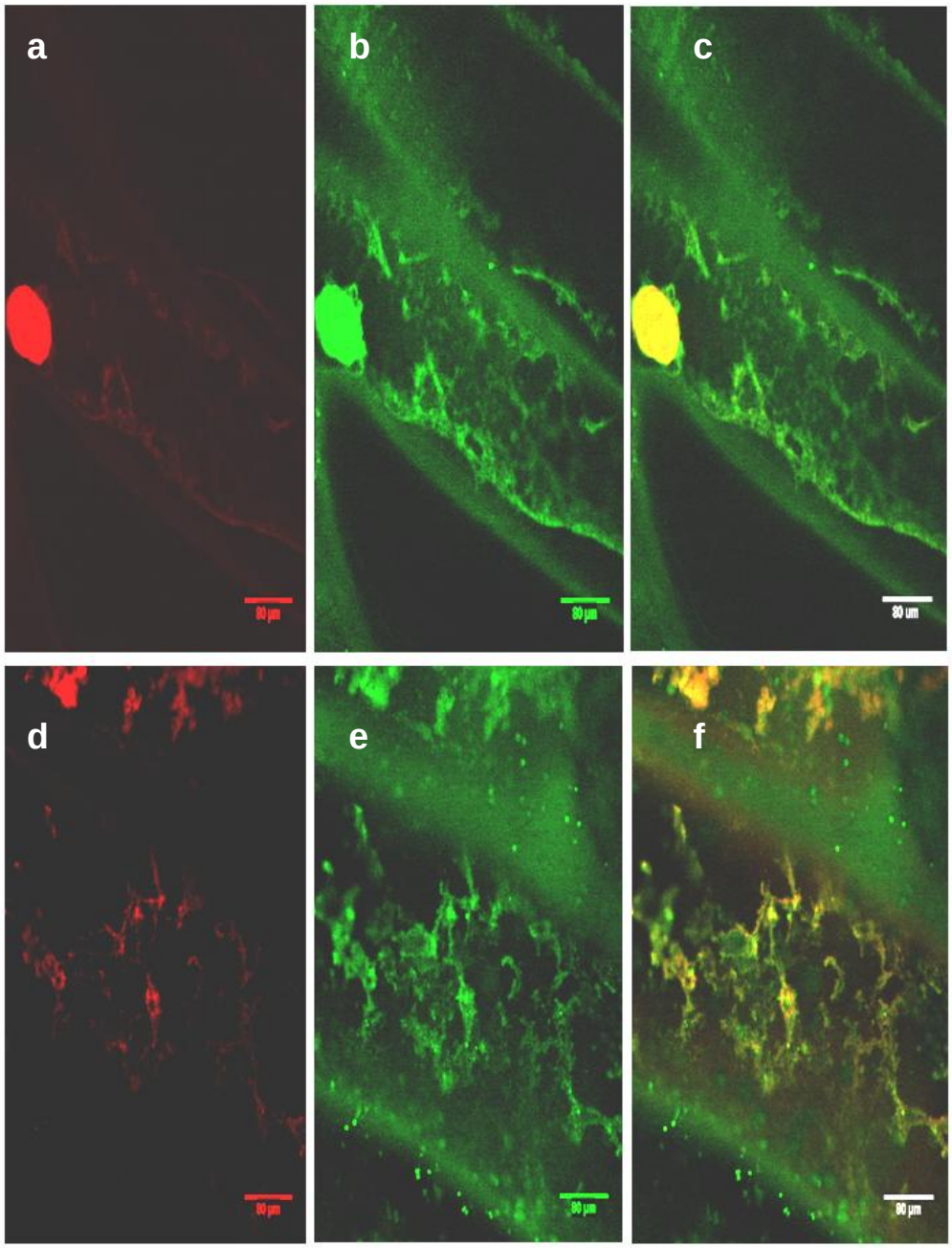


**Figure 5.4: Localisation of the ETR1–CTR1 interaction as an internal positive control in the BiFC assay.** a-c) Onion peel cell showing YPF fluorescence (in green) due to interaction between YPFn-ETR1 and CTR1-YFPc, predicted to be localised to the endoplasmic reticulum, and background stained with red propidium iodide. d-f) Higher magnification image showing YFP fluorescence (in green) in a reticulated membrane compartment (presumed to be ER) as a result of reconstitution of YFP due to interaction between ETR1 and CTR1.

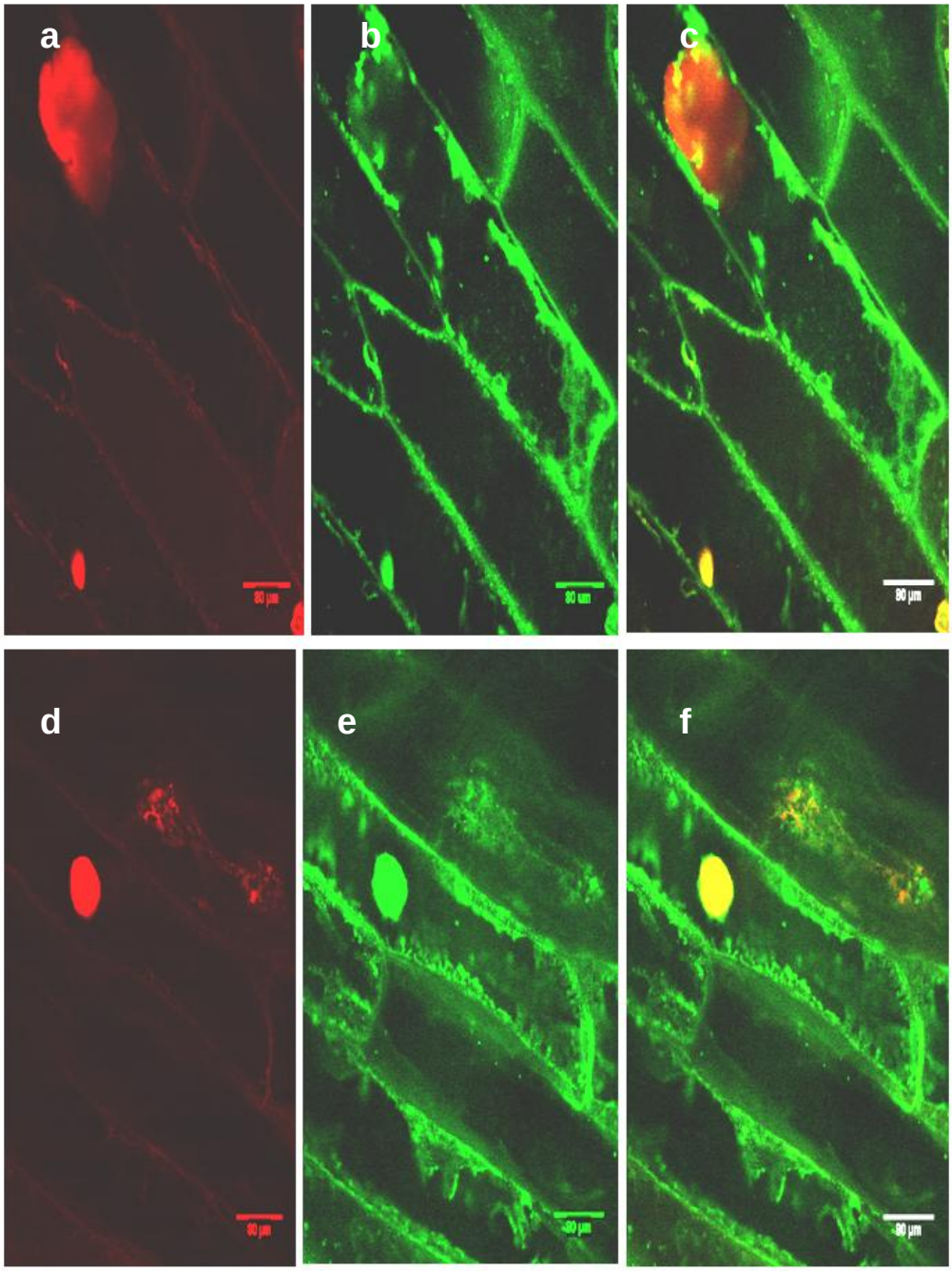


**Figure 5.5: PLS- ETR1 interaction suggested by BiFC assay.** a- f) Onion peel cells showing YFP expression (in green) as a result of interaction between YFPn – ETR1 and PLS-YFPc putatively localised in the ER, but showing also some localization in the cell periphery.

further analysis of the association between PLS with other components of the ethylene signalling pathways needs to be carried out.

## 5.2: The *pls* mutant shows upregulation of ethylene responsive genes

Ethylene binding to the receptor causes inactivation of CTR1, and the consequent derepression of EIN2, a protein of unknown biochemical function that is essential for the ethylene response. Downstream of EIN2, a family of transcription factors including EIN3 and EIN3-like proteins triggers a transcriptional cascade that results in the activation/ repression of hundreds of target genes (Alonso and Stepanova, 2004; Guo and Ecker, 2004). Since the *pls* mutant seedling is known to show upregulation of two ethylene regulated genes (*GSTF2* and *ERF10*; Chilley et al., 2006), it was decided to investigate the expression of ethylene signalling pathway genes and other ethylene-regulated genes in the *pls* mutant, and in PLS-overexpressing (*PLS*Ox) and *pls etr1* double mutant backgrounds. The overexpression of the *PLS* gene and *pls etr1* double mutant rescues the *pls* phenotype, and therefore the expression of genes in these mutant background are expected to be the opposite to that seen in the *pls* mutant.

Transcriptional analysis of seven ethylene pathway regulator or regulated genes, *ETR1*, *ERS1*, *CTR1*, *GST1*, *HSL1, EIN2* and *EIN3*; and one control gene, *ACTIN2,* was carried out by Real-time PCR and confirmed by semi-quantitative PCR. Primers were designed for the all the eight genes (Section 2.10.6) for expression analysis. cDNA was prepared from 1µg total RNA from seven day old seedlings of Col-O, C24, *pls*, *PLSOx*, *pls etr1*, *etr1*, *ctr1*, and *eto1* (Sections 2.6.4 and 2.10.5). Quantitative RT-PCR was performed with eight primers each corresponding to eight different ethylene regulated genes on eight cDNA samples in quadruplicates as described in Section 2.11.

The results of the quantitative RT-PCR were plotted as mRNA level in the eight different cDNA samples. The results showed up-regulation of ethylene receptors, *ETR1* and *ERS1* (Figure 5.6) and of the ethylene-regulated genes *CTR1*, *HSL1*, *GST2*, *EIN2*, and *EIN3* in *pls* (Figure 5.7), but down-regulation in *PLSOx* and *pls etr1.* Interestingly, the expression of *ETR1*, *ERS1*, *CTR1*, *GST2*, *EIN2* and *EIN3* are up-regulated in *eto1* mutant background, but down-regulated in *etr1* mutant background. The result of semi-quantitative PCR analysis further confirmed these results (Figure 5.9). The overall comparison of relative transcript abundance of seven ethylene regulated genes in eight different cDNA background is illustrated in Figure 5.9. Two major expression patterns

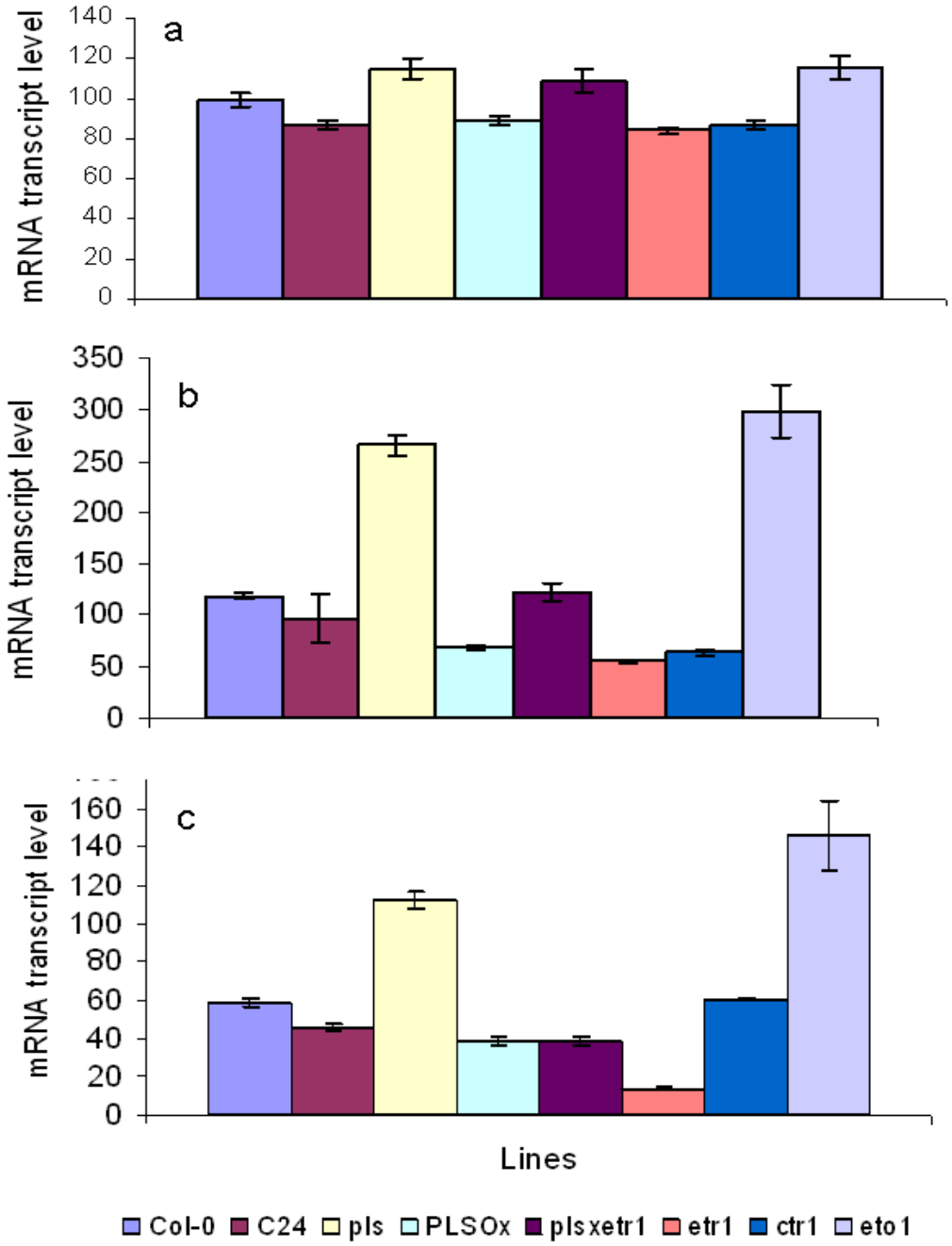


**Figure 5.6 (a): Transcriptional analysis of the genes *ACTIN2* (a), *ETHYLENE RESISTANT 1* (*ETR1*) (b) and *ETHYLENE RECEPTOR1* (*ERS1*) (c) in eight different RNA samples (Col-0, C24, *pls*, *PLS*Ox, *pls etr1*, *etr1*, *ctr1* and *eto1*, as indicated in colour).**

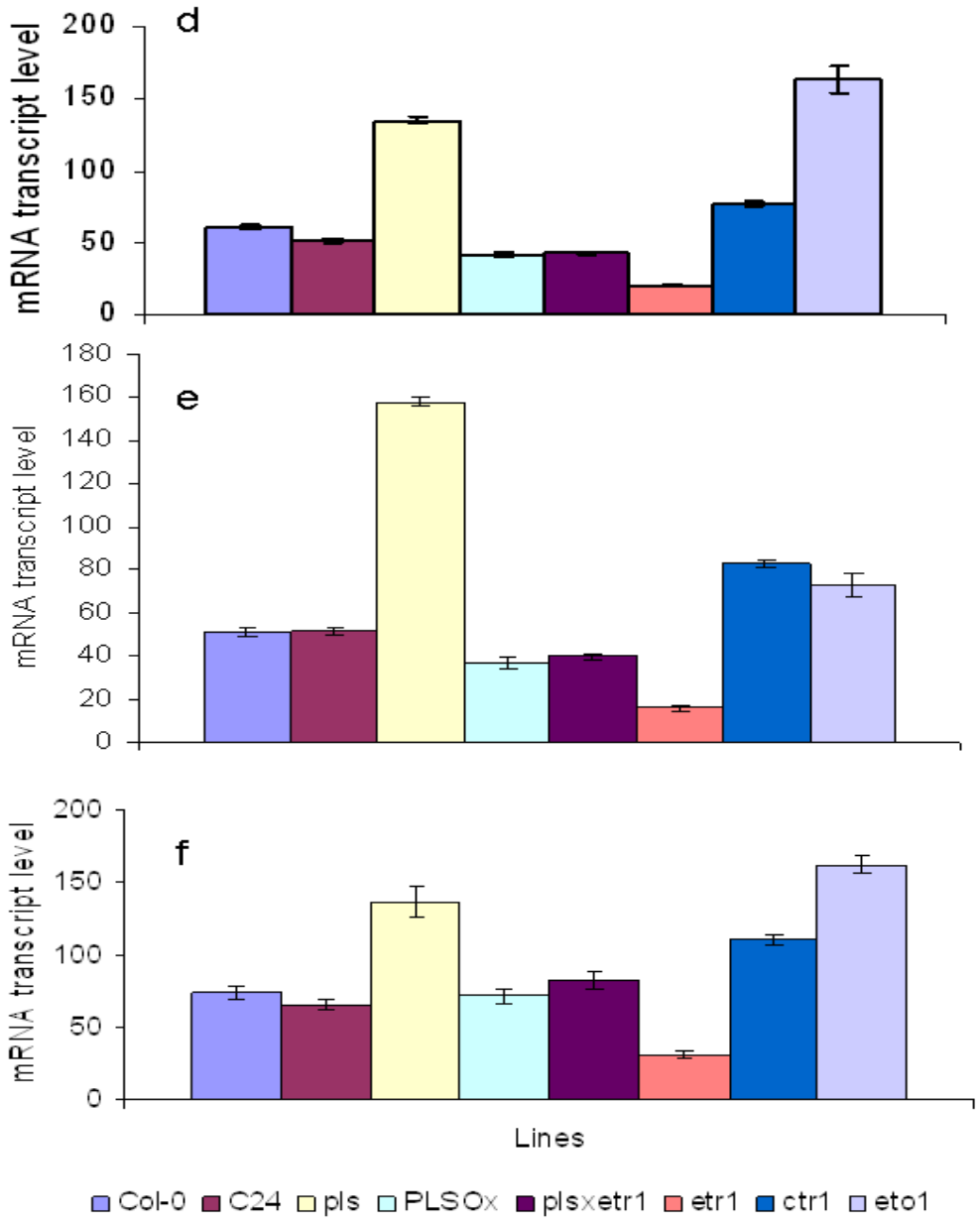


**Figure 5.7 (b): Transcriptional analysis of *CONSTITUTIVE TRIPLE RESPONSE1* (*CTR1*) (d), *GLUTATHIONE S-TRANSFERASE2* (*GST2*) (e) and *HOOKLESS1* (*HLS1*) (f) in eight different RNA samples (Col-0, C24, *pls*, *PLS*Ox, *pls etr1*, *etr1*, *ctr1* and *eto1*, as indicated in colour).**

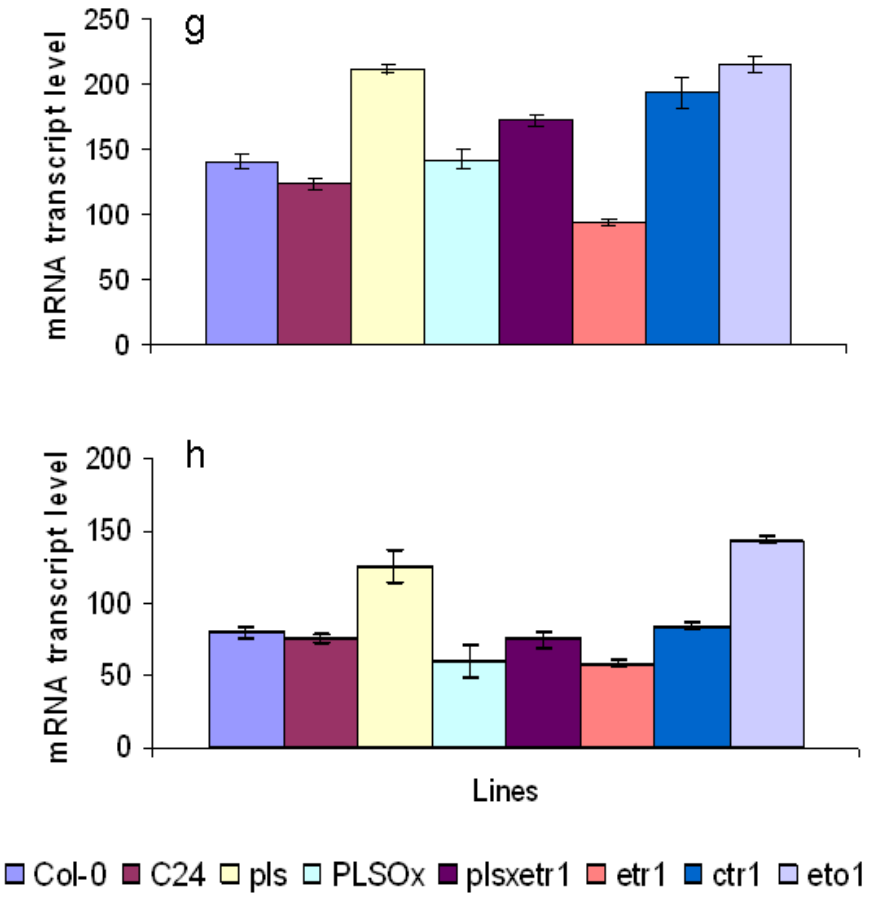


**Figure 5.8 (c): Transcriptional analysis of *ETHYLENE INSENSITIVE2* (*EIN2*) (g) and *ETHYLENE INSENSITIVE3* (*EIN3*) (c) in eight different RNA samples (Col-0, C24, *pls*, *PLS*Ox, *pls etr1*, *etr1*, *ctr1* and *eto1*, as indicated in colour).**

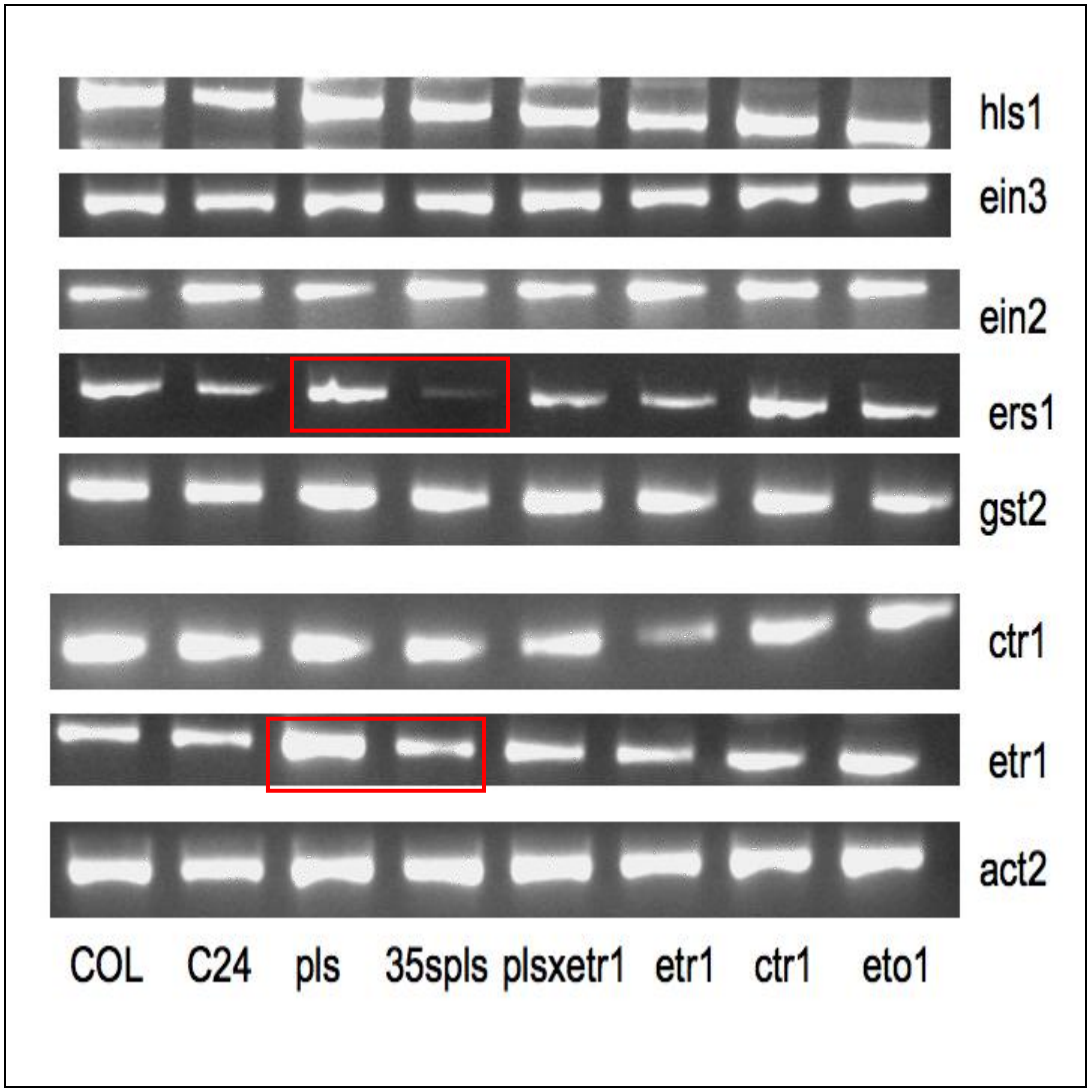


**Figure 5.9: Ethylene receptors are upregulated in *pls* but downregulated in *35S::pls*.** Result of semi-quatitative RT-PCR analysis. Highlighted in red is the expression of *ETR1* and *ERS1* in *pls* and *35S::pls*. Both *ETR1* and *ERS1* are upregulated in *pls* but downregulated in *35S::pls*.

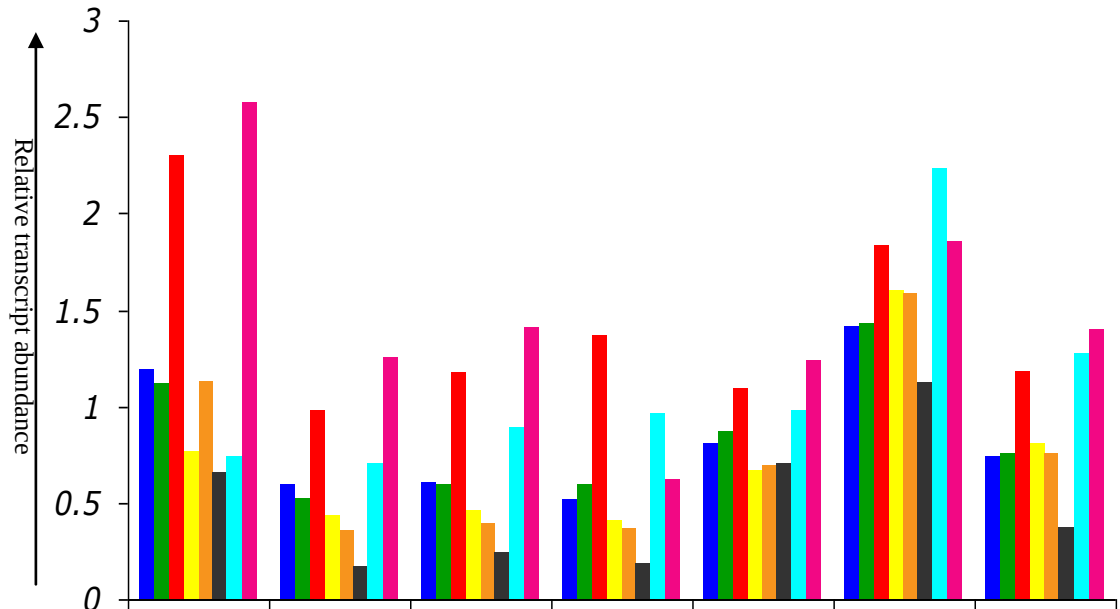


| | etr1 | ers1 | ctr1 | gst2 | ein3 | ein2 | hls1 |
|---|---|---|---|---|---|---|---|
| Col-0 | 1.19257 | 0.59277 | 0.60582 | 0.51419 | 0.80593 | 1.411 | 0.73814 |
| C24 | 1.11734 | 0.5289 | 0.59682 | 0.59711 | 0.87514 | 1.43353 | 0.76069 |
| pls | 2.3087 | 0.97609 | 1.17391 | 1.37391 | 1.09348 | 1.83696 | 1.18696 |
| plsOx | 0.76735 | 0.43383 | 0.46249 | 0.4136 | 0.66592 | 1.60157 | 0.80725 |
| plsxetr1 | 1.13208 | 0.35435 | 0.39485 | 0.36838 | 0.69052 | 1.58537 | 0.75863 |
| etr1 | 0.65943 | 0.16805 | 0.23736 | 0.18709 | 0.69899 | 1.12255 | 0.37359 |
| ctr1 | 0.73497 | 0.69942 | 0.88728 | 0.96127 | 0.97775 | 2.23121 | 1.27168 |
| eto1 | 2.57112 | 1.25431 | 1.40948 | 0.62716 | 1.24138 | 1.84914 | 1.39871 |



**Figure 5.10: Relative transcript abundance of seven ethylene regulator/regulated genes (on X-axis) in eight different plant lines indicated by various colours**. Results of semi-quantitative PCR are confirmed by Real time PCR analysis. Ethylene regulated genes (*ETR1, ERS1*, *CTR1*, *GST2*, *HSL1*, *EIN2* and *EIN3*) are upregulated in the *pls* mutant (red).

were observed in the examined transcripts: (i) ethylene receptors and ethylene regulated genes are up-regulated in each of the *pls* and *eto1* mutant lines, and (ii) ethylene-regulated genes are back to wild-type level in *PLSOx*, and in the *pls etr1* double mutant. The relative mRNA levels of these genes are further reduced in the *etr1-1* mutant.

## 5.3: Summary

This chapter outlined the possible role of the PLS peptide in the ethylene signalling pathway. The results suggest a physical interaction between PLS and the ethylene receptor ETR1, as determined by both GAL4 Yeast Two-Hybrid assay and BiFC. The spilt YFP assay (BiFC) indicated the possible localization of PLS-ETR1 interaction in the ER of the cell, using the known ER-localised ETR1-CTR1 interaction as a positive control. It further suggests the sub-cellular localisation of PLS in the ER (discussed in Chapter 3) shown in Figure 5.5. Described in the latter half of the chapter are the transcription profiles of seven ethylene regulator or regulated genes, *ETR1, ERS1, CTR1, HSL1, GST2, EIN2* and *EIN3* in eight different cDNA populations derived from different mutant or transgenic lines altered in ethylene response (Figure 5.10). The results revealed up-regulation of all the seven ethylene regulated genes in the *pls* mutant and down-regulation in the *PLSOx* and *pls etr1* plants, supporting the idea of a role for PLS as a negative regulator of the ethylene signalling pathway.

# Chapter 6:

# Discussion

This study has been concerned with the further understanding of the function of the PLS peptide in Arabidopsis, its subcellular localisation and establishing the role of PLS in auxin-ethylene crosstalk. The *PLS* gene was initially identified as a promoter trap transgenic line, showing β-glucuronidase (GUS) fusion gene expression in the heart-stage embryo, in the basal region of the embryo; and in the seedling root tip (Topping *et al*., 1994; Topping and Lindsey, 1997). The *pls* mutant shows a semi-dominant phenotype, characterised by relatively short and radially expanded cells in the root with reduced division, leading to short roots; it also shows altered responses to exogenous auxins and cytokinins (Casson *et al*., 2002). Further, cloning and characterisation of the *PLS* gene revealed that it encodes a polypeptide of 36 amino acids and is required for correct auxin-cytokinin homeostasis to modulate root growth and leaf vascular patterning (Casson *et al*., 2002). Chilley *et al*. (2006) established a link between PLS, ethylene signalling and auxin homeostasis. This work suggested that PLS negatively regulates ethylene responses to modulate cell division and expansion via downstream effects on auxin signalling and microtubule dynamics, influencing normal root growth and lateral root formation.

Phytohormones play a vital role in determining the fate of a cell division and expansion in the root tip. Auxin, cytokinins, ethylene, gibberellins and abscisic acid interact either synergistically or antagonistically to regulate normal growth and development in the plants. For example, auxin and cytokinins can each trigger ethylene biosynthesis and in turn ethylene can modify auxin responses and meristem function (Vogel *et al*., 1998; Souter *et al*, 2004; Stepanova *et al*., 2005). Ethylene can either inhibit or promote cell division, influencing cell fate, depending upon the exposure (Kazama *et al*., 2004). Many of the genes involved in cellular patterning and development are either transcriptionally upregulated or downregulated in response to these hormones. Auxin signalling is necessary for QC initiation in the embryo (Hardtke and Berleth, 1998; Harmann *et al*., 2002), and directs expression of the *PLETHORA1 (PLT1*) and *PLT2* transcription factors, which function redundantly in specifying QC fate (Aida *et al*., 2004). The *SCR* and *SHR* transcriptional factor genes were initially identified for their role in radial patterning (Benfey *et al*., 1993), but are also required for QC function (Sabatini *et al*., 2003). In *plt1*, *plt2, scr* and *shr* mutants, some QC markers are not expressed, and the root meristem loses its ability to undergo cell division. Therefore stem cell function in the Arabidopsis root involves regulation by transcription factors (SCR, SHR or PLT) in response to signal transduction pathways that produce transcriptional changes via auxin.

This chapter discusses the results of the work described in the preceding chapters, aims to connect it with previous work on PLS and endeavours to develop a more advanced

model for the role of PLS in Arabidopsis root growth and development. The chapter concludes by suggesting future work in order to clarify further the link between PLS, ethylene signalling and auxin homeostasis.

## 6.1: PLS is a membrane-localised peptide expressed in the root tip

Casson *et al*. (2002) demonstrated that the *PLS* gene encodes a 36 amino acid polypeptide. The 24 amino acids on the N-terminal of the peptide were predicted to form two beta sheets, and the remaining 12 amino acid to form an alpha helix. The presence of three arginine residues in between the two beta sheets suggested the possibility of either a cleavage site or formation of a turn region, converting these beta sheets into beta barrels. Most transmembrane proteins contain either beta barrels or alpha helices, indicating the possibility of PLS being attached to a membrane, or possibly interacting with hydrophobic regions of other proteins. In this present study, the subcellular localisation of PLS revealed that the peptide is indeed membrane associated, but the precise nature of the membrane is not yet clear, and needs further colocalisation studies to confirm this. Nevertheless, the BiFC assay, designed to explore the possible interaction of PLS with the ER-bound ethylene receptor ETR1, indicated the possibility of this membrane to be ER.

Although the PLS peptide is yet to be detected in vivo by western blotting or immunolocalization, it has been detected in cell extracts following a proteomic analysis of the APM1 protein (Angus Murphy and Wendy Peer, personal communication). *Aminopeptidase M1* (*APM1*) encodes a metallopeptidase originally identified by its affinity for, and hydrolysis of, the auxin transport inhibitor 1-naphthylphthalamic acid (NPA). APM1 is localised at the margins of Golgi cisternae, plasma membrane, tonoplast, dense intravacuolar bodies and metaxylem cells. APM1 is also associated with brefeldin A-sensitive endomembrane structures and the plasma membrane in cortical and epidermal cells (Peer *et al*., 2009). Thus, considering all the above evidence, it would be valid to predict that PLS is a protein- and membrane-associated peptide expressed in the Arabidopsis root tip.

## 6.2: The *pls* mutant shows defective cellular patterning in the root tip

The coordinated expression of genes determines cellular characteristics which in turn direct root morphogenesis, and in this thesis, it is shown that the *pls* mutant shows reduced expression of QC marker lines (QC12::GFP and QC6::GFP) and a reduction in the number of cell layers of the columella.

Several genes important for development and cellular patterning of the root were first identified by their mutant phenotypes. As described above, the *SCR* and *SHR* genes encode GRAS-type transcription factors required for asymmetrical division of the ground tissue stem cell and for endodermis specification. In the mutant lines, instead of cortex and endodermis there is a single mutant cell layer between the epidermis and stele, with characteristics of both endodermis and cortex (Benfey *et al*., 1993, 2000, Scheres *et al*., 1995, 2000). The *cobra* (*cob*) and *lion's tail* (*lit*) mutants exhibit abnormal expansion in epidermis and stele respectively; the *sabre* mutants have abnormal cell expansion in the root cortex (Benfey *et al*., 1994; Aeschbacher *et al*., 1995**,** Schindelman *et al*., 2001); and the *PLETHORA 1* (*PLT1*) and *PLT2* genes are essential for QC specification and the stem cell activity (Aida *et al*., 2004). The role of the *PLT* genes in particular, which in turn are auxin-inducible in their expression, is essential for correct auxin distribution (via regulation of *PIN* gene expression). The defective expression in *pls* of QC markers may be the consequence of the reduced auxin accumulation in the *pls* root tip, seen as the reduced DR5::GFP signal (Chapter 4) and consistent with previous auxin transport and concentration measurements (Chilley *et al.*, 2006).

Ethylene also influences the activity of the QC and surrounding initials. The roots of the ethylene-insensitive mutant *ein2* and wild-type treated with AVG (aminoethoxyvinly glycine), an inhibitor of ethylene biosynthesis, were also reported to have fewer columella layers; and mutants with enhanced ethylene responses, or wild-type plants treated with ACC, showed defective QC division, indicating a role of ethylene in the cell division of the QC cells and initials (Ortega-Martinez *et al*., 2007). PLS acts as a negative regulator of ethylene signalling, and so the *pls* mutant (with enhanced ethylene responses) might be expected to have additional QC divisions and more layers of columella cells. In fact the opposite in observed. A possible explanation is that a critical level of ethylene response, or specific ethylene response targets, are required to be activated to modulate cell division activation or inhibition. It is also possible that PLS may regulate a subset of ethylene signalling responses.

The loss of ability to undergo mitotic cell division in the root tip was also described before in *scr-1*, *plt1* and *shr* mutants (Sabatini *et al*., 2003; Aida *et al*., 2004). The SCR::GFP, J1092 and J2341 expression markers were also found to be defective in the *pls* mutant, further showing a requirement for *PLS* in correct gene expression levels in particular cell types.

## 6.3: PLS is a component of the ethylene signalling pathway

The *pls* mutant seedling exhibits enhanced ethylene signalling, seen as the triple-response phenotype when grown in air, and the enhanced expression of both the endogenous *AtGSTF2*, an ethylene unregulated gene (Smith *et al*., 2003), and the primary ethylene response gene *ERF10* (Ohta *et al*., 2001). The defective *pls* mutant phenotype of short primary root, reduced polar auxin transport and low auxin accumulation are rescued by the pharmacological or genetic inhibition of ethylene signalling (Chilley *et al*., 2006). Overexpression of the *PLS* gene reduces the inhibitory effects of exogenous ACC on primary root growth. Chilley *et al*. (2006) showed that PLS action does not require ACC synthase5 (ACS5), an essential enzyme catalysing the first step of cytokinin-mediated ethylene biosynthesis by ACS5/CIN5 (Vogel *et al*., 1998). Both the *pls* mutant and *pls cin5* double mutant show a strong triple response phenotype in presence of cytokinin, which indicated that ethylene response of *pls* is independent of cytokinin-mediated ethylene biosynthesis. Furthermore, *pls* does not overproduce ethylene and the enhanced ethylene response of *pls* is not rescued by the ethylene synthesis inhibitor aminoethoxyvinylglycine, pointing towards ethylene signalling defects in *pls* rather than defects in ethylene biosynthesis control (Chilley *et al*., 2006). The rescue of the effects of the *pls* mutation by the introduction of *etr1-1* and the failure of *pls* to suppress the *etr1-1* phenotype, together with the failure of the *PLS*-overexpression phenotype to completely suppress the *ctr1-1* mutant phenotype, strongly suggests a role for PLS in the ethylene signalling pathway positioned close to ETR1 and its interaction with CTR1.

The results from the yeast two-hybrid and Bimolecular Fluorescence Complementation (BiFC) studies performed in this project provided evidence that PLS interacts directly with ETR1, although the possible interaction between CTR1 and PLS still needs to be tested. As is the case for *pls*, the *rte1* mutant cannot suppress the ethylene resistance phenotype of *etr1-1* and it also seems to act as a negative regulator of ethylene responses and is required for correct ethylene receptor function (Resnick *et al*., 2006). However, no evidence of direct interactions of RTE1 with any of the components of the ethylene signalling pathway have yet been shown.

Gene expression studies showed that the *pls* mutant exhibits up-regulation of the ethylene receptor genes *ETR1* and *ERS1* and of the other ethylene signalling pathway genes *CTR1*, *EIN2* and *EIN3.* These data would suggest a feedback regulation of the transcription of genes encoding components of the ethylene signalling pathway in response to alterations in the activity of the pathway, as mediated by changes in *PLS* expression levels. The increase in ethylene responses in the *pls* mutant is consistent with upregulation of the *EIN2* and *EIN3* proteins that positively mediate ethylene signal transduction (Li and Guo, 2007). Upregulation of *ETR1*, *ERS1* and *CTR1*, which are each negative regulators of ethylene responses (reviewed by Klee 2002), may represent a cellular mechanism aimed at reducing ethylene responses as a consequence of the enhanced ethylene signalling produced in the *pls* mutant. It has also been shown previously that ACC negatively regulates *PLS* transcription, though auxin upregulates it (Casson *et al.* 2002; Chilley *et al*., 2006).

## 6.4: PLS is required for ACC-mediated auxin synthesis in the root

The plant hormone auxin is a simple molecule similar to tryptophan, yet it elicits a diverse array of biological responses and is involved in the regulation of growth and development throughout the plant life cycle. The ability of auxin to bring about such diverse responses appears to result partly from the existence of several independent mechanisms for auxin perception and signal transduction, and partly because of its interactions with other hormones, including ethylene and cytokinins. However, our understanding of the molecular mechanisms by which auxin interacts with other hormones to control growth and development in plants is far from complete.

Normal growth and development of roots results from postembryonic activity of cells within the root meristem that is controlled by coordinated action of auxin, ethylene, cytokinins, gibberellins and abscisic acid. For example, synergistic effects of auxin and ethylene have been well defined in the regulation of hypocotyl elongation (Smalle *et al*., 1997; Vandenbussche *et al*., 2003), root hair growth and differentiation (Pitts *et al*., 1998), apical hook formation (Lehman *et al*., 1996; Li *et al*., 2004), root gravitropism (Lee *et al*., 1990; Buer *et al*., 2006; Swarup *et al*., 2007), and root growth (Pickett *et al*., 1990; Rahman *et al*., 2001; Swarup *et al*., 2007) suggesting that these two signalling pathways interact at the molecular level. Recently, it was shown that the effect of ethylene on root growth is largely mediated by the local regulation of auxin biosynthesis and transport-dependent local auxin distribution (Ruzicka *et al.*, 2007; Swarup *et al*., 2007; Stepanova *et al*., 2007). In mutants affected in auxin perception and or basipetal auxin transport, ethylene cannot activate the auxin responses nor regulate root growth.

In the *pls* mutant, enhanced ethylene signalling causes repression in auxin transport in the inflorescence stem and auxin accumulation in the root, resulting in reduced lateral root formation and DR5 signal (Chilley *et al*., 2006 and this thesis). This contrasts to the effects of ethylene in increasing auxin transport at the root tip, via increased PIN levels (Ruzicka *et al*. 2007), suggesting ethylene has different effects on polar auxin traport in the root and inflorscence stem. Similarly, the *aux1* mutant has defective inflorescence stem and root polar auxin transport, reduced levels of auxin in the root tip and reduced lateral root formation (Swarup et al., 2001; Marchant *et al*., 2001). In this thesis it is shown that not only does the *pls* mutant show reduced *DR5::GFP* expression, it also exhibits a failure of the ACC-mediated induction of auxin synthesis (and reflected in enhanced DR5 expression) seen in the wild-type root tip (Ruzicka *et al.*, 2007; Swarup *et al*., 2007; Stepanova *et al*., 2007). This indicates a requirement for PLS in ACC-mediated auxin synthesis and accumulation. Interestingly, in the *aux1* mutant the inhibition of root elongation by ACC is lost (Rahman *et al*., 2001; Ruzicka *et al.,* 2007), but in the *aux1 pls* double mutant, the *aux1* mutation only partially rescues the short root phenotype of *pls* or the inhibitory effect of ACC on *pls*. This further suggests that PLS is required for ACC-mediated auxin biosynthesis.

Stepanova *et al*. (2005) found that inhibition of root growth by ethylene is regulated by action of *WEI2*, which encodes an essential enzyme in auxin biosynthesis. Upregulation in its expression mediated ethylene-mediated auxin synthesis in roots, whereas downregulation prevents this increase. *WEI2* expression is downregulated in the *ctr1* mutant, which suggests that ethylene-mediated auxin synthesis and *WEI2* expression is dependent on CTR1-mediated ethylene signalling (Stepanova *et al*., 2005). Intriguingly, there is upregulation of *WEI2* expression in the *pls* mutant, but the *pls* mutant does not show the normal increase in DR5-GFP expression in the presence of ACC. It is possible that PLS has a function downstream of WEI2 to regulate ACC-mediated auxin biosynthesis, and the observed upregulation of WEI2 may reflect a feedback effect to increase synthesis on ACC treatment. It is also possible that any increased auxin in the root tip following ACC treatment of *pls* is removed by enhanced PIN2 levels, as the *pls* mutant shows upregulation of PIN2. However, since there is no observed DR5-GFP activation further up the root following ACC treatment, this seems unlikely. Taken together, the evidence that PLS both interacts with ETR1, and is required for ACC-mediated auxin synthesis, indicates two distinct roles for PLS, in repression of ethylene signalling and in ethylene-mediated auxin synthesis.

Furthermore, the *pls* mutant shows upregulation of PIN1 and PIN2, but downregulation in both *PLS* overexpression lines and in the *pls etr1* double mutant (Chapter 4). This would

suggest that the PIN upregulation in *pls* is the secondary consequence of the enhanced ethylene responses in the mutant, consistent with the observed effect of ACC and ethylene on PIN levels in wild-type roots (Ruzicka *et al.*, 2007; ), rather than a direct effect of the PLS peptide in the regulation of PIN levels.

Galinha *et al*. (2007) demonstrated that the PLETHORA gradient may work as a read-out of an auxin gradient in the root and *PLT* genes control the expression of *PIN* genes, indicating that there is no linear relationship between the auxin gradient and the PLETHORA gradient. This opens the possibility that other genes like *PLS* either directly or indirectly regulate the complex interaction between *PIN* and *PLT.* It is possible that PLS might be involved in either regulation of these transcription factors (SCR, SHR or PLT) or have a role in the auxin signalling pathway, either directly or via effects on ethylene signalling. Further analysis of a role for PLS in specifying the QC fate and in turn role in cellular patterning of root tip needs detailed study of transcription expression pattern of *PLT*, *PIN*, *SCR* and *SHR* in the *pls* mutant background. Generation of *PLT*::*GFP* marker lines and interaction studies of PLS with PLT, SCR and SHR will provide further insight into the function of *PLS*.

## 6.5: *PLS* is required for correct gravitropic responses in the root

The gravitropic response in roots proceeds in four steps: first, sensing the direction of gravity; second, conversion of a biophysical signal to a biochemical one; third, transmission of the signal to the columella; and fourth, cell expansion in the lower side of the elongation zone is reduced relative to the upper side, which causes the root to bend downwards (Mullen *et al.*, 1991, Morita *et al*., 2004, Swarup *et al*., 2005). Auxin is believed to provide the signal which mediates the gravitropic response, as a large number of auxin transport and response mutants exhibit root gravitropic defects (Mullen *et al*., 1991; Bennett *et al*., 1996; Chen *et al*., 1998; Luschnig *et al*., 1998). Both the auxin influx and efflux carriers AUX1, PIN2 and PIN3 seem to be required for channelling the auxin from the root cap to the elongation zone for the correct gravitropic response. Other signalling molecules such as cytokinin and nitric oxide have recently been reported to be required during the gravitropic response (Aloni *et al*., 2004; Hu *et al*., 2005).

It has been shown in this thesis that the *pls* mutant shows a reduced DR5 signal in the root tip, exhibits upregulation of PIN2 and has gravitropic defects, and it is hypothesized that PIN2 upregulation is a consequence of the enhanced ethylene response in *pls*, as ACC similarly enhances PIN2 levels in wild-type (Ruzicka *et al.*, 2007; Swarup *et al*., 2007; Stepanova *et al*., 2007). It is therefore likely that the ethylene defects in *pls*

contribute to altered auxin transport and accumulation, and these may lead to defective gravitropic responses. This view is supported by the observation that overexpression of the *PLS* gene, or inhibition of ethylene signalling in the *pls etr1* double mutant, rescues the gravitropic defects in the *pls* mutant. It is known that prolonged ethylene exposure stimulates negative gravitropic responses in inflorescence stems and in hypocotyls (Lu *et al*., 2002). Further, work from this project indicates the *eto1* ethylene overproducing mutant shows agravitropism, whereas other ethylene signalling mutants show normal gravitropic responses.

## 6.6: Auxin-PLS-Ethylene cross-talk - where does PLS fit?

Hormones participate in the regulation of almost every aspect of the plant life cycle and do so with an unusual functional plasticity. For example it is not rare to find that the same hormone controls a variety of completely different biological processes, yet at the same time, a particular biological process is similarly affected by several hormones (Gazzarrini and McCourt, 2003). Therefore, it is difficult to define a function of a hormone without specifying its tissue type, developmental stage and environmental conditions affecting it. In other words, understanding the function of a hormone requires comprehension of a complex network of interaction between multiple signals. The results presented in this thesis suggest PLS may act as an important component in modulating the cross-talk between ethylene and auxin responses in Arabidopsis.

With respect to the interaction between ethylene and auxin in roots, several independent studies have reported a dramatically altered responsiveness of auxin mutants to ethylene (Swarup *et al*., 2002). *PLS* transcription is positively affected by auxin and negatively by ethylene. Furthermore, correct patterning of proPLS-GUS expression is dependent on GNOM activity (Topping and Lindsey, 1997), which in turn is required for correct PIN protein localisation, local auxin accumulation and intracellular auxin signalling (Steinmann *et al*., 1999; Geldner *et al*., 2003; Kleine-Vehn *et al*., 2008). Also, the defects in auxin biosynthesis transport or response can all lead to altered ethylene responsiveness in roots (Stepanova *et al*., 2007). Although it is clear that auxin is required for the normal ethylene responses in roots and ethylene is able to stimulate auxin levels in these tissues (Stepanova *et al*., 2005), this does not imply that auxin acts downstream of ethylene in the control of root growth. Some recent studies support the role of ethylene in boosting the rate of auxin biosynthesis in roots; this auxin is then transported to transition zones by an AUX1- and PIN2-dependent mechanism (Ruzicka

et al., 2007; Swarup et al., 2007). Stepanova et al. (2007) suggested that in addition to the auxin-mediated and auxin-dependent ethylene responses, there might be a third type of response that would be dependent on the levels of auxin but would not be directly mediated by this hormone. At this point, PLS may come into play, acting as a negative regulator of ethylene responses, a positive regulator of auxin responses and is required for ACC-mediated auxin biosynthesis (Chilley *et al*., 2006, this work). PLS is required for correct gravitropic responses, correct expression of PINs and correct expression of the ethylene-regulated auxin synthesis gene, *WEI2*. It is tempting to speculate that PLS might be acting to control the interaction between auxin and ethylene for normal root growth and development; and, given its semi-dominant phenotype, in a dose-dependent manner, in part at least through direct interaction with ETR1.

## 6.7: Model of PLS function in the root

As suggested by this work, PLS is hypothesized to be membrane-associated. This membrane could be plasmamembrane or ER, and both of these represent sites of significant signalling activities. The results of the interaction studies PLS and ETR1, and of expression studies on components of the ethylene signalling pathway, provide further support for a role for PLS as working in a dose-dependent manner to regulate the ethylene response. It can be speculated that PLS interactions with ETR1 might alter ethylene binding to ETR1, ETR1-CTR1 interactions, or ETR1 stability, each of which would affect ethylene signal transduction. It is also possible that PLS may additionally interact with other ethylene receptors, to modulate downstream responses. Enhanced ethylene responses can trigger auxin synthesis, and evidence from this thesis suggests that PLS is also required for this response.

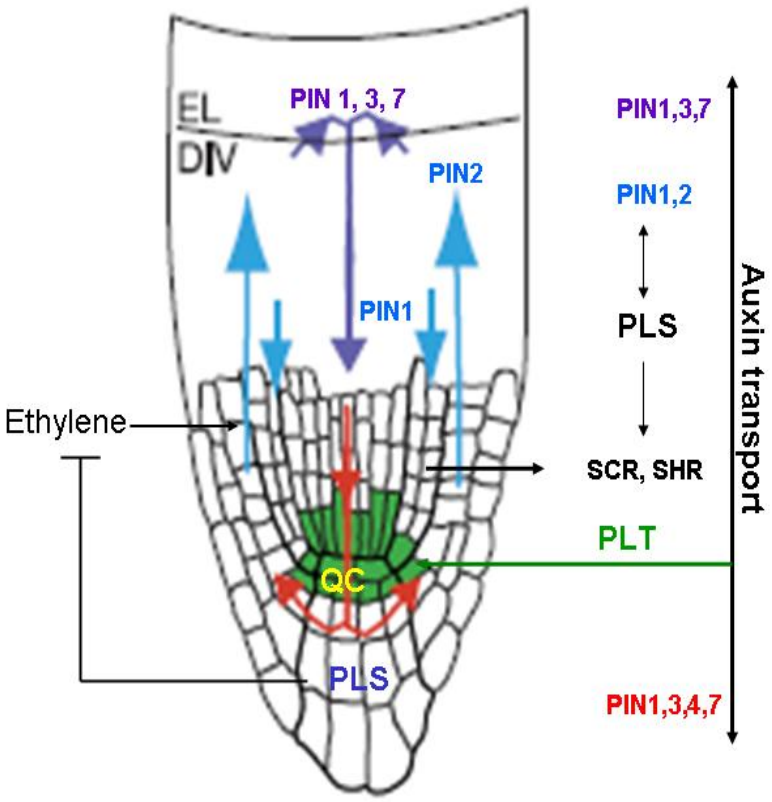


**Figure 6.1: Role of PLS in the specification of root stem cells by auxin** (adapted from Blilou *et al*., 2005; Kepinski, 2006)

An auxin maximum in the root meristem is maintained by directional auxin transport. This auxin maximum induces *PLT* gene expression that controls the function of PIN protein. There is an overlap of auxin-induced PLT with that of SCR and SHR (which are expressed in the endodermis and QC). The auxin maximum could lead to ethylene production in the root tip. PLS presence in the root tip inhibits ethylene production and PLS might be required for correct expression of auxin-regulated genes in the root tip.

.

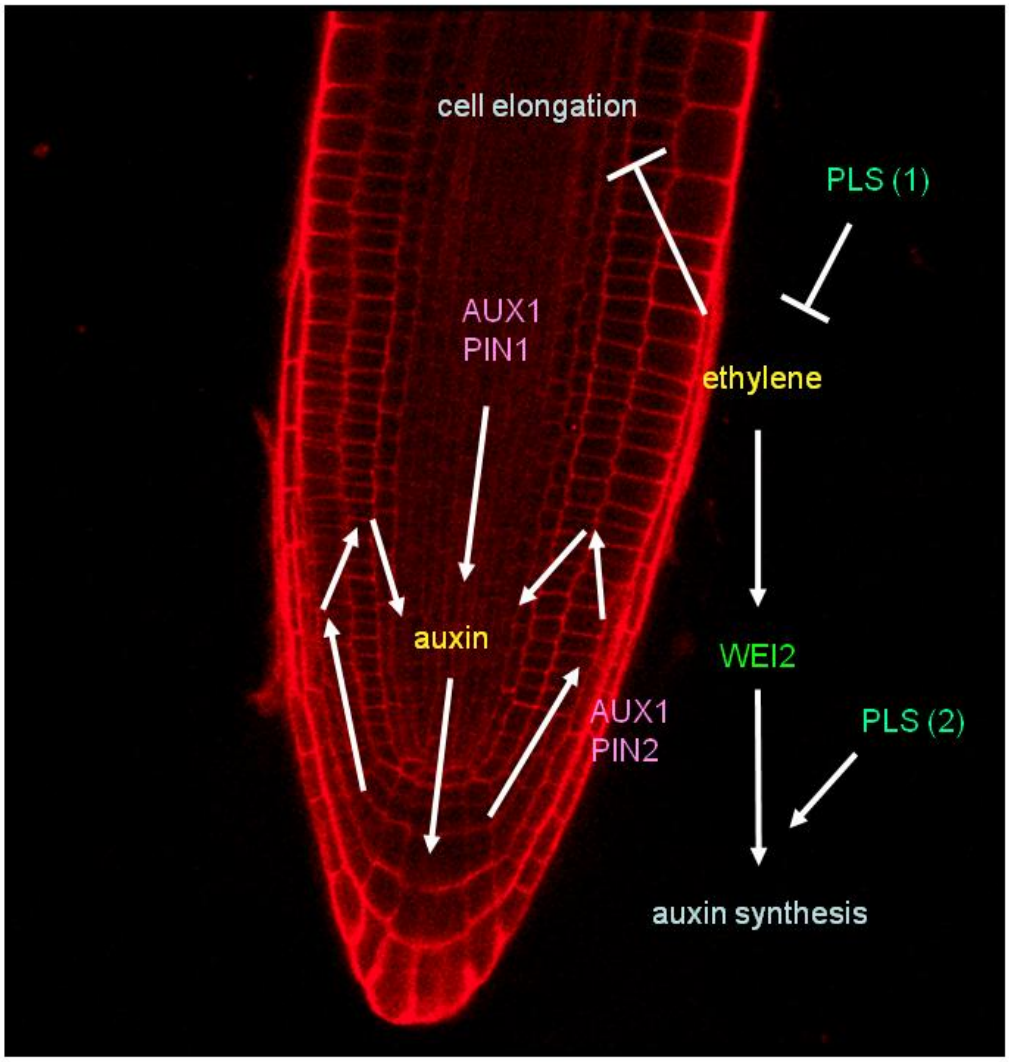


**Figure 6.2: A model of PLS action in the root tip.** Auxin accumulates to a maximum at the QC and columella initials in the root, to a large extent due to the action of the auxin influx and efflux transporters (here only AUX, PIN1 and PIN2 are indicated). Ethylene inhibits anisotropic cell elongation, and PLS negatively regulates ethylene responses, so that the *pls* mutant exhibits reduced cell elongation. This is one role for PLS (PLS 1), proposed to be mediated through its direct interaction with the ethylene receptor ETR1. Ethylene also induces auxin biosynthesis in the root tip via WEI2, and PLS is required for this pathway to function, acting downstream of WEI2 (PLS2) by an as yet unknown mechanism. The two roles of PLS must be distinct, to account for the lack of enhanced auxin synthesis in the root tip in response to the high ethylene responses in the *pls* mutant. Ethylene also enhances PIN protein levels, seen in both wild type and in the *pls* mutant, and for *pls* this may be the result of the enhanced ethylene responses in the mutant.

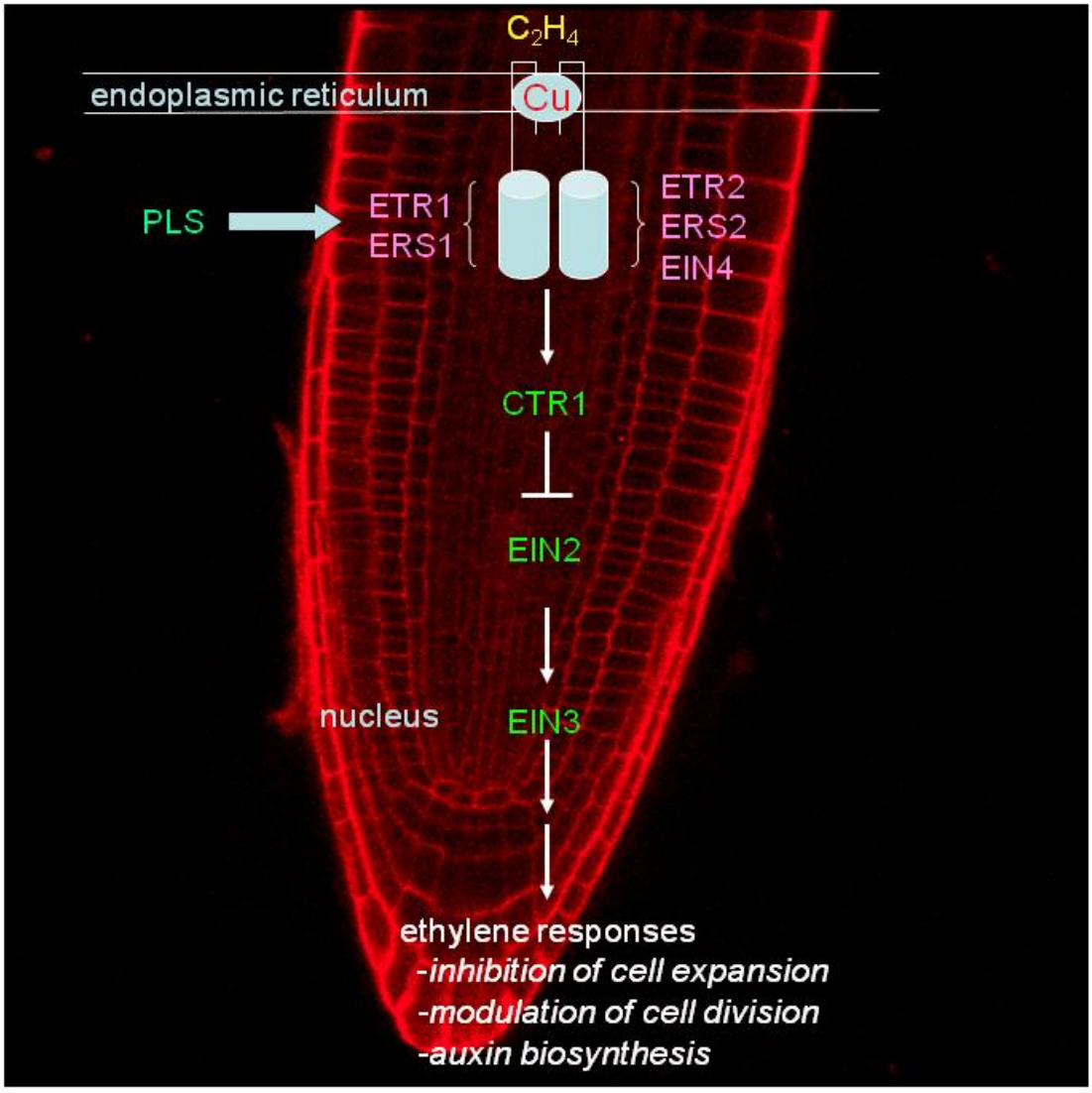


**Figure 6.3: A model of *PLS* action in the ethylene signalling pathway**

In air, the ethylene receptor complex interacts with CTR1 in the endoplasmic reticulum to inhibit downstream responses via EIN2 and the transcription factor EIN3. In the presence of ethylene, which binds the receptor complex, CTR1 dissociates, resulting in the release of inhibition of the downstream pathway. PLS functions as a negative regulator of the pathway, and evidence suggests it interacts with ETR1. It may therefore act to 'reset' the receptor following ethylene binding. The mechanism is unknown, but possibilities include the induction of a conformational change in the receptor to displace ethylene or disrupt the interaction with CTR1; or modulate the stability or dimerization of the receptor complex.

Since *PLS* gene expression is inhibited by ethylene and promoted by auxin (Casson *et al*. 2002, Chilley *et al.* 2006), and yet PLS at the same inhibits ethylene responses and promotes auxin synthesis, it seems possible that PLS has at least two distinct roles, one in repressing the ethylene response and a second in promoting auxin biosynthesis. Mathematical modelling techniques have been used to investigate this further, and further support a dual role for PLS (J. Liu et al., manuscript submitted). PLS might be acting at a cross-point between ethylene and auxin responses to infuence cell growth in roots, by modulating ethylene-mediated auxin transport into and out of the root, and auxin biosynthesis in the root in response to ethylene. Auxin in turn is key to the control of cell division and expansion, primary root growth and tropism, and lateral root architecture.

According to this model, a high ethylene response suppress auxin entry and promote its exit at the root tip and in turn therefore decreases the auxin concentration in the root tip. This would lead to a reduction in *PLS* transcription and interaction with ethylene receptor and hence may release CTR1 to trigger ethylene signalling and allowing ethylene to alter the root architecture via auxin effects.

## 6.8: Future work

This work has raised a number of avenues for future investigation both at the molecular and phenotypic levels. Certainly one of the most important points is to clarify the precise mode of action of PLS with regard to the ethylene and auxin signalling pathways. Biochemical analysis (eg pull-down studies and proteomic analysis, stability sudies) of ethylene receptors could be done to search for associated PLS peptide and to detemine whether PLS interactions affect receptor stability or localization. Interaction studies between PLS and CTR1 could also be carried out.

It was demonstrated that *WEI2* expression was altered in *pls*, but study of the expression levels of other genes involved in auxin synthesis might provide new clues to the relation of PLS with them. If genes are identified that are down-regulated in the *pls* mutant background, these may indicate a point of control by PLS (possibly by PLS peptide acting as a 'cofactor' or accessory peptide), and one-to-one interaction studies could be performed to come to some conclusion.

Furthermore, the function of the PLS peptide needs to be probed in detail. This could be started by generating new mutants of PLS by site directed mutagenesis to identify the function domains of the protein – the *pls* null mutant could be tested for complementation by various mutant forms of the PLS peptide.

Monoclonal antibodies against the PLS peptide need to be generated to perform *in situ* immunolocalisation studies. Conservation of PLS function in other plant species needs to be tested as well. Results from initial experiments in tobacco indicated a possible conservation of PLS function (data not shown), but this needs further evidence to confirm the results.

It is interesting, given the rarity of small peptides in plants compared to animals that PLS are required for controlling a major developmental function, by interaction with at least two key signal transduction pathways of auxin and ethylene response regulation. It is also interesting to speculate that there might be several other small proteins and peptides performing vital function that have yet to be identified.

# References

Abas L, Benjamins R, Malenica N, Paciorek T, Wiśniewska J, Moulinier-Anzola JC, Sieberer T, Friml J, Luschnig C (2006), Intracellular trafficking and proteolysis of the Arabidopsis auxin-efflux facilitator PIN2 are involved in root gravitropism, *Nat Cell Biol*, **3**:249-56.

Abeles FB, Morgan PW, Saltveit MEJr . 1992. *Ethylene in Plant Biology*. San Diego, CA: Academic.414 pp.2nd ed.

Abel S, Nguyen MD, Chow W, Theologis A(1995), ACS4, a primary indoleacetic acid-responsive gene encoding 1-aminocyclopropane-1-carboxylate synthase in Arabidopsis thaliana. Structural characterization, expression in Escherichia coli, and expression characteristics in response to auxin, *J Biol Chem*., **270**:19093-9.

Adams-Phillips L, Barry C, Kannan P, Leclercq J, Bouzayen M, Giovannoni J (2004), Evidence that CTR1-mediated ethylene signal transduction in tomato is encoded by a multigene family whose members display distinct regulatory features, *Plant Mol Biol*., **54**:387-404.

Aida M, Beis D, Heidstra R, Willemsen V, Blilou I, Galinha C, Nussaume L, Noh YS, Amasino R, Scheres B (2004),The PLETHORA genes mediate patterning of the Arabidopsis root stem cell niche, *Cell*, **119**:109-20.

Alonso JM, Stepanova AN (2004), The ethylene signaling pathway, *Science*, **306** (5701):1513-5.

Alonso JM, Hirayama T, Roman G, Nourizadeh S, Ecker JR(1999), EIN2, a bifunctional transducer of ethylene and stress responses in Arabidopsis, Science, **284**(5423):2148-52.

Amerik AY, Hochstrasser M (2004), Mechanism and function of deubiquitinating enzymes*, Biochim Biophys Acta*, **1695**(1-3):189-207.

Avsian-Kretchmer O, Cheng JC, Chen L, Moctezuma E, Sung ZR (2002), .Indole acetic acid distribution coincides with vascular differentiation pattern during Arabidopsis leaf ontogeny, *Plant Physiol*., **130**(1):199-209.

Bartel B (1997), Auxin Biosynthesis, *Annu. Rev. Plant Physiol*., **48**:51-66.

Bauby H, Divol F, Truernit E, Grandjean O, Palauqui JC (2007), Protophloem differentiation in early Arabidopsis thaliana development, *Plant Cell Physiol*., **48**(1):97-109.

Benfey PN, Linstead PJ, Roberts K, Schiefelbein JW, Hauser MT, Aeschbacher RA (2000), Root development, *Current Biol*., **10**(22):R813-5.

Benfey PN, Mitchell-Olds T (2008), From genotype to phenotype: systems biology meets natural variation, *Science*, **320**(5875):495-7.

Benjamins R, Quint A, Weijers D, Hooykaas P, Offringa R (2001), The PINOID protein kinase regulates organ development in Arabidopsis by enhancing polar auxin transport.. *Development*, **128**(20):4057-67

Benková E, Michniewicz M, Sauer M, Teichmann T, Seifertová D, Jürgens G, Friml J.(2003), Local, efflux-dependent auxin gradients as a common module for plant organ formation, *Cell,* **115**(5):591-602

Bennett MJ, Marchant A, Green HG, May ST, Ward SP, Millner PA, Walker AR, Schulz B, Feldmann KA (1996), *Arabidopsis AUX1* gene: a permease-like regulator of root gravitropism, *Science*, **273**: 948-50.

Blakeslee JJ, Peer WA, Murphy AS (2005), Auxin transport, *Curr Opin Plant Biol*., **8**(5):494-500.

Blakeslee JJ, Bandyopadhyay A Lee OR, Mravec J, Sauer M, Titapiwatanakun B, Makam SN, Bouchard R, Geisler M, Martinoia E, Friml J, Peer WA, Murphy AS (2007), Interactions of PIN and PGP auxin transport mechanisms, *Biochem Soc Trans*., **35**(Pt 1):137-41.

Bleecker AB (1999), Ethylene perception and signaling: an evolutionary perspective, *Trends Plant Sci*., **4**(7):269-274.

Bleecker AB, Estelle MA, Somerville C, Kende H. (1988) Insensitivity to ethylene conferred by a dominant mutation in *Arabidopsis thaliana*. *Science*. **241**:1086-1089

Blilou I, Xu J, Wildwater M, Willemsen V, Paponov I, Friml J, Heidstra R, Aida M, Palme K, Scheres B (2005), The PIN auxin efflux facilitator network controls growth and patterning in Arabidopsis roots, *Nature,* **433**(7021):39-44.

Brown K, Gallagher K, Smith LG (1997), Asymmetric cell division and cell fate in plants, *Curr Opin Cell Biol*., **9**(6):842-8.

Brukhin V, Gheyselinck J, Gagliardini V, Genschik P, Grossniklaus U (2005), The RPN1 subunit of the 26S proteasome in Arabidopsis is essential for embryogenesis, *Plant Cell*, **17**(10):2723-37.

Cancel JD, Larsen PB (2002), Loss-of-function mutations in the ethylene receptor ETR1 cause enhanced sensitivity and exaggerated response to ethylene in Arabidopsis, *Plant Physiol.*, **129**(4):1557-67.

Casimiro I, Marchant A, Bhalerao RP, Beeckman T, Dhooge S, Swarup R, Graham N,Inzé D, Sandberg G, Casero PJ, Bennett M. (2001) Auxin transport promotes Arabidopsis lateral root initiation. *Plant Cell.* 2001 **13**: 843-52.

Casson SA, Topping JF, Lindsey K (2009), MERISTEM-DEFECTIVE, an RS domain protein, is required for the correct meristem patterning and function in Arabidopsis, *Plant J*., **57**(5):857-69.

Casson SA, Chilley PM, Topping JF, Evans IM, Souter MA, Lindsey K(2002), The POLARIS gene of Arabidopsis encodes a predicted peptide required for correct root growth and leaf vascular patterning, *Plant Cell*, **14**(8):1705-21.

Casson Stuart A. and Keith Lindsey (2003), Erratum: Genes and Signalling in Root Development, *New Phytologist*, **158** :11-417.

Chang C, Kwok SF, Bleecker AB, Meyerowitz EM(1993), Arabidopsis ethylene-response gene ETR1: similarity of product to two-component regulators, *Science*, **262**(5133):539-44.

Chao Q, Rothenberg M, Solano R, Roman G, Terzaghi W, Ecker JR (1997), Activation of the ethylene gas response pathway in Arabidopsis by the nuclear protein ETHYLENE-INSENSITIVE3 and related proteins, *Cell*, **89**(7):1133-44.

Chen YF, Randlett MD, Findell JL, Schaller GE (2002), Localization of the ethylene receptor ETR1 to the endoplasmic reticulum of Arabidopsis, *J Biol Chem*., **277**(22):19861-6.

Chen ZJ, Wang J, Tian L, Lee HS, Wang JJ (2004), The development of an *Arabidopsis* model system for genome-wide analysis of polyploidy effects, *Biol. J. Linn. Soc.,* **82:** 689–700.

Chilley PM, Casson SA, Tarkowski P, Hawkins N, Wang KL, Hussey PJ, Beale M, Ecker JR, Sandberg GK, Lindsey K(2006), The POLARIS peptide of Arabidopsis regulates auxin transport and root growth via effects on ethylene signaling, *Plant Cell*, **18**(11):3058-72.

Christensen SK, Dagenais N, Chory J, Weigel D (2000), Regulation of auxin response by the protein kinase PINOID, *Cell*, **4**:469-78.

Chang C, Clark K, Wang X, Stewart R (1998), 'Two-component' ethylene signaling in Arabidopsis, *Symp Soc Exp Biol*., **51**:59-64.

Clough SJ, Bent AF (1998), Floral dip: a simplified method for Agrobacterium-mediated transformation of Arabidopsis thaliana, *Plant J*., 16(6):735-43.

Clark KL, Larsen PB, Wang X, Chang C (1998), Association of the Arabidopsis CTR1 Raf-like kinase with the ETR1 and ERS ethylene receptors, *Proc Natl Acad Sci*., **95**(9):5401-6.

Demartino GN, Gillette TG(2007), Proteasomes: machines for all reasons, *Cell*, **129**(4):659-62.

de Billy F, Grosjean C, May S, Bennett M, Cullimore JV (2001), Expression studies on AUX1-like genes in Medicago truncatula suggest that auxin is required at two steps in early nodule development, *Mol Plant Microbe Interact.*, **14**(3):267-77

Dharmasiri N, Dharmasiri S, Weijers D, Lechner E, Yamada M, Hobbie L, Ehrismann JS, Jürgens G, Estelle M (2005), Plant development is regulated by a family of auxin receptor F box proteins, *Dev. Cell*, **9**(1):109-19.

Dharmasiri N, Dharmasiri S, Estelle M(2005), The F-box protein TIR1 is an auxin receptor, *Nature*, **435**(7041):441-5.

Dharmasiri N, Dharmasiri S, Jones AM, Estelle M (2003), Auxin action in a cell-free system, *Curr. Biol*., **13**(16):1418-22.

Dharmasiri S, Swarup R, Mockaitis K, Dharmasiri N, Singh SK, Kowalchyk M, Marchant A, Mills S, Sandberg G, Bennett MJ, Estelle M (2006), AXR4 is required for localization of the auxin influx facilitator AUX1, *Science*, **312**(5777):1218-20.

Di Laurenzio L, Wysocka-Diller J, Malamy JE, Pysh L, Helariutta Y, Freshour G, Hahn MG, Feldmann KA, Benfey PN (1996), The SCARECROW gene regulates an asymmetric cell

division that is essential for generating the radial organization of the Arabidopsis root, *Cell*, **86**(3):423-33.

Dolan L, Janmaat K, Willemsen V, Linstead P, Poethig S, Roberts K, Scheres B(1993), Cellular organisation of the Arabidopsis thaliana root, *Development*, **119**(1):71-84

Dolan L, Scheres B (1998), Root development in Arabidopsis: four mutants with dramatically altered root morphogenesis, *Development,* **119**(1):57-70.

Dolan L, Duckett C M, Grierson C, Linstead P, Schneider K,Lawson E, Dean C, Poethig S and Roberts K (1994), Clonal originand patterning in the root epidermis of *Arabidopsis*, *Development*, **120**, 2465-2474.

Dolan L (2006), Positional information and mobile transcriptional regulators determine cell pattern in the Arabidopsis root epidermis, *J Exp Bot.*, **57**(1):51-4.

Ellis CM, Nagpal P, Young JC, Hagen G, Guilfoyle TJ, Reed JW (2005), AUXIN RESPONSE FACTOR1 and AUXIN RESPONSE FACTOR2 regulate senescence and floral organ abscission in Arabidopsis thaliana, *Development*, **132**(20):4563-74.

Friml J, Yang X, Michniewicz M, Weijers D, Quint A, Tietz O, Benjamins R, Ouwerkerk PB, Ljung K, Sandberg G, Hooykaas PJ, Palme K, Offringa R (2004), A PINOID-dependent binary switch in apical-basal PIN polar targeting directs auxin efflux, *Science*, **306**(5697):862-5.

Friml J, Vieten A, Sauer M, Weijers D, Schwarz H, Hamann T, Offringa R, Jürgens G (2003), Efflux-dependent auxin gradients establish the apical-basal axis of Arabidopsis, *Nature*, **426**(6963):147-53.

Friml J (2003), Auxin transport - shaping the plant, *Curr. Opin. Plant Biol*., **6**(1):7-12.

Friml J, Palme K (2002) , Polar auxin transport--old questions and new concepts?, *Plant Mol Biol*., **49**(3-4):273-84.

Friml J, Benková E, Blilou I, Wisniewska J, Hamann T, Ljung K, Woody S, Sandberg G, Scheres B, Jürgens G, Palme K (2002), AtPIN4 mediates sink-driven auxin gradients and root patterning in Arabidopsis, *Cell*, **108**(5):661-73.

Friml J Vieten A, Sauer M, Brewer PB (2007), Molecular and cellular aspects of auxin-transport-mediated development, *Trends Plant Sci.,* **12**(4):160-8.

Galinha C, Hofhuis H, Luijten M, Willemsen V, Blilou I, Heidstra R, Scheres B (2007), PLETHORA proteins as dose-dependent master regulators of Arabidopsis root development, *Nature*, **449**(7165):1053.

Gälweiler L, Guan C, Müller A, Wisman E, Mendgen K, Yephremov A, Palme K (1998), Regulation of polar auxin transport by AtPIN1 in Arabidopsis vascular tissue, *Science*, **282**(5397):2226-30.

Gamble RL, Coonfield ML, Schaller GE(1998), Histidine kinase activity of the ETR1 ethylene receptor from Arabidopsis, *Proc. Natl. Acad. Sci. U S A*, **95**(13):7825-9.

Gallagher KL, Benfey PN (2009), Both the conserved GRAS domain and nuclear localization are required for SHORT-ROOT movement, *Plant J*. **57**(5):785-97.

Gälweiler L ,Müller A, Guan C, , Tänzler P, Huijser P, Marchant A, Parry G, Bennett M, Wisman E, Palme K (1998), AtPIN2 defines a locus of Arabidopsis for root gravitropism control, *EMBO J.*, **7**(23):6903-11.

Guo H, Ecker JR (2004), The ethylene signaling pathway: new insights, *Curr. Opin. Plant Biol.*, 7(1):40-9.

Guo H, Ecker JR (2003), Plant responses to ethylene gas are mediated by SCF(EBF1/EBF2)-dependent proteolysis of EIN3 transcription factor, Cell,**115**(6):667-77.

Gao Z, Chen YF, Randlett MD, Zhao XC, Findell JL, Kieber JJ, Schaller GE(2003), Localization of the Raf-like kinase CTR1 to the endoplasmic reticulum of Arabidopsis through participation in ethylene receptor signaling complexes, *J Biol Chem*., **278**(36):34725-32.

Geisler M, Blakeslee JJ, Bouchard R, Lee OR, Vincenzetti V, Bandyopadhyay A, Titapiwatanakun B, Peer WA, Bailly A, Richards EL, Ejendal KF, Smith AP, Baroux C, Grossniklaus U, Müller A, Hrycyna CA, Dudler R, Murphy AS, Martinoia E(2005), Cellular efflux of auxin catalyzed by the Arabidopsis MDR/PGP transporter AtPGP1, *Plant J*, **4**(2):179-94.

Geldner N, Friml J, Stierhof YD, Jürgens G, Palme K (2001), Auxin transport inhibitors block PIN1 cycling and vesicle trafficking, *Nature*, **413**(6854):425-8.

Geldner N, Anders N, Wolters H, Keicher J, Kornberger W, Muller P, Delbarre A, Ueda T, Nakano A, Jürgens G (2003), The Arabidopsis GNOM ARF-GEF mediates endosomal recycling, auxin transport, and auxin-dependent plant growth, *Cell*, **112**(2):219-30.

Gray WM, del Pozo JC, Walker L, Hobbie L, Risseeuw E, Banks T, Crosby WL, Yang M, Ma H, Estelle M (1999), Identification of an SCF ubiquitin-ligase complex required for auxin response in Arabidopsis thaliana, *Genes Dev*. **13**(13):1678-91.

Grebe M, Xu J, Möbius W, Ueda T, Nakano A, Geuze HJ, Rook MB, Scheres B (2003), Arabidopsis sterol endocytosis involves actin-mediated trafficking via ARA6-positive early endosomes, *Curr Biol*., **13**(16):1378-87.

Grieneisen VA, Xu J, Marée AF, Hogeweg P, Scheres B (2007), Auxin transport is sufficient to generate a maximum and gradient guiding root growth, *Nature*, **449**(7165):1008-13.

Guo H, Ecker JR (2004), The ethylene signaling pathway: new insights, *Curr Opin Plant Biol*., **7**(1):40-9.

Guzmán P, Ecker JR (1990), Exploiting the triple response of Arabidopsis to identify ethylene-related mutants, *Plant Cell*, **2**(6):513-23.

Hauser MT, Morikami A, Benfey PN (1995), Conditional root expansion mutants of Arabidopsis, *Development*, **121**(4):1237-52.

Heisler MG, Ohno C, Das P, Sieber P, Reddy GV, Long JA, Meyerowitz EM (2005), Patterns of auxin transport and gene expression during primordium development revealed by live imaging of the Arabidopsis inflorescence meristem, *Curr Biol.*, **15**(21):1899-911.

Helariutta Y, Lim J, Specht CD, Jung J, Sims L, Bruce WB, Diehn S, Benfey PN(2000), Molecular analysis of the SCARECROW gene in maize reveals a common basis for radial patterning in diverse meristems. *Plant Cell*, **12**(8):1307-18.

Helariutta Y, Fukaki H, Wysocka-Diller J, Nakajima K, Jung J, Sena G, Hauser MT, Benfey PN(2000), The SHORT-ROOT gene controls radial patterning of the Arabidopsis root through radial signaling, *Cell*, **101**(5):555-67.

Helariutta Y (2007), Cell signalling during vascular morphogenesis, *Biochem Soc Trans*. **35**(Pt 1):152-5.

Hershko A, Ciechanover A (1998), The ubiquitin system, *Annu Rev Biochem*., **67**:425-79.

Hirayama T, Kieber JJ, Hirayama N, Kogan M, Guzman P, Nourizadeh S, Alonso JM, Dailey WP, Dancis A, Ecker JR (1999), RESPONSIVE-TO-ANTAGONIST1, a Menkes/Wilson dis-

ease-related copper transporter, is required for ethylene signaling in Arabidopsis, *Cell*, **97**(3):383-93.

Hobbie L, McGovern M, Hurwitz LR, Pierro A, Liu NY, Bandyopadhyay A, Estelle M (2000), The axr6 mutants of Arabidopsis thaliana define a gene involved in auxin response and early development, *Development*, **127**(1):23-32

Hochstrasser M( 2006), Lingering mysteries of ubiquitin-chain assembly, Cell,**124**(1):27-34.

Hua J, Meyerowitz EM (1998), Ethylene responses are negatively regulated by a receptor gene family in Arabidopsis thaliana, *Cell*, **94**(2):261-71.

Huang Y, Li H, Hutchison CE, Laskey J, Kieber JJ (2003), Biochemical and functional analysis of CTR1, a protein kinase that negatively regulates ethylene signaling in Arabidopsis, *Plant J*, **33**(2):221-33.

Jensen PJ, Hangarter RP, Estelle M( 1998), Auxin transport is required for hypocotyl elongation in light-grown but not dark-grown Arabidopsis, Plant Physiol., **116**(2):455-62.

Jiang Xu, Hao-Dong Li, Li-Qing Chen, Yi Wang, Li-Li Liu, Liu He, Wei-Hua Wu (2006), Protein Kinase, Interacting with Two Calcineurin B-like Proteins, Regulates $K^+$ Transporter AKT1 in *Arabidopsis*, Cell - 125:1347-1360.

Kazama H, Dan H, Imaseki H, Wasteneys GO. Transient exposure to ethylene stimulates cell division and alters the fate and polarity of hypocotyl epidermal cells. *Plant Physiol*. 2004 Apr;**134**(4):1614-23.

Kepinski S, Leyser O (2003), SCF-mediated proteolysis and negative regulation in ethylene signaling, *Cell*, **115**(6):647-8.

Kende H Peck SC, Olson DC A(1993), cDNA sequence encoding 1-aminocyclopropane-1-carboxylate oxidase from pea., *Plant Physiol.,* **101**(2):689-90.

Kepinski S, Leyser O ( 2005), Plant development: auxin in loops, *Curr Biol*. **15**(6):R208-10.

Kepinski S, Leyser O (2005), The Arabidopsis F-box protein TIR1 is an auxin receptor, *Nature*, **435**(7041):446-51.

Kerk NM, Jiang K, Feldman LJ (2000), Auxin metabolism in the root apical meristem, *Plant Physiol.*, **122**(3):925-32.

Kieber JJ, Rothenberg M, Roman G, Feldmann KA, Ecker JR ( 1993), CTR1, a negative regulator of the ethylene response pathway in Arabidopsis, encodes a member of the raf family of protein kinases, *Cell*, **72**(3):427-41.

Kieber JJ, Ecker JR (1993), Ethylene gas: it's not just for ripening any more!. *Trends Genet*., **9**(10):356-62.

Kieber JJ, Deruère J, Maxwell BB, Morris VF, Hutchison CE, Ferreira FJ, Schaller GE (2007), Cytokinin regulates type-A Arabidopsis Response Regulator activity and protein stability via two-component phosphorelay, *Plant Cell,* **19**(12):3901-14.

Kionka C, Amrhein N (1984), The enzymatic malonylation of 1-aminocyclopropane-1-carboxylic acid in homogenates of mung bean hypocotyls, *Planta*, **194:**226-235.

Kolch W, Weissinger E, Mischak H, Troppmair J, Showalter SD, Lloyd P, Heidecker G, Rapp UR (1990), Probing structure and function of the raf protein kinase domain with monoclonal antibodies, *Oncogene*, **5**(5):713-20.

Klee HJ (2002)Control of ethylene-mediated processes in tomato at the level of receptors..J *Exp Bot*., **53**(377):2057-63.

Klee HJ (2004), Ethylene signal transduction: Moving beyond Arabidopsis, *Plant Physiol.,* **135**(2):660-7.

Kleine-Vehn J, Dhonukshe P, Swarup R, Bennett M, Friml J (2006), Subcellular trafficking of the Arabidopsis auxin influx carrier AUX1 uses a novel pathway distinct from PIN1, *Plant Cell*, **18**(11):3171-81.

Kleine-Vehn J, Friml J (2008), Polar targeting and endocytic recycling in auxin-dependent plant development, *Annu Rev Cell Dev Biol*., **24**:447-73.

Koizumi K, Naramoto S, Sawa S, Yahara N, Ueda T, Nakano A, Sugiyama M, Fukuda H (2005), VAN3 ARF-GAP-mediated vesicle transport is involved in leaf vascular network formation, *Development*, **132**(7):1699-711.

Kwak SH, Shen R, Schiefelbein J (2005), Positional signaling mediated by a receptor-like kinase in Arabidopsis, *Science*, **307**(5712):1111-3.

Li H, Johnson P, Stepanova A, Alonso JM, Ecker JR (2004), Convergence of signaling pathways in the control of differential cell growth in Arabidopsis, *Dev Cell,* **2**:193-20.

Laskowski MJ, Williams ME, Nusbaum HC, Sussex IM (1995), Formation of lateral root meristems is a two-stage process, *Development*, **121**(10):3303-10.

Laux T, Würschum T, Breuninger H (2004), Genetic regulation of embryonic pattern formation, *Plant Cell*., **16** Suppl:S190-202.

Lehman A, Black R, Ecker JR (1996), HOOKLESS1, an ethylene response gene, is required for differential cell elongation in the Arabidopsis hypocotyl, *Cell*, **85**(2):183-94.

Levesque MP, Vernoux T, Busch W, Cui H, Wang JY, Blilou I, Hassan H, Nakajima K, Matsumoto N, Lohmann JU, Scheres B, Benfey PN. (2006) Whole-genome analysis of the SHORT-ROOT developmental pathway in Arabidopsis. *PLoS Biol*. **4**,739-752

Leyser HM, Lincoln CA, Timpte C, Lammer D, Turner J, Estelle M (1993), Arabidopsis auxin-resistance gene AXR1 encodes a protein related to ubiquitin-activating enzyme E1, *Nature*, **364**(6433):161-4.

Leyser O (2005), The fall and rise of apical dominance, *Curr Opin.Genet Dev*., 15(4):468-71.

Leyser HM, Pickett FB, Dharmasiri S, Estelle M (1996), Mutations in the AXR3 gene of Arabidopsis result in altered auxin response including ectopic expression from the SAUR-AC1 promoter, *Plant J*., **10**(3):403-13.

Li J, Yang H, Peer WA, Richter G, Blakeslee J, Bandyopadhyay A, Titapiwantakun B, Undurraga S, Khodakovskaya M, Richards EL, Krizek B, Murphy AS, Gilroy S, Gaxiola R (2005), Arabidopsis H+-PPase AVP1 regulates auxin-mediated organ development, *Science*, **310**(5745):121-5

Lincoln C, Britton JH, Estelle M (1990), Growth and development of the axr1 mutants of Arabidopsis, *Plant Cell*, **2**(11):1071-80.

Liu Y, Zhang S (2004), Phosphorylation of 1-aminocyclopropane-1-carboxylic acid synthase by MPK6, a stress-responsive mitogen-activated protein kinase, induces ethylene biosynthesis in Arabidopsis, Plant Cell, **16**(12):3386-99.

Ljung K, Hull AK, Kowalczyk M, Marchant A, Celenza J, Cohen JD, Sandberg G (2002), Biosynthesis, conjugation, catabolism and homeostasis of indole-3-acetic acid in Arabidopsis thaliana, Plant Mol Biol., **49**(3-4):249-72.

Ljung K, Hull AK, Celenza J, Yamada M, Estelle M, Normanly J, Sandberg G (2005)Sites and regulation of auxin biosynthesis in Arabidopsis roots, *Plant Cell*, **17**(4):1090-104.

Luschnig C, Gaxiola RA, Grisafi P, Fink GR (1998), EIR1, a root-specific protein involved in auxin transport, is required for gravitropism in *Arabidopsis thaliana*, *Genes Dev,* **12**(14):2175-87.

Maher EP, Martindale SJ (1980), Mutants of Arabidopsis thaliana with altered responses to auxins and gravity, *Biochem Genet*., **18**(11-12):1041-53.

Malcolm J. Bennett, Alan Marchant, Haydn G. Green, Sean T. May, Sally P. Ward, Paul A. Millner, Amanda R. Walker, Burkhard Schulz, Kenneth A (1996), Arabidopsis AUX1 Gene: A Permease-Like Regulator of Root Gravitropism, *Science*, **948**.

Marchant A, Kargul J, May ST, Muller P, Delbarre A, Perrot-Rechenmann C, Bennett MJ (1999), AUX1 regulates root gravitropism in Arabidopsis by facilitating auxin uptake within root apical tissues, *EMBO J*., **18**(8):2066-73.

Menke FL, van Pelt JA, Pieterse CM, Klessig DF (2004), Silencing of the mitogen-activated protein kinase MPK6 compromises disease resistance in Arabidopsis, *Plant Cell*, **16**(4):897-907.

Mittler R, Del Pozo O, Meisel L, Lam E (1997), Pathogen-induced programmed cell death in plants, a possible defense mechanism, *Dev Genet*., **21**(4):279-89.

Miséra S, Müller AJ, Weiland-Heidecker U, Jürgens G (1999), The FUSCA genes of Arabidopsis: negative regulators of light responses, *Mol Gen Genet*., **244**(3):242-52.

Mockaitis K, Estelle M (2008), Auxin receptors and plant development: a new signaling paradigm, *Annu Rev Cell Dev Biol.*, **24**:55-80.

Moon J, Parry G, Estelle M (2004), The ubiquitin-proteasome pathway and plant development, *Plant Cell*, **16**(12):3181-95.

Morris ER & Walker JC (2003), Receptor-like protein kinases: the keys to response, *Curr Opin Plant Biol*., **6**(4):339-42.

Mouchel CF, Briggs GC, Hardtke CS (2004), Natural genetic variation in Arabidopsis identifies BREVIS RADIX, a novel regulator of cell proliferation and elongation in the root, *Genes Dev*., **18**(6):700-14.

Mouchel CF, Osmont KS, Hardtke CS (2006), BRX mediates feedback between brassinosteroid levels and auxin signalling in root growth, *Nature*, **443**(7110):458-61.

Moussatche P, Klee HJ (2004), Autophosphorylation activity of the Arabidopsis ethylene receptor multigene family, *J Biol Chem*., **279**(47):48734-41.

Mravec J, Skůpa P, Bailly A, Hoyerová K, Krecek P, Bielach A, Petrásek J, Zhang J, Gaykova V, Stierhof YD, Dobrev PI, Schwarzerová K, Rolcík J, Seifertová D, Luschnig C, Benková E, Zazímalová E, Geisler M, Friml J (2009), Subcellular homeostasis of phytohormone auxin is mediated by the ER-localized PIN5 transporter, *Nature*, **459**:1136-40.

Müller A, Hillebrand H, Weiler EW (1998), Indole-3-acetic acid is synthesized from L-tryptophan in roots of Arabidopsis thaliana, *Planta*, **206**(3):362.

Müller A, Guan C, Gälweiler L, Tänzler P, Huijser P, Marchant A, Parry G, Bennett M, Wisman E, Palme K (1998), AtPIN2 defines a locus of Arabidopsis for root gravitropism control, *EMBO J*.,**17**(23):6903-11.

Nakajima K, Sena G, Nawy T, Benfey PN (2001), Intercellular movement of the putative transcription factor SHR in root patterning, *Nature*, **413** (6853): 307-11.

Noh B, Murphy AS, Spalding EP (2001), Multidrug resistance-like genes of Arabidopsis required for auxin transport and auxin-mediated development, *Plant Cell*, **13** (11): 2441-54.

Ohashi-Ito K, Bergmann DC (2007), Regulation of the Arabidopsis root vascular initial population by LONESOME HIGHWAY, *Development*, **134**(16):2959-68.

Okada K, Ueda J, Komaki MK, Bell CJ, Shimura Y (1991), Requirement of the Auxin Polar Transport System in Early Stages of Arabidopsis Floral Bud Formation, *Plant Cell*, 3(7):677-684.

OR, Fink GR, Geisler M, Murphy AS, Luschnig C, Zazímalová E, Friml J(2006), PIN proteins perform a rate-limiting function in cellular auxin efflux, *Science*, **312**(5775):914-8.

Ouaked F, Rozhon W, Lecourieux D, Hirt H (2003), A MAPK pathway mediates ethylene signaling in plants. *EMBO J., 22*(6):1282-8.

Petricka JJ, Benfey PN (2008), Root layers: complex regulation of developmental patterning, *Current Opin. Genetic Dev.*, **18**(4):354-61.

Petrásek J, Mravec J, Bouchard R, Blakeslee JJ, Abas M, Seifertová D, Wisniewska J, Tadele Z, Kubes M, Covanová M, Dhonukshe P, Skupa P, Benková E, Perry L, Krecek P, Lee

Parry G, Delbarre A, Marchant A, Swarup R, Napier R, Perrot-Rechenmann C, Bennett MJ (2001), Novel auxin transport inhibitors phenocopy the auxin influx carrier mutation aux1, *Plant J*., **25**(4):399-406.

Peer WA, Bandyopadhyay A, Blakeslee JJ, Makam SN, Chen RJ, Masson PH, Murphy AS (2004), Variation in expression and protein localization of the PIN family of auxin efflux facilitator proteins in flavonoid mutants with altered auxin transport in Arabidopsis thaliana, *Plant Cell*, **16**(7):1898-911.

Peer WA, Hosein FN, Bandyopadhyay A, Makam SN, Otegui MS, Lee GJ, Blakeslee JJ, Cheng Y, Titapiwatanakun B, Yakubov B, Bangari B, Murphy AS. Mutation of the membrane-associated M1 protease APM1 results in distinct embryonic and seedling developmental defects in Arabidopsis. *Plant Cell*. 2009 **21**(6):1693-721.

Perry P, Linke B, Schmidt W. (2007) Reprogramming of root epidermal cells in response to nutrient deficiency. *Biochem Soc Trans*. **35**: 161-163.

Petroski MD, Deshaies RJ (2005), Mechanism of lysine 48-linked ubiquitin-chain synthesis by the cullin-RING ubiquitin-ligase complex SCF-Cdc34, *Cell*, **123**(6):1107-20.

Pickart CM (2001), Ubiquitin enters the new millennium, *Mol. Cell*, **8**(3):499-504.

Pickett FB, Wilson AK, Estelle M (1990), The aux1 Mutation of Arabidopsis Confers Both Auxin and Ethylene Resistance, *Plant Physiol*., **94**(3):1462-1466.

Pitts RJ, Cernac A, Estelle M (1998), Auxin and ethylene promote root hair elongation in Arabidopsis, *Plant J*., **16**(5):553-60.

Ponce G, Luján R, Campos ME, Reyes A, Nieto-Sotelo J, Feldman LJ, Cassab GI (2000), Three maize root-specific genes are not correctly expressed in regenerated caps in the absence of the quiescent center, *Planta*, **211**(1):23-33.

Rahman A, Amakawa T, Goto N, Tsurumi S (2001), Auxin is a positive regulator for ethylene-mediated response in the growth of Arabidopsis roots, *Plant Cell Physiol*., **42**(3):301-7.

Rahman A, Hosokawa S, Oono Y, Amakawa T, Goto N, Tsurumi S (2002), Auxin and ethylene response interactions during Arabidopsis root hair development dissected by auxin influx modulators, *Plant Physiol*., **130**(4):1908-17.

Reinhardt D, Mandel T, Kuhlemeier C (2000), Auxin regulates the initiation and radial position of plant lateral organs, *Plant Cell*, **12**(4):507-18.

Reinhardt D, Pesce ER, Stieger P, Mandel T, Baltensperger K, Bennett M, Traas J, Friml J, Kuhlemeier C (2003), Regulation of phyllotaxis by polar auxin transport, *Nature*, **6**(6964):255-60.

Resnick JS, Wen CK, Shockey JA, Chang C (2006), REVERSION-TO-ETHYLENE SENSITIVITY1, a conserved gene that regulates ethylene receptor function in Arabidopsis, Proc Natl Acad Sci U S A, **103**(20):7917-22.

Roman G, Ecker JR(1995), Genetic analysis of a seedling stress response to ethylene in Arabidopsis, *Philos Trans R Soc Lond B Biol Sci.,***350**(1331):75-81.

Rubery PH, Sheldrake AR (1974) Carrier-mediated auxin transport,*Planta*, **118**:101–121.

Ruegger M, Dewey E, Gray WM, Hobbie L, Turner J, Estelle M (1998), The TIR1 protein of Arabidopsis functions in auxin response and is related to human SKP2 and yeast grr1p, *Genes Dev*. ,**12**(2):198-207.

Ruzicka, K., Ljung, K., Vanneste, S., Podhorska, R., Beeckman, T., Friml, J.,and Benkova, E. (2007), Ethylene Regulates Root Growth through Effects onAuxin Biosynthesis and Transport-Dependent Auxin Distribution, *Plant Cell*,**19**, 2197–2212.

Sabatini S, Beis D, Wolkenfelt H, Murfett J, Guilfoyle T, Malamy J, Benfey P, Leyser O, Bechtold N, Weisbeek P, Scheres B (1999), An auxin-dependent distal organizer of pattern and polarity in the Arabidopsis root, *Cell*, **99**(5):463-72.

Sabatini S, Heidstra R, Wildwater M, Scheres B (2003), SCARECROW is involved in positioning the stem cell niche in the Arabidopsis root meristem, *Genes Dev*., **17**(3):354-8.

Saiga S, Furumizu C, Yokoyama R, Kurata T, Sato S, Kato T, Tabata S, Suzuki M, Komeda Y (2008), The Arabidopsis OBERON1 and OBERON2 genes encode plant homeodomain finger proteins and are required for apical meristem maintenance, *Development*, 35(10):1751-9.

Sakai H, Hua J, Chen QG, Chang C, Medrano LJ, Bleecker AB, Meyerowitz EM (1998),ETR2 is an ETR1-like gene involved in ethylene signaling in Arabidopsis, *Proc Natl Acad Sci USA*., **95**(10):5812-7.

Sanders, I.O., Smith, A.R., and Hall, M.A (1989), Ethylene metabolism in *Pisum* safivum L, *Planta*, **179**:104-114.

Santelia D, Vincenzetti V, Azzarello E, Bovet L, Fukao Y, Düchtig P, Mancuso S, Martinoia E, Geisler M (2005), MDR-like ABC transporter AtPGP4 is involved in auxin-mediated lateral root and root hair development, *FEBS Lett*., **579**(24):5399-5406.

Schaller, G.E., and Kieber, J.J. (September 30, 2002). Ethylene. InThe Arabidopsis Book, C.R. Somerville and E.M. Meyerowitz, eds(Rockville, MD: American Society of Plant Biologists), doi/10.1199/tab.0071, http://www.aspb.org/publications/arabidopsis.

Scheres B (2002), Plant patterning: TRY to inhibit your neighbors, *Curr Biol*., **12**(23):R804-6.

Scheres B Dolan L, Janmaat K, Willemsen V, Linstead P, Poethig S, Roberts K (1993), Cellular organisation of the Arabidopsis thaliana root, *Development*, **119**(1):71-84.

Scheres B van den Berg C, Willemsen V, Hage W, Weisbeek P(1995), Cell fate in the Arabidopsis root meristem determined by directional signalling, *Nature*, **378**(6552):62-5.

Scheres B, van der Kop DA, Schuyer M, van der Zaal BJ(1996), Isolation and characterization of an auxin-inducible glutathione S-transferase gene of Arabidopsis thaliana, *PJ.Plant Mol Biol.,* **30**(4):839-44.

Scheres B , Benfey PN (2000), Root development, *Curr Biol*., **10**(22):R813-5.

Schiefelbein JW, Masucci JD, Wang H (1997), Building a root: the control of patterning and morphogenesis during root development, *Plant Cell*, **9**(7):1089-98.

Schrick K, Mayer U, Martin G, Bellini C, Kuhnt C, Schmidt J, Jürgens G(2002), Interactions between sterol biosynthesis genes in embryonic development of Arabidopsis, Plant J., 31(1):61-73.

Sena G, Jung JW, Benfey PN(2004), A broad competence to respond to SHORT ROOT revealed by tissue-specific ectopic expression, *Development*, **131**(12):2817-26.

Shevell DE, Leu WM, Gillmor CS, Xia G, Feldmann KA, Chua NH (1994), EMB30 is essential for normal cell division, cell expansion and cell adhesion in Arabidopsis and encodes a protein that has similarity to Sec7, *Cell*, 77(7):1051-62.

Sieberer T, Seifert GJ, Hauser MT, Grisafi P, Fink GR, Luschnig C (2000), Post-transcriptional control of the Arabidopsis auxin efflux carrier EIR1 requires AXR1, *Curr Biol*., **10**(24):1595-8.

Sieburth LE, Muday GK, King EJ, Benton G, Kim S, Metcalf KE, Meyers L, Seamen E, Van Norman JM (2006), SCARFACE encodes an ARF-GAP that is required for normal auxin efflux and vein patterning in Arabidopsis, *Plant Cell*, **18**(6):1396-411.

Smalle J, Vierstra RD (2004), The ubiquitin 26S proteasome proteolytic pathway, *Annu Rev Plant Biol*., **55**:555-90.

Smalle J, Kurepa J, Yang P, Babiychuk E, Kushnir S, Durski A, Vierstra RD (2002), Cytokinin growth responses in Arabidopsis involve the 26S proteasome subunit RPN12, Plant Cell, **14**(1):17-32.

Smith AM, Zeeman SC, Thorneycroft D, Smith SM (2003), Starch mobilization in leaves, *J Exp Bot*., **54:** 577–583.

Souter M, Topping J, Pullen M, Friml J, Palme K, Hackett R, Grierson D, Lindsey K(2002), hydra Mutants of Arabidopsis are defective in sterol profiles and auxin and ethylene signaling, *Plant Cell*, **14**(5):1017-31.

Souter MA, Pullen ML, Topping JF, Zhang X, Lindsey K (2004), Rescue of defective auxin-mediated gene expression and root meristem function by inhibition of ethylene signalling in sterol biosynthesis mutants of Arabidopsis, *Planta*, **219**(5):773-83.

Steinmann T, Geldner N, Grebe M, Mangold S, Jackson CL, Paris S, Gälweiler L, Palme K, Jürgens G (1999), Coordinated polar localization of auxin efflux carrier PIN1 by GNOM ARF GEF, *Science*, **286**(5438):316-8.

Stepanova AN, Alonso JM (2005), Arabidopsis ethylene signaling pathway, *Sci STKE*, **2005**(276):cm4.

Stepanova AN, Hoyt JM, Hamilton AA, Alonso JM (2005), A Link between ethylene and auxin uncovered by the characterization of two root-specific ethylene-insensitive mutants in Arabidopsis, *Plant Cell*, **17**(8):2230-42.

Stepanova AN, Yun J, Likhacheva AV, Alonso JM (2007), Multilevel interactions between ethylene and auxin in Arabidopsis roots, *Plant Cell*, **19**(7):2169-85.

Stepanova AN, Robertson-Hoyt J, Yun J, Benavente LM, Xie DY, Dolezal K, Schlereth A, Jürgens G, Alonso JM (2008), TAA1-mediated auxin biosynthesis is essential for hormone crosstalk and plant development, *Cell*, **133**(1):177-91.

Swarup R, Friml J, Marchant A, Ljung K, Sandberg G, Palme K, Bennett M (2001), Localization of the auxin permease AUX1 suggests two functionally distinct hormone transport pathways operate in the Arabidopsis root apex, *Genes Dev*., **15**(20):2648-53.

Swarup R, Parry G, Graham N, Allen T, Bennett M (2002), Auxin cross-talk: integration of signalling pathways to control plant development, *Plant Mol Biol.,* **49**(3-4):411-26.

Swarup R, Kramer EM, Perry P, Knox K, Leyser HM, Haseloff J, Beemster GT, Bhalerao R, Bennett MJ (2005), Root gravitropism requires lateral root cap and epidermal cells for transport and response to a mobile auxin signal, *Nat Cell Biol*., **7**(11):1057-65.

Swarup R, Perry P, Hagenbeek D, Van Der Straeten D, Beemster GT, Sandberg G, Bhalerao R, Ljung K, Bennett MJ (2007), Ethylene upregulates auxin biosynthesis in Arabidopsis seedlings to enhance inhibition of root cell elongation, *Plant Cell*, **19**(7):2186-96.

Swarup K, Benková E, Swarup R, Casimiro I, Péret B, Yang Y, Parry G, Nielsen E, De Smet I, Vanneste S, Levesque MP, Carrier D, James N, Calvo V, Ljung K, Kramer E, Roberts R, Graham N, Marillonnet S, Patel K, Jones JD, Taylor CG, Schachtman DP, May S, Sandberg G, Benfey P, Friml J, Kerr I, Beeckman T, Laplaze L, Bennett MJ(2008), The auxin influx carrier LAX3 promotes lateral root emergence*, Nat. Cell Biol*., **10**(8):946-54.

Tan DX, Manchester LC, Terron MP, Flores LJ, Reiter RJ (2007), One molecule, any derivatives: a never-ending interaction of melatonin with reactive oxygen and nitrogen species?, *J Pineal Res* **42:** 28-42.

Tanaka H, Dhonukshe P, Brewer PB, Friml J(2006), Spatiotemporal asymmetric auxin distribution: a means to coordinate plant development, *Cell Mol Life Sci*., **63**(23):2738-54.

Tao Y, Ferrer JL, Ljung K, Pojer F, Hong F, Long JA, Li L, Moreno JE, Bowman ME, Ivans LJ, Cheng Y, Lim J, Zhao Y, Ballaré CL, Sandberg G, Noel JP, Chory J (2008), Rapid synthesis of auxin via a new tryptophan-dependent pathway is required for shade avoidance in plants, Cell, **133**(1):164-76.

Tatematsu K, Kumagai S, Muto H, Sato A, Watahiki MK, Harper RM, Liscum E, Yamamoto KT (2004), MASSUGU2 encodes Aux/IAA19, an auxin-regulated protein that functions together with the transcriptional activator NPH4/ARF7 to regulate differential growth responses of hypocotyl and formation of lateral roots in Arabidopsis thaliana, *Plant Cell*, **16**(2):379-93.

Teale WD, Paponov IA, Palme K (2006), Auxin in action: signalling, transport and the control of plant growth and development, *Nat Rev Mol Cell Biol*., **7**(11):847-59.

Thimann K.V ( 1938), Hormones and the analysis of growth, *Plant Physiol.* **13**:437–449.

Tian D, Araki H, Stahl E, Bergelson J, Kreitman M (2002), Signature of balancing selection in Arabidopsis, *Proc Natl Acad Sci U S A.,* **99**(17):11525-30.

Topping JF, Lindsey K (1997), Promoter trap markers differentiate structural and positional components of polar development in Arabidopsis, *Plant Cell*, **9**(10):1713-25.

Topping JF, Agyeman F, Henricot B, Lindsey K (1994), Identification of molecular markers of embryogenesis in Arabidopsis thaliana by promoter trapping, *Plant J*., **5**(6):895-903.

Topping J F, Wei W and Lindsey K (1991), Functional taggingof regulatory elements in the plant genome, Development, 112:1009-1.

Ulmasov T, Murfett J, Hagen G, Guilfoyle TJ(1997), Aux/IAA proteins repress expression of reporter genes containing natural and highly active synthetic auxin response elements, *Plant Cell*, **9**(11):1963-71.

van den Berg C, Willemsen V, Hendriks G, Weisbeek P, Scheres B (1997), Short-range control of cell differentiation in the Arabidopsis root meristem, *Nature*, **390**(6657):287-9.

Vanneste S, Friml J(2009), Auxin: a trigger for change in plant development, *Cell*, **136**(6):1005-16.

van den Berg C,Willemsen V, HageW,Weisbeek P and Scheres B(1995), Cell fate in the *Arabidopsis* rootmeristem determined by directional signalling, *Nature,* **378,** 62–65 (1995).

Vieten A, Vanneste S, Wisniewska J, Benková E, Benjamins R, Beeckman T, Luschnig C, Friml J (2005), Functional redundancy of PIN proteins is accompanied by auxin-dependent cross-regulation of PIN expression, *Development*, **132**(20):4521-31.

Vieten A, Sauer M, Brewer PB, Friml J (2007), Molecular and cellular aspects of auxin-transport-mediated development, *Trends Plant Sci.,* **12**(4):160-8.

Vogel JP, Schuerman P, Woeste K, Brandstatter I, Kieber JJ (1998), Isolation and characterization of Arabidopsis mutants defective in the induction of ethylene biosynthesis by cytokinin, *Genetics*, **149**(1):417-27.

Walker L, Estelle M(1998), Molecular mechanisms of auxin action, *Curr Opin Plant Biol*., **1**(5):434-9.

Walsh TA, Neal R, Merlo AO, Honma M, Hicks GR, Wolff K, Matsumura W, Davies JP (2006), Mutations in an auxin receptor homolog AFB5 and in SGT1b confer resistance to synthetic picolinate auxins and not to 2,4-dichlorophenoxyacetic acid or indole-3-acetic acid in Arabidopsis, *Plant Physiol*.,**142**(2):542-52.

Wada T Tominaga R, Iwata M, Sano R, Inoue K, Okada K (2008), Arabidopsis CAPRICE-LIKE MYB 3 (CPL3) controls endoreduplication and flowering development in addition to trichome and root hair formation, *Development*, **135**(7):1335-45.

Welch D, Hassan H, Blilou I, Immink R, Heidstra R, Scheres B(2007), Arabidopsis JACK-DAW and MAGPIE zinc finger proteins delimit asymmetric cell division and stabilize tissue boundaries by restricting SHORT-ROOT action, *Genes Dev*., **21**(17):2196-204.

Willemsen V, Friml J, Grebe M, van den Toorn A, Palme K, Scheres B (2003), Cell polarity and PIN protein positioning in Arabidopsis require STEROL METHYLTRANSFERASE1 function, *Plant Cell*, **15**(3):612-25.

Wisniewska J, Xu J, Seifertová D, Brewer PB, Ruzicka K, Blilou I, Rouquié D, Benková E, Scheres B, Friml J (2006), Polar PIN localization directs auxin flow in plants, *Science*, **312**(5775):883.

Wisniewska J, Xu J, Seifertová D, Brewer PB, Ruzicka K, Blilou I, Rouquié D, Benková E, Scheres B, Friml J(2006), Polar PIN localization directs auxin flow in plants, *Science*, **2312**(5775):883.

Willemsen V, Wolkenfelt H, de Vrieze G, Weisbeek P, Scheres B(1998), The HOBBIT gene is required for formation of the root meristem in the Arabidopsis embryo, Development, **125**(3):521-31.

Willemsen V, Friml J, Grebe M, van den Toorn A, Palme K, Scheres B(2003), Cell polarity and PIN protein positioning in Arabidopsis require STEROL METHYLTRANSFERASE1 function, *Plant Cell*, **15**(3):612-25.

Woodward AW, Bartel B(2005), A receptor for auxin, *Plant Cell*, **17**(9):2425-9.

Wysocka-Diller JW, Helariutta Y, Fukaki H, Malamy JE, Benfey PN (2000), Molecular analysis of SCARECROW function reveals a radial patterning mechanism common to root and shoot, *Development*, **127**(3):595-603.

Yamamoto M, Yamamoto K(1998), Differential effects of 1-naphathaleneacetic acid and 2,4-dichlorophenoxyacetic acid on the gravitropic response of roots in an auxin resistant mutant of Arabidopsis, aux1, *Plant Cell Physiol*., **39**:660.

Yang S, Hoffman N (1987), Ethylene biosynthesis and its regulation in higher plants, Ann. Rev. Plant Physiol., 35:155-189.

Zarembinski TI, Theologis A(1994), Ethylene biosynthesis and action: a case of conservation, Plant Mol Biol., **26**(5):1579-97.

Zemach A, Li Y, Wayburn B, Ben-Meir H, Kiss V, Avivi Y, Kalchenko V, Jacobsen SE, Grafi G( 2005), DDM1 binds Arabidopsis methyl-CpG binding domain proteins and affects their subnuclear localization, *Plant Cell*, **17**(5):1549-58.

# Appendix

## Appendix 1: Data of Figure 4.8: Comparison of *pls* root length on different media

| | | | | | | | | | | | | | | | | | | | |
|---|---|---|---|---|---|---|---|---|---|---|---|---|---|---|---|---|---|---|---|
| wt on 1/2 MS10 | 6.3 | 5.78 | 6.5 | 5.9 | 6.7 | 6 | 6.6 | 5.34 | 7.3 | 7.8 | 5.66 | 5.5 | 5.55 | 5.34 | 6.1 | 5.78 | 6.134375 | 0.701769 | 0.175442 |
| pls on 1/2 MS10 | 3.1 | 3.5 | 2.9 | 3.7 | 3 | 3.2 | 3.8 | 4 | 3.1 | 4.1 | 3.8 | 3.2 | 3.6 | 4 | 3.8 | 4.5 | 3.58125 | 0.460751 | 0.115188 |
| pls on ACC | 3.1 | 2.9 | 2.8 | 3.2 | 2.9 | 3.9 | 2.9 | 2.7 | 3.2 | 3.5 | 3.1 | 3 | 3.9 | 3.7 | 3.77 | 3.22 | 3.236875 | 0.39695 | 0.099238 |
| pls on AgNO3 | 4.4 | 3.5 | 5 | 3.76 | 4.1 | 4.5 | 4.44 | 4.5 | 4.33 | 5.4 | 4.34 | 4.9 | 5 | 4.56 | 4.89 | 4.13 | 4.484375 | 0.485413 | 0.121353 |
| pls on NAA | 3.4 | 3.22 | 3.44 | 3.89 | 3.67 | 4.1 | 3.5 | 3.76 | 3.66 | 3.11 | 3 | 4.2 | 3.44 | 3 | 3.89 | 3.97 | 3.578125 | 0.378351 | 0.094588 |

## Appendix 2 : Data of Figure 4.9: Rescue of *pls* root length on ACC using *aux1*

| | 1 | 2 | | 3 | 4 | 5 | 6 | 7 | Mean | st dev. | std error |
|---|---|---|---|---|---|---|---|---|---|---|---|
| *aux1* | 5 | 4 | 3.8 | 6 | 4.5 | 4.2 | 3.6 | 4.4 | 4.4375 | 0.7670677 | 0.27395275 |
| *pls* | 1.5 | 3 | 2 | 2.2 | 2.3 | 2.4 | 2.7 | 3 | 2.3875 | 0.51112621 | 0.18254507 |
| *aux1x pls* | 2.8 | 3 | 2.8 | 3.6 | 2.5 | 2.9 | 4 | 2.6 | 3.025 | 0.51478151 | 0.18385054 |
| | | | | | | | | | | | |

# Appendix 3: Data for Figure 4.17: Relative transcript abundance of WEI2 in *pls* and ethylene mutants

**Actin**

| | 1 | 2 | 3 | 4 | Mean | STD Dev. | Std Error |
|---|---|---|---|---|---|---|---|
| col | 126 | 107 | 113 | 113 | 114.75 | 8.01561 | 4.007805 |
| C24 | 101 | 113 | 90.1 | 100 | 101.025 | 9.377411 | 4.688705 |
| pls | 130 | 141 | 141 | 117 | 132.25 | 11.41271 | 5.706356 |
| plsOX | 95.3 | 96.2 | 100.1 | 109.1 | 100.175 | 6.304165 | 3.152083 |
| plsxetr1 | 117 | 134 | 112 | 121 | 121 | 9.416298 | 4.708149 |
| etr1 | 92 | 95.3 | 100.6 | 107 | 98.725 | 6.556104 | 3.278052 |
| eto1 | 117 | 147 | 121 | 132 | 129.25 | 13.42572 | 6.712861 |

**WEI2**

| | 1 | 2 | 3 | 4 | Mean | STDEV | STD Error | wei2/act |
|---|---|---|---|---|---|---|---|---|
| col | 9.8 | 9.8 | 10.4 | 8.75 | 9.6875 | 0.686021 | 0.343011 | 0.010349 |
| C24 | 8.6 | 8.76 | 9 | 6.6 | 8.24 | 1.105622 | 0.552811 | 0.010233 |
| pls | 11.5 | 11.6 | 9.8 | 9.8 | 10.675 | 1.011187 | 0.505594 | 0.018015 |
| plsOX | 15.4 | 11 | 10.8 | 13.4 | 12.65 | 2.180978 | 1.090489 | 0.010931 |
| plsxetr1 | 20.1 | 14.5 | 19.8 | 11 | 16.35 | 4.397348 | 2.198674 | 0.008682 |
| etr1 | 8.75 | 7.39 | 6.6 | 7.39 | 7.5325 | 0.893024 | 0.446512 | 0.007769 |
| eto1 | 19 | 17.2 | 16.3 | 15.4 | 16.975 | 1.537043 | 0.768521 | 0.014952 |

## Appendix 4: Data for Figure 4.18 Root length of the *ctr1* mutant is rescued on 1- NAA

| | 1 | 2 | 3 | 4 | 5 | 6 | 7 | 8 | 9 | 10 | 11 | 12 | 13 | 14 | 15 | 16 | mean | Std Dev | STD ERROR |
|---|---|---|---|---|---|---|---|---|---|---|---|---|---|---|---|---|---|---|---|
| ctr1 on NAA | 2 | 2.5 | 2.8 | 2.9 | 3.5 | 3 | 2.7 | 2.1 | 3 | 3.1 | 2.9 | 2.7 | 2.6 | 2.5 | 3 | 2.5 | 2.7375 | 0.37572153 | 0.0939308 |
| ctr1 on 1/2 MS10 | 0.9 | 0.9 | 2 | 0.8 | 1.5 | 1.2 | 2 | 1.1 | 1.5 | 2 | 1.2 | 3 | 2.2 | 2.3 | 2 | 2 | 1.6625 | 0.619542844 | 0.1548857 |
| | | | | | | | | | | | | | | | | | | | |

## Appendix 5: Data for Figures 5.6-5.10

| act2 | | | | | | | |
|---|---|---|---|---|---|---|---|
| Lines | 1 | 2 | 3 | 4 | Mean | STD Dev | STD Error |
| Col-0 | 94.1 | 94.1 | 105.1 | 105 | 99.575 | 6.322117 | 3.161059 |
| C24 | 88.9 | 79.3 | 88.9 | 88.9 | 86.5 | 4.8 | 2.4 |
| pls | 111 | 125 | 123 | 101 | 115 | 11.19524 | 5.597619 |
| PLSOx | 94.1 | 88.9 | 88.9 | 84 | 88.975 | 4.124217 | 2.062109 |
| plsxetr1 | 125 | 105 | 105 | 99.6 | 108.65 | 11.1933 | 5.596651 |
| etr1 | 88.9 | 79.3 | 84 | 84 | 84.05 | 3.919609 | 1.959804 |
| ctr1 | 79.3 | 88.9 | 88.9 | 88.9 | 86.5 | 4.8 | 2.4 |
| eto1 | 125 | 112 | 125 | 102 | 116 | 11.16542 | 5.582711 |
| | | | | | | | |
| ctr1 | | | | | | | |
| Lines | 1 | 2 | 3 | 4 | Mean | STD Dev | STD Error |
| Col-0 | 56.1 | 59.4 | 62.9 | 62.9 | 60.325 | 3.264327 | 1.632164 |
| C24 | 56.1 | 50.1 | 47.3 | 53 | 51.625 | 3.783627 | 1.891814 |
| pls | 139 | 131 | 139 | 131 | 135 | 4.618802 | 2.309401 |
| PLSOx | 44.7 | 37.7 | 42.3 | 39.9 | 41.15 | 3.021589 | 1.510794 |
| plsxetr1 | 42.3 | 42.3 | 42.3 | 44.7 | 42.9 | 1.2 | 0.6 |
| etr1 | 19.1 | 19.1 | 21.4 | 20.2 | 19.95 | 1.096966 | 0.548483 |
| ctr1 | 74.5 | 74.5 | 74.5 | 83.5 | 76.75 | 4.5 | 2.25 |
| eto1 | 185 | 147 | 175 | 147 | 163.5 | 19.48504 | 9.742518 |
| | | | | | | | |
| etr1 | | | | | | | |
| Lines | 1 | 2 | 3 | 4 | Mean | STD Dev | STD Error |
| Col-0 | 110 | 117 | 124 | 124 | 118.75 | 6.70199 | 3.350995 |
| C24 | 166 | 82.3 | 73.2 | 65.1 | 96.65 | 46.76412 | 23.38206 |
| pls | 250 | 250 | 281 | 281 | 265.5 | 17.89786 | 8.948929 |
| PLSOx | 73.2 | 69 | 61.9 | 69 | 68.275 | 4.68855 | 2.344275 |

| | | | | | | | |
|---|---|---|---|---|---|---|---|
| ***plsxetr1*** | ***117*** | ***117*** | ***148*** | ***110*** | ***123*** | ***16.99019*** | ***8.495097*** |
| ***etr1*** | ***57.9*** | ***54.6*** | ***54.6*** | ***54.6*** | ***55.425*** | ***1.65*** | ***0.825*** |
| ***ctr1*** | ***65.1*** | ***73.2*** | ***54.6*** | ***61.4*** | ***63.575*** | ***7.75129*** | ***3.875645*** |
| ***eto1*** | ***300*** | ***335*** | ***223*** | ***335*** | ***298.25*** | ***52.81019*** | ***26.4051*** |
| | | | | | | | |
| ***ers1*** | | | | | | | |
| ***Lines*** | ***1*** | ***2*** | ***3*** | ***4*** | ***Mean*** | ***STD Dev*** | ***STD Error*** |
| ***Col-0*** | ***61.3*** | ***52.2*** | ***61.3*** | ***61.3*** | ***59.025*** | ***4.55*** | ***2.275*** |
| ***C24*** | ***49.5*** | ***44.5*** | ***46.9*** | ***42.1*** | ***45.75*** | ***3.176476*** | ***1.588238*** |
| ***pls*** | ***123*** | ***116*** | ***105*** | ***105*** | ***112.25*** | ***8.845903*** | ***4.422952*** |
| ***PLSOx*** | ***40*** | ***42.1*** | ***32.3*** | ***40*** | ***38.6*** | ***4.31509*** | ***2.157545*** |
| ***plsxetr1*** | ***34*** | ***40*** | ***37.9*** | ***42.1*** | ***38.5*** | ***3.455431*** | ***1.727715*** |
| ***etr1*** | ***13*** | ***13.7*** | ***13.7*** | ***16.1*** | ***14.125*** | ***1.357387*** | ***0.678694*** |
| ***ctr1*** | ***61.3*** | ***61.3*** | ***58.1*** | ***61.3*** | ***60.5*** | ***1.6*** | ***0.8*** |
| ***eto1*** | ***123*** | ***137*** | ***199*** | ***123*** | ***145.5*** | ***36.27212*** | ***18.13606*** |
| | | | | | | | |
| ***ein3*** | | | | | | | |
| ***Lines*** | ***1*** | ***2*** | ***3*** | ***4*** | ***Mean*** | ***STD Dev*** | ***STD Error*** |
| ***Col-0*** | ***84.5*** | ***84.5*** | ***84.5*** | ***67.5*** | ***80.25*** | ***8.5*** | ***4.25*** |
| ***C24*** | ***71.4*** | ***84.5*** | ***75.5*** | ***71.4*** | ***75.7*** | ***6.176838*** | ***3.088419*** |
| ***pls*** | ***153*** | ***132*** | ***112*** | ***106*** | ***125.75*** | ***21.2975*** | ***10.64875*** |
| ***PLSOx*** | ***89.4*** | ***63.8*** | ***40.7*** | ***43.1*** | ***59.25*** | ***22.61747*** | ***11.30874*** |
| ***plsxetr1*** | ***89.4*** | ***71.4*** | ***63.8*** | ***75.5*** | ***75.025*** | ***10.73945*** | ***5.369726*** |
| ***etr1*** | ***63.8*** | ***53.9*** | ***60.3*** | ***57*** | ***58.75*** | ***4.261846*** | ***2.130923*** |
| ***ctr1*** | ***89.4*** | ***79.9*** | ***84.5*** | ***84.5*** | ***84.575*** | ***3.879326*** | ***1.939663*** |
| ***eto1*** | ***140*** | ***148*** | ***148*** | ***140*** | ***144*** | ***4.618802*** | ***2.309401*** |

| ***gst2*** | | | | | | | |
|---|---|---|---|---|---|---|---|
| Lines | 1 | 2 | 3 | 4 | Mean | STD Dev | STD Error |
| Col-0 | 49.7 | 55.1 | 44.9 | 55.1 | 51.2 | 4.911212 | 2.455606 |
| C24 | 49.7 | 46.7 | 55.1 | 55.1 | 51.65 | 4.167733 | 2.083867 |
| pls | 154 | 162 | 154 | 162 | 158 | 4.618802 | 2.309401 |
| PLSOx | 44.9 | 32.9 | 32.9 | 36.5 | 36.8 | 5.660389 | 2.830194 |
| plsxetr1 | 40.5 | 42.6 | 36.5 | 40.5 | 40.025 | 2.55 | 1.275 |
| etr1 | 18.7 | 13.8 | 15.2 | 15.2 | 15.725 | 2.090255 | 1.045128 |

| | | | | | | | |
|---|---|---|---|---|---|---|---|
| ctr1 | 83.1 | 87.5 | 78.9 | 83.1 | 83.15 | 3.51141 | 1.755705 |
| eto1 | 58 | 75 | 75 | 83 | 72.75 | 10.5317 | 5.265849 |
| | | | | | | | |
| ***hls1*** | | | | | | | |
| Lines | 1 | 2 | 3 | 4 | Mean | STD Dev | STD Error |
| Col-0 | 82.7 | 66.4 | 78.5 | 66.4 | 73.5 | 8.375759 | 4.187879 |
| C24 | 59.4 | 59.4 | 74.2 | 70.2 | 65.8 | 7.568355 | 3.784178 |
| pls | 137 | 162 | 137 | 110 | 136.5 | 21.23676 | 10.61838 |
| PLSOx | 83 | 66.4 | 78.5 | 59.4 | 71.825 | 10.85123 | 5.425614 |
| plsxetr1 | 83 | 70.2 | 78.5 | 98 | 82.425 | 11.65858 | 5.82929 |
| etr1 | 24.4 | 40.2 | 30.5 | 30.5 | 31.4 | 6.533503 | 3.266752 |
| ctr1 | 104 | 104 | 116 | 116 | 110 | 6.928203 | 3.464102 |
| eto1 | 153 | 181 | 162 | 153 | 162.25 | 13.20038 | 6.600189 |
| | | | | | | | |
| | | | | | | | |
| ***ein2*** | | | | | | | |
| Lines | 1 | 2 | 3 | 4 | Mean | STD Dev | STD Error |
| Col-0 | 131 | 131 | 154 | 146 | 140.5 | 11.44 | 5.72 |
| C24 | 131 | 131 | 117 | 117 | 124 | 8.082904 | 4.041452 |
| pls | 214 | 214 | 214 | 203 | 211.25 | 5.5 | 2.75 |
| PLSOx | 138 | 138 | 131 | 163 | 142.5 | 14.0594 | 7.029699 |
| plsxetr1 | 172 | 163 | 172 | 182 | 172.25 | 7.762087 | 3.881044 |
| etr1 | 89.2 | 99.5 | 89.2 | 99.5 | 94.35 | 5.946708 | 2.973354 |
| ctr1 | 226 | 192 | 182 | 172 | 193 | 23.46629 | 11.73314 |
| eto1 | 203 | 226 | 203 | 226 | 214.5 | 13.27906 | 6.639528 |

***Relative transcript abundunce***

| ***LINES*** | ***etr1*** | ***ers1*** | ***ctr1*** | ***gst2*** | ***ein3*** | ***ein2*** | ***hls1*** |
|---|---|---|---|---|---|---|---|
| ***Col-0*** | ***1.192568*** | ***0.592769*** | ***0.605825*** | ***0.514185*** | ***0.805925*** | ***1.410997*** | ***0.738137*** |
| ***C24*** | ***1.117341*** | ***0.528902*** | ***0.596821*** | ***0.59711*** | ***0.875145*** | ***1.433526*** | ***0.760694*** |
| ***pls*** | ***2.308696*** | ***0.976087*** | ***1.173913*** | ***1.373913*** | ***1.093478*** | ***1.836957*** | ***1.186957*** |
| ***PLSOx*** | ***0.76735*** | ***0.43383*** | ***0.462489*** | ***0.413599*** | ***0.665917*** | ***1.601573*** | ***0.807249*** |

| | | | | | | | |
|---|---|---|---|---|---|---|---|
| ***plsxetr1*** | ***1.132075*** | ***0.354349*** | ***0.394846*** | ***0.368385*** | ***0.69052*** | ***1.585366*** | ***0.758629*** |
| ***etr1*** | ***0.659429*** | ***0.168055*** | ***0.237359*** | ***0.187091*** | ***0.698989*** | ***1.122546*** | ***0.373587*** |
| ***ctr1*** | ***0.734971*** | ***0.699422*** | ***0.887283*** | ***0.961272*** | ***0.977746*** | ***2.231214*** | ***1.271676*** |
| ***eto1*** | ***2.571121*** | ***1.25431*** | ***1.409483*** | ***0.627155*** | ***1.241379*** | ***1.849138*** | ***1.398707*** |